

**Physiological and Structural Characterization of a Manganese  
Catalase (KatB) from the Filamentous, Heterocystous, N<sub>2</sub>-fixing  
Cyanobacterium *Anabaena* PCC 7120**

*By*

**DHIMAN CHAKRAVARTY**

**Enrolment Number: LIFE01201504005**

**Bhabha Atomic Research Centre, Mumbai**

*A thesis submitted to the*

*Board of Studies in Life Sciences*

*In partial fulfillment of requirements*

*for the Degree of*

**DOCTOR OF PHILOSOPHY**

*of*

**HOMI BHABHA NATIONAL INSTITUTE**

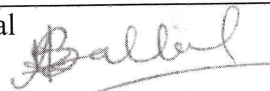
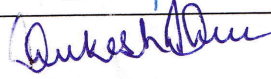


**November, 2020**

# Homi Bhabha National Institute<sup>1</sup>

## Recommendations of the Viva Voce Committee

As members of the Viva Voce Committee, we certify that we have read the dissertation prepared by Mr. Dhiman Chakravarty entitled "Physiological and Structural Characterization of a Manganese Catalase (KatB) from the Filamentous, Heterocystous, N<sub>2</sub>-fixing Cyanobacterium *Anabaena* PCC 7120" and recommend that it may be accepted as fulfilling the thesis requirement for the award of Degree of Doctor of Philosophy.

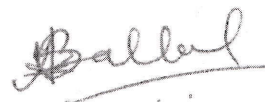
Chairman : Dr. Hema Rajaram		Date: 18/11/2020
Guide / Convener : Dr. Anand Ballal		Date: 27/10/2020
Examiner: Prof. Sudhir Kumar Sopory		Date: 27/10/2020
Member: Dr. Mukesh Kumar		Date: 17/11/2020
Member: Dr. S. N. Jamdar		Date: 17/11/2020

Final approval and acceptance of this thesis is contingent upon the candidate's submission of the final copies of the thesis to HBNI.

I hereby certify that I have read this thesis prepared under my direction and recommend that it may be accepted as fulfilling the thesis requirement.

Date: 27/10/2020

Place: Mumbai



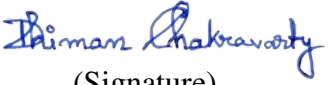
Dr. Anand Ballal  
Guide

<sup>1</sup> This page is to be included only for final submission after successful completion of viva voce.

## STATEMENT BY AUTHOR

This dissertation has been submitted in partial fulfillment of requirements for an advanced degree at Homi Bhabha National Institute (HBNI) and is deposited in the Library to be made available to borrowers under rules of the HBNI.

Brief quotations from this dissertation are allowable without special permission, provided that accurate acknowledgement of source is made. Requests for permission for extended quotation from or reproduction of this manuscript in whole or in part may be granted by the Competent Authority of HBNI when in his or her judgment the proposed use of the material is in the interests of scholarship. In all other instances, however, permission must be obtained from the author.

  
(Signature)

Dhiman Chakravarty

## DECLARATION

I, hereby declare that the investigation presented in the thesis has been carried out by me. The work is original and has not been submitted earlier as a whole or in part for a degree/diploma at this or any other Institution/University.



(Signature)

Dhiman Chakravarty

## List of publications arising from the thesis

### Journal

1. “Gazing into the remarkable world of non heme-catalases through the window of the cyanobacterial Mn-catalase ‘KatB’” Anand Ballal, Dhiman Chakravarty\*, Subhash C. Bihani and Manisha Banerjee, *Free Radical Biology and Medicine*, **2020**, *160*, 480-487.  
(\* Equal first author)
2. “Facile generation of a biotechnologically-relevant catalase showcases the efficacy of a blue-green algal biomass as a suitable bioresource for protein overproduction” Dhiman Chakravarty, Manisha Banerjee and Anand Ballal, *Bioresource Technology*, **2019**, *293*, 122013.
3. “Novel molecular insights into the anti-oxidative stress response and structure-function of a salt-inducible cyanobacterial Mn-catalase” Dhiman Chakravarty, Subhash C. Bihani, Manisha Banerjee and Anand Ballal, *Plant, Cell & Environment*, **2019**, *42*(8), 2508-2521.
4. “A salt-inducible Mn-catalase (KatB) protects cyanobacterium from oxidative stress” Dhiman Chakravarty, Manisha Banerjee, Subhash C. Bihani and Anand Ballal, *Plant Physiology*, **2016**, *170*(2), 761-773.
5. “Cyanobacterial Mn-catalase ‘KatB’: Molecular link between salinity and oxidative stress resistance” Dhiman Chakravarty, Manisha Banerjee, Namrata Waghmare and Anand Ballal, *Communicative & Integrative Biology*, **2016**, *9*(5), p.e1216738.
6. “KatB, a cyanobacterial Mn-catalase with unique active site configuration: Implications for enzyme function” Subhash C. Bihani, Dhiman Chakravarty and Anand Ballal, *Free Radical Biology and Medicine*, **2016**, *93*, 118-129.

## Chapters in books and lectures notes

Nil

## Conferences

1. **New Phytologist Next Generation Scientist-2019** held from 22<sup>nd</sup>-25<sup>th</sup> July, 2019 at University College Dublin, Ireland.
2. DAE-BRNS Life Science Symposium-2019 (**LSS-2019**) on 'Molecular and Cellular Responses to Stresses and Cancer Therapeutics', held from 28<sup>th</sup>-30<sup>th</sup> January, 2019 at Anushaktinagar, Mumbai. (**Won the best poster award**)
3. 88<sup>th</sup> Annual Meeting of the Society for Biological Chemists, India (**SBCI-2019**) and Conference on 'Advances at the Interface of Biology & Chemistry', held from 31<sup>st</sup> October-3<sup>rd</sup> November, 2019 at Anushaktinagar, Mumbai.
4. 59<sup>th</sup> Annual Conference of Association of Microbiologists of India (**AMI- 2018**) & International Symposium on 'Host Pathogen Interactions', held from 9<sup>th</sup>-12<sup>th</sup> December, 2018 at Hyderabad.
5. 15<sup>th</sup> Annual Meeting of Society for Free Radical Research-India (**SFRR-INDIA-17**) and conference on 'Basic and Applied Aspects of Health Management using Radiation, Antioxidants & Nutraceuticals' & One Day School on 'Radiation and Redox Process in Health', held from 9<sup>th</sup>-12<sup>th</sup> January, 2017 at Anushaktinagar, Mumbai. (**Won the best poster award**)
6. DAE-BRNS Life Sciences Symposium (**LSS-2015**) on 'Advances in Microbiology of Food, Agriculture, Health and Environment', held from 3<sup>rd</sup>-5<sup>th</sup> February, 2015 at Anushaktinagar, Mumbai

## Others

Nil

  
(Signature)

Dhiman Chakravarty

# **DEDICATION**

**Dedicated to my parents whose blessings have  
brought me here....**

## ACKNOWLEDGEMENTS

First and foremost, I would like to thank my PhD supervisor Dr. Anand Ballal for guiding me to sail through the journey of science so far. I am indebted to him for all his teaching, training and nurturing the naive mind of mine. His inclination towards better and better science and the importance of scientific attitude are the two main inspirations that have driven me this far. He always stands by me under all circumstances, be it professional or personal. He is the one mentor with whom I share my joy and sorrow.

Dr. Hema Rajaram, the chairman of my doctoral committee, has always carefully scrutinized my work and given me timely suggestions for the betterment of the thesis. I take this opportunity to thank her for the much needed support that I got from her. I thank the members of my doctoral committee, Dr. Mukesh Kumar and Dr. S. N. Jamdar, for the valuable inputs in biophysics and biochemistry which made the thesis a multidisciplinary piece of work. I am deeply indebted to Dr. Subhash C. Bihani for all the structural biology based analyses.

I would like to specially thank Dr. Manisha Banerjee for all the molecular biology techniques that I have learnt from her. A special thank to Mr. Prakash Kalwani for always standing by me with a 'May I Help You' sign. Mrs. Namrata Waghmare and Mr. Narendra Tekade have always provided indispensable scientific and technical supports related to the work. I thank my other lab members, Dr. Rajanikant Chittela, Dr. Rachna Agarwal, Dr. Alka Gupta, Ms. Vinayiki Pillai, Dr. Vijay Tailor, Dr. Anuradha Nair and Mr. V. R. Jadhav for making my journey a smooth and joyful one.

I sincerely thank Dr. H. S. Misra, Head, Molecular Biology Division for the constant support and encouragement throughout the study. The encouragement that I got from Dr. S. K Apte, former Head of our division, in my initial days fuelled me ahead in my career.

Big thanks to all my training school batchmates who became my family and provided all the supports I needed throughout.

It cannot be expressed in words the sacrifice my parents and my family back home made to put me here. Our parrot Mithu played the role of stressbuster with his sweet melodies whenever I needed. My wife Sujata has always stood by my side during this wonderful journey. I am fortunate to be with Sujata with whom I share not only my life, but science too. I also acknowledge everyone who directly or indirectly helped me during course of my PhD.

It feels my heart with joy and my mind with delight to share the arrival of our twin daughter and son, Aabriti and Aabahan at the time when I am writing my thesis.



Dhiman Chakravarty

# CONTENTS

<b>SUMMARY .....</b>	<b>15</b>
<b>LIST OF FIGURES .....</b>	<b>17</b>
<b>LIST OF TABLES .....</b>	<b>23</b>
<b>CHAPTER 1: General Introduction .....</b>	<b>25</b>
<b>1.1 Reactive Oxygen Species (ROS) .....</b>	<b>27</b>
<b>1.1.1 Types of ROS .....</b>	<b>28</b>
<b>1.1.2 Sources of ROS.....</b>	<b>29</b>
<b>1.1.2.1 Endogenous Sources.....</b>	<b>29</b>
<b>1.1.2.2 Exogenous Factors.....</b>	<b>30</b>
<b>1.2 Oxidative Stress.....</b>	<b>31</b>
<b>1.2.1 Damage due to Oxidative Stress: Biomolecular Damage .....</b>	<b>32</b>
<b>1.2.2 Sensing Oxidative Stress in Bacteria .....</b>	<b>34</b>
<b>1.2.2.1 Transcriptional Regulators .....</b>	<b>34</b>
<b>1.2.2.2 Two Component Systems .....</b>	<b>35</b>
<b>1.3 Mitigation of Oxidative Stress .....</b>	<b>36</b>
<b>1.3.1 Non-enzymatic Antioxidants .....</b>	<b>37</b>
<b>1.3.2 Enzymatic Antioxidants .....</b>	<b>38</b>
<b>1.3.2.1 Superoxide Dismutase (SOD) .....</b>	<b>38</b>

	<b>1.3.2.2</b> Peroxidases and Peroxiredoxins .....	39
	<b>1.3.2.3</b> Catalases .....	41
<b>1.4</b>	Clinical Importance of the Oxidative Stress Response .....	42
<b>1.5</b>	Catalase .....	43
	<b>1.5.1</b> Types of Catalase.....	44
	<b>1.5.1.1</b> Typical Mono-functional Catalases.....	44
	<b>1.5.1.2</b> Bifunctional Catalase Peroxidases (KatGs) .....	44
	<b>1.5.1.3</b> Binuclear Mn-catalase .....	45
	<b>1.5.2</b> Use of Catalase Enzyme.....	45
	<b>1.5.2.1</b> Industrial Use.....	45
	<b>1.5.2.2</b> Therapeutic Use .....	46
<b>1.6</b>	Mn-Catalase .....	46
	<b>1.6.1</b> Occurrence .....	47
	<b>1.6.2</b> Structure of Mn-catalases .....	49
	<b>1.6.3</b> Reaction Mechanism .....	51
<b>1.7</b>	Cyanobacteria .....	53
	<b>1.7.1</b> Morphology .....	54
	<b>1.7.2</b> Habitat .....	55

1.7.3	Cyanobacterial Oxidative Stress Management System.....	53
1.7.4	Economic Importance of Cyanobacteria.....	58
1.8	<i>Anabaena</i> PCC 7120 .....	59
1.9	Oxidative Stress Management in <i>Anabaena</i> .....	60
1.10	The Current Study .....	63
<b>CHAPTER 2: Materials &amp; Methods .....</b>		<b>65</b>
2.1	Materials .....	67
2.1.1	Chemicals used in this study .....	67
2.1.2	Primers used in the study .....	68
2.1.3	Plasmids used or generated in the study .....	71
2.1.4	Restriction enzymes used in the study .....	74
2.1.5	<i>E. coli</i> strains used or generated in the study .....	74
2.1.6	<i>Anabaena</i> strains used or generated in the study.....	76
2.2	Bioinformatic tools used .....	77
2.2.1	Designing of primers .....	77
2.2.2	Nucleotide or amino acid sequence analysis, multiple sequence alignment and phylogenetic analyses .....	78
2.3	Medium and growth condition .....	78
2.3.1	Medium and growth condition for <i>Anabaena</i> strains .....	78

2.3.2	Medium and growth condition for <i>E. coli</i> strains .....	79
2.4	Measurement Colony Forming Units (CFUs) .....	79
2.5	Recombinant DNA technology .....	79
2.5.1	Ligation of the <i>katB</i> DNA fragment into pET21a .....	79
2.5.2	Ligation of the <i>katB</i> variants into pET21a .....	80
2.5.3	Construction of pAMkatB or pAMkatBF2V or pAMkatB6His and Over-expression of KatB/KatBF2V/KatB6His Protein in <i>Anabaena</i> PCC 7120.....	80
2.5.4	Construction of <i>katB</i> Promoter- <i>gfp</i> Fusion .....	81
2.5.5	Construction of the <i>katB</i> Mutant ( <i>AnKatB</i> <sup>-</sup> ) .....	81
2.6	Rapid Amplification of cDNA Ends (RACE) .....	82
2.7	Protein expression in <i>E. coli</i> and purification of recombinant protein.....	82
2.8	Purification of the KatB protein from <i>AnKatB6H</i> <sup>+</sup> strain .....	84
2.9	Microscopic techniques .....	85
2.10	RNA isolation from <i>Anabaena</i> PCC 7120 .....	85
2.11	Northern blotting hybridization .....	86
2.12	Protein electrophoresis .....	86
2.13	Western blot hybridization and immuno-detection .....	87
2.14	Biophysical methods used in the study .....	87

2.14.1	Size exclusion chromatography .....	87
2.14.2	Circular Dichroism spectropolarimetry .....	87
2.14.3	Dynamic Light Scattering (DLS) .....	88
2.15	Enzyme assays.....	88
2.15.1	In-Gel Catalase Activity (Zymogram).....	88
2.15.2	Spectrophotometric H <sub>2</sub> O <sub>2</sub> decomposition assay.....	89
2.15.3	Effect of GuHCl on KatB activity.....	90
2.15.4	Effect of temperature on KatB activity.....	90
2.15.5	Estimation of residual H <sub>2</sub> O <sub>2</sub> in catalase assay performed at high temperature.....	90
2.15.6	Ability of <i>Anabaena</i> strains to decompose externally added H <sub>2</sub> O <sub>2</sub> .....	91
2.16	Methods for assessing oxidative stress in <i>Anabaena</i> cultures.....	91
2.16.1	DCHFDA assay for ROS estimation.....	91
2.16.2	MDA assay for lipid peroxidation.....	91
2.16.3	Protein oxidation and estimation of total peroxide.....	92
2.16.4	Measurement of maximum photosynthetic efficiency.....	92
2.17	Determination of oxidative stress tolerance of <i>Anabaena</i> strains.....	92
2.18	Transmission electron microscopy.....	93

2.19	Determination of crystal structure.....	94
2.20	Analysis interaction energies between residues.....	94
<b>CHAPTER 3: Physiological Role of the Mn-Catalase ‘KatB’ From <i>Anabaena</i>.....</b>		<b>95</b>
3.1	Introduction.....	97
3.2	Effect of NaCl pre-treatment on H <sub>2</sub> O <sub>2</sub> tolerance.....	98
3.2.1	Survival of NaCl pre-treated <i>Anabaena</i> cultures after exposure to H <sub>2</sub> O <sub>2</sub> .....	98
3.2.2	Molecular damage in NaCl pre-treated <i>Anabaena</i> after exposure to H <sub>2</sub> O <sub>2</sub> .....	100
3.3	Expression of catalase in NaCl pre-treated <i>Anabaena</i> PCC 7120 culture...	102
3.4	Over-expression of KatB through genetic manipulation in <i>Anabaena</i> and its effect on H <sub>2</sub> O <sub>2</sub> tolerance.....	103
3.5	Generation of KatB deficient <i>Anabaena</i> strain by insertional gene inactivation strategy.....	105
3.5.1	Cloning of 300 bp fragment internal to <i>katB</i> gene into <i>Anabaena</i> suicide vector, pRL271.....	105
3.5.2	Generation and confirmation of <i>Anabaena katB</i> mutant of KatB down-regulation.....	106
3.6	Sensitivity of the KatB deficient <i>Anabaena</i> strain to salt stress.....	108

3.6.1	Growth of the wild-type or the <i>AnKatB<sup>-</sup></i> <i>Anabaena</i> strain in the presence of NaCl.....	108
3.6.2	Molecular changes associated with NaCl treatment in wild-type <i>Anabaena</i> or the <i>AnKatB<sup>-</sup></i> strain.....	109
3.7	NaCl induced cross-protection to externally added H <sub>2</sub> O <sub>2</sub> in <i>AnKatB<sup>-</sup></i> .....	111
3.8	Ultra-structural changes associated with H <sub>2</sub> O <sub>2</sub> stress in salt pre-treated <i>katB</i> mutant.....	113
3.9	Expression analyses of <i>katB</i> /KatB under various abiotic stresses.....	114
3.9.1	Detection of <i>katB</i> transcript by Northern blotting-hybridization.....	114
3.9.2	Assessment of KatB protein content in <i>Anabaena</i> by Western blot analyses.....	115
3.10	Nitrogen status-dependent expression of <i>katB</i> /KatB .....	116
3.11	Identification of <i>katB</i> promoter region by 5' RACE analysis .....	117
3.12	Generation of <i>katB</i> promoter-GFP fusion <i>Anabaena</i> strain and analysis of the <i>katB</i> promoter activity under various stresses .....	118
3.12.1	Cloning of <i>katB</i> promoter upstream of <i>gfp</i> reporter in pAM1956 vector and generation of <i>katB</i> promoter- <i>gfp</i> fusion <i>Anabaena</i> strain.....	118
3.12.2	Assessment of <i>katB</i> promoter activity in response to various stresses by monitoring GFP fluorescence.....	120
3.13	Vegetative cell specific expression <i>katB</i> promoter.....	121

3.14	Discussion.....	122
<b>CHAPTER 4: Biochemical, Biophysical &amp; Structural Characterization of the KatB Protein.....</b>		<b>131</b>
4.1	Introduction.....	133
4.2	Cloning of <i>alr3090</i> ORF ( <i>katB</i> gene) from <i>Anabaena</i> in pET21a expression vector and over-expression in <i>E. coli</i> .....	134
4.3	Purification of KatB protein from KatB over-producing <i>E. coli</i> strain.....	135
4.4	Effect of Manganese supplementation the <i>E. coli</i> growth medium.....	136
4.4.1	Solubility of the over-produced protein in recombinant <i>E. coli</i> grown on Mn-supplemented medium .....	136
4.4.2	Enzymatic activity of KatB purified from Mn-supplemented or Mn-lacking <i>E. coli</i> cultures .....	137
4.5	Biophysical properties of the purified KatB protein.....	138
4.5.1	Gel filtration and native PAGE analyses of purified KatB protein.....	138
4.5.2	Determination of secondary structure of KatB protein by CD spectropolarimetry.....	139
4.5.3	DLS spectroscopy of KatB protein.....	139
4.6	Biochemical characterization of the purified KatB protein.....	140
4.6.1	Zymographic and spectrophotometric H <sub>2</sub> O <sub>2</sub> decomposition assay.....	140

4.6.2	Determination of the kinetic parameters of KatB enzyme.....	141
4.6.3	Determination of the pH optima of KatB.....	142
4.6.4	Enzyme inhibition studies.....	143
4.6.5	Effect of NaCl on KatB function.....	144
4.7	Thermostability of the KatB protein.....	145
4.8	Sensitivity of the KatB protein to chemical denaturant (GuHCl).....	146
4.9	Crystal structure of the KatB protein.....	147
4.9.1	Four-helix bundle type architecture of KatB.....	148
4.9.2	Hexameric assembly of the KatB protein.....	149
4.9.3	Bi-manganese core structure of KatB.....	149
4.9.4	Comparison of KatB active site with that of LPC or TTC.....	150
4.10	Site directed mutagenesis of the important second shell interacting residues..	152
4.10.1	Substitution of Tyr-42 by phenyl alanine.....	153
4.10.2	Substitution of Tyr-140 by phenyl alanine.....	154
4.11	Discussion.....	155
<b>CHAPTER 5: Role of N-Terminal Region in Maintenance of KatB Structure-Function .....</b>		<b>165</b>
5.1	Introduction .....	167

<b>5.2</b>	Localization and importance of the N-terminal residues at the subunit interface.....	168
<b>5.3</b>	Sequence conservation of the N-terminal region.....	169
<b>5.4</b>	Site directed mutagenesis of the N-terminal amino acid residues.....	170
<b>5.5</b>	Effect of the N-terminal residues on compactness of the KatB protein.....	172
<b>5.6</b>	Activity of KatB N-terminal amino acid substitution mutants.....	173
<b>5.7</b>	Effect of mutating the N-terminal residues on sensitivity to chemical denaturant.....	174
<b>5.8</b>	Detailed analysis of the N-terminal second amino acid.....	175
<b>5.8.1</b>	Sequence analysis .....	176
<b>5.8.2</b>	Substitution of the second amino acid with amino acid of different sizes by site directed mutagenesis and purification of the corresponding proteins.....	177
<b>5.8.3</b>	Effect of second amino acid mutation on compactness of KatB.....	178
<b>5.8.4</b>	Catalase activity of the KatB variants at different pH.....	179
<b>5.8.5</b>	Kinetic properties of the 2 <sup>nd</sup> residue variants of KatB.....	180
<b>5.8.6</b>	Sensitivity of the KatB variants to thermal or chemical denaturation.....	182
<b>5.9</b>	Over-expression of an N-terminal second amino acid variant (KatBF2V) of KatB in <i>Anabaena</i> .....	184

5.9.1	Cloning of <i>katBF2V</i> ORF into <i>E. coli/ Anabaena</i> shuttle vector pAM1956 and transfer to <i>Anabaena</i> .....	184
5.9.2	Production of KatB in the <i>AnKatBF2V<sup>+</sup></i> strain.....	186
5.9.3	Ability of KatBF2V over-producing <i>Anabaena</i> strain to decompose externally added H <sub>2</sub> O <sub>2</sub> .....	188
5.10	Crystal structure of the KatBF2V protein.....	189
5.11	Comparison of KatBWT and KatBF2V structures.....	190
5.11.1	Involvement of second residue in hydrophobic interactions at the oligomer interface.....	190
5.11.2	Interaction between the second amino acid and Phe-66.....	191
5.11.3	Interaction of Phe-2 with structurally important residue Trp-43.....	193
5.11.4	Calculation of interaction energies.....	194
5.12	Discussion.....	194

## **CHAPTER 6: Facile Production of the Thermostable Catalase KatB using**

### ***Anabaena* as a Production Platform: Biotechnological Implications.....201**

6.1	Introduction .....	203
6.2	Over-expression of the his tagged KatB protein in <i>Anabaena</i> PCC 7120.....	204

6.2.1	Cloning of <i>katB</i> ORF with 6 in-frame <i>His</i> codons into <i>E. coli/Anabaena</i> shuttle vector pAM1956.....	205
6.2.2	Generation of <i>Anabaena</i> strain over-producing his-tagged KatB protein.....	206
6.2.3	Confirmation of recombinant protein production by SDS-PAGE and Western blot analysis.....	207
6.2.4	Localization of the over-expressed An-KatB protein.....	208
6.3	Purification of his-tagged An-KatB protein using affinity chromatography.....	210
6.4	Facile purification of the overproduced KatB by simple physical downstream processes involving heat treatment and ammonium sulphate precipitation.....	211
6.5	Biophysical and biochemical characteristics of the purified An-KatB .....	215
6.6	Comparison of biophysical properties of An-KatB and KatB purified from <i>E. coli</i> (Ec-KatB).....	217
6.6.1	Compactness of An-KatB and Ec-KatB.....	217
6.6.2	Secondary structure and thermostability.....	218
6.7	Comparison of the biochemical properties of An-KatB and Ec-KatB.....	219
6.8	Comparison of the total KatB protein yield obtained from <i>Anabaena</i> or <i>E. coli</i> expression host.....	221

<b>6.9</b>	Comparison of An-KatB with a commercially procured heme-catalase.....	221
<b>6.9.1</b>	Biochemical properties.....	221
<b>6.9.2</b>	CD spectropolarimetric analyses.....	222
<b>6.9.3</b>	Effect of high temperature on catalase activity.....	223
<b>6.10</b>	Discussion .....	225
 <b>CHAPTER 7: Overall Findings of the Thesis and Future Directions.....</b>		<b>231</b>
<b>7.1</b>	Overall Findings of the Thesis.....	233
<b>7.2</b>	Future Directions.....	238
 <b>REFERENCES.....</b>		<b>241</b>
 <b>ANNEXURE.....</b>		<b>283</b>
<b>A1.</b>	Vector map of pET21a plasmid.....	285
<b>A2.</b>	Vector map of pAM1956 plasmid.....	286
<b>A3.</b>	Media constituents of Luria-Bertani broth.....	287
<b>A4.</b>	Media constituents of Luria-Bertani agar.....	288
<b>A5.</b>	Media constituents of BG11.....	289
<b>A6.</b>	Published articles.....	291

## **CHAPTER 7**

### **Overall Findings of the Thesis and Future Directions**



## 7.1 Overall Findings of the Thesis

Heterocystous, nitrogen-fixing, filamentous cyanobacterium *Anabaena* PCC 7120 is tolerant to stresses like desiccation, radiation, which generate reactive oxygen species (ROS). If ROS level exceeds certain threshold, it can damage all the cellular macromolecules, resulting in cell death. The cyanobacterium *Anabaena* is endowed with an arsenal of ROS scavenging proteins which are deployed under various circumstances to combat oxidative stress. Genome of this ancient photosynthetic organism shows the presence of multiple genes for peroxiredoxins (Prx), Superoxide dismutases (SODs), DPS protein (DNA Protection during starvation), Universal Stress Protein (USP) etc [148]. Notably, typical catalase or bifunctional catalase-peroxidase (KatG) genes are absent in *Anabaena*, but two genes (*katA* and *katB*) encoding a Mn-catalase are present in this organism.

Catalases are ubiquitous ROS scavenging enzymes present in all spheres of life. These enzymes detoxify H<sub>2</sub>O<sub>2</sub>, one of the most important ROS in living organisms. If not scavenged, H<sub>2</sub>O<sub>2</sub>, in presence of Fe<sup>2+</sup>, undergoes Fenton reaction to generate the hydroxyl radical (·OH), the most deleterious ROS that can damage all biomolecules. In *Anabaena*, peroxidases and catalases are the enzymes dedicated to detoxify H<sub>2</sub>O<sub>2</sub>. Induction of peroxidases in response to H<sub>2</sub>O<sub>2</sub> challenge has been reported in past [95]. On the other hand, expression of catalase was not detected in *Anabaena* even on treatment with H<sub>2</sub>O<sub>2</sub> [200]. Among the two Mn-catalases, KatB (230 amino acids in length) was found to be expressed in response to iron starvation, arsenic stress or UV-B stress [206, 207, 208]. It is also up-regulated in desiccation stress [205]. However, detailed physiological analysis or structural characterization of this important stress-responsive protein had not been performed when this work was initiated.

Interestingly, as described in Chapter 3, the wild-type *Anabaena*, pre-treated with NaCl, showed unusual resistance to H<sub>2</sub>O<sub>2</sub> compared to the control cells (i.e. not pre-treated with NaCl). After exposure to H<sub>2</sub>O<sub>2</sub>, the NaCl pre-treated cultures exhibited less formation of ROS and peroxides, decreased malonaldehyde formation and reduced content of oxidized proteins, indicating diminished levels of oxidative stress as compared to control cultures. Interestingly, the NaCl pre-treatment was found to be associated with increased accumulation of Mn-catalase, KatB.

To conclusively prove the role of KatB in the above-mentioned protective effect, production of the KatB protein in *Anabaena* was modulated by genetic manipulation and the response of these genetically altered strains to H<sub>2</sub>O<sub>2</sub> was carefully analyzed. When KatB was over-expressed, the recombinant *Anabaena* strain showed better tolerance to H<sub>2</sub>O<sub>2</sub> than the wild-type cells, indicating that elevated levels of the KatB protein makes this organism resistant to H<sub>2</sub>O<sub>2</sub>. To prove the involvement of KatB in NaCl-mediated cross protection, KatB deficient *Anabaena* strain was generated. The mutant strain could not tolerate H<sub>2</sub>O<sub>2</sub> stress after pre-treatment with NaCl, thereby, proving that it was indeed the *katB* gene that was responsible for NaCl-induced cross-protection. Moreover, the mutant strain was also found to be very susceptible to the oxidative effects of salt stress.

KatB was found to be up-regulated under conditions of osmotic or desiccation stress. However, surprisingly, it was not induced by H<sub>2</sub>O<sub>2</sub>, the direct substrate of the enzyme. In nature, cyanobacteria are periodically exposed to stresses like salinity or desiccation which are known to increase the intracellular levels of H<sub>2</sub>O<sub>2</sub>. Apparently, nature has tuned expression of *katB* gene in such a way that the protein is produced in response to

salinity or desiccation, making the cells competent to combat the H<sub>2</sub>O<sub>2</sub> that is eventually generated due to these stresses.

The promoter region of this gene (*P<sub>katB</sub>*), identified by 5'RACE analysis, was ligated upstream of the *gfp* reporter gene in pAM1956 vector and the construct was transferred to *Anabaena*. Analyses of this *Anabaena* strain revealed that the promoter was a genuine osmo-inducible one and that its expression was limited to only vegetative cells, but absent in the heterocysts i.e. the site of nitrogen-fixation.

The KatB protein was over-produced in *E. coli* and purified therefrom by affinity chromatography. The protein was found to be largely  $\alpha$ -helical with a single oligomeric form. Purified protein showed catalase activity and its enzyme kinetic parameters were determined. Sensitivity to hydroxylamine and resistance to sodium azide-mediated inhibition proved that the purified protein was indeed a Mn-catalase. The protein was found to be highly thermostable and could function under conditions of high ionic strength or under alkaline conditions.

The crystal structure revealed that the KatB protein to be hexameric in nature with the individual monomers adopting a four-helix bundle fold architecture specific to the ferritin-like superfamily. Two monomer come together to form the core dimer and the trimer of dimers forms the hexameric assembly of KatB. The two manganese ions at the active site are held together at the centre of the helix core by a Glu<sub>4</sub>His<sub>2</sub> coordination geometry. The active site of KatB is distinctly different from LPC or TTC in terms of coordination environment with two unique amino acids (Tyr-140 and Glu-163) in the active site region.

The N-terminal region of KatB is extensively involved in oligomerization. The first few residues of the N-terminus form a  $\beta$ -strand, which interacts (in antiparallel fashion)

with the corresponding  $\beta$ -strand of the neighbouring subunit, creating a  $\beta$ -sheet at the dimer interface. Moreover, these residues are relatively conserved in all cyanobacterial Mn-catalases, indicating the N-terminal  $\beta$ -sheet to play an important structural role. To decipher the role of this structural element, the 2<sup>nd</sup> to 7<sup>th</sup> amino acid residues from the N-terminal end were deleted to generate an N-terminally truncated version of KatB. The truncated protein was found to be less compact than the wild-type protein and importantly, did not show any catalase activity. To investigate the contribution of the individual amino acids within the  $\beta$ -strand, 2<sup>nd</sup> to 7<sup>th</sup> amino acid residues was individually mutated to alanine and the variant proteins were purified after over-expression in *E. coli*. Analyses with the N-terminal variants suggested that alteration in the 2<sup>nd</sup> or 4<sup>th</sup> residue affected the biochemical and biophysical properties of KatB the most.

Interestingly, the N-terminal 2<sup>nd</sup> amino acid was always a bulky aromatic amino acid (Phe, Tyr or Trp) in all Mn-catalases across the genera. Our initial mutagenesis also indicated that among the 6 residues in the  $\beta$ -strand, mutation of the second residue (Phe) affected the enzyme most. Hence, the Phe-2 residue was replaced by smaller (Gly or Ala), intermediate (Val) or bulky aromatic (Tyr or Trp) amino acids and corresponding variant proteins were purified after over-expression in *E. coli*. Analyses with the 2<sup>nd</sup> amino acid variants revealed that KatB with smaller or intermediate (Gly, Ala or Val) 2<sup>nd</sup> amino acid were less compact and less stable to thermal or chemical denaturation compared to the wild-type protein. Variant with Val at 2<sup>nd</sup> position showed only marginal catalase activity but, the ones with Gly or Ala were totally inactive. On the other hand the variants with Tyr or Trp at the second position showed appreciable catalase activity with compactness and stability comparable to the wild-type protein.

Also, *Anabaena* strain over-expressing a 2<sup>nd</sup> amino acid variant (KatBF2V) was inefficient in decomposition of externally added H<sub>2</sub>O<sub>2</sub> when compared to the strain over-expressing the wild-type KatB protein.

To shed light on the implications of the 2<sup>nd</sup> amino acid in KatB structure-function, crystal structure of KatBF2V variant was compared with that of the wild-type protein. In the wild-type protein the second amino acid (Phe) forms extensive hydrophobic interactions at the dimer interface which are important to hold the dimer together. Phe-2 also interacts with structurally important Phe-66 and Trp-43 residues in the active site region through its bulky hydrophobic side chain. In KatBF2V these important interactions were not possible due to the much shorter side chain length of Val-2, leading to the formation of a less compact hexamer and a severe reduction in the catalase activity.

Due to photoautotrophic nature and minimal culture requirements, cyanobacteria offer a distinct advantage over the heterotrophic expression hosts like *E. coli* for over-expression of recombinant proteins. Catalase enzyme has in great demand enzymes in industries pertaining to textile, leather, and food. Attempts were made to over-produce and purify KatB enzyme using *Anabaena* PCC 7120 as the expression host to demonstrate the utility of this nitrogen-fixing cyanobacterium as an alternate and viable protein production platform. Using suitable genetic manipulation techniques, *Anabaena* was bioengineered to produce the KatB protein (An-KatB). Interestingly, the over-produced protein could be easily purified by a simple downstream process involving heat treatment followed by ammonium sulphate precipitation thereby obviating the need of chromatographic steps. The purified An-KatB protein retained all the properties of Mn-catalases and showed a robust ability to decompose H<sub>2</sub>O<sub>2</sub>. Interestingly, An-KatB

showed four-fold more activity compared to the KatB protein (Ec-KatB) purified after over-expression in *E. coli*. An-KatB was found to be active in a broader range of pH than Ec-KatB. An-KatB was stable and functioned at temperature as high as 85°C, whereas a commercially procured heme-catalase showed significant drop at temperature above 50°C. Unlike the heme-catalase which showed maximal activity around neutral pH, An-KatB was active at alkaline pH. The study demonstrated that *Anabaena* can be used as a competent microbial platform for overproduction of proteins and also highlighted the advantages of An-KatB over heme-catalases in processes where H<sub>2</sub>O<sub>2</sub> has to be removed at elevated temperatures and pH (e.g. textile industry).

## **7.2 Future Directions**

Although, a detailed characterization of KatB was carried out in this study, several interesting questions remain to be answered. Firstly, the transcriptional regulation of this important salt and desiccation-inducible gene needs to be explored. Our study has revealed that osmotic stress in general is able to induce *katB*. But, the presence of combined nitrogen is also an important factor that modulates *katB* expression. Other studies show that iron starvation, arsenic stress or UV-B stress also up-regulates *katB* expression [206, 207, 208]. Clearly, regulation of this gene expression is complex and several environmental cues are integrated in the process. In unicellular cyanobacterium *Synechocystis* PCC 6803, a bulk of the osmo-inducible genes are regulated by two component systems comprising of sensor histidine kinases and response regulators. Homologues of many of those kinases and regulators are present in *Anabaena* too. Role of these systems in perceiving environmental stimuli and subsequently transmission of those signals to gene level is worth pursuing. Another interesting area for research is to

understand the regulatory mechanisms which suppress expression of *katB* in heterocysts.

The unique active site of Mn-catalase KatB offers a scope to study detailed mechanisms of catalase reaction. The active site region of Mn-catalase is thought to be the precursor of the oxygen evolving complex (OEC) in photosystem II (PSII) [301]. Earlier, the Mn-catalase active site was probed to understand the complexities of chemistry behind the OEC [138]. With a novel type of active site configuration, KatB can offer new understandings related to OEC. Also, the active site can be studied and modified to design novel catalase mimetics for potential therapeutic usage.

Although a comprehensive study was done to decipher the role of the Phe-2 residue, more detailed analyses of the other residues in the N-terminal region needs to be carried out. Structural biology-based analyses can also answer the reason for biophysical and biochemical differences between An-KatB and Ec-KatB.

The unique properties of KatB, like thermostability or ability to function at high pH or at high ionic strength, make this enzyme a suitable candidate for industrial applications. Use of this enzyme may offer benefit over the conventional heme-catalases for applications where H<sub>2</sub>O<sub>2</sub> has to be decomposed at elevated temperatures or at high pH (e. g. textile industry). Other than industrial applications, KatB can be used for biotechnological purposes such as improvement of environmental stress resistance in plants. Heterologous expression of *E. coli* KatE (a hemecatalase) increased tolerance of rice to withstand salt stress [302]. However, in many parts of the world, the temperature reaches 40-45°C regularly during summer months, limiting the activity of the thermolabile heme catalases. Thus, being a thermo and halo-tolerant enzyme, KatB

may be a promising option for transfer to crop plants for improving their stress resistance capabilities.

# **CHAPTER 1**

## **General Introduction**



Molecular oxygen (O<sub>2</sub>) is required by the aerobic organisms for respiration i.e. oxidation of nutrients to obtain energy. Association with oxygen is a double edged sword; at one end, oxygen ensures complete oxidation of food so that maximum energy can be harvested whereas on the other hand it is connected with generation of reactive oxygen species (ROS) that threatens the survival of cells. ROS are invariably generated as by-products of respiration or other enzymatic reactions involving oxygen. Apart from cellular processes, various biotic and abiotic stresses also lead to ROS generation in biological systems. Cells counteract ROS by employing a variety of mechanisms that include enzymatic as well as non-enzymatic pathways. When ROS content increases to a level that cannot be handled by the cellular defense machinery, cell experiences oxidative stress. In this chapter, various aspects of ROS/oxidative stresses, types of damage caused by ROS, strategies adopted for detoxification of ROS etc. are discussed with a special emphasis on the cyanobacterial oxidative stress management systems.

### **1.1 Reactive Oxygen Species (ROS)**

The atmospheric oxygen that we breathe is stable in nature due to the presence of two unpaired electrons in the  $\pi$ -antibonding orbitals, which exist in the same spin state [1]. This arrangement makes oxygen a relatively weak electron acceptor. It can accept only one electron at a time and after accepting one electron at a time it generates radical intermediates that are highly reactive in nature. These radical intermediates, along with the other oxygen-containing free radicals and reactive molecules that can directly or indirectly generate radicals are collectively called as ROS [2, 3].

The oxygen free radicals and ROS directly or indirectly damage the cellular macromolecules thereby, threatening cell survival. Some ROS form secondary radicals by enzymatic or non-enzymatic reactions which can cause biomolecular damage [4].

ROS primarily damages nucleic acids, lipids and proteins thereby affecting cellular viability [5].

### 1.1.1 Types of ROS

Majority of the ROSs are generated due to stepwise reduction of molecular oxygen. Production of principle ROS like superoxide anion radical ( $O_2^{\cdot-}$ ), hydrogen peroxide ( $H_2O_2$ ) and hydroxyl radical ( $OH^{\cdot}$ ) by stepwise reduction is schematically shown in Fig. 1.1.1 [6].

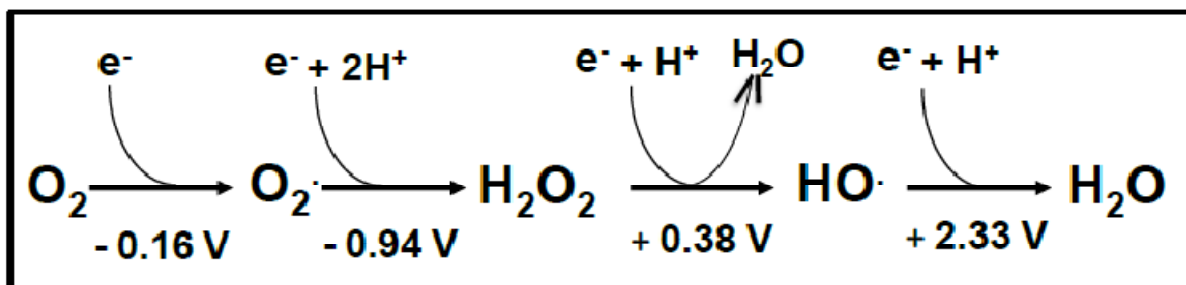


Fig. 1.1.1 Generation of ROS due to stepwise partial reduction of molecular oxygen (From Warren et al., 1987, [6]). Redox potential of each step is mentioned in the figure.

Apart from the above-mentioned ROS, singlet oxygen ( $^1O_2$ ) is also one of the most important biologically relevant molecules generated due to spin flip of the unpaired electron [1]. This is an excited state of oxygen where the  $\pi$ -antibonding electrons get paired because of spin flip [7]. Singlet oxygen is mainly generated in the photosynthetic organisms [8].

The primary ROS undergo reactions with various cellular components and lead to the formation of secondary ROS. Organic hydroperoxides (ROOH) are generated when oxygen radicals react with cellular biomolecules like DNA, RNA, lipid or protein. Alkoxy ( $RO^{\cdot}$ ) or peroxy radicals ( $ROO^{\cdot}$ ) are generated in the presence of oxygen by the addition of radicals to double bonds or hydrogen abstraction. These radicals are relatively long lived and can damage lipid molecules. Hypochlorous acid (HOCl) is

formed from  $\text{H}_2\text{O}_2$  by the action of enzymes like myeloperoxidases while rapid reaction between  $\cdot\text{O}_2^-$  and  $\text{NO}\cdot$  radicals generates the peroxynitrite radical ( $\text{ONOO}\cdot$ ), which can damage protein molecules by reacting with the thiol and amino groups [9].

### **1.1.2 Sources of ROS**

Most of the cellular ROS are generated as a consequence of aerobic metabolism or by enzymatic reactions. There are multiple modes by which ROS are generated in a cell or in a particular tissue in any organism [10]. ROS are generated by regular metabolic processes or in response to external stimuli.

#### **1.1.2.1 Endogenous sources**

Mitochondrial and photosynthetic electron transport chains (ETC) are the major sources of endogenous ROS. In the mitochondrial ETC, electron is transported through a series of oxidation-reduction cycles to the final acceptor  $\text{O}_2$ , resulting in its eventual reduction to  $\text{H}_2\text{O}$ . However, leakage of electrons in course of transfer through this chain leads to the occasional formation of ROS. Under normal metabolism, roughly 1-5% of the electrons passing through the ETC are accepted by oxygen at respiratory complex I and complex III, which results in the formation of superoxide anion radical ( $\cdot\text{O}_2^-$ ), that is eventually converted to hydrogen peroxide ( $\text{H}_2\text{O}_2$ ) [11]. In *E. coli*, the respiratory chain alone can account for as much as 87% of the total  $\text{H}_2\text{O}_2$  produced [12].

In photosynthetic organisms, chloroplast/thylakoids serves as the principal source of ROS generation [13]. Electron leakage from respiratory electron transport chain (ETC) or reduction of oxygen at the end of the non-cyclic photosynthetic ETC [14] are the major sources of superoxide radicals ( $\text{O}_2^{\cdot-}$ ) in cyanobacteria.  $\text{O}_2^{\cdot-}$  thus produced is dismutated to  $\text{H}_2\text{O}_2$  by the action of superoxide dismutases (SODs) [15]. This is the

principal source of intracellular  $\text{H}_2\text{O}_2$ . Apart from this,  $\text{H}_2\text{O}_2$  is also generated from the  $\text{O}_2^{\bullet-}$  produced at the reducing side of PSI by Mehler reaction [16, 17]. In the reaction centre of PSII, singlet oxygen is generated from the ground (triplet) state oxygen due to excess harvest of light energy [18, 19, 20]. In animal cells, mitochondria serves as the main source of ROS, whereas, chloroplasts and peroxisomes are the principal site of ROS generation in plant cells [21].

Apart from these sources, many oxidases catalyzing oxidation-reduction reaction involving molecular  $\text{O}_2$  generate  $\text{H}_2\text{O}_2$  as by-product [22].  $\text{H}_2\text{O}_2$  is produced by the action of plasma membrane-bound NADPH oxidase or xanthine oxidases in cytoplasmic environment [23, 24, 25]. In neutrophils and monocytes,  $\text{H}_2\text{O}_2$  is converted to hypochlorous acid (HOCl), which helps in phagocytosis [26].  $\text{H}_2\text{O}_2$ , generated from metabolism, is relatively stable, but in presence of  $\text{Fe}^{2+}$  (even traces) it undergoes Fenton reaction to form the hydroxyl radical ( $\cdot\text{OH}$ ), which is the most harmful ROS that can damage all cellular macromolecules [27, 28, 29].

#### **1.1.2.2 Exogenous factors**

Apart from cellular metabolism, exogenous factors also contribute to ROS generation, consequently disturbing the redox homeostasis [13]. These factors include exposure to radiation, salinity, osmotic shock, desiccation, UV, drought, cold shock, metal toxicity, high light intensity, etc. Increased ROS accumulation under these conditions indicates a positive correlation between oxidative stress and these factors. Ionizing radiation results in radiolysis of water molecules, which generates a variety of ROS that harm cells [30]. Production of ROS in response to pathogen attack is also a well established fact [31]. Direct or indirect ROS production in response to various abiotic stresses in plasma

membrane, apoplast, chloroplasts, mitochondria, endoplasmic reticulum and peroxisomes is schematically depicted in Fig. 1.1.2.2 [32].

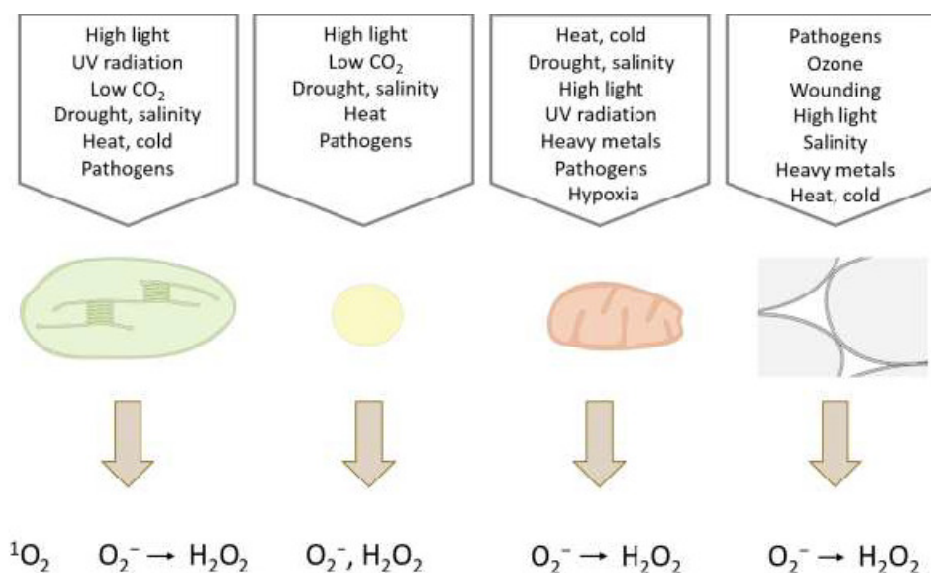


**Fig. 1.1.2.2 ROS generation in chloroplasts, peroxisomes, mitochondria, and the apoplast in response to different environmental stresses (From Czarnocka & Karpiński, 2018, [13]).**

Although singlet oxygen is constantly generated at the photosynthetic reaction centre, its production significantly increases in the presence of high intensity light [33]. Environmental factors like drought, salinity, high light intensity, temperature rise etc. that affect photorespiration are also known to cause marked elevation of the ROS level in plant cells [34]. Photochemistry triggered by solar energy results in accumulation of H<sub>2</sub>O<sub>2</sub> at micromolar level in oceans or freshwater bodies, which can cause oxidative stress to the aquatic life forms [27].

## 1.2 Oxidative stress

Cells respond to oxidative stresses by employing various enzymatic and non-enzymatic approaches. Cellular antioxidants play an important role of combating the ROS burden. These substances significantly delay or inhibit ROS action [35]. An imbalance between

oxidants and antioxidants, in favour of the oxidants, potentially leading to damage, is termed as 'oxidative stress' [36]. Under normal conditions, there is balance between ROS burden of the cell and the cellular antioxidant pool. In other word, oxidative stress can be termed as interference in the balance between the production of reactive oxygen species (ROS), and the ability of biological systems to readily detoxify ROS or repair the resulting damage. Oxidative stress depends upon the inherent ability of an organism to counter the damaging effect of ROS. In bacteria a rise in H<sub>2</sub>O<sub>2</sub> concentration to just 2 μM can cause oxidative stress [37].

### **1.2.1 Damage due to Oxidative Stress: Biomolecular Damage**

Biomolecules like DNA, RNA, protein and lipids are the targets of ROS action. Free radicals can directly attack lipid molecules, making it one of the main targets during oxidative stress. The primary effects of lipid peroxidation are decreased membrane fluidity, altered membrane properties, disruption of membrane-bound proteins, formation of reactive alkyl hydroperoxide etc. ROS also attacks nucleic acids by forming single and double-strand breaks. *In vitro* and *in vivo* studies have identified more than 20 different types of oxidized DNA adducts along with damaged bases and pyrimidine cross-links [38]. Different types of oxidative damage to proteins also challenges cell survival under oxidative stress [39, 40]. The oxidative stress induced biomolecular damage causes serious alteration in normal functioning of cellular metabolism and thus limits cell survival.

Among the various ROS, superoxide radical (O<sub>2</sub><sup>•-</sup>) can act as both oxidizing or reducing agent and damage biomolecules by directly interacting with them, e.g. lipid peroxidation, inactivation of proteins, especially iron-sulphur proteins like aconitase,

dehydratase etc. [41, 42, 43]. This radical is also known to damage the cytochrome-c and transketolase enzyme [44], which in turn prevents synthesis of erythrose-4-phosphate, a biosynthetic precursor of aromatic amino acids. The  $O_2^{\cdot-}$  radical can oxidize triose sugars, forming highly reactive methyl glyoxal that can react with and damage proteins or nucleic acids [9].

In biological systems, hydrogen peroxide ( $H_2O_2$ ) is a key ROS that threatens cell survival.  $H_2O_2$  is produced by dismutation of  $O_2^{\cdot-}$  by superoxide dismutases or directly by several oxidases [22].  $H_2O_2$  can directly permeate into cells; hence,  $H_2O_2$  toxicity arises whenever  $H_2O_2$  is present in the medium. Inside cells,  $H_2O_2$  is known to directly inactivate enzymes such as dehydratases which contain iron-sulphur clusters [45].  $H_2O_2$  can oxidize Cys (-SH) or Met (-SCH<sub>3</sub>) residues in enzymes like Cu/Zn-SOD or Fe-SOD. In the presence of  $Fe^{2+}$ ,  $H_2O_2$  produces  $\cdot OH$  (Fenton reaction) that can damage molecules in its vicinity at diffusion-limited rates [29].  $\cdot OH$  is the most deleterious ROS with a very short life time and strong positive redox potential (+2 V). The effects of this radical are more pervasive because cell has no machinery to detoxify  $\cdot OH$  directly. DNA single and double strand breaks, protein oxidation, lipid peroxidation etc. can be caused by  $\cdot OH$  radicals.

It is important to note here that at low concentration of  $H_2O_2$  plays an important role in cellular signaling, thereby, acting as a second messenger [46]. But when the level of  $H_2O_2$  exceeds the critical limit that the cellular defense cannot manage, pathological conditions like cancer, ageing, neurodegenerative processes etc. may arise [47, 48].  $H_2O_2$  generated within cells is detoxified by several enzymes of which peroxidases and catalases are the two major classes.

## 1.2.2 Sensing Oxidative Stress in Bacteria

Bacteria have evolved with various sensory systems to perceive oxidative stress. The stress signals are finally transduced to desired genes, resulting in expression of proteins involved in the anti-oxidative stress response results. The types of sensory mechanisms vary, depending on with the type and magnitude of stress.

### 1.2.2.1 Transcriptional Regulators

There are many transcriptional regulators which contain the stress sensory and the response domain within the same protein itself. These single transcriptional regulators perceive oxidative stress directly and modulate gene expression through the response domain. OxyR is the most extensively studied transcriptional activator of this kind in various Gram-negative and Gram-positive bacteria [49, 50]. This H<sub>2</sub>O<sub>2</sub> sensing regulator is activated by the redox dependent formation of an intramolecular disulfide bond [51]. Once activated, it up-regulates several genes like catalase, glutaredoxin, glutathione reductase, NADPH-dependent alkyl hydroperoxide reductase, protective DNA-binding protein (Dps) etc. through specific DNA promoter recognition. Often, the target genes are located downstream of the *oxyR* gene forming an operon [52].

Under normal condition, Zinc-containing redox regulator FurS represses transcription of catalase-peroxidase, *cpeB*, in *Streptomyces reticuli* by binding the operator site of *furS-cpeB* orperon. But under oxidative stress it is released from the operator site due to the formation of an intra-molecular disulfide bond formation, which causes a conformational change in the protein, ultimately leading to the transcriptional induction of the *cpeB* gene [53]. Similarly, FurA, a close relative of FurS, regulates *katG* transcription in *Mycobacterium tuberculosis* [54] and its involvement in isoniazide (one

of the most widely used anti-Tuberculosis drug) resistance was investigated recently [55]. In *Staphylococcus aureus*, SarA acts as a negative regulator for genes responsible combating oxidative stress tolerance. The *sarA* mutant showed increased expression of superoxide dismutases, SodM and SodA, and thioredoxin reductase, which protects the organism against oxidative stress. In both cases purified SarA protein was found to bind the promoter region of the genes it regulated [56, 57].

#### **1.2.2.2 Two Component Systems**

Two component systems are the most important sensory and adaptation systems in bacteria. It comprises of a membrane bound sensor kinase, which activates or deactivates its cognate response regulator. The sensor kinase is autophosphorylated upon signal recognition, and the phosphoryl group is subsequently passed to one or more cognate response regulators. It should be noted that phosphorylation alters the DNA-binding behaviour of response regulators [58]. As many as 200 two component systems may be present in a single bacterium [59]. *Escherichia coli* genome encodes 32 sensor kinases and 23 response regulators along with hybrid sensor kinases [60]. SoxRS system is the one of the most extensively studied system which regulates at least 10 genes including Mn-SOD, endonuclease IV, glucose-6-phosphate dehydrogenase, fumarase, aconitase, ferredoxin reductase, *micF* RNA etc. [61]. Gram-positive *Streptomyces avermitilis* genome contains 67 sensor kinases and 68 response regulators [62], suggesting that *Streptomyces sp.* are well equipped to respond to highly variable environmental conditions. Presence of large number of different two-component systems in *Actinobacteria* appears to reflect their responsiveness to a wide range of rapidly changing environmental stimuli. Very recently, a bacterial two component

phosphorelay has been successfully recruited for artificial signal transduction in mammalian system [63].

In some cases, apart from the two partners, there exists a third component which acts as an accessory protein to respond to the environmental conditions and thereby influences the kinase activity of its cognate sensor kinase. YycFG is one of the best studied two component system whose activity is modulated by accessory proteins [64]. This system is highly conserved and specific to low-G+C content bacteria like *Bacillus subtilis*, *Streptococcus pneumoniae*, *Staphylococcus aureus*, and *Enterococcus faecalis* [65]. In *Bacillus subtilis*, the activity of YycG, the sensor kinase, is modulated by YycH or YyvI that have N-terminal transmembrane helices. All the four genes are clustered in a single operon [66]. In *Mycobacterium tuberculosis*, accessory lipoprotein (LpqB) is known to interact with MtrB sensor and affect the phosphotransfer to MtrA, the response regulator [67].

### **1.3 Mitigation of Oxidative Stress**

To counteract the deleterious effects of oxidative stress, bacteria have evolved highly complex and well regulated defense, repair and detoxification mechanisms [68, 69]. Bacterial cell responds to oxidative stress by regulation of gene expression in a coordinated manner [70]. Primary defense is through detoxification of deleterious ROS into harmless products, while secondary response is the effective repair of the ROS induced biomolecular damage. There are several ways to mitigate oxidative stress through detoxification of ROS. While some of these defenses are non-enzymatic (glutathione, vitamin A, C, E, carotenoids, etc.), others depend on specific enzymes (catalases, SOD, peroxidases etc) [71, 72].

### 1.3.1 Non-enzymatic antioxidants

Non-enzymatic antioxidant molecules such as glutathione (GSH), carotenes, ascorbic acid,  $\alpha$ -tocopherol, NADPH and NADH pool etc. are constitutively present in cells to maintain a reducing intracellular environment or to scavenge chemically reactive oxygen species. GSH, at high intracellular concentrations, maintains a strong reducing environment in the cell. GSH is maintained in its reduced form by glutathione reductase using NADPH as a source of reducing power. The main protective roles of glutathione against oxidative stress are (1) acts as co-factors for several ROS detoxifying enzymes (2) participates in amino acid transport across plasma membrane (3) scavenges ROS directly and (4) regenerates vitamins C and E back to their active forms [73]. The ratio of oxidized to reduced GSH serves a marker of oxidative stress where a higher value is indicative of increased level of oxidative stress.  $\gamma$ -glutamylcysteine, the immediate precursor GSH, can also function as antioxidant to protect the mitochondria from excess ROS [74]. Carotenoids act as antioxidants to inhibit oxidative damage by scavenging free radicals generated during the transfer of electrons through ETC. The antioxidant mechanisms of ascorbic acid are based on hydrogen atom donation to lipid radicals, quenching of singlet oxygen, and removal of molecular oxygen. Scavenging aqueous radicals and regeneration of  $\alpha$ -tocopherol from the tocopheroxyl radical species are the well known antioxidant mechanisms of ascorbic acid [75].

Genome analysis of a highly radiation resistant bacterium, *Deinococcus radiodurans* showed presence of biosynthetic pathways for common antioxidant metabolites like, carotenoids, lipoic acid, folates etc. Mutant strain of *D. radiodurans* that fails to synthesize carotenoids became sensitive to ionizing radiation and hydrogen peroxide indicating the importance of carotenoids in radiation/oxidative stress resistance in this

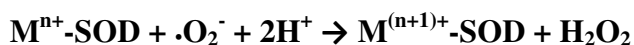
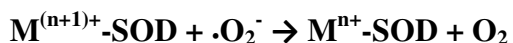
bacterium [76]. Antioxidant effects of lipoic acid and folate have been well documented in mammalian systems [77, 78, 79]. Presence of lipoic acid and folate biosynthesis pathway in *D. radiodurans* strongly suggests the importance of these non-enzymatic antioxidants in radioresistance too.

### 1.3.2 Enzymatic antioxidants

Several enzymes are involved in oxidative stress mitigation and maintenance of redox homeostasis in the cellular systems. The network of antioxidant enzyme includes enzymes like superoxide dismutases, catalase, peroxidases, alkylhydroperoxide reductases etc.

#### 1.3.2.1 Superoxide dismutase (SOD)

These enzymes catalyse the conversion of superoxide anions to molecular oxygen and hydrogen peroxide. Superoxide dismutase (EC 1.15.1.1) neutralizes the superoxide ions by successive oxidative and reductive cycles of transition metal ions at its active site [80]. The general reaction of SOD is stated below:



M is the metal cofactor. When metal ion is Cu, n=1; when M is Fe/Ni/Mn, n=2

SODs are generally classified into three types depending on the metal species located at the redox-active centre. The iron-containing (Fe-SOD) and the manganese-containing (Mn-SOD) enzymes are characteristically present in prokaryotes [81]. The third group, Cu/Zn-SOD is mainly found in eukaryotes. In *E. coli*, Fe-SOD expression is modulated

by intracellular iron levels [82] while, Mn-SOD, is the predominant enzyme during aerobic growth. A eukaryotic Cu/Zn-SOD like enzyme has been reported to be present in the *E. coli* periplasmic space [44]. *Mycobacterium tuberculosis* possesses Mn-SOD (SodA) as well as Cu/Zn-SOD (SodC), and both have been associated with the detoxification of ROS during phagocytosis [83]. SOD containing Ni at the active site (Ni-SOD) has been reported from some *Streptomyces* species [84, 85]. There are reports of cambialistic SODs that can function with Mn or Fe in their active site [86]. Cu-only SOD is a new type of SOD, which are specifically found in fungi and oomycetes and are released in the extracellular environment [87].

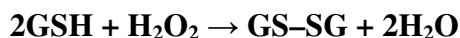
### 1.3.2.2 Peroxidases and Peroxiredoxins

Peroxidases (EC.1.11.1.x) are ubiquitous enzymes found in bacteria, fungi, algae, plants and animals [88]. These enzymes detoxify hydrogen peroxide (H<sub>2</sub>O<sub>2</sub>) into water in a reaction that is coupled to oxidation of a wide range of phenolic as well as non-phenolic substrates. Apart from hydrogen peroxide, some of these enzymes also act on organic hydroperoxides (e.g. t-butyl hydroperoxide) or even lipid hydro-peroxide (linoleic acid hydroperoxide). The general reaction of peroxidases is given as below:



Based on presence of co-factor heme, peroxidases are broadly classified under two groups: heme peroxidases and non-heme peroxidases [89]. As per the PeroxiBase database, the majority of peroxidases are heme peroxidase (80%), while the non heme peroxidases are represented by some thiol peroxidases, alkyl hydroperoxidases, FNR-dependent peroxidases, NADPH peroxidases etc. During the peroxidase reaction, peroxidases use diverse electron donors depending on the nature of the enzyme. For

example, the horseradish peroxidase uses a wide variety of organic compounds as electron donors because of an accessible active site. In contrast, Cytochrome c peroxidase is able to use small only small molecules as electron donor because of its closed active site conformation. Glutathione peroxidases (GPX) are the principal peroxidases in animals. These are seleno-enzymes that use reduced glutathione (GSH) as the electron donor [90, 91]. During the reaction cycle, GSH gets oxidized to GS-SG, which is subsequently converted back to its reduced form by glutathione reductase using NADPH as the electron donor. The general reaction of glutathione peroxidase is as follows:



Apart from  $\text{H}_2\text{O}_2$ , mammalian GPXs can also decompose lipid and alkyl hydroperoxides. Homologues of GPX have been identified in higher plants. However, they exhibit lower activity compared to their mammalian counterparts as they carry a cysteine residue in place of selenocysteine in their active site [92].

In higher plants, ascorbate peroxidases play a crucial in role detoxification of  $\text{H}_2\text{O}_2$  [93]. Using ascorbate as electron donor, these enzymes reduce  $\text{H}_2\text{O}_2$  into water and monodehydroascorbate which is spontaneously converted to ascorbate and dehydroascorbate. Dehydroascorbate is eventually reduced by dehydroascorbate reductase that uses glutathione. NADPH-dependent glutathione reductase finally regenerates glutathione to complete the reaction cycle.

Peroxiredoxins are capable of detoxifying hydrogen peroxide, alkylhydroperoxides and peroxyxynitrites using thioredoxin and other thiol containing reducing agents as electron donors [94]. Peroxiredoxins (Prxs) are characterized by a conserved alkylhydroperoxide C (AhpC) or Thiol-Specific Antioxidant (TSA) domain containing

the thioredoxin fold. These proteins usually contain two highly conserved cysteine residues, the peroxidatic cysteine and the resolving cysteine, which are essential for peroxidase activity [95]. Peroxide substrate is neutralized on reaction with the peroxidatic cysteine residue, which in turn is oxidized to sulfenic acid (RSOH) intermediate. Subsequently the reduced form of the protein is regenerated with the help of resolving cysteine that accepts electrons from a suitable electron donor such as thioredoxin, glutaredoxin, glutathione etc [96].

### **1.3.2.3 Catalases**

The ubiquitous enzyme catalase is present in all aerobic organisms and in some anaerobes too. It is one of the most important oxidative stress alleviating enzymes that performs dismutation of  $H_2O_2$  into water and oxygen, consequently preventing the Fenton reaction. Unlike peroxidase, the catalase reaction is a direct dismutation without any requirement of additional reductants. Details of catalase enzyme are described separately in Section 1.5.

It should be mentioned here that apart from enzymatic or non-enzymatic ROS detoxification pathways, cells employ multiple strategies to limit ROS generation. For example, photosynthetic organisms deploy a number of methods to quench excess of solar energy, which otherwise would increase the ROS burden. Maintaining the levels of free transition metals like  $Fe^{2+}$  is one of the prime strategies to reduce the ROS level in cells [3, 97]. Uncontrolled rise in  $Fe^{2+}$  ions leads formation of the highly toxic hydroxyl radical ( $\cdot OH$ ) via the Fenton reaction [1].

#### 1.4. Clinical importance of the oxidative stress response

There is an intricate relationship between oxidative stress response and pathogenicity of microbes that cause disease. ROS generation is a common phenomenon found during host pathogen interaction. In humans 'oxidative burst' is the natural defense process against pathogens. Oxidative burst is generated during phagocytosis where imported substances or pathogens are rapidly oxidized. The rapid burst of oxygen consumption related to ROS generation in phagocyte is associated with microbial killing. Pathogenicity of an organism is depends on how best the organism can defend itself from the adverse effects of this oxidative burst.

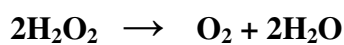
The common human pathogenic bacteria are from the genera such as *Staphylococcus*, *Streptococcus*, *Enterococcus*, *Bacillus*, *Corynebacterium*, *Nocardia*, *Clostridium*, *Listeria* etc. In the case of *Mycobacterium tuberculosis* infection, human immune system responds through interferon- $\gamma$  mediated macrophage activation resulting in generation of ROS and RNS which limits the efficacy of infection by the bacteria [98]. To counteract the adverse effect of oxidative bursts, the bacterium has evolved with multiple strategies [99]. The bacterium under this condition produces and secretes antioxidant enzymes like catalase-peroxidase (KatG), superoxide dismutases (SodA and SodC), and alkylhydroperoxide reductase (Ahp) etc. which help it to evade the host defense system.

However, the use of intracellular oxidative burst as a major tool of cellular defense may cause problems as ROS generated during this burst may damage cellular macromolecules. To avoid this, cells maintain a reducing environment. In this case, small proteins like thioredoxin, low molecular weight thiols like glutathione etc play a

key role in maintaining a reducing environment within the cell, which in turn, also controls the extent of the oxidative burst [100].

### **1.5 Catalase**

As mentioned earlier, catalases (EC 1.11.1.6) are an integral component of oxidative stress management in all aerobic organisms as well as in some anaerobes. The reaction of catalase is as follows:



This reaction is highly exergonic ( $\Delta H = -47$  kcal/mol;  $\Delta S = +34$  kcal/mol K;  $\Delta G = -57$  kcal/mol) and is favourable under physiological condition [101]. This very favourable reaction led to the discovery of catalase by Thenard from the observation that molecular oxygen is liberated upon treatment of animal tissues with dilute solution of  $\text{H}_2\text{O}_2$  without the tissue being consumed [102]. The term 'catalase' was given by Loew who defined it as the enzyme which can convert  $\text{H}_2\text{O}_2$  into water and oxygen [103]. He reported the presence of catalase enzyme in many organisms ranging from plants to mammals. Later, in 1923, Warburg suggested that this enzyme might contain the iron atom at the active site as its activity was inhibited by cyanide treatment. More than a decade later it was found that the hemin group of the enzyme can react with compounds like cyanides, fluorides, sulfides etc. It was observed that the ferric complex present in the enzyme active group was similar to the ferric complex present in the protoporphyrin found in the haemoglobin protein [104]. Around the same time bovine catalase was purified and crystallized [105].

### **1.5.1 Types of catalase**

Based on the structure and function, catalases are classified into three groups; (1) Typical mono-functional catalases, (2) Bifunctional catalase peroxidases (KatG) and (3) binuclear manganese catalases (Mn-catalases) [106, 107]. Of the three, the first two, which are heme-containing, have been extensively characterized from several organisms, both prokaryotic and eukaryotic. The distribution of Mn-catalases is restricted to prokaryotes [108].

#### **1.5.1.1 Typical mono-functional catalases**

The typical mono functional catalases that form the largest group of catalases are prevalent in aerobic organisms. Most of these proteins are homotetramers with a four heme prosthetic group. These enzymes are often referred to as the true catalases. In most cases the active site contains a ferric protoporphyrin IX (heme *b*) similar to the human haemoglobin. However, there are few typical catalases where other variant heme group such as heme *d* has been found [109].

#### **1.5.1.2 Bifunctional catalase peroxidases (KatGs)**

The bifunctional catalases can carry out both catalase and peroxidase function. These enzymes are found in fungi, archeobacteria and bacteria. In general the bifunctional catalases are homodimeric. Although less efficient compared to the typical catalases, bifunctional catalase-peroxidases have better substrate binding affinity. Compared to the typical catalases, the catalase-peroxidases are more sensitive to inactivation by pH or temperature [109]. The commonly used immunoblotting reagent horseradish peroxidase is an example of bifunctional catalase-peroxidase.

### **1.5.1.3 Binuclear Mn-catalase**

While the heme containing typical mono-functional and bifunctional catalase peroxidases are widespread across the phyla, Mn-containing catalases are restricted to bacteria and archae. This type of catalase is altogether different from the other two types in terms of sequence homology and reaction mechanism. Instead of Fe-porphyrin, they harbour two manganese atom atoms at the catalytic core which undergoes reversible oxidation-reduction cycle to carry out catalysis reaction. Since the thesis deals with characterization of a Mn-catalase, a detailed discussion pertaining to this group of enzyme is stated in Section 1.6.

## **1.5.2 Use of catalase enzyme**

### **1.5.2.1 Industrial use**

Catalases are one of the most industrially utilized enzymes. These enzymes have found applications in various industries like dairy, leather, cosmetic, textile and semiconductor industries [110]. Bioremediation is another upcoming field where catalase enzyme has potential applications. Use of catalase as indicator for hydrocarbon degradation in soil is a very crucial aspect in bioremediation of crude oil pollution. The enzyme can act as oxygen generator in aerobic bioremediation processes. Treatment of effluents for detoxification of residual  $H_2O_2$  from leather or textile bleaching industry is performed by catalase enzymes [111]. Catalases are also used in lens cleaning solutions to remove residual  $H_2O_2$ . Co-immobilization of catalase and glucose oxidase is used in food packaging material to reduce oxygen content inside the package [112]. This combination also has potential to remove glucose contamination from commercial isomaltooligosaccharide (IMO) [113].

### **1.5.2.2 Therapeutic use**

Numerous studies have established that  $H_2O_2$  is involved in biological processes like cancer, aging, neurodegenerative diseases etc. These studies led intensive search for new generation catalysts that can detoxify  $H_2O_2$  so that effective therapeutic interventions can be designed for those ailments [114]. In this line, many synthetic catalase mimetics are being developed as curative agents for disorders such as Alzheimer's, cancer, aging, inflammatory and heart diseases [114, 115]. A number of diseases have been found to be directly or indirectly linked to catalase deficiency and/or modification. Diabetes mellitus, Parkinson's disease, vitiligo, and acatalasemia are some of these. Hence, the possibility of using the catalase protein as therapeutic agent for management of these pathological conditions is being explored. Very recently, gold and silver nanoparticles mediated delivery of catalase enzyme was found to reduce UV-induced oxidative stress in rat skin [116]. In all these studies heme-based catalases have been exploited. However, Mn-catalases, which are distinctly different from the heme-containing catalases, can serve as novel templates for designing synthetic catalysts for potential therapeutic usages [117]. Being one of the principal ROS scavenging enzymes, catalase serves as a major candidate protein for research pertaining to anti-ageing. Studies with mice model suggested that expression of catalase protein in mitochondria could enhance the median lifespan by 20% [118].

### **1.6 Mn-catalase**

Presence and the role of heme cofactor in catalase enzymes was established long ago. However, it was found that in spite of the lack of heme or cytochromes, some bacteria exhibited weak catalase activity. This phenomenon led to the discovery of the non-heme catalases in lactic acid bacteria. The heme-independent catalase activity was

reported to be present in the strains of *Pediococci* [119] and *Lactobacilli* [120]. Finally, the manganese metal specificity for the catalase activity was demonstrated when the heme-independent catalase protein from *Lactobacillus plantarum* was purified and characterized [121]. This established the fact that there is a third group of catalase which contains 2 Mn atoms at the active site instead of heme and subsequently this catalase was named as Mn-catalase. Unlike the widespread heme containing catalases, Mn-catalases are poorly characterized and due to the absence of the heme group, these are also sometimes referred as pseudocatalases.

In recent years, there has been an explosion in data generated from sequencing of genomes worldwide. From the sequence homology, a total of 101 putative Mn-catalase sequences have been identified (RedoxiBase: <http://peroxibase.toulouse.inra.fr/>). Among these putative Mn-catalase genes only a few have been actually demonstrated as Mn-catalases.

### **1.6.1 Occurrence**

Unlike the heme catalases, the Mn-catalases are restricted to prokaryotes and archae [106]. Phylogenetic analysis revealed the presence of 7 rooted clades showing the occurrence of Mn-catalases in various kinds of bacteria (Fig. 1.6.1) [122]. Presence of putative Mn-catalase in anaerobes is also documented. Mn-catalases are present not only in mesophilic organisms (such as cyanobacteria), but also occur in halophilic or thermophilic bacteria/archaea. Mn-catalases from thermophilic eubacteria like *Thermus thermophilus*, or hyperthermophilic archae like *Pyrobaculum calidifontis* VA1 and *Geobacillus thermopakistanensis* have been biochemically characterized [123, 108, 124]. These enzymes are distributed in both Gram positive and Gram negative bacteria.

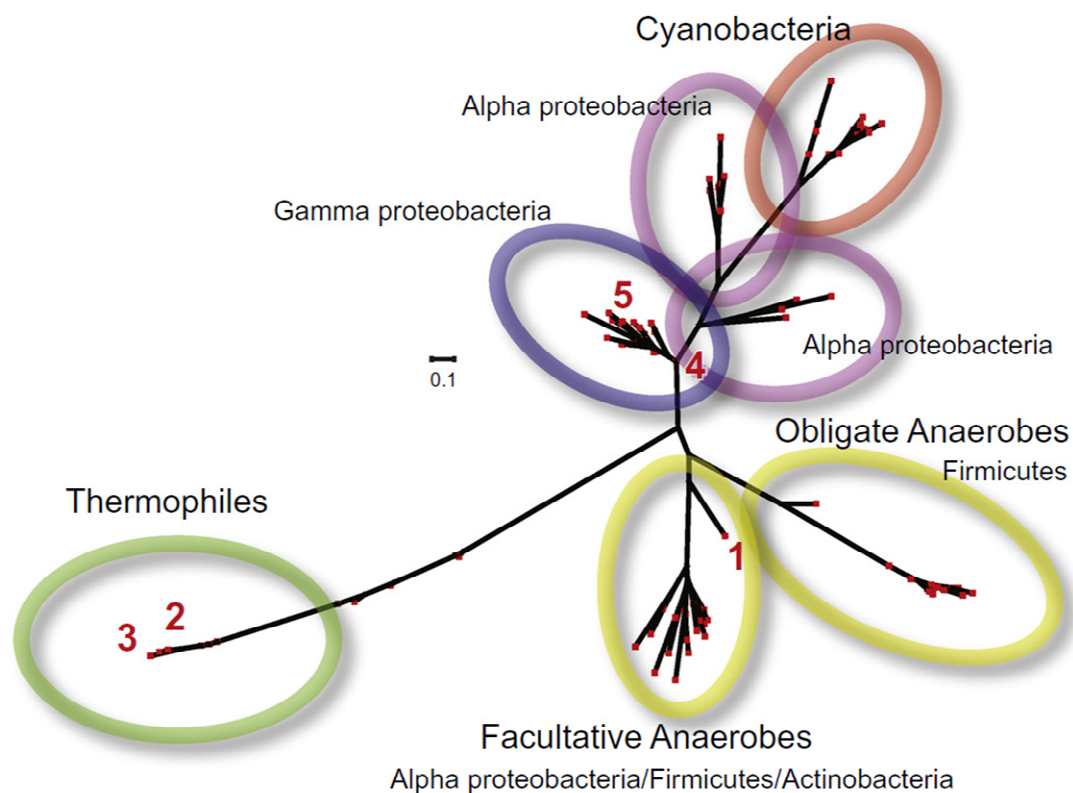


**Fig. 1.6.1 Radial phylogenetic tree for putative manganese catalases in genomic databases (from Whittaker, 2012, [122]).** (1) *Lactobacillus plantarum* manganese catalase (LPC); (2) *Thermus thermophilus* manganese catalase (TTC); (3) *Pyrobaculum caldifontis* manganese catalase; (4) *Salmonella enterica katNp*; (5) *Escherichia coli* O157:H7 Z1921p.

Phylogenetic studies suggest that Mn-catalases have originated very early in the evolution. Its presence in strictly anaerobic organism *Halothermothrix orneii* suggests that Mn-catalases evolved long before oxygenation of earth's atmosphere [125].

The putative Mn-catalase genes have been identified in a number of pathogenic bacteria too. The notable examples are KatN from *Salmonella enterica* subsp. *enterica* serovar Typhimurium [126], locus Z1921 in *E. coli* O157:H7 [127], KatN from *Pseudomonas aeruginosa* [128] etc. Role of KatN in the stress response of pathogenic bacterium *S. enterica* has been demonstrated through knock-out experiments [129].

### 1.6.2 Structure of Mn-catalases

Mn-catalases have been relatively poorly characterized and the crystal structures of only two Mn-catalases (from *Thermus thermophilus* and *Lactobacillus plantarum*) was known when this work was initiated [130, 131]. The individual monomers of Mn-catalases show 4-helix bundle type architecture which is specific to the Ferritin-like superfamily [132] that includes ferritin [133], monooxygenase [134] and ribonucleotide reductase [135]. All these proteins have four-helix bundle coiled-coil domain with a binuclear metal complex at the active site [136]. However, in Mn-catalases, instead of diiron complex, manganese atoms are complexed at the catalytic core. The binuclear catalytic active site undergoes two-electron oxidation–reduction cycle during the process of catalysis [122].

The Mn-catalases from *Lactobacillus plantarum* and *Thermus thermophilus* Mn-catalase (hereafter, referred as LPC and TTC respectively) are homohexameric in nature. In both the proteins, the N-terminal region extends out of the core helix-bundle and forms an antiparallel  $\beta$ -sheet linkage with the neighbouring subunit. These interactions are thought to be crucial for stabilization of the multimer (Fig. 1.6.2). In LPC and TTC, the C-terminal region is also extended out of the helix core. This region includes an important binding site for divalent cation ( $\text{Ca}^{++}$ ) that plays an important structural role in maintaining oligomeric integrity [122]. Both LPC and TTC have a catalytic core consisting of two Mn atoms (bi-metallocore) which are coordinated with the protein with  $\text{Glu}_3\text{His}_2$  coordination geometry instead of canonical  $\text{Glu}_4\text{His}_2$  coordination generally found in the ferritin superfamily [131, 137, 122]. Due to this altered coordination geometry, the Mn atoms in these enzymes are connected by two single-atom solvent bridges. Based on the crystal structures of LPC and TTC, a

comprehensive mechanism of  $\text{H}_2\text{O}_2$  decomposition has been proposed. This mechanism involves two-electron redox cycle which renders both the metal centres to be in reduced or oxidized states at a given time [131, 122].

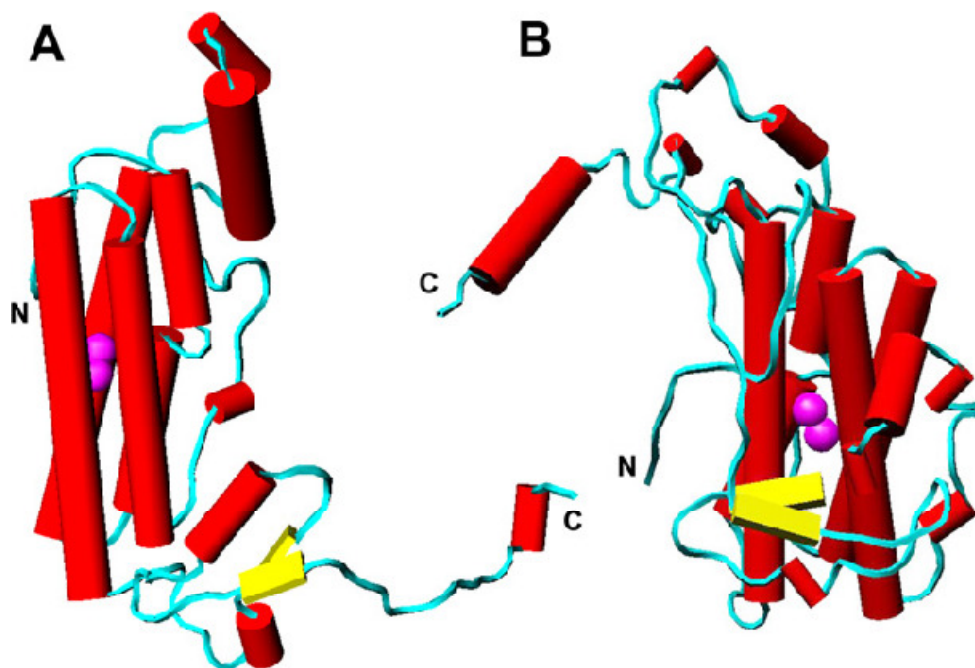


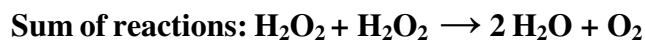
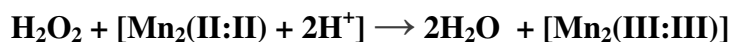
**Fig. 1.6.2 Structure of manganese catalase subunits (from Whittaker, 2012, [122]).** (A) The secondary structural elements of Mn-catalase from *Lactobacillus plantarum* (based on PDB ID: 1JKU). (B) The secondary structural elements of *Thermus thermophilus* Mn-catalase (based on PDB ID: 2V8U).  $\alpha$ -helices are shown in red colour;  $\beta$ -sheet in yellow and turns are shown in blue colour. The manganese ions at the active site are indicated as magenta spheres.

The apical and the two bridging solvent molecules present in the active site have been suggested to facilitate the catalytic process. The location and chemical nature of these solvent molecules is considered to be essential for  $\text{H}_2\text{O}_2$  decomposition. Active sites of Mn-catalases have been extensively studied as templates for designing synthetic catalysts [117]. An evolutionary relationship between Mn-catalases and the oxygen evolving complex (OEC) has been suggested and the active site of Mn-catalases has

been studied to understand the complexity of the underlying chemistry of the OEC [138].

### 1.6.3 Reaction mechanism

Catalytic reaction of the Mn-catalase is mediated by transfer of two electrons and two protons from one H<sub>2</sub>O<sub>2</sub> molecule to the other. Thus, decomposition of H<sub>2</sub>O<sub>2</sub> to H<sub>2</sub>O and O<sub>2</sub> by Mn-catalase is a dismutation reaction. Under uncatalyzed conditions, this intermolecular redox reaction has a large activation barrier (estimated to be 18 kcal/mol) if the reaction has to happen by simple bimolecular collision. The Mn-catalase active site acts as a storage site for electrons and protons to facilitate the process of catalysis. The Mn-catalyzed reaction can be expressed by two half reactions:



In the first half of the reaction, the substrate H<sub>2</sub>O<sub>2</sub> is oxidized to molecular oxygen. In the course of this oxidative reaction, the manganese cluster gets reduced [Mn<sub>2</sub>(III:III) to Mn<sub>2</sub>(II:II)]. The second step is a reductive half reaction where the reduced bimetallocore donates the electrons and protons to second molecule of H<sub>2</sub>O<sub>2</sub>. This results in breakage of O-O bond of H<sub>2</sub>O<sub>2</sub> and generation of two water molecules.

Structural and biochemical analyses of the Mn-catalase from *Lactobacillus plantarum* suggest that the substrate H<sub>2</sub>O<sub>2</sub> reaches the deeply buried active site through an access channel made of series of water molecules connected through network of hydrogen bonds. Upon reaching the active site, the substrate molecules initially coordinates with the Mn1 by displacing the bound water molecule in the oxidized Mn complex (III:III, where both the Mn atoms are in +III oxidation state) (Fig. 1.6.3, Complex 2) [131]. The

electrons are transferred to the Mn(III) centers during this process which lowers the activation energy significantly. Molecular oxygen is generated during this proton coupled electron transfer process and the reaction centre moves to a reduced state (Fig. 1.6.3, Complex 3). After dissociation from the reaction centre, the oxygen molecule exits from the active site either through the same access channel or by diffusion through the protein, with solvent replacing dioxygen in the axial position of Mn1 (Fig. 1.6.3, Complex 4).

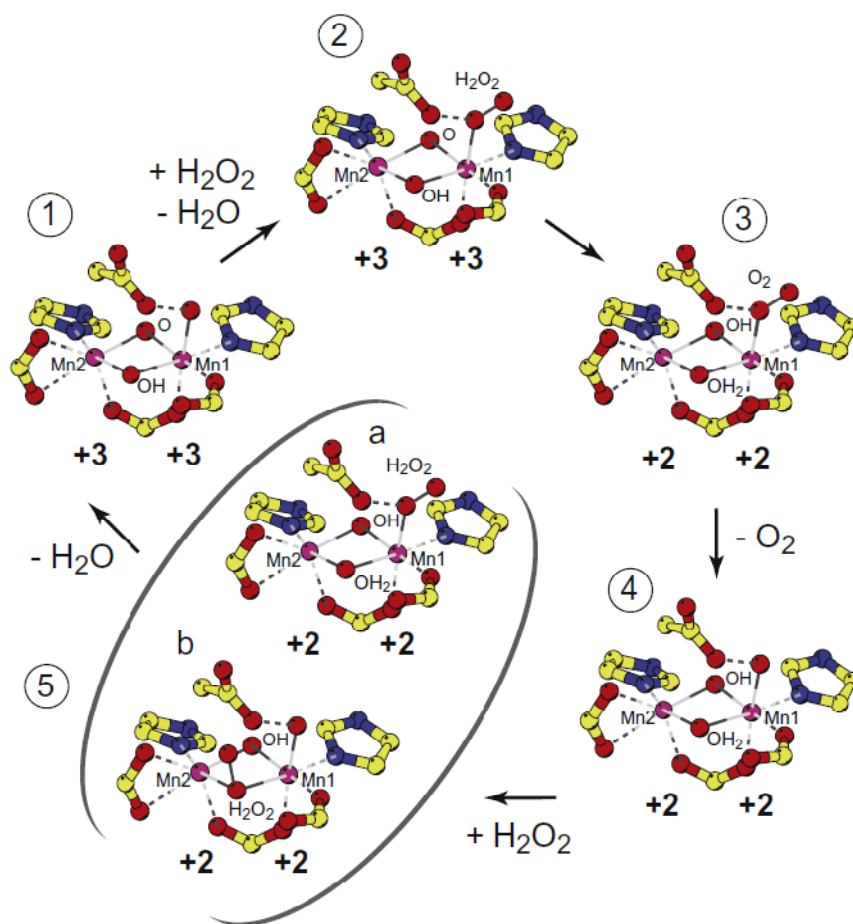


**Fig. 1.6.3 Reaction mechanism of *Lactobacillus plantarum* Mn-catalase (from Whittaker, 2012, [122]).** Oxidative half-reaction: (1) Resting oxidized Mn (III,III) state (2) Terminal peroxide adduct (3) Terminal dioxygen adduct. Reductive half-reaction: (4) Resting reduced Mn (II,II) state. (5) Activated hydrogen peroxide complexes: (a) Terminally bound substrate; (b) Peroxy-complexed substrate.

In the next step of reaction, the second molecule of hydrogen peroxide enters the active site and binds to the Mn1 terminally (Fig. 1.6.3, Complex 5a), or, alternatively, gets inserted into the cluster core to form a peroxy complex (Fig. 1.6.3, Complex 5b). This binding results in activation of the O–O bond. Reductive cleavage of the O–O bond is coupled with the oxidation of the two metal centers back to the Mn(III) state, thereby completing the catalytic cycle (Fig. 1.6.3, Complex 1) [122].

It should be noted here that the heme containing catalases exhibit higher turnover number compared to the Mn-catalases. The  $k_{\text{cat}}$  of heme catalase has been reported as high as  $4 \times 10^7 \text{ s}^{-1}$  [139], while, the Mn-catalases from *Lactobacillus plantarum* and *Thermus thermophilus* have a  $k_{\text{cat}}$  value of  $2 \times 10^5 \text{ s}^{-1}$  and  $2.6 \times 10^5 \text{ s}^{-1}$  respectively [121, 140].

## 1.7 Cyanobacteria

Cyanobacteria, the group of photosynthetic prokaryotic organisms, are often called as blue green algae (BGA) due to their characteristic bluish green colour. Studies of the fossil records indicate that they are very ancient organisms evolved about 3.5 billion years ago [141]. These organisms are characterized as Gram-negative bacteria and are the first photosynthetic organisms to evolve oxygen by coupling the two photosystems [142, 143, 144]. Evolution of oxygen by the cyanobacteria is responsible for the sudden rise in atmospheric oxygen level during the ‘Great Oxidation Event’ that altered the course of evolution of life on the Earth [145, 146]. It is generally well accepted that these organisms are the progenitors of plant chloroplasts [147]. Some cyanobacteria are endowed with the capability to fix atmospheric nitrogen. Thus, cyanobacteria are the only organism that can harness solar energy to fix atmospheric nitrogen [148].

### 1.7.1 Morphology

Cyanobacteria are morphologically diverse organisms. They can be unicellular or multicellular in nature. The multicellular ones are filamentous in nature, wherein individual cells are joined end to end to form long filaments. In some species, branching of filaments is seen. Fig. 1.7.1 illustrates only a subset of the vast morphological diversity of cyanobacteria belonging to various orders [149]. Strains of cyanobacteria show the presence of intercellular connections or microplasmodesmata, thus, they are considered to be multicellular [150]. Some nitrogen fixing cyanobacteria like *Anabaena* possess specialized cells known as heterocysts, which protect the nitrogenase enzyme from oxygen toxicity [151]. Some cyanobacteria form akinetes, which are resting phase cells. These functional differentiations of specific cells further establish the phenomenon of multicellularity in cyanobacteria [152].



**Fig. 1.7.1 Morphological diversity in cyanobacteria belonging to various orders (from Dvořák et al., 2015, [149]). I. Chroococcales:** a) *Chroococcus subnudus*, b) *C. limneticus*, c) *Cyanothece aeruginosa*, d) *Snowella litoralis*, e) *Microcystis aeruginosa*. **II. Pleurocapsales:** f) *Pleurocapsa minor*. **III. Oscillatoriales:** g) *Planktothrix agardhii*, h) *Limnothrix redekei*, i) *Arthrospira jenneri*, j) *Johanseninema constrictum*, k) *Phormidium* sp., l) & m) *Oscillatoria* sp., n) *Schizothrix* sp., o) *Tolypothrix* sp., p) *Katagnymene accurata*, **IV. Nostocales:** q) *Dolichospermum planctonicum*, r) *Dolichospermum* sp., s) *Nostoc* sp., t) *Nodularia moravica*. **V. Stigonematales:** u) & v) *Stigonema* sp. Scale bar a–u = 10 µm, v = 20 µm.

### 1.7.2 Habitat

Cyanobacteria are present in wide range of natural habitats. These can be also found in some of the extreme ecological niches such as the cold waters of Arctic and Antarctic regions, hot springs or in extreme dry conditions like desert ecosystem, rock surfaces etc. [153]. They are found both in marine as well as in fresh water ecosystems. Their unusual ability to tolerate extreme environmental conditions such as drought, salinity, desiccation, temperature shock, high intensity light, UV, anaerobiosis, photo-oxidation etc. makes them extremely resilient species [154, 155, 156, 152], capable of thriving in some of the most extreme environmental conditions [157]. Cyanobacteria and the eukaryotic algae share similar habitats too [146]. Cyanobacteria can exist as free living organisms or can be in symbiotic association with others (e.g. *Anabaena-Azollae*). Often, cyanobacterial species (such as *Microcystis*) forms a toxic algal bloom over a vast area in marine or fresh water bodies.

### 1.7.3 Cyanobacterial oxidative stress management system

As mentioned earlier, ROS are generated in all living organism during the course of normal metabolism and in response to environmental stresses. Owing to their photosynthetic activity, harvesting of excess solar energy itself is associated with excess ROS generation in cyanobacteria. Intimate association with oxygen further

contributes to the rise of intracellular ROS pool in these organisms. Also, during the course of their evolution, cyanobacteria have been exposed to virtually all natural (high-intensity light, salinity, desiccation etc.) and anthropogenic stresses (heavy metals, herbicides etc.), many of which ultimately culminate in oxidative stress [158]. Naturally, cyanobacteria have developed several strategies to overcome the deleterious effects caused by the reactive oxygen species (ROS), which are formed due to the partial reduction of oxygen [148, 159]. For these reasons, cyanobacteria have been proposed to be excellent model systems to study mechanisms of oxidative stress resistance [160].

Cyanobacteria employ various strategies to mitigate the ROS burden. The first line of defense is to dissipate the excess solar energy by non photochemical quenching (NPQ). This is accomplished by carotenoids and few other specialized proteins such as high light-inducible proteins (HLIPs), small CAB-like proteins (SCPs) and the CP43' protein [71]. Non-enzymatic antioxidants like  $\alpha$ -tocopherol and carotenoids too play an important role in ROS mitigation in cyanobacteria. Cyanobacterial carotenoids like myxoxanthophyll,  $\beta$ -carotene, and its derivatives (zeaxanthin, echinenone) aid in dissipation of energy from photosensitized chlorophyll [161]. Enzymatic ROS removal pathways include SODs, peroxidases, catalases etc. Among the various types of SODs, Cu/Zn-SODs are rare in cyanobacteria while, Mn-SODs and Fe-SODs are well represented [162]. Some unicellular cyanobacteria also show the presence of Ni-SODs [71]. Interestingly, except for a probable heme-catalase gene in *Nostoc punctiforme* PCC 73102, the typical mono-functional heme-catalases are virtually absent in cyanobacteria whereas the bifunctional catalase-peroxidases (KatGs) are very common [106]. Mn-catalases, on the other hand, are rare in cyanobacteria, but interestingly, all

the heterocystous nitrogen-fixing strains of cyanobacteria show the presence of at least one gene corresponding to Mn-catalase [163].

Although common in higher plants, ascorbate peroxidases are rare in cyanobacteria [16]. In *Nostoc muscorum* PCC 7119 and *Synechococcus* PCC 6311, ascorbate peroxidase-like activities have been reported. In another unicellular cyanobacterium *Synechococcus* PCC 7942, dehydroascorbate reductase and glutathione reductase were found to be involved in the regeneration of ascorbate and glutathione, respectively indicating presence of functional ascorbate/glutathione peroxidase system [164]. Peroxiredoxins (Prxs) are widely present in all cyanobacteria and constitute the major class of enzyme that manages the ROS burden [71]. Exhaustive bioinformatic searches revealed the presence of total 244 probable Prxs in 37 cyanobacterial genomes which have been sequenced. Number of Prxs in the genome varies widely species to species. The marine cyanobacterium *Prochlorococcus marinus* SS120 has only 3 Prx genes while, *Acaryochloris marina* MBIC 11017 has 12 genes corresponding to Prxs. In general, filamentous nitrogen-fixing cyanobacteria show more number of Prxs compared to the unicellular non-nitrogen fixing cyanobacteria [148, 165].

Apart from these principal ROS scavenging enzymes, cyanobacterial genome contains proteins like Dps, USPs, Suf proteins etc. which are directly or indirectly involved in management of oxidative stress. The DNA-binding proteins from starved cells (Dps), originally identified from *E. coli*, are a group of proteins that are tasked with protection of DNA under oxidative stress [166]. Presence of Dps homologues in many cyanobacterial genomes strongly suggests their role in oxidative stress management [71].

#### **1.7.4 Economic importance of cyanobacteria**

Nitrogen fixing strains of cyanobacteria such as *Anabaena* PCC 7120 are economically important because they are extensively used as nitrogen biofertilizers for cultivating rice in South-East Asia [167, 168]. Growing cyanobacteria in agricultural land is useful for reclamation of salinity affected soils and improvement of fertility for subsequent cultivation of crop plants [169]. Many bioactive compounds like phenolics, alkaloids, steroids, peptides, phytohormones, polyketides, terpenoids and halogenated compounds are present in cyanobacteria [170, 171]. Thus, cyanobacteria have been considered as a potential source for drug development [172, 173]. Production of biofuels using cyanobacterial biomass is another thrust area towards cleaner alternative to fossil fuels [174]. Cyanobacteria are also considered to be rich source of nutraceuticals and are being used as food or feed supplements [175].

Bioremediation is one of the potential fields where cyanobacteria can be used to harness their photoautotrophic nature. Sequestration of uranium by the acid soluble polyphosphate bodies in nitrogen-fixing marine cyanobacterium *Anabaena torulosa* has been demonstrated [176]. Detection and removal of heavy metal contaminants from waste water from industrial effluents using microalgal and cyanobacterial biofilms are gaining increasing attention for potential applications [177, 178]. Recently, axenic culture of cyanobacterium *Nostoc muscorum* was shown to form biofilms which could sequester Cd(II) from waste water [179].

With the advent of genetic manipulation techniques, the potential application of cyanobacteria has widened. With rational engineering of the genome, cyanobacteria can be used as potential bio-factories for sustainable production of high value chemicals [180]. To make the production process commercially viable, system-biology

approaches are being undertaken for isolation and development of improved cyanobacterial strains [181]. Cyanobacterial cells are considered to be excellent host for production of recombinant proteins. They can be grown in minimal medium without the requirement of sugar source. Cyanobacterial cells have been successfully engineered to produce recombinant enzymes, biopharmaceuticals, therapeutic proteins etc. [182].

### **1.8 *Anabaena* PCC 7120**

*Anabaena* PCC 7120 is a fresh water strain of cyanobacteria that can fix atmospheric nitrogen. As mentioned earlier, it is a heterocystous, filamentous cyanobacterium (Fig. 1.8). This organism has been extensively used as model system for studying nitrogen-fixation and to understand the molecular basis of cellular differentiation [183].

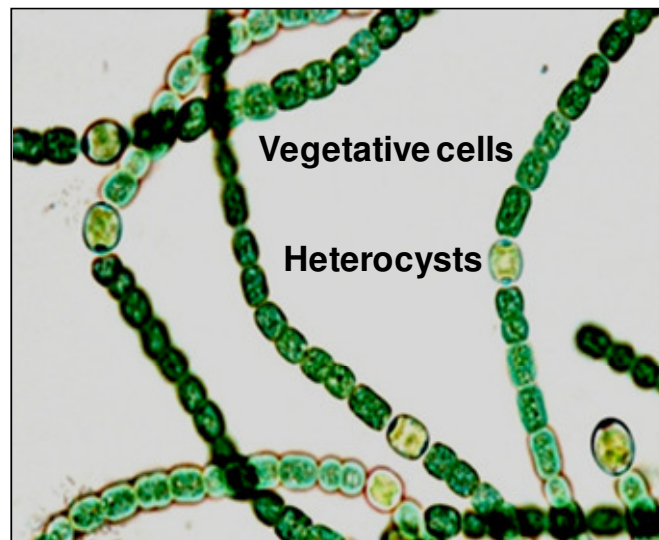


**Fig. 1.8 Filaments of *Anabaena* PCC 7120 under microscope.** Vegetative cells and the heterocysts are marked. Image courtesy of Dr. Manisha Banerjee, BARC.

When grown in the absence combined nitrogen (i.e. under nitrogen-fixing conditions), one cell after every 11-13 cells in an *Anabaena* filament is differentiated into heterocysts, which carries out the task of converting atmospheric nitrogen into its bio-available form [184]. Nitrogenase enzyme is selectively expressed in heterocyst

because of its unique structure and metabolic activities that lead to a reduced O<sub>2</sub> tension. Heterocysts employ multiple mechanisms, such as absence of photosystem II or thickening of cell wall with impervious glycolipids, to protect nitrogenase from oxygen [185]. By virtue of its nitrogen fixing capability, strains of *Anabaena* have found widespread application as natural nitrogen biofertilizers in the paddy fields of South-East Asia [167].

Various abiotic stresses (heavy metals, drought, salt, herbicides etc.) that affect plant growth and limit crop production worldwide, also adversely affect the biofertilizer potential of *Anabaena*. It should be noted that all these stresses cause over-production of ROS too [186]. Thus, studying the detailed basis of oxidative stress resistance in *Anabaena* is essential for development of novel biofertilizers, which may be used under adverse conditions. The role played by various proteins in overcoming oxidative stress in the filamentous, heterocystous, nitrogen-fixing, cyanobacterium *Anabaena* PCC 7120 has garnered remarkable interest in the recent past [95, 187, 188, 189, 190, 191, 192]. With fully sequenced and annotated genome [193] and ease of genetic manipulation [194, 195], *Anabaena* serves as an excellent model to study various genes and pathways.

### **1.9 Oxidative stress management in *Anabaena***

*Anabaenas* PCC 7120 can tolerate a variety of abiotic stresses like drought, salinity, nutrient deficiency and temperature up shift [196]. This organism is highly resistant to ionizing radiation with a LD<sub>50</sub> value of 6 kGy for gamma radiation [197]. It can also tolerate desiccation which can be considered to be an extreme form of osmotic stress. Apart from these, *Anabaena* shows remarkable resistance to other stresses like heavy metal toxicity, herbicide treatment, high-intensity light etc. Most of the above-

mentioned stresses are known to generate excess ROS which are toxic to cells. Given their long history of evolution and intimate relationship with oxygen, *Anabaena* PCC 7120 is endowed with an elaborate oxidative stress management system [148]. In animals and plants, the primary  $H_2O_2$  decomposing enzymes are glutathione peroxidases and ascorbate peroxidases respectively. Interestingly, these two groups of enzymes are very rare in cyanobacteria [164]. The genome of *Anabaena* showed this organism to possess 2 superoxide dismutases (SODs), 10 peroxiredoxins (Prxs), 6 DPS-type proteins, ruberythrin, universal stress proteins (USPs) and 2 Mn-catalases [148]. The major ROS removal pathways in *Anabaena* are schematically depicted in Fig. 1.9.

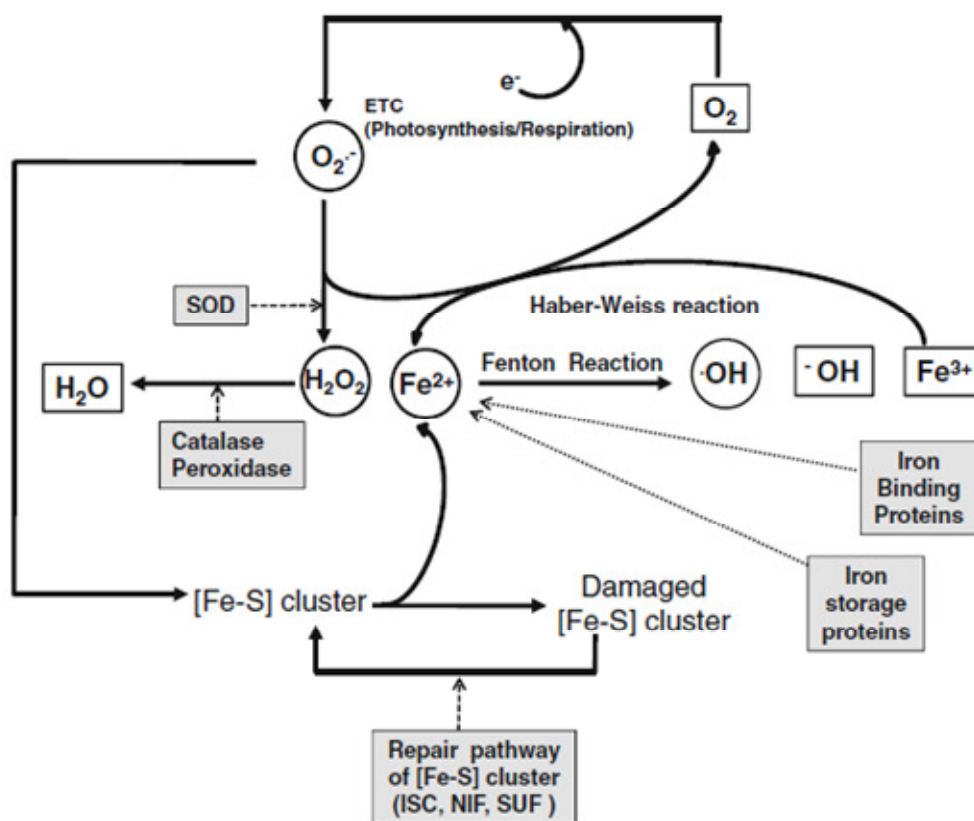


**Fig. 1.9** Schematic representation of major ROS removal pathways in *Anabaena* (from Banerjee et al., 2013, [148]). The toxic species/free radicals are indicated in circles and the nontoxic products in square boxes. The detoxifying/repair enzymes (grey boxes) are shown by dotted arrows. ETC, electron transport chain; SOD, superoxide dismutase.

The first line of enzymatic antioxidant defense is accomplished by superoxide dismutases (SODs). Of the two SODs present in *Anabaena*, the Mn-SOD was found to protect the organism from oxidative stress mediated by methyl viologen under nitrogen fixing conditions. This enzyme was shown to be involved in acclimation to high-intensity light and protection of the nitrogenase enzyme [14]. The Fe-SOD, on the other hand, was found to play an important role when the organism was grown under nitrogen-supplemented conditions. Over-expression of this protein under nitrogen fixing conditions was found to be lethal even in absence of any stress [198]. The two enzymes also showed differential localization. The Fe-SOD was a cytosolic protein while, the Mn-SOD was present in cytosol as well as in periplasmic lumen [199]. All these reports indicates that the two forms of SOD have distinct roles in combating oxidative stress in *Anabaena* depending on nitrogen status of the culture and their subcellular localization [148].

Although two ORFs encoding Mn-catalase are present in the genome of *Anabaena* PCC 7120, cell extracts from the control or H<sub>2</sub>O<sub>2</sub>-treated *Anabaena* failed to show any catalase activity on zymograms [200], suggesting a rather limited expression of catalases under these conditions. Presence and expression of multiple peroxiredoxins strongly suggest that Prxs are the principal enzymes that are employed for H<sub>2</sub>O<sub>2</sub> decomposition in *Anabaena* PCC 7120 in the absence of stresses or on exposure to H<sub>2</sub>O<sub>2</sub> [95, 165, 190, 191, 200, 201, 202]. A heme-dependent peroxidase from *Anabaena* has been biochemically characterized [203]. Role of an FNR-dependent peroxidase, (ruberythrin, RbrA) in detoxification of H<sub>2</sub>O<sub>2</sub>, specifically in heterocyst has also been investigated in past [204].

Apart from these major antioxidant enzymes, many other proteins that are directly or indirectly involved in managing the burden of oxidative stress are present in *Anabaena*. Presence of multiple Dps (DNA protection under starvation) proteins and universal stress proteins strongly suggest their contribution in ROS detoxification [148]. Role of Suf (sulfur uptake) proteins in reducing ROS content has been demonstrated in recent past. These proteins are involved in Fe-S cluster formation in various redox-active enzymes thus, playing a major role in iron homeostasis which is an important factor for maintaining oxidative status of any cell [192].

### **1.10 The current study**

As mentioned in previous sections, heterocystous cyanobacterium *Anabaena* PCC 7120 harbours a robust oxidative stress management system. Interestingly, this organism lacks typical or bifunctional catalase, instead, two ORFs, *alr0998* (*katA*) and *alr3090* (*katB*), that encode Mn-catalase each are present. As per the nucleotide sequence, the *katA* gene encodes for a 304 amino acid long protein while, *katB* encodes for a 230 amino acid long protein. Although expression of these proteins was not detected even after treatment with H<sub>2</sub>O<sub>2</sub>, over-expression of KatA, resulted in increased tolerance to oxidative stress mediated by H<sub>2</sub>O<sub>2</sub> in *Anabaena* PCC 7120. KatB was found to be up-regulated under desiccation stress [205] and other proteomic screens showed KatB to accumulate under iron starvation or arsenic stress [206, 207]. The protein was also found to be synthesized under in response to treatment with herbicide butachlor [187] or under UV-B stress [208].

However, in spite of its apparent importance, its detailed physiological role, biochemistry or structural aspects had not been studied at all. Keeping this in mind, the objectives of the thesis were framed with the aim of biophysical/biochemical

characterization of the KatB protein and elucidation of structural features of this protein by X-ray crystallography. It was also desired to carry out detailed expression analysis of the *katB* gene and to modulate KatB levels in *Anabaena* to demarcate its *in vivo* role in oxidative stress management. Finally, *Anabaena* was used as a platform for production of the KatB protein and the biotechnological potential of this protein/strain was evaluated.

On the basis of the research work carried out to fulfil these objectives, the thesis is organized into 7 chapters followed by the references section. The first chapter (Chapter 1) is the General Introduction to the research work described in the thesis. It provides the background to this study with detailed review of the related literature. The second chapter (Chapter 2) states the materials and methods employed during the study. The next four chapters (Chapters 3, Chapter 4, Chapter 5 and Chapter 6) describe the results obtained during the study along with the relevant discussion. Chapter 3 deals with the role of *katB* gene in the physiology of the cyanobacterium *Anabaena* PCC 7120. The biochemistry and the structure of the KatB protein are explained in Chapter 4. Chapter 5 details the role of the N-terminal region in maintenance of KatB structure-function. Chapter 6 states the results related to production of KatB protein using *Anabaena* as an expression platform demonstrating the biotechnological potential of the protein/strain. The final chapter (Chapter 7) is the summary of major findings of this work along with the concluding remarks. The future perspectives emanating from this study is also mentioned in this chapter. All the previous studies referred to in the text are cited in the 'References' section.

## **CHAPTER 2**

### **Materials & Methods**



## 2.1 Materials

### 2.1.1 Chemicals used in this study

The list of chemicals used in the study are mentioned in the Table 2.1.

**Table 2.1 List of chemicals used in the study**

Name of the chemical	Source	Name of the chemical	Source
Acrylamide	Sigma	Neomycin	Sigma
Agarose	Sigma	Chloroform	Sigma
Ammonium per sulfate	Sigma	Ethidium bromide	Sigma
Boric acid	Sigma	Thiobarbituric acid	Sigma
CaCl <sub>2</sub>	Sigma	K <sub>2</sub> HPO <sub>4</sub>	Sigma
CDP-star	Roche	Sorbitol	Sigma
Coommassie Brilliant Blue	Sigma	Carbenicillin	Sigma
DNaseI	Sigma	H <sub>2</sub> SO <sub>4</sub>	Sigma
FeCl <sub>3</sub>	Sigma	C <sub>6</sub> N <sub>6</sub> FeK <sub>3</sub>	Sigma
Glycine	Sigma	KMnO <sub>4</sub>	Sigma
Imidazole	Sigma	Ampicillin	Sigma
KCl	Sigma	Trichloroacetic acid	Sigma
Lenox LB medium	Sigma	Ethanol	Haymann
LiCl <sub>2</sub>	Sigma	Acetone	Sigma
Lowry's reagent	Sigma	Iso-propanol	Sigma
Malic acid	Sigma	NaNO <sub>3</sub>	Sigma
Methyl viologen	Sigma	Chloramphenicol	Sigma
Methylene bis-acrylamide	Sigma	Kanamycin	Sigma

MgCl <sub>2</sub>	Sigma	PEG	Sigma
Na <sub>2</sub> EDTA	Sigma	KH <sub>2</sub> PO <sub>4</sub>	Sigma
NaCl	Sigma	H <sub>2</sub> O <sub>2</sub>	Sigma
NBT-BCIP	Roche	Mannitol	Sigma
Quick ligase	NEB	HCl	Sigma
RbCl <sub>2</sub>	Sigma	Na-acetate	Sigma
Sucrose	Sigma	Glycerol	Sigma
Tris-HCl	Sigma	NaOH	Sigma
Trizol reagent	Invitrogen	Methanol	Sigma
MOPS	Sigma	Formaldehyde	Sigma
Sodium acetate	Sigma	Acetone	Sigma

### 2.1.2 Primers used in the study

Primers were designed as per requirement of the study and were synthesized at commercial facilities. Names, nucleotide sequences and restriction site present in those primers are stated in Table 2.2.

**Table 2.2 List of primers used in the study**

<b>Primer</b>	<b>Sequence</b>	<b>Restriction enzyme site</b>
KatB_Nde_Fwd	GGAC <u>CATATG</u> TTTTTTCACAAGAAAGAAC CG	<i>NdeI</i>
KatB_BamHI_Rev	GGGGATCCTTAGGAATGTTTTTCTAGTGG GT	<i>BamHI</i>
KatB_prom_Fwd	GCGAGCTCAAAGCTGCCTTGGGGGGAAT	<i>SacI</i>

	TAGG	
KatB_prom_Rev	GGGGTACCCTCAAAAATTA <del>ACTCGCAT</del>	<i>KpnI</i>
	CTG	
pAM1956Kan_Rev	CCGCTCGAGTCCCGCTCAGAAGAACTCG	<i>XhoI</i>
	TCAAG AAG	
Kan_3090_Olap_Rev	CTTGCGCCCTGAGTGCTGAGGAGATGAA	-
	CTAGAG	
3090_Kan_Olap_Fwd	AAACTCTAGTTCATCTCCTCAGCACTCAG	-
	GGCGC AAGGGCTGCTAAAG	
3090_sacI_Fwd	GCC GAGCTCAAAAACGTGG	<i>SacI</i>
	ATCAAACAGAGG	
RACE_KatB_Ext	AACGAGGGTTTGCTTCACCG	-
RACE_KatB_Int	CGTGAATCGGTTCTTTCTTG	-
KatB_BamHis_Rev	GGGGATCCTCCAGTTAGTGATGGTGATG	<i>BamHI</i>
	GTGATGGGAATGTTTTTCTAGTGGGTTAG	
KatB_F2G_Fwd	GGAC <u>CATAT</u> GGGCTTTCACAAGAAAGAAC	<i>NdeI</i>
	CG	
KatB_F2A_Fwd	GGAC <u>CATAT</u> GGCGTTTCACAAGAAAGAAC	<i>NdeI</i>
	CG	
KatB_F2V_Fwd	GGAC <u>CATAT</u> GGTTTTTCACAAGAAAGAAC	<i>NdeI</i>
	CG	
KatB_F2Y_Fwd	GGAC <u>CATAT</u> GTACTTTCACAAGAAAGAAC	<i>NdeI</i>
	CG ATTCACG	
KatB_F2W_Fwd	GGAC <u>CATAT</u> GTGGTTTCACAAGAAAGAAC	<i>NdeI</i>

	CGATTCACG	
KatB_F3A_Fwd	GGAC <u>CATATG</u> TTTGCGCACAAGAAAGAAC	<i>NdeI</i>
	CGATTCACG	
KatB_H4A_Fwd	GGAC <u>CATATG</u> TTTTTTGCGAAGAAAGAAC	<i>NdeI</i>
	CGATTCACG	
KatB_K5A_Fwd	GGAC <u>CATATG</u> TTTTTTCACGCGAAAGAACC	<i>NdeI</i>
	GATTCACG	
KatB_K6A_Fwd	GGAC <u>CATATG</u> TTTTTTCACAAGGCGGAACC	<i>NdeI</i>
	GATTCACG	
KatB_Truncated_Fwd	GGAC <u>CATATG</u> CCGATTCACGTTGTAAATAT	<i>NdeI</i>
	CGG	
KatBY42F_Fwd	CTGCAAGATCAAGCCTGGGTGCAATCAT	-
	TC	
KatBY42F_Rev	GAATGATTGCACCCAGGCTTGATCTTGCA	-
	G	
KatBY140F_Fwd	GCGCGTCAAACCGCCGAAGAGCTAATC	-
KatBY140F_Rev	GATTAGCTCTTCGGCGGTTTGACGCGC	-

### 2.1.3 Plasmids used or generated for the study

Following plasmid constructs were used or generated for the study (Table 2.3).

**Table 2.3 List plasmids used or generated in the study**

Plasmid	Description	Source/reference
pAM1956	<i>kan<sup>R</sup></i> , promoterless vector with <i>gfpmut2</i> reporter gene	Lab collection
pFPN	<i>amp<sup>R</sup></i> , <i>kan<sup>R</sup></i> , integrative expression vector	[195]
pRL271	<i>cm<sup>R</sup></i> , <i>kan<sup>R</sup></i> suicide vector for <i>Anabaena</i>	Lab collection
pRL3090Kan	Internal 300 bp <i>katB</i> sequence along with <i>nptII</i> expression cassette (1.2 kb) cloned into <i>SacI</i> and <i>KpnI</i> sites of pRL271	This study
pFPNkatB	0.693 kb <i>alr3090</i> fragment cloned in pFPN at <i>NdeI</i> - <i>BamHI</i> restriction sites	This study
pAMKatB	1.3 kb <i>XmaI</i> - <i>SalI</i> fragment from pFPNkatB cloned in pAM1956 vector	This study
pAM3090Prom	300 bp <i>KpnI</i> - <i>SacI</i> fragment containing the <i>katB</i> promoter	This study
pFPNkatF2V	0.693 kb <i>katBF2V</i> PCR product introduced into <i>NdeI</i> and <i>BamHI</i> sites of pFPN.	This study
pAMkatF2V	0.693 kb <i>katBF2V</i> PCR product along with light inducible <i>P<sub>psbA1</sub></i> promoter cloned into <i>SalI</i> and <i>XmaI</i> sites of pAM1956.	This study
pFPNkatB6His	0.693 kb <i>katB</i> PCR product with six in-	This study

	frame C-terminal histidine codons cloned downstream of P <sub>psbA1</sub> promoter in <i>NdeI</i> and <i>BamHI</i> sites of pFPN vector.	
pAMkatB6His	0.693 kb <i>katB</i> PCR product with six in-frame C-terminal histidine codons along with light inducible P <sub>psbA1</sub> promoter cloned into <i>SalI</i> and <i>XmaI</i> sites of pAM1956 vector.	This study
pET21a	Amp <sup>R</sup> , expression vector.	Novagen
pETkatB	0.693 kb <i>katB</i> PCR product with six in-frame C-terminal His codons cloned into <i>NdeI</i> and <i>BamHI</i> sites of pET21a.	This study
pETkatF2V	0.693 kb <i>katBF2V</i> PCR product with six in-frame C-terminal His codons cloned into <i>NdeI</i> and <i>BamHI</i> sites of pET21a.	This study
pETkatF2G	0.693 kb <i>katBF2G</i> PCR product with six in-frame C-terminal His codons cloned into <i>NdeI</i> and <i>BamHI</i> sites of pET21a.	This study
pETkatF2A	0.693 kb <i>katBF2A</i> PCR product with six in-frame C-terminal His codons cloned into <i>NdeI</i> and <i>BamHI</i> sites of pET21a.	This study
pETkatF2Y	0.693 kb <i>katBF2Y</i> PCR product with six in-frame C-terminal His codons cloned into <i>NdeI</i> and <i>BamHI</i> sites of pET21a.	This study

pETkatF2W	0.693 kb <i>katBF2W</i> PCR product with six in-frame C-terminal His codons cloned into <i>NdeI</i> and <i>BamHI</i> sites of pET21a.	This study
pETkatF3A	0.693 kb <i>katBF3A</i> PCR product with six in-frame C-terminal His codons cloned into <i>NdeI</i> and <i>BamHI</i> sites of pET21a.	This study
pETkatH4A	0.693 kb <i>katBH4A</i> PCR product with six in-frame C-terminal His codons cloned into <i>NdeI</i> and <i>BamHI</i> sites of pET21a.	This study
pETkatK5A	0.693 kb <i>katBK5A</i> PCR product with six in-frame C-terminal His codons cloned into <i>NdeI</i> and <i>BamHI</i> sites of pET21a.	This study
pETkatK6A	0.693 kb <i>katBK6A</i> PCR product with six in-frame C-terminal His codons cloned into <i>NdeI</i> and <i>BamHI</i> sites of pET21a.	This study
pETkatE7A	0.693 kb <i>katE7A</i> PCR product with six in-frame C-terminal His codons cloned into <i>NdeI</i> and <i>BamHI</i> sites of pET21a.	This study
pETkatB_Trunc	0.675 kb <i>katB_Truncated</i> PCR product with six in-frame C-terminal His codons cloned into <i>NdeI</i> and <i>BamHI</i> sites of pET21a.	This study
pETkatY42F	0.693 kb <i>katY42F</i> PCR product with six in-frame C-terminal His codons cloned	This study

---

	into <i>NdeI</i> and <i>BamHI</i> sites of pET21a.	
pETkatY140F	0.693 kb <i>katY140F</i> PCR product with six in-frame C-terminal His codons cloned into <i>NdeI</i> and <i>BamHI</i> sites of pET21a.	This study

---

#### 2.1.4 Restriction endonucleases used in the study

Following restriction enzymes were used for the study (Table 2.4). All the enzymes were procured from New England Biolabs.

**Table 2.4 List of restriction enzymes used in the study**

Name of the enzyme	Recognition sequence
<i>NdeI</i>	CATATG
<i>BamHI</i>	GGATCC
<i>XmaI</i>	CCCGGG
<i>SalI</i>	GTCGAC
<i>KpnI</i>	GGTACC
<i>SacI</i>	GAGCTC
<i>XhoI</i>	CTCGAG

#### 2.1.5 *E. coli* strains used or generated in the study

**Table 2.5 List of *E. coli* strains used or generated in the study**

Strain	Description	Reference
JM109	endA1 glnV44 thi-1 relA1 gyrA96 recA1 mcrB <sup>+</sup> Δ (lac-proAB) e14- [F' traD36 proAB <sup>+</sup> lacI <sup>q</sup>	Lab collection

---

	lacZΔM15] hsdR17 ( $r_K^- m_K^+$ )	
DH5α	$F^-$ <i>endA1 glnV44 thi-1 recA1 relA1 gyrA96 deoR nupG purB20</i> φ80 <i>lacZΔM15</i> Δ( <i>lacZYA-argF</i> ) U169, hsdR17( $r_K^- m_K^+$ ), λ <sup>-</sup>	Lab Collection
BL21 (DE3) pLysS	$Cm^r F^-$ <i>ompT hsdS<sub>B</sub> (r<sub>B</sub><sup>-</sup> m<sub>B</sub><sup>-</sup>) gal dcm</i> (DE3) pLysS	Novagen
HB 101	$F^-$ <i>mcrBmrr hsdS20(rB<sup>-</sup> mB<sup>-</sup>) recA13 leuB6 ara-14 proA2 lacY1 galK2 xyl-5 mtl-1 rpsL20(SmR) glnV44</i> λ <sup>-</sup>	Lab Collection
HB101R2	Donor strain carrying pRL623(encoding methylase) and pRL443 (conjugal plasmid)	[209]
BL21(DE3)pLysSpETkatB	BL21(DE3) pLysS expression host carrying pETkatB plasmid	This study
BL21(DE3)pLysSpETkatF2G	BL21(DE3) pLysS expression host carrying pETkatF2G plasmid	This study
BL21(DE3)pLysSpETkatF2A	BL21(DE3) pLysS expression host carrying pETkatF2G plasmid	This study
BL21(DE3)pLysSpETkatF2V	BL21(DE3) pLysS expression host carrying pETkatF2V plasmid	This study
BL21(DE3)pLysSpETkatF3A	BL21(DE3) pLysS expression	This study

	host carrying pETkatF3A plasmid	
BL21(DE3)pLysSpETkatH4A	BL21(DE3) pLysS expression host carrying pETkatH4A plasmid	This study
BL21(DE3)pLysSpETkatK5A	BL21(DE3) pLysS expression host carrying pETkatK5A plasmid	This study
BL21(DE3)pLysSpETkatK6A	BL21(DE3) pLysS expression host carrying pETkatK6A plasmid	This study
BL21(DE3)pLysSpETkatE7A	BL21(DE3) pLysS expression host carrying pETkatE7A plasmid	This study
BL21(DE3)pLysSpETkatBTrunc	BL21(DE3) pLysS expression host carrying pETkatB_Trunc plasmid	This study
BL21(DE3)pLysSpETkatY42F	BL21(DE3) pLysS expression host carrying pETkatY42F plasmid	This study
BL21(DE3)pLysSpETKatY140F	BL21(DE3) pLysS expression host carrying pETkatY140F plasmid	This study

### 2.1.6 *Anabaena* strains used or generated in the study

**Table 2.6 List of *Anabaena* strains used or generated in the study**

Strain	Description	Source/reference
<i>Anabaena</i> PCC 7120	Wild-type strain	Lab collection
<i>AnKatB</i> <sup>+</sup>	<i>Anabaena</i> PCC 7120 harboring pAMKatB	This study

<i>AnKatB</i> <sup>-</sup>	Insertional inactivation of <i>katB</i> in <i>Anabaena</i> PCC 7120	This study
<i>An3090Prom</i>	<i>Anabaena</i> PCC 7120 harbouring pAM3090Prom	This study
<i>AnKatBF2V</i> <sup>+</sup>	<i>Anabaena</i> PCC 7120 harboring pAMKatBF2V	This study
<i>AnKatB6His</i> <sup>+</sup>	<i>Anabaena</i> PCC 7120 harbouring pAMKatB6His	This study

## 2.2 Bioinformatic tools used

### 2.2.1 Designing of primers

For ligation of the ORFs into the expression vector for production of recombinant proteins or for cloning the promoter region of the gene, the desired DNA fragment was first PCR amplified using *Anabaena* PCC 7120 genomic DNA as the template. For PCR amplification the primers were designed manually. The *Anabaena* DNA sequence information was obtained from the Kazusa genome database ([www.kazusa.or.jp/cyanobase](http://www.kazusa.or.jp/cyanobase)). The manually designed primers were subjected to quality control where, the GC content, probable hairpin formation, self primer complementarity etc. were carefully verified using the software DNAMAN (Lynnon Biosoft, Germany). To facilitate ligation of the PCR-amplified fragment in the vector of choice and to assure the orientation of the cloned fragment, suitable restriction endoclease recognition sequences were put at the end of the primer sequences. Presences of those recognition sequences in fragment of interest were checked using the NEB cutter online web tool ([http://www.tools.neb.com/NEB\\_cutter2/index.php](http://www.tools.neb.com/NEB_cutter2/index.php)) from the New England Biolab's official website. The complete list of the primers used in the study is mentioned in the Table 2.2.

## **2.2.2 Nucleotide or amino acid sequence analysis, multiple sequence alignment and phylogenetic analyses**

The Redoxibase database [210] was used to retrieve the available Mn-catalase sequences from various bacterial species. The nucleotide sequence or the amino acid sequences were handled and analyzed using softwares and web tools like DNAMAN (Lynnon Biosoft, Germany), NCBI BLAST tool (<http://blast.ncbi.nlm.nih.gov/blast>), Clustal W (<http://www.ch.embnet.org/software/ClustalW.html>), Nucleic Acid Sequence Massager (<http://www.attotron.com/cybertory/analysis/seqMassager.html>) etc.

## **2.3 Media and growth conditions**

### **2.3.1 Medium and growth condition for *Anabaena* strains**

The wild-type *Anabaena* PCC 7120 cultures were grown in BG11 liquid medium, pH 7.0 in presence of combined nitrogen (17 mM NaNO<sub>3</sub>, BG11 N+). The medium were not supplemented with the combined nitrogen salt whenever diazotrophic growth was desired (BG11 N-). The composition of BG11 medium is stated in Table 2.6. For the growth of recombinant *Anabaena* strains generated in this study the BG11 medium was supplemented with the antibiotic neomycin at a final concentration of 12.5 µg/ml (Neo<sub>12.5</sub>) or 25 µg/ml (Neo<sub>25</sub>) in liquid medium or in solid medium respectively. BG11 plates were made by addition of 1.5% agar.

*Anabaena* cultures were grown under constant illumination 30 µE m<sup>-2</sup>s<sup>-1</sup> with or without shaking (100 rpm) at 27°C ± 2°C. Growth of the culture was assessed by measuring the chlorophyll *a* content from 1 ml of the culture suspension [211]. For spot assay, 20 µl of the culture suspension was spotted on an appropriate BG11 agar plate and incubated under above-mentioned conditions for 15 days and photographed.

### **2.3.2 Medium and growth condition for *E. coli* strains**

Luria-Bertani (LB, Annexure A3 & A4) medium was used for the growth of *Escherichia coli* cells. Liquid cultures were grown at 37°C with shaking at 150 rpm in the presence of appropriate antibiotics. The antibiotics used were chloramphenicol (34 mg/ml, Cm<sub>34</sub>), kanamycin (50 mg/ml, Kan<sub>50</sub>), or carbenicillin (100 mg/ml, Cb<sub>100</sub>). 1.5% agar was used as solidifying agent whenever cultures were required to be grown on solid medium.

### **2.4 Measurement Colony Forming Units (CFUs)**

Three days old wild-type *Anabaena* cultures were reinoculated in fresh BG11N+ medium at chlorophylla density of 1.5 mg/ml and subjected to NaCl and/or H<sub>2</sub>O<sub>2</sub> stress for 2 days. 150 µl of the culture was then spread on BG11N+ agar plate and incubated under constant illumination for 14 days at 27°C ± 2°C. The plates were photographed and number of colonies was counted manually and the values were represented as bar diagram.

### **2.5 Recombinant DNA technology**

#### **2.5.1 Ligation of the *katB* DNA fragment into pET21a**

The *katB*<sup>WT</sup> ORF was PCR amplified from the *Anabaena* genomic DNA (using KatB\_Nde\_Fwd and KatB\_Bam\_His\_Rev; Table 2.2). The reverse primer also contained six in-frame histidine codons. The PCR amplified product was digested with *Nde*I and *Bam*HI restriction endonuclease and subsequently ligated to similarly digested pET21a vector. The resultant plasmid (pETKatB) was sequenced to confirm the nucleotide identity.

### **2.5.2 Ligation of the *katB* variants into pET21a**

DNA corresponding to the different *katB* variants (where N-terminal 2<sup>nd</sup> to 7<sup>th</sup> residue were individually replaced with alanine) was PCR-amplified from *Anabaena* genomic DNA with the respective custom-designed mutagenic forward primers and KatB\_Bam\_His\_Rev reverse primer (Table 2.2) which contained six in-frame histidine codons. Along with these, a variant *katB* ORF, wherein the original 2<sup>nd</sup> to 7<sup>th</sup> N-terminal residues were deleted, was also generated by performing PCR with KatB\_Trunc\_Fwd forward primer (Table 2.2) and the same reverse primer (KatB\_BamHis\_Rev). Similarly, DNA corresponding to the *katB* variants differing at the second amino acid position (Phe-2 replaced with Gly or Ala or Val or Tyr or Trp) was also PCR amplified with the respective custom designed mutagenic forward primer and the KatB\_Bam\_His\_Rev primer (Table 2.2). All the mutated ORFs were individually ligated to pET21a as *NdeI-BamHI* digested fragments. The presence of desired mutation and nucleotide integrity was confirmed by sequencing the resultant plasmids. All these plasmids were transformed into *E. coli* BL21(DE3)pLysS expression host for the expression of respective protein.

### **2.5.3 Construction of pAMkatB or pAMkatBF2V or pAMkatB6His and Over-expression of KatB/KatBF2V/KatB6His Protein in *Anabaena* PCC 7120**

The *katB* DNA fragment (693 bp) or the *katBF2V* (where Phe-2 codon was replaced by Val codon) was PCR amplified from *Anabaena* PCC 7120 genomic DNA using KatB\_Nde\_Fwd or KatBF2V\_Nde\_Fwd forward primer respectively. In both cases, KatB\_Bam\_Rev was used as reverse primer (Table 2.2). For amplification of *katB6His* DNA fragment, KatB\_Nde\_Fwd and KatB\_Bam\_His\_Rev was used as forward and reverse primers respectively (Table 2.2). The PCR products were then cloned

downstream of a strong light-inducible  $P_{psbA1}$  promoter, in pFPN [195] using *NdeI* and *BamHI* restriction endonucleases (plasmid called pFPNkatB or pFPNkatBF2V or pFPNkatB6His respectively). The *katB/katBF2V/katB6His* DNA fragment along with the  $P_{psbA1}$  promoter was then excised out from pFPNkatB/pFPNkatBF2V/pAMkatB6His using *SalI* and *XmaI* restriction endonucleases and ligated into *E. coli/Anabaena* shuttle vector pAM1956 [212] to generate pAMkatB or pAMkatBF2V plasmid. A conjugal *E. coli* donor [HB101 (pRL623 + pRL443)] [194, 213] strain was utilized to transfer the pAMkatB/pAMkatB into *Anabaena* PCC 7120 through tri-parental mating as described earlier [194]. The exconjugants were selected on BG11N+ plates supplemented with neomycin (25  $\mu$ g/ml) antibiotic and repeated subculturing was performed to obtain the desired transformants. The strains thus obtained were maintained on BG11N+ plates constantly under neomycin selection pressure.

#### **2.5.4 Construction of *katB* Promoter-*gfp* Fusion**

A 300 bp DNA fragment containing the *katB* promoter region, as identified by RACE analysis, was PCR amplified using KatB\_prom\_Fwd/KatB\_prom\_Rev primers (Table 2.2) and subsequently cloned just upstream of *gfp* reporter gene in pAM1956 vector employing *KpnI* and *SacI* restriction endonucleases. The construct thus generated was named as pAM3090prom). The construct was conjugally transferred into *Anabaena* PCC 7120 and the exconjugants (*An3090prom*) were selected on BG11N+ plates containing Neo<sub>25</sub> and subjected to microscopic analysis.

#### **2.5.5 Construction of the *katB* Mutant (*AnKatB*<sup>-</sup>)**

For generation of *katB* mutant *Anabaena* strain, single recombination-based strategy using a suicide plasmid was employed [214]. A 300-bp DNA fragment internal to the

*katB* ORF was PCR amplified from *Anabaena* genomic DNA using 3090\_SacI\_Fwd (containing *SacI* site) and Kan\_3090\_Olap\_Rev primers (Table 2.2). Kanamycin expression cassette was PCR amplified from pAM1956 vector by primers 3090\_Kan\_Olap\_Fwd and pAM1956Kan\_Rev (containing *XhoI* site). Subsequently, the above-mentioned two fragments were combined by overlap extension PCR using 3090\_SacI\_Fwd and pAM1956Kan\_Rev primers. The resultant PCR product, which contained 300-bp *katB* fragment + Kanamycin expression cassette, was cloned into a suicide vector pRL271 by using *XhoI* and *SacI* restriction endonucleases and the construct generated was named as pRLkatBkan. This construct was conjugally transferred to *Anabaena* PCC 7120, and the putative mutants (*AnKatB*<sup>-</sup>) were selected on BG11N+ plates supplemented with Neo<sub>25</sub>. Repeated subculturing in presence of neomycin was performed to obtain the *katB* mutant *Anabaena* strain.

## **2.6 Rapid Amplification of cDNA Ends (RACE)**

The total RNA was isolated from the control wild-type *Anabaena* PCC 7120 cells or cells stressed with NaCl for 16 h, followed by DNase-I treatment and repurification using spin columns (Nucleospin RNA clean-up XS, Macherey Nagel). For synthesis of cDNA, KatB\_RACE\_Ext (Table 2.2) was used as the reverse primer. The cDNA was subjected to poly-A tailing using dATP and terminal transferase enzyme. The product was used for PCR amplification with oligo dT-anchor primer and an internal gene specific primer (KatB\_RACE\_Int) as described (5'/3' RACE kit, 2<sup>nd</sup> Generation, Roche).

## **2.7 Protein expression in *E. coli* and purification of recombinant protein**

Over-expression of recombinant proteins in *E. coli* and subsequent purification by NiNTA column chromatography was performed as described earlier [215]. The *E. coli*

BL21 (DE3) pLysS strains carrying appropriate recombinant plasmids were grown at 37°C with shaking at 180 rpm in Luria–Bertani (LB) medium supplemented with carbenicillin (100 µg/ml) and chloramphenicol (34 µg/ml). When the OD<sub>600</sub> of the culture reached 0.6, 100 µM MnCl<sub>2</sub> was added to the culture and the temperature was brought down to 20°C. 1 mM isopropyl β-D-1-thiogalactopyranoside (IPTG) was then added to the culture and the cells were incubated for further 16 hours at 20°C. The recombinant *E. coli* cells were then harvested by centrifugation at 6500Xg for 5 minutes. The cell pellets were resuspended in pre-chilled lysis buffer (50 mM Tris pH 8.0, 200 mM NaCl, and 5 mM imidazole). After 3-4 cycles of freeze-thawing in liquid nitrogen, the cells were lysed by sonication with a Branson digital sonifier for three cycles (each cycle was of 2 min with 2 s ‘on’ and 2 s ‘off’ pulse, 40% amplitude) while maintaining temperature at 4°C by jacketing the cell suspension with ice water. Cell lysate was subjected to centrifugation at 10000 rpm for 30 minutes at 4°C. The pellet, which contained the inclusion bodies was discarded and the supernatant was allowed to bind Ni<sup>2+</sup>-NTA (nitrilotriacetic acid) agarose matrix with gentle shaking at 4°C for 2.5 h. After that, the slurry was thoroughly washed with cold lysis buffer for at least 3 times to remove the unbound proteins and other components of the cell lysate. Following this, the slurry was further washed with lysis buffer supplemented with increasing concentration of imidazole (10, 20 and 30 mM) to wash off the non-specific proteins bound to the slurry. The bound protein was then eluted by increasing the imidazole concentration in the lysis buffer to 100 mM and 250 mM. The protein thus obtained in the elution fraction was dialyzed against 20 mM Tris buffer pH 8.0 overnight to remove imidazol. All the protein fractions were resolved on 14% SDS-PAGE and stained with Coomassie Brilliant Blue G-250 for visualization.

## 2.8 Purification of the KatB protein from *AnKatB6H<sup>+</sup>* strain

The *AnKatB6H<sup>+</sup>* strain over-expressing the his-tagged KatB protein was grown in BG11 liquid medium supplemented with combined nitrogen (17 mM NaNO<sub>3</sub>) and neomycin (12.5 µg/ml) for 7-10 days under constant illumination. Once sufficient biomass was attained, the *AnKatB6H<sup>+</sup>* cells were harvested by centrifugation and resuspended in cold lysis buffer (50 mM Tris, 200 mM NaCl and 5mM imidazole). The cell suspension was subjected to repeated freeze-thaw cycles (at least thrice) followed by sonication (Branson digital sonifier) for three cycles (each cycle was of 2 min with 2 s 'on' and 2 s 'off' pulse at 40% amplitude). The sample tube was jacketed with ice water to maintain low temperature while performing sonication. Cell lysate thus obtained was centrifuged at 8500×g for 30 min for separation of the soluble fraction from the insoluble cellular debris/inclusion bodies. The soluble fraction, which contained the his-tagged KatB protein, was allowed to interact with His-select NiNTA slurry (Sigma, pre-equilibrated with cold lysis buffer) for 3 h with gentle shaking. After discarding the flow-through, the slurry was subjected to repeated washing with lysis buffer containing 10 mM imidazole to remove unbound or non-specifically bound proteins. Elution of the bound his-tagged-KatB protein was performed by increasing the imidazol concentration of the lysis buffer to 100 mM or 250 mM.

For purification of An-KatB without NiNTA resin, the soluble fraction obtained after centrifugation of *AnaKatB6His<sup>+</sup>* cell lysate was subjected to heat treatment (80°C) in a water bath for 20 min, followed by centrifugation (8500×g for 30 min) to pellet down the debris accumulated due to coagulation of the heat labile cellular proteins. The supernatant thus obtained was then subjected to stepwise (NH<sub>4</sub>)<sub>2</sub>SO<sub>4</sub> precipitation (30%,

60% and 90%) to obtain sufficiently pure An-KatB preparation. The precipitate obtained after each step of  $(\text{NH}_4)_2\text{SO}_4$  treatment was dissolved in lysis buffer and dialyzed later against 20 mM Tris. All the fractions were resolved on 14% SDS-PAGE and stained with Coomassie Brilliant Blue G-250 for visualization.

## **2.9 Microscopic techniques**

The wild-type or the recombinant *Anabaena* strains grown under various conditions were visualized and photographed at 400X magnification on a Carl Zeiss Axioscop microscope. CCD AxioCamMRC (Zeiss) camera fitted with the microscope was used for capturing the microscopic field. Fluorescence microscopy of the same microscopic field was carried out using GFP filter (Zeiss filter set 9) with the Hg-Arc lamp (excitation BP, 450–490 nm and emission LP, 515 nm).

Nikon Eclipse Ti microscope was used for taking the light microscopic pictures of the recombinant AnKatBF2V+ strain. Images were captured at 400X magnification and the fluorescence micrograph of the same microscopic fields were captured using GFP filter (excitation filter 465–495 nm, dichroic mirror DM505, barrier filter 515–555 nm).

## **2.10 RNA isolation from *Anabaena* PCC 7120**

The total RNA was isolated from *Anabaena* PCC 7120 cultures as per the modified Trizol method as described earlier [216] with minor modifications. Briefly, the wild-type *Anabaena* PCC 7120 cells were harvested from 50 ml culture (chlorophyll *a* concentration 4  $\mu\text{g}/\text{ml}$ ) and mixed with Trizol reagent. Cells were lysed by bead beating and few cycles of freeze-thaw. The total RNA was isolated from the cell lysate as per the recommended protocol. The RNA quality was assessed by resolving the product on formaldehyde agarose gel. The RNA was subjected to DNaseI (Roche) treatment as per manufacturer's instruction. At the end of DNaseI treatment, 2 M lithium chloride was

added and the samples were incubated at 20°C for at least an hour. The RNA was pelleted down by centrifugation at 15000xg for 20 minutes at 4°C. Following this, the RNA pellet was washed thoroughly with 75% ethanol, dried in air and re-dissolved in nuclease-free water.

### **2.11 Northern blotting hybridization**

Northern blotting hybridization with the digoxigenin (DIG)-labeled *katB* DNA probe was performed as described earlier [216]. In short, 15 µg of the DNaseI treated total RNA was resolved on denaturing formaldehyde agarose gels. After completion of electrophoresis, the gel was washed with diethyl pyrocarbonate (DEPC)-treated water and RNA was transferred to positively charged nylon membrane by capillary blotting (in 10X SSC buffer). The blot was pre-hybridized in DIG Easy Hyb buffer (Roche) for an hour at 50°C. The *katB* gene was PCR amplified from *Anabaena* genomic DNA, labelled with DIG and allowed to hybridize (in DIG Easy Hyb Buffer) with the RNA blot for 16 hours at 50°C. The membrane was washed with 2X SSC, 0.1% SDS twice for 15 minutes at room temperature followed by two washes (15 min each) at 65°C with 0.1X SSC, 0.1% SDS. The blot was then subjected to chemiluminescent detection with CDP-STAR substrate as per the manufacturer's (Roche) instructions.

### **2.12 Protein electrophoresis**

The purified KatB protein or variants were resolved by electrophoresis on denaturing sodium dodecyl sulphate–polyacrylamide gels (14% acrylamide) or on native polyacrylamide gels (10% acrylamide). The resolved proteins were visualized as bands by staining with Coomassie Brilliant Blue G-50. Laemmli's buffer [217] was used to isolate the total cellular proteins from various *Anabaena* cultures (i.e., the wild-type *Anabaena*/*AnKatB*<sup>+</sup>/*AnKatBF2V*<sup>+</sup>/*AnKatB6His*<sup>+</sup>). The extracted total cellular protein

preparations were electrophoretically separated on denaturing 14% polyacrylamide gel and subjected to Western blotting analyses. The cell free extracts were also resolved on native 10% polyacrylamide gels for subsequent zymographic or Western blot analyses.

### **2.13 Western blot hybridization and immuno-detection**

Purified proteins or cell free *Anabaena* extracts that were resolved on SDS or Native polyacrylamide gels were transferred on to a nitrocellulose membrane (Sigma) by electroblotting. The blots were subsequently probed with the KatB antiserum or the monoclonal anti-poly histidine antibody. All Western blots were repeated at least thrice with consistent results.

### **2.14 Biophysical methods used in the study**

#### **2.14.1 Size exclusion chromatography**

Size exclusion chromatography (AKTA purifier, GE Healthcare) was performed using GE Superdex 200 10/300 GL column equilibrated with buffer A (20 mM Tris, 50 mM NaCl, pH 7.2) at 25°C.

#### **2.14.2 Circular Dichroism spectropolarimetry**

For recording of circular dichroism spectra, purified proteins (0.1 mg/ml, in 20 mM Tris buffer) were taken in cuvette of 1 mm path length and the CD spectra in the far ultraviolet range (200–260 nm) were recorded in a Jasco J-815 CD spectropolarimeter equipped with a peltier-type thermostatic cell holder. Change in dichroic intensity at 222 nm with respect to increasing temperature was monitored for thermal denaturation of the purified proteins to identify their melting point ( $T_m$ ). The heating rate was fixed at 2°C/min. For representation purposes, change in dichroic intensity at 222 nm was plotted as a function of temperature and in few cases first-order derivative of response unit (mDegree) was plotted as a function of temperature. For CD based chemical

denaturation assays, guanidine-HCl of different concentration was mixed with the protein of interest of in a quartz cuvette of 2-mm path length and immediately put into CD machine for measurement of changes in dichroic intensity. Rise in the CD signal at 222 nm (which is indicative of the loss of secondary structure) was monitored with respect to time in a Biologic MOS-500 CD spectropolarimeter.

### **2.14.3 Dynamic Light Scattering (DLS)**

DLS spectroscopy was carried out to assess the hydrodynamic volume of the purified protein. Purified proteins (0.4 µg/µl in 20 mM Tris, pH 8) were taken in 1 ml cuvettes and the hydrodynamic sizes were determined by DLS using the Malvern Zetasizer nanoseries instrument.

## **2.15 Enzyme assays**

### **2.15.1 In-Gel Catalase Activity (Zymogram)**

Purified proteins or cell-free extracts of *Anabaena* cultures were subjected to in-gel catalase activity assay. Cell-free extracts were prepared by resuspending the cyanobacterial cells in a buffer (20mM Tris-HCl, pH 8.0) followed by repeated cycles of freeze-thaw and vortexing (in the presence of glass beads, 600 µm diameter). The lysate was subjected to centrifugation at 14,000 g for 8 min to obtain cell-free extracts. The cell-free extracts or the purified proteins were electrophoretically separated on native 10% polyacrylamide gels and the gel was subjected to in-gel catalase activity. Once resolved, the gel was treated with 0.003% H<sub>2</sub>O<sub>2</sub> for 10 min, washed with distilled water, and stained with 1% ferric chloride and 1% potassium ferricyanide. The catalase activity was observed as a zone of clearance on a greenish-yellow background of the gel [218].

### 2.15.2 Spectrophotometric H<sub>2</sub>O<sub>2</sub> decomposition assay

The purified protein or cell free extracts from *Anabaena* cultures were assayed for H<sub>2</sub>O<sub>2</sub> decomposition activity in a spectrophotometer as described earlier [219]. In short, purified proteins or cell free extracts were mixed with various concentrations of H<sub>2</sub>O<sub>2</sub> in 1 ml of buffer (20 mM Tris, pH 8.5) and decomposition of H<sub>2</sub>O<sub>2</sub> with time was monitored by following the decrease in absorbance at 240 nm in a spectrophotometer (Chemito, SPETRASCAN UV2600). A molar extinction coefficient of 43.6 was used for determination of H<sub>2</sub>O<sub>2</sub> concentration [220]. For assaying the effect of inhibitors on KatB activity, a known concentration of H<sub>2</sub>O<sub>2</sub> was incubated with the purified protein in presence or absence of inhibitors (NaN<sub>3</sub> or NH<sub>2</sub>OH) in 1 ml of reaction buffer (20 mM Tris-HCl, pH8.0) and H<sub>2</sub>O<sub>2</sub> decomposition was monitored by following the decrease in absorbance at 240 nm with time in spectrophotometer. Rate of the reaction was calculated as mM of H<sub>2</sub>O decomposed per minute. For representation purpose the rate of reaction under control condition (without inhibitor) was considered as 100% and rests were calculated accordingly.

KatB activity at different pH was determined by measuring the relative activity of the purified protein in buffers with different pH. Buffer systems used for various pH ranges were; sodium acetate (pH 4.5 to 5.5), potassium phosphate (pH 5.5 to 7.5), Tris-HCl (pH 7.5 to 9.0) and glycine-NaOH (pH 9.0 to 10.0).

Effect of presence of calcium on catalytic activity of KatB was monitored by assaying the catalase activity in presence of 200 mM calcium acetate in 100 mM imidazole buffer (pH 8.0). For determination of the kinetic parameters, various concentrations of substrate (H<sub>2</sub>O<sub>2</sub>) were incubated with a fixed amount of the purified protein (10 µg) in

20 mM Tris-HCl buffer (pH8.0) and corresponding rates were calculated. The rate of reaction was plotted against substrate concentration in the form of Lineweaver-Burk plot and  $K_m$  value was determined from the plot.

### **2.15.3 Effect of GuHCl on KatB activity**

The purified KatB protein or variants were incubated in different concentrations of GuHCl (0.1-0.5M) for 15 minutes and their activity was monitored spectrophotometrically after diluting them in 20 mM Tris, pH 8.0. For calculating the relative catalase activity, activity of the protein in the absence of GuHCl was considered as 100% and rest were calculated accordingly.

### **2.15.4 Effect of temperature on KatB activity**

The purified proteins were exposed to different temperatures (50-100°C) for 10 min in a water bath or in a PCR machine and their activities were monitored immediately at room temperature in a spectrophotometer using 5 mM  $H_2O_2$  as substrate. The activity of the protein incubated at room temperature was considered to be 100% and rest was calculated accordingly.

### **2.15.5 Estimation of residual $H_2O_2$ in catalase assay performed at high temperature**

A fixed amount of catalase protein (10  $\mu$ g) was incubated for 15 min at 85 °C in 200  $\mu$ l of assay buffer (20 mM Tris, pH 8) followed by addition of  $H_2O_2$  substrate (10 mM final concentration) while maintaining the temperature of the bath at 85 °C. From the ongoing reaction mixture, samples were aliquoted at various time points and the

concentration of residual H<sub>2</sub>O<sub>2</sub> in those samples was determined by using the peroxide assay kit (MAK311, SIGMA) as per the manufacturer's instructions.

#### **2.15.6 Ability of *Anabaena* strains to decompose externally added H<sub>2</sub>O<sub>2</sub>**

The wild-type *Anabaena* or the *AnKatBF2V*<sup>+</sup> strain was treated with 1 mM H<sub>2</sub>O<sub>2</sub> and residual H<sub>2</sub>O<sub>2</sub> content was measured at various time points using FOX assay system as described by Lindahl and Cejudo [221].

### **2.16 Methods for assessing oxidative stress in *Anabaena* cultures**

#### **2.16.1 DCHFDA assay for ROS estimation**

The extent of ROS content in various *Anabaena* strains after treatment with H<sub>2</sub>O<sub>2</sub> and/or NaCl was measured using DCHFDA probe [222]. In short, 10 μM of DCHFDA dye was added to cells suspended in BG11 medium (3 μg chlorophyll/ml) followed by incubation at 25°C for 20 min in dark with shaking. Fluorescence emission ( $\lambda_{\text{ex}} = 490$  nm,  $\lambda_{\text{em}} = 520$  nm) of the control or treated cells was measured immediately in a spectrofluorimeter. Biological and experimental replicates were taken into account and average values were reported.

#### **2.16.2 MDA assay for lipid peroxidation**

For the estimation of MDA, the product of lipid peroxidation, 300 μl of cell free *Anabaena* extract (corresponding to 500 μg of total protein) was taken in 10 mM potassium phosphate buffer (pH 7.4) and allowed to react with 900 μl of TBA reagent (0.375% 2-thiobarbituric acid, 0.25 M HCl, 15% trichloroacetic acid, and 6mM Na<sub>2</sub>EDTA). The reaction mixture was incubated for 20 min at 95°C, cooled to room

temperature and centrifuged at 10,000 rpm for 5 min at 25°C. The supernatant was used to assess the MDA equivalents by measuring the fluorescence ( $\lambda_{\text{ex}} = 530 \text{ nm}$ ;  $\lambda_{\text{em}} = 590 \text{ nm}$ ). 1, 1, 3, 3-tetra methoxy propane was used as standard and the lipid peroxidation values were expressed as nmoles of MDA equivalents per mg protein.

### **2.16.3 Protein oxidation and estimation of total peroxides**

OxyBlot oxidation detection kit (Millipore, S7150) was used to assess the extent of oxidized proteins in *Anabaena* cultures after H<sub>2</sub>O<sub>2</sub> and/or NaCl treatment. Cell free extracts corresponding to 40  $\mu\text{g}$  of protein was used for the assay performed as described in the manufacturer's instruction manual.

Total peroxide content following H<sub>2</sub>O<sub>2</sub> and/or NaCl treatment was estimated by the Peroxoquant kit (Thermo Scientific, 23280) as per the protocol provided by the manufacturer. Solutions of known H<sub>2</sub>O<sub>2</sub> concentration were used to generate standard curve, which was used for determining the peroxide content in *Anabaena* cell extracts.

### **2.16.4 Measurement of maximum photosynthetic efficiency**

The photosynthetic efficiency of the *Anabaena* cultures was measured by assessing the variable photosynthetic efficiency ( $F_v$ ) and maximum photosynthetic efficiency ( $F_m$ ) in a hand held PAM fluorimeter with an attachment for liquid culture.

### **2.17 Determination of oxidative stress tolerance of *Anabaena* strains**

Different *Anabaena* strains (wild-type *Anabaena* PCC 7120, *AnKatB*<sup>+</sup> or *AnKatB*<sup>-</sup>) were grown for three days in BG11N+ medium followed by re-inoculation in fresh growth medium at a chlorophyll *a* density of 3 mg/ml in tubes (in triplicates). These

were subjected to treatment with H<sub>2</sub>O<sub>2</sub> (1 mM) or NaCl (100 mM). The tubes were kept without shaking under constant illumination. Growth of these cultures was monitored by determination the chlorophyll *a* content [211] and photography.

## **2.18 Transmission electron microscopy**

Sample preparation and capture of TEM images of *Anabaena* cells were performed as described earlier [223] with minor modifications. In short, the NaCl pre-treated wild-type or the *katB* mutant *Anabaena* cells were treated with 1 mM H<sub>2</sub>O<sub>2</sub> for 16 hours, harvested by centrifugation and washed with 0.1 N cacodylate buffer (pH 7.4) thrice. Fixation was carried out by treating the cells overnight at 4°C with 0.1 N cacodylate buffer containing 2.5% glutaraldehyde and 0.5% para-formaldehyde. Following this, a post fixation treatment was performed with 1% KMnO<sub>4</sub> for 1 hour at 4°C. The cells were then entrapped into 1% agarose blocks. The agarose blocks containing *Anabaena* cells were subjected to dehydration with graded series of ethanol (30%, 60%, 75%, 90%, and 100%). Samples were kept at each dehydration step for 15-20 minutes. Ethanol was then removed by treatment with propylene oxide and the cells were subjected to stepwise infiltration with spurr reagent on incubation with 1:3, 1:1 and 3:1 volume by volume spurr reagent: propylene oxide) for 3 hours each followed by overnight treatment with spurr resin only. Finally, the samples were embedded in the resin by incubation at 60°C for 72 hours. Sectioning of the resin embedded solidified samples was carried out with a microtome (Leica, Germany) and the sections were positioned in 200 mesh formvar-coated copper grids and visualized with the Libra 120 plus transmission electron microscope (Carl Zeiss).

## **2.19 Determination of crystal structure**

The KatB protein or the KatBF2V variant was crystallized and the X-ray crystal structures of these were solved by our collaborator, Dr. Subhash C. Bihani, Radiation Biology & Health Sciences Division, Bhabha Atomic Research Centre. Briefly, the purified proteins were sufficiently concentrated (6-8 mg/ml) and initial screens were performed by hanging drop vapour-diffusion method. The conditions where crystals formed were further optimized by sitting drop vapour-diffusion method. X-ray diffraction was performed at protein crystallography beamline at Indus-2 synchrotron, RRCAT, Indore, India. For solving the crystal structure, molecular replacement method was adopted. KatBF2V structure was determined using *Lactobacillus plantarum* Mn-catalase structure as template while, the structure of the wild-type KatB protein was solved using KatBF2V as the template.

## **2.20 Analysis interaction energies between residues**

Interaction energies between specific residues were calculated using the INTAA web server (<http://bioinfo.uochb.cas.cz/INTAA/>) [224].

## **CHAPTER 3**

### **Physiological Role of the Mn-catalase 'KatB' from *Anabaena***



### 3.1 Introduction

Cyanobacteria, the first photosynthetic organisms, appeared more than 3 billion years ago and are believed to be the progenitors of plant chloroplasts [147, 225]. Few cyanobacteria are endowed with the unique ability to fix atmospheric nitrogen, and so far, cyanobacteria remain the only group whose members can harvest solar energy for both carbon as well as nitrogen fixation [226]. The initial oxygenation of the earth's atmosphere and consequent evolution of aerobic organisms was possible due to the massive quantities of oxygen produced by cyanobacterial photosynthesis [227]. Due to their close association with molecular oxygen, it is very likely that cyanobacteria have evolved elaborate mechanisms to combat the detrimental effects caused by reactive oxygen species (ROS), which are the products of partial reduction of oxygen [148, 159]. Moreover, given their long history of evolution, cyanobacteria have also experienced all kinds of natural (like salinity, desiccation, high light intensity etc.) and anthropogenic stresses (like herbicides, heavy metals etc). Almost all these stresses lead to generation of ROS, resulting oxidative stress [158]. Due to these reasons, cyanobacteria serve as excellent model systems to study the cellular defence mechanisms against oxidative stress.

Hydrogen peroxide ( $H_2O_2$ ) is an important ROS whose presence above a threshold limit is detrimental for cellular components. There are several ways by which  $H_2O_2$  is produced intra-cellularly. Primarily, it is generated by dismutation of  $O_2^-$  by superoxide dismutases or by oxidase enzymes that directly utilize molecular oxygen [22]. Being a small molecule,  $H_2O_2$  easily permeates into cells directly, causing toxicity. Although  $H_2O_2$  can cause direct damage to enzymes like dehydratases, which contain iron-sulphur clusters [45],  $H_2O_2$  by itself it is not very detrimental. However, in the presence

of  $\text{Fe}^{2+}$ , it undergoes Fenton reaction to generate hydroxyl radical ( $\text{OH}\cdot$ ) that can destroy any molecule in its vicinity at diffusion-limited rates [29]. Therefore, to protect themselves, all live forms have evolved efficient  $\text{H}_2\text{O}_2$  detoxification systems. Peroxidases and catalases are the principal group of enzymes that detoxify  $\text{H}_2\text{O}_2$  in living beings. In cyanobacteria, catalases and peroxidases (particularly the peroxiredoxin proteins) are well represented [106].

The genome of the cyanobacterium *Anabaena* PCC 7120, lacks the presence of any gene representing typical catalases or KatGs, instead, there exist two ORFs *all0998* (*katA*) and *alr3090* (*katB*), which encode Mn-catalase each [193]. However, on zymographic analyses, no detectable catalase activity was observed under control (i.e. unstressed) or under  $\text{H}_2\text{O}_2$  stress in *Anabaena* PCC 7120. But overexpression of KatA could protect *Anabaena* from  $\text{H}_2\text{O}_2$ -mediated oxidative stress [200]. On the other hand, other studies showed KatB/*katB* protein to be induced by stresses such as salinity, iron limitation, metal stress and desiccation. As it was likely that KatB, but not KatA, played important physiological role under those conditions, it was desired to characterize the *katB* gene from *Anabaena* PCC 7120 and evaluate its role in resistance to environmental stresses.

### **3.2 Effect of NaCl pre-treatment on $\text{H}_2\text{O}_2$ tolerance**

As NaCl is known to induce the catalase KatB in *Anabaena*, it was desired to verify if pre-treatment of *Anabaena* with common salt would protect it from subsequent challenge with  $\text{H}_2\text{O}_2$ .

#### **3.2.1 Survival of NaCl pre-treated *Anabaena* cultures after exposure to $\text{H}_2\text{O}_2$**

To test the above-mentioned hypothesis, the wild-type *Anabaena* culture was split into two parts. One part was subjected to NaCl pre-treatment for 16 hours while the other

part was left without any treatment to serve as control. Subsequently, the cultures were exposed to different concentrations of H<sub>2</sub>O<sub>2</sub> (0, 1, 2 and 3 mM) and monitored (Fig. 3.2.1). The control cells (without NaCl pre-treatment) showed enhanced bleaching of pigments when exposed to higher concentration of H<sub>2</sub>O<sub>2</sub> (2 or 3 mM).

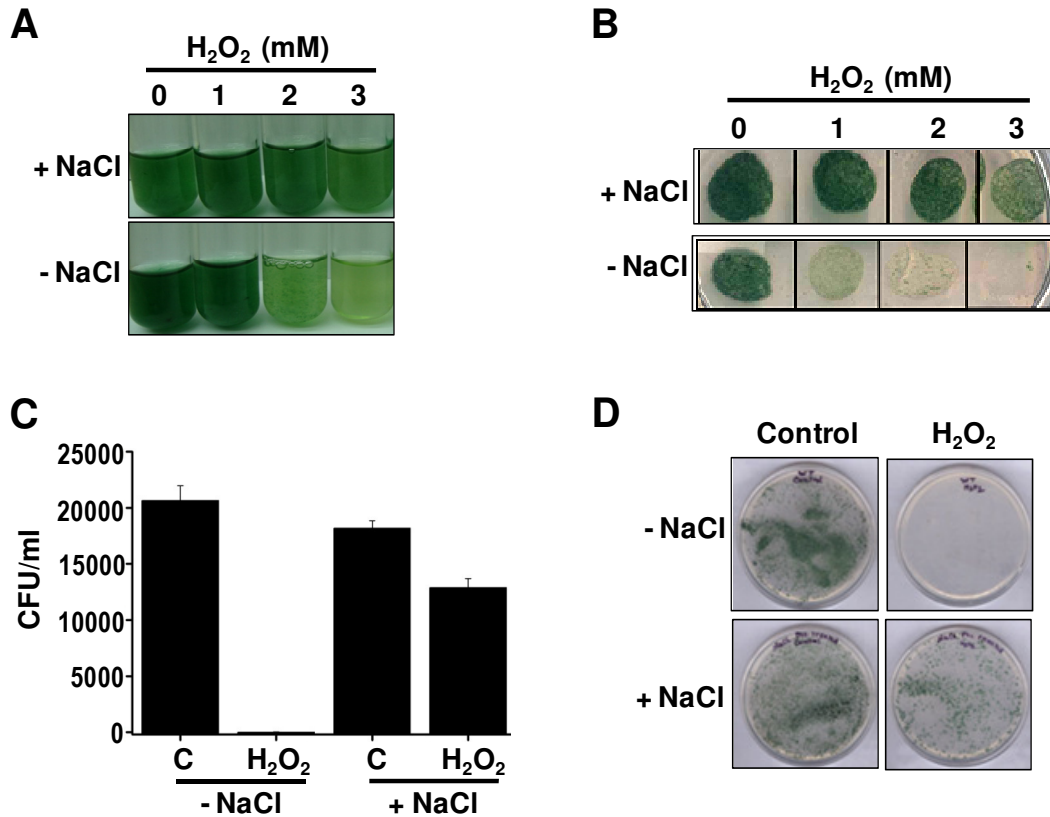


**Fig. 3.2.1 NaCl induced H<sub>2</sub>O<sub>2</sub> stress tolerance in *Anabaena* PCC 7120.** (A) Three-day-old *Anabaena* culture was re-inoculated in fresh BG11N+ medium and divided into two parts. One part was subjected to pre-treatment with 100 mM NaCl (+NaCl) for 16 hours, while the other part served as the control (-NaCl). Both the cultures were then exposed to different concentrations of H<sub>2</sub>O<sub>2</sub> as indicated in the figure and photographed after 2 days. (B) 20  $\mu$ l of the above-mentioned cultures after 2 days of H<sub>2</sub>O<sub>2</sub> treatment were spotted on BG11N+ agar plate, kept under continuous illumination for 14 days and photographed. (C) 3 day old NaCl pre-treated (+NaCl) or control wild-type *Anabaena* (-NaCl) culture was subjected to 1 mM H<sub>2</sub>O<sub>2</sub> treatment for 2 days and 150  $\mu$ l of the culture was spread on BG11N+ agar plate. Number of foci was counted manually after 14 days of incubation under constant illumination and number of CFUs was represented as bar diagram. Error bars represent SE. (D) Photograph of the above-mentioned plates at the time of colony counting (14 days of incubation).

On the other hand, considerably less bleaching, even with higher concentration of H<sub>2</sub>O<sub>2</sub>, was observed in the NaCl pre-treated cells (Fig. 3.2.1 A). There was significant loss of viability of in the H<sub>2</sub>O<sub>2</sub>-exposed control cells as they showed considerably reduced growth on BG11N+ plates. On the contrary, the salt-treated cultures could grow on BG11N+ plates (Fig. 3.2.1 B). After exposure to H<sub>2</sub>O<sub>2</sub>, the NaCl pre-treated culture showed a high number of colony forming units (CFUs), thus confirming the observation that pre-treatment with NaCl protected *Anabaena* from H<sub>2</sub>O<sub>2</sub>-mediated damage (Fig. 3.2.1 B and C).

### **3.2.2 Molecular damage in NaCl pre-treated *Anabaena* after exposure to H<sub>2</sub>O<sub>2</sub>**

The level of cellular oxidative stress in the above-mentioned cells was monitored by probing the cultures with dichloro dihydro fluorescein diacetate (DCHFDA) dye. In the NaCl pre-treated cultures, significantly decreased ROS were observed at all concentrations of H<sub>2</sub>O<sub>2</sub> (1, 2 or 3 mM) tested, which was in contrast to the ROS levels observed in control cells exposed to H<sub>2</sub>O<sub>2</sub> (Fig. 3.2.2 A). In line with this observation, considerably higher amount of total peroxides were detected in the control cells (i.e. not pre-treated with NaCl) compared to cells pre-treated with NaCl (Fig. 3.2.2 B). As increased lipid peroxidation and amount of oxidized proteins are often considered to be markers for oxidative stress, these parameters were also assessed. The control *Anabaena* cells showed significantly higher amount of malondialdehyde (MDA, an end product of lipid peroxidation) after exposure to H<sub>2</sub>O<sub>2</sub> when compared to the NaCl pre-treated cells (Fig. 3.2.2 C). Considerably higher amount of oxidized proteins were detected in the control cells after 24 h of H<sub>2</sub>O<sub>2</sub> exposure whereas, less oxidative damage of the cellular proteins was observed in NaCl pre-treated cells (Fig. 3.2.2 D).

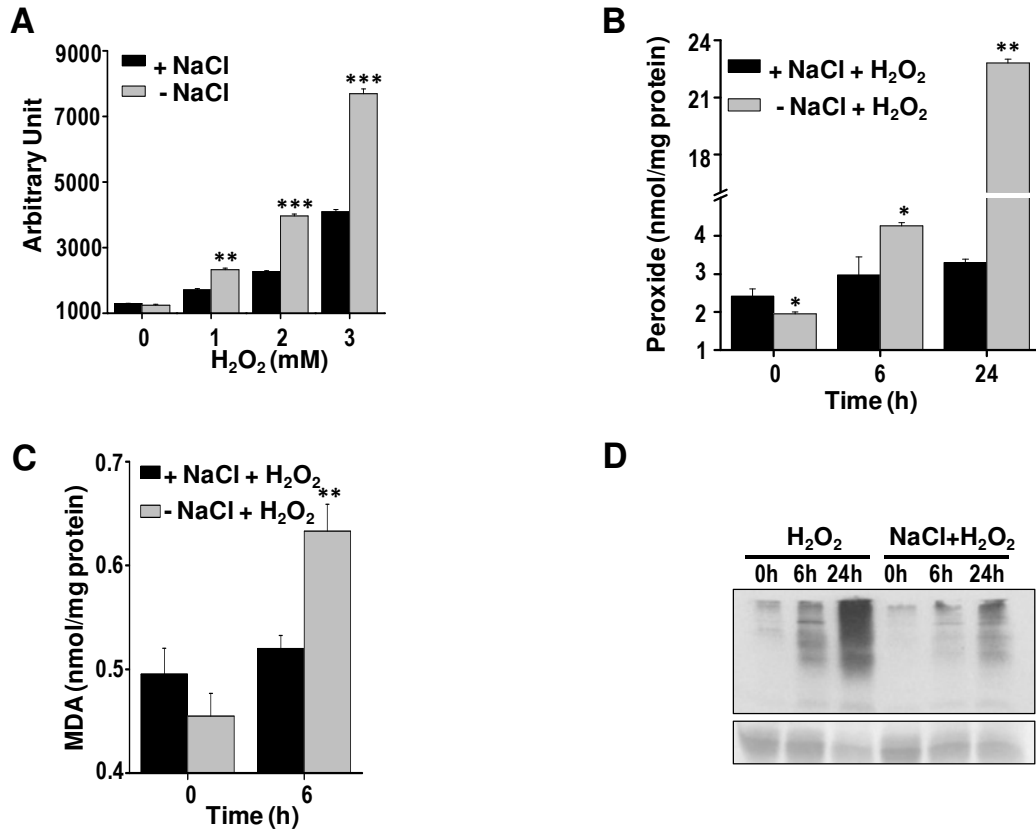


**Fig. 3.2.2 Molecular changes associated with H<sub>2</sub>O<sub>2</sub> treatment in control or NaCl pre-treated *Anabaena* cells.** (A) Production of ROS after exposure to H<sub>2</sub>O<sub>2</sub>. The control (-NaCl) or NaCl-treated (+NaCl) *Anabaena* cultures were subjected to H<sub>2</sub>O<sub>2</sub> treatment for 16 hours followed by incubation with 10 μM DCHFDA for 20 minutes in dark. Fluorescence emission ( $\lambda_{\text{ex}}=490$  nm,  $\lambda_{\text{em}}=520$  nm) from cells was measured immediately on a spectrofluorimeter. The relative fluorescence in arbitrary units (AUs) of both types of cultures is shown in the figure. Error bars show SE (n = 5). \*\* indicates significant differences at P<0.01 compared with the corresponding control (-NaCl) cells (Student's t test). (B) Total peroxide content in cells pre-treated with NaCl (+NaCl) or control (-NaCl) cells after exposure to 1 mM H<sub>2</sub>O<sub>2</sub> at time points as indicated in the figure. Error bars represent SE (n = 3). Asterisks indicate significant differences (\*P<0.05 and \*\*P<0.01) compared with the corresponding control (-NaCl) cells. (C) The MDA produced in the control or the NaCl pre-treated cells after exposure to H<sub>2</sub>O<sub>2</sub>. Error bars represent SE (n = 3). \*\* indicates significant differences at P<0.01 compared with the corresponding control (-NaCl) cells (Student's t test). (D) Detection of protein oxidation. Protein extracts were prepared from H<sub>2</sub>O<sub>2</sub> exposed control (H<sub>2</sub>O<sub>2</sub>) or NaCl pre-treated (NaCl+H<sub>2</sub>O<sub>2</sub>) *Anabaena* cultures at time point indicated, derivatized with dinitrophenol (DNP), resolved on SDS-PAGE and transferred onto nitrocellulose membrane. The blot was then probed with the monoclonal DNP antiserum and chemiluminescent detection was performed. A part of the Ponceau S-stained blot is shown as loading control. The experiment was repeated thrice with consistent results.

To summarize, severe oxidative stress was experienced by the control *Anabaena* cells on treatment with H<sub>2</sub>O<sub>2</sub>, which resulted in cell death. On the other hand, NaCl pre-treated cells were remarkably protected from the detrimental effects of H<sub>2</sub>O<sub>2</sub> exposure.

### 3.3 Expression of catalase in NaCl pre-treated *Anabaena* PCC 7120 culture

As the salt pre-treated *Anabaena* PCC 7120 showed considerable tolerance to oxidative stress mediated by H<sub>2</sub>O<sub>2</sub>, expression of the common H<sub>2</sub>O<sub>2</sub>-detoxifying enzyme i.e. catalase was monitored (Fig. 3.3). On staining for catalase activity on zymograms, the salt-stressed *Anabaena* showed a distinct zone of clearance, indicating the presence of active catalase enzyme. On the other hand, the control cells (i.e. without NaCl pre-treatment) did not show any zone of clearance, suggesting lack of catalase expression (Fig. 3.3 A, upper panel). To identify whether the expressed catalase was KatA or KatB, the native gel was subjected to Western blotting analysis with KatA or KatB antiserum. The zone of clearance in NaCl pre-treated culture perfectly matched the signal from the KatB (but not KatA) antiserum (Fig. 3.3 A, lower panel), demonstrating that KatB was the catalase induced in response to salt stress in *Anabaena*.

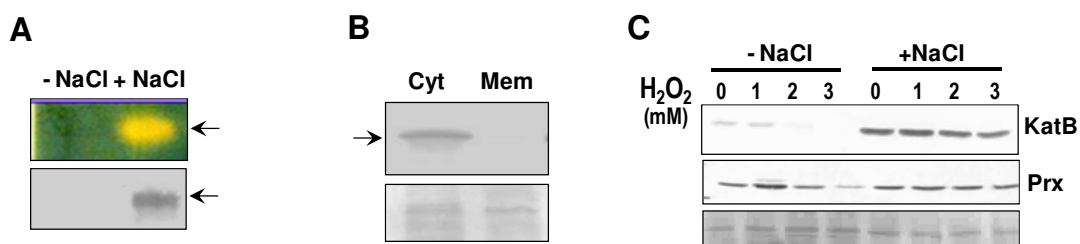


**Fig. 3.3 Expression of catalase and Prx in NaCl and/or H<sub>2</sub>O<sub>2</sub> stressed *Anabaena*.** (A) The cell free extracts control (-NaCl) or 100 mM NaCl-treated (+NaCl) *Anabaena* cultures were subjected in-gel catalase activity assay (zymography, top) or Western blot hybridization with KatB antisera (bottom). (B) Localization of KatB protein. The cell lysate of the NaCl pre-treated *Anabaena* cells were centrifuged to separate the membrane fraction (Mem) and the cytosolic content (Cyt). These fractions were resolved on SDS-PAGE and subjected to western blot hybridization with KatB antiserum. A Ponceau S-stained part of the blot is shown as loading control at the bottom. (C) The cell-free extracts of control (-NaCl) or salt pre-treated (+NaCl) *Anabaena* stressed with various concentrations of H<sub>2</sub>O<sub>2</sub> were resolved on 14% SDS-PAGE, transferred onto nitrocellulose membrane and probed with the KatB antiserum (KatB, top) or the

Alr4641 (2-Cys-Prx) antiserum (Prx, middle). Part of the Ponceau S-stained nitrocellulose membrane is shown as loading control at the bottom.

Further, it was found that the KatB protein was cytosolic in nature as it was detected only in the soluble fraction of *Anabaena* whole cell extracts i.e. absent in the membrane fractions (Fig. 3.3 B). Interestingly, in the control *Anabaena* cells treated with H<sub>2</sub>O<sub>2</sub>, KatB could hardly be detected, whereas, the KatB level was virtually unchanged in the NaCl pre-treated cells even in presence of H<sub>2</sub>O<sub>2</sub> (Fig. 3.3 C, upper panel). Alr4641, a 2-Cys-Peroxiredoxin (2-Cys-Prx) in *Anabaena*, is known to be induced under H<sub>2</sub>O<sub>2</sub> stress [95]. Expression of this protein was monitored in salt pre-treated *Anabaena* subjected to H<sub>2</sub>O<sub>2</sub> stress. In control *Anabaena* cells, a distinct increase in the oxidative stress-inducible 2-Cys-Prx protein was detected after treatment with 1 mM H<sub>2</sub>O<sub>2</sub>. However, no such induction was observed in the NaCl pre-treated cells even on treatment with 3 mM H<sub>2</sub>O<sub>2</sub> (Fig. 3.3 C, middle panel).

#### **3.4 Over-expression of KatB through genetic manipulation in *Anabaena* and its effect on H<sub>2</sub>O<sub>2</sub> tolerance**

Earlier experiments showed that NaCl pre-treatment protected *Anabaena* from H<sub>2</sub>O<sub>2</sub> stress and also resulted in accumulation of the Mn-catalase, KatB. Further, to shed light on the contribution of KatB in combating the oxidative stress mediated by H<sub>2</sub>O<sub>2</sub>, it was desired to over-express KatB in *Anabaena* using an *E. coli*-*Anabaena* PCC 7120 shuttle vector, pAM1956 [212]. For cloning the *katB* ORF into this vector, the *katB* DNA fragment (693 bp) was PCR-amplified from *Anabaena* PCC 7120 genomic DNA and cloned downstream of strong light inducible P<sub>*psbA1*</sub> promoter, in pFPN vector [195]. Subsequently, the *katB* gene along with the P<sub>*psbA1*</sub> promoter was excised out and

subcloned into *E. coli/Anabaena* shuttle vector pAM1956 vector to generate pAMKatB plasmid. The details of pAMKatB are pictorially depicted in Fig. 3.4 A.

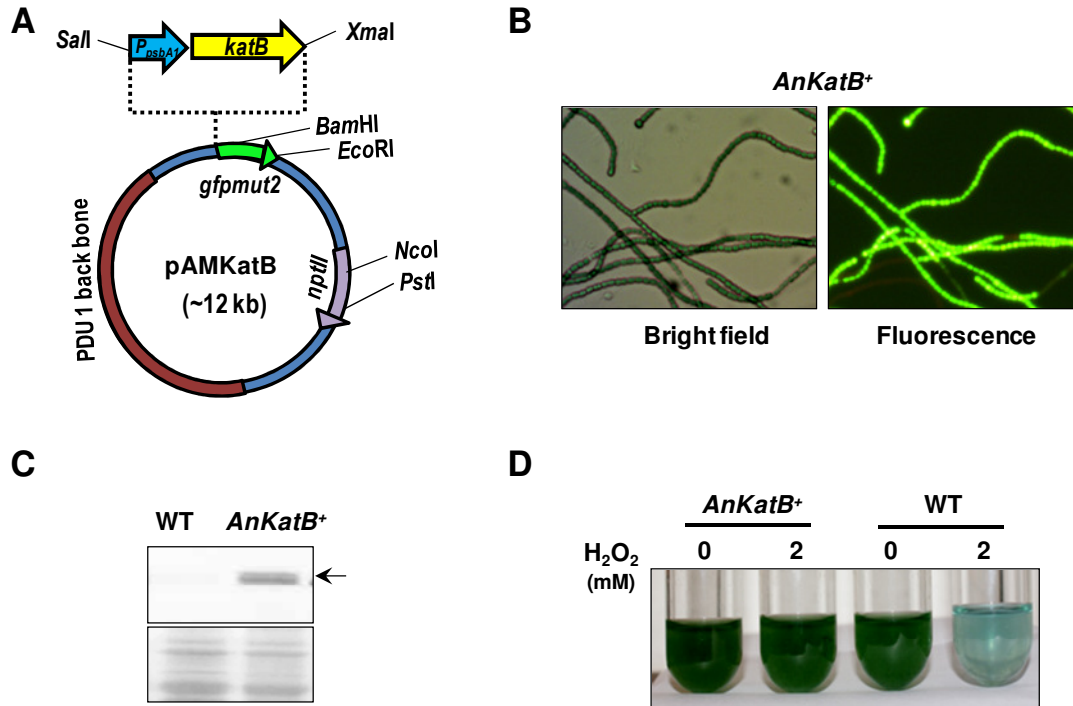


**Fig. 3.4 KatB over-expression in *Anabaena*.** (A) Schematic vector map of pAMKatB plasmid. The *katB* ORF along with *psbA1* promoter is cloned into pAM1956 vector using *XmaI* and *SaI* restriction endonucleases. (B) Bright field and fluorescence micrograph of *KatB* over-expressing *Anabaena* strain (*AnKatB*<sup>+</sup>). (C) Expression of *KatB* protein in *AnKatB*<sup>+</sup> cultures. The cell-free extracts of the wild-type *Anabaena* PCC 7120 (WT) or the *KatB* over-expressing strain (*AnKatB*<sup>+</sup>) were resolved by SDS-PAGE, transferred onto nitrocellulose membrane and probed with anti-KatB antiserum. A part of the Ponceau S-stained blot is shown at the bottom as loading control. (D) The *KatB* over-expressing *Anabaena* strain (*AnKatB*<sup>+</sup>) or the wild-type *Anabaena* (WT) were exposed to 2 mM H<sub>2</sub>O<sub>2</sub> for 2 days and photographed.

The pAMKatB plasmid was conjugally transferred into *Anabaena* PCC 7120 using a conjugal *E. coli* donor [HB101 (pRL623 + pRL443)] [194, 213] as described earlier [194]. Exconjugants were selected on BG11N+ plates containing neomycin and repeatedly sub-cultured. The transformed *Anabaena* strain thus obtained (designated *AnKatB*<sup>+</sup>) was maintained on BG11N+ plates under neomycin selection pressure.

In *AnKatB*<sup>+</sup> strain (*Anabaena* strain carrying pAMKatB), both *katB* and *gfp* (driven by the *P<sub>PsbAI</sub>* promoter) are co-transcribed but translated separately, resulting in co-production of both the proteins. The *AnKatB*<sup>+</sup> cells were monitored for expression of GFP under a fluorescence microscope (Fig. 3.4 B), wherein bright green fluorescence of GFP was observed. The *AnKatB*<sup>+</sup> cells were probed with the KatB antiserum (1:15000) to confirm the over-production of KatB protein. Considerable amount of KatB protein could be detected in the recombinant *AnKatB*<sup>+</sup> strain (Fig. 3.4 C). When the KatB over-expressing strain was subjected to treatment with 2 mM H<sub>2</sub>O<sub>2</sub>, significant protection was observed as compared to the wild-type *Anabaena*, which was markedly bleached after two days of H<sub>2</sub>O<sub>2</sub> treatment (Fig. 3.4 D). This result clearly demonstrated the ability of KatB to protect *Anabaena* from oxidative effects of H<sub>2</sub>O<sub>2</sub>.

### **3.5 Generation of KatB deficient *Anabaena* strain by insertional gene inactivation strategy**

To evaluate its *in vivo* contribution, insertional inactivation of the *katB* gene in *Anabaena* was carried out.

#### **3.5.1 Cloning of 300 bp fragment internal to *katB* gene into *Anabaena* suicide vector, pRL271**

For generating the *katB* mutant of *Anabaena*, a strategy described by Neunuebel and Golden in 2008 [214] was employed. A 300 bp DNA fragment from *katB* ORF was PCR amplified from genomic DNA using suitable primers (Table 2.2). Kanamycin expression cassette was PCR amplified from pAM1956 vector by primers 3090\_Kan\_Olap\_Fwd and pAM1956Kan\_Rev (containing *XhoI* site).

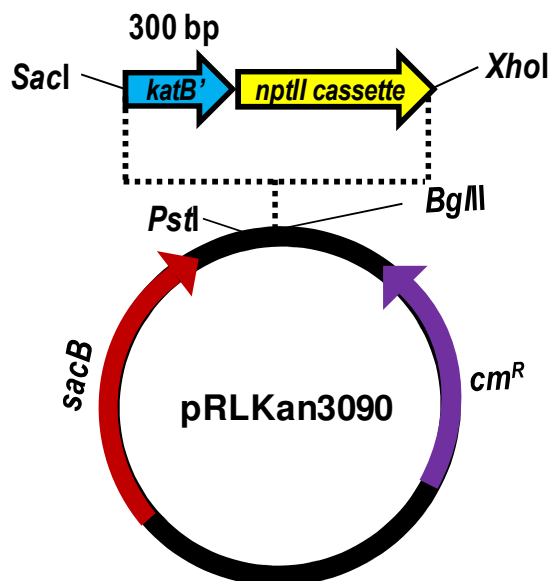


**Fig. 3.5.1 Schematic diagram of the pRLkatBKan.** A 300 bp DNA fragment internal to *katB* gene was fused to kanamycin expression cassette and subsequently ligated to pRL271 vector employing *SacI* and *XhoI* restriction sites.

These two fragments were combined by overlap extension PCR using 3090\_*SacI*\_Fwd and pAM1956Kan\_Rev primers (Table 2.2). The resultant DNA (300 bp *katB* fragment + Kanamycin expression cassette) was cloned into suicide vector pRL271 by employing *XhoI* and *SacI* restriction endonucleases (construct named as pRLKan3090). The schematic diagram of the pRLkatBKan is depicted in Fig. 3.5.1.

### 3.5.2 Generation and confirmation of *Anabaena katB* mutant

pRLkatBKan was conjugally transferred to *Anabaena* PCC 7120 and the exconjugants (*AnKatB<sup>-</sup>*) that came up were selected by repeatedly subculturing on BG11N+ plates containing neomycin. The mutant nature of the *AnKatB<sup>-</sup>* strain was confirmed by performing PCR with isolated genomic DNA. The primers used for the PCR reactions were chosen from various genetic elements as per Fig. 3.5.2 A. When the PCR was performed (with KatB\_*SacI*\_Fwd and KatB\_*Bam*\_Rev primers, Table 2.2) for a 500 bp

product specific to *katB* gene, no amplification was detected in *AnKatB*<sup>-</sup> strain (Fig. 3.5.2 B)

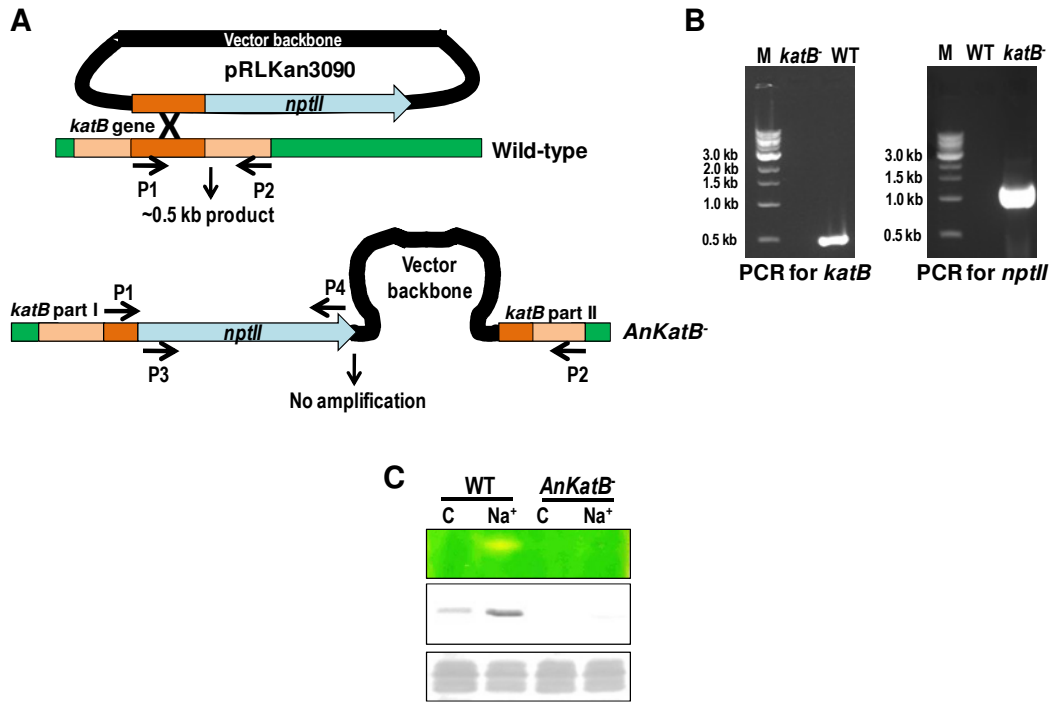


**Fig. 3.5.2 Generation of *Anabaena katB* mutant.** (A) Schematic diagram of single cross-over based insertional inactivation of *katB* gene. Position of cross over within *katB* gene in *Anabaena* genome is depicted by 'X' (upper panel). Genomic organization of the *AnKatB*<sup>-</sup> strain where the *katB* gene is disrupted by the vector backbone and the neomycin expression cassette (shown in black color, bottom panel). Various primers used for confirmation of the mutant nature are P1:KatB\_SacI\_Fwd; P2: KatB\_Bam\_Rev; P3: *nptII*\_Fwd and P4: *nptII*\_Rev. (B) PCR for presence of intact *katB* gene fragment in the *katB* mutant (*katB*<sup>-</sup>) or in the wild-type *Anabaena* (WT). Primer pair P1 and P2 was used for this amplification (left panel). PCR for presence of *nptII* gene in *katB* mutant (*katB*<sup>-</sup>) or in the wild-type *Anabaena* (WT). Primer pair P3 and P4 was used for this amplification (right panel). (C) Expression of KatB in the wild-type *Anabaena* (WT) cells or the *katB* mutant (*AnKatB*<sup>-</sup>) was monitored on zymogram (top) and on western blots probing with the KatB antiserum (middle). A Ponceau S-stained part of the blot is shown as loading control (bottom). C, Control cells; Na<sup>+</sup>, cells treated with 100 mM NaCl for 16 hours.

However, the wild-type *Anabaena* showed a 500 bp product after PCR (Fig. 3.5.2 B, left panel). Unlike the wild-type *Anabaena*, the *AnKatB*<sup>-</sup> showed the presence of

kanamycin cassette when PCR was performed with kanamycin specific primers (*nptII\_Fwd* and *nptII\_Rev*, Table 2.2) (Fig. 3.5.2 B, right panel). The presence of *nptII* cassette and the absence of the *katB*-specific fragment demonstrated the mutant nature of the *AnKatB*<sup>-</sup>. Zymographic and Western blot analysis using KatB specific antiserum were performed to further validate the absence of KatB protein in the mutant strain. Catalase activity was detected only in the NaCl-treated wild-type *Anabaena* but not in the *AnKatB*<sup>-</sup> strain even after treatment with NaCl (Fig. 3.5.2 C, upper panel). Western-blotting analysis also showed the presence of KatB protein only in the wild-type *Anabaena* PCC 7120 cells but not in the mutant (*AnKatB*<sup>-</sup>) strain (Fig. 3.5.2 C middle panel). All this results clearly showed that the *Anabaena katB* mutant failed to express the KatB protein.

### **3.6 Sensitivity of the KatB deficient *Anabaena* strain to salt stress**

#### **3.6.1 Growth of the wild-type or the *AnKatB*<sup>-</sup> *Anabaena* strain in the presence of NaCl**

In the presence of NaCl (100 mM), the wild-type *Anabaena* showed a small reduction in growth as compared to control cells, but no growth was observed in *AnKatB*<sup>-</sup> cells (**Fig. 3.6.1 A**). In contrast to the wild-type *Anabaena* PCC 7120, the *AnKatB*<sup>-</sup> strain was severely bleached after prolonged exposure to NaCl (**Fig. 3.6.1 B**). The level of oxidative stress imposed upon treatment with NaCl was assessed with DCHFDA. Within three hours of NaCl treatment, a sharp rise in the ROS levels was observed in the *katB* mutant (**Fig. 3.6.1 C**). After 48 hours of NaCl treatment, increase in ROS was observed in the wild-type cells too, however, these levels were many fold lower than those seen in the *katB* mutant at that corresponding time point.

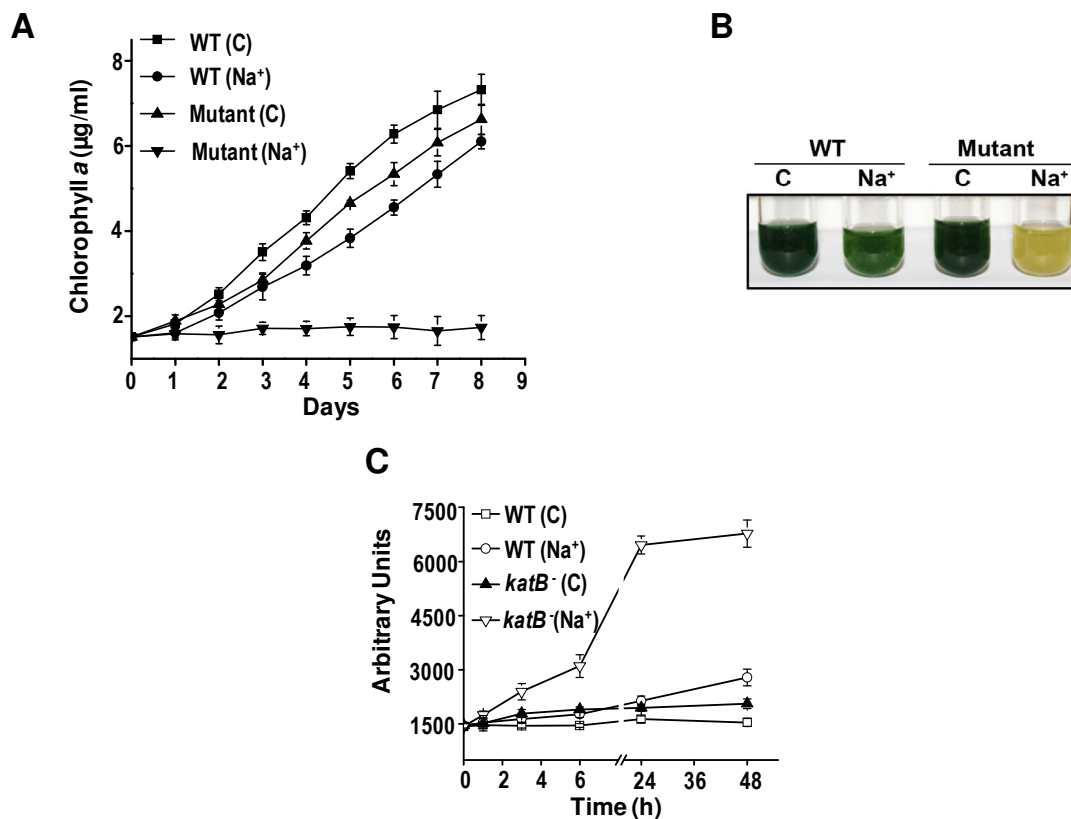


**Fig. 3.6.1 Sensitivity of the *AnKatB*<sup>-</sup> strain to NaCl stress.** (A) Growth of the wild-type *Anabaena* (WT) or the *katB* mutant (Mutant) in response to NaCl stress. 3 day old *Anabaena* cultures were reinoculated in fresh BG11N+ liquid medium in presence of 100 mM NaCl (Na<sup>+</sup>) or under control condition (C) at a chlorophyll *a* density of 1 µg/ml of culture. The chlorophyll *a* content of these cultures was monitored each day for 8 days and plotted. Error bars represent the SE. (B) The wild-type (WT) or the *AnKatB*<sup>-</sup> cells were grown in presence of 100 mM NaCl (Na<sup>+</sup>) or under control conditions (C) for 15 days and photographed. (C) Production of ROS in response to NaCl. The above-mentioned cultures were treated with 100 mM NaCl and the total ROS content was measured with the DCHFDA probe at time points indicated in the figure. The fluorescence values are depicted in arbitrary units (AUs). Error bars represent SE (n = 4).

### 3.6.2 Molecular changes associated with NaCl treatment in wild-type *Anabaena* or the *AnKatB*<sup>-</sup> strain

The level of peroxides, which serves as a marker for oxidative damage, in response to NaCl treatment in the wild-type or the *AnKatB*<sup>-</sup> strain was compared (Fig. 3.6.2).

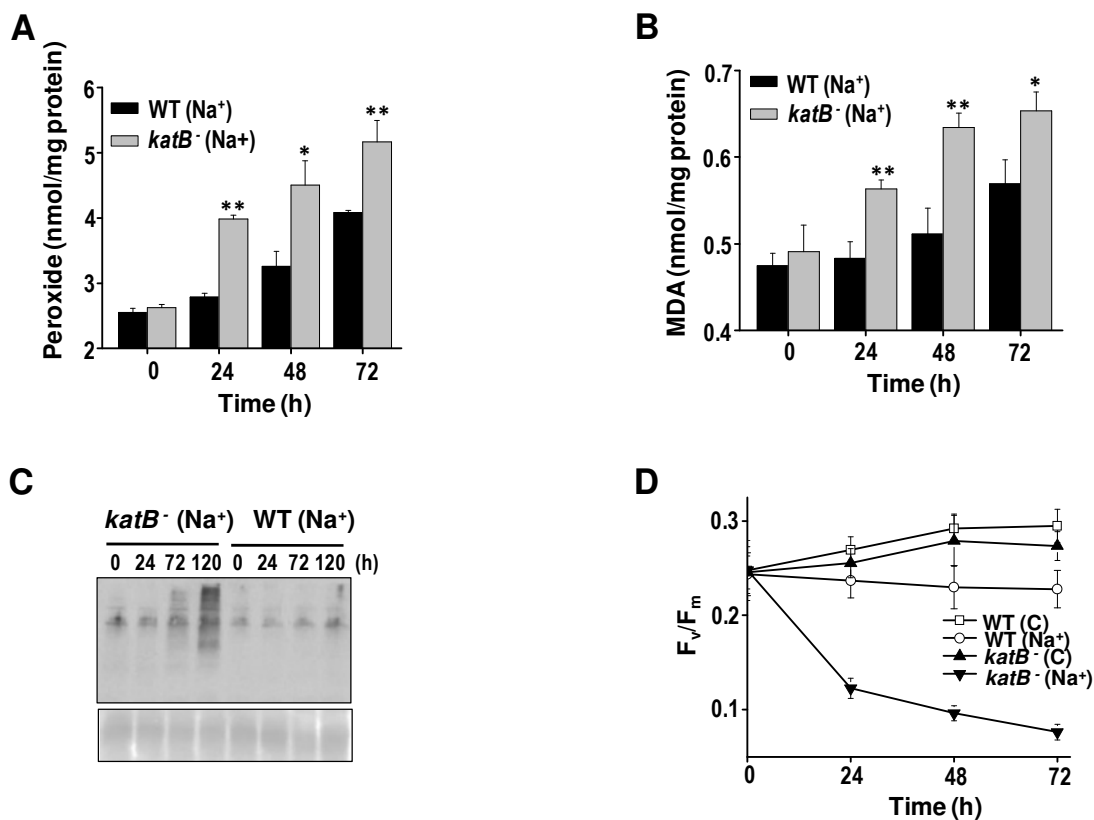


**Fig. 3.6.2 Molecular changes associated with NaCl treatment in *katB* mutant.** (A) Content of total peroxides in the wild-type *Anabaena* (WT) or *katB* mutant (*katB*<sup>-</sup>) cells after treatment with 100 mM NaCl (Na<sup>+</sup>). Error bars represent SE (n = 3). Asterisks indicate significant differences (\*P<0.05 and \*\*P<0.01) compared with the corresponding wild-type cells. (B) Extent of lipid peroxidation in terms of MDA equivalent in the wild type (WT) or the *katB* mutant (*katB*<sup>-</sup>) after treatment with 100 mM NaCl. Error bars represent SE (n = 3) and asterisks indicate significant differences (\*P<0.05 and \*\*P<0.01) compared to the corresponding wild-type cells. (C) Detection of oxidized proteins. Cell free extracts were prepared from the above-mentioned two different cell types at the time points indicated. The proteins were derivatized with DNP, resolved on SDS-PAGE, transferred to nitrocellulose membrane and probed with the monoclonal DNP antiserum followed by chemiluminescence detection. (D) F<sub>v</sub>/F<sub>m</sub> of the wild-type (WT) or the *katB* mutant (*katB*<sup>-</sup>) at various time points after treatment with 100 mM NaCl (Na<sup>+</sup>). C, Control. Error bars show the SE (n = 4).

After treatment with NaCl, higher levels of peroxide were observed in *AnKatB*<sup>-</sup> than the corresponding wild-type cells at all the time points tested (Fig. 3.6.2 A). Similarly, the *katB* mutant showed higher level of malonaldehyde equivalent, indicating increased lipid peroxidation than the wild-type *Anabaena* (Fig. 3.6.2 B). The mutant also showed more amount of oxidized proteins than the wild-type (Fig. 3.6.2 C). After treatment

with NaCl, the *katB* mutant showed a severe reduction in the quantum yield of PSII, i.e.  $F_v/F_m$  values compared to the wild-type *Anabaena*, wherein only a minor reduction of the same was recorded (Fig. 3.6.2 D).

### **3.7 NaCl induced cross-protection to externally added H<sub>2</sub>O<sub>2</sub> in *AnKatB***

The *katB* mutant was subjected to NaCl pre-treatment followed by exposure to H<sub>2</sub>O<sub>2</sub> to conclusively prove the involvement of the *katB* gene in NaCl-induced cross-protection phenomenon (Fig. 3.7). After exposure to H<sub>2</sub>O<sub>2</sub>, more than 8-fold excess of total peroxides and ROS were observed in the NaCl pre-treated *katB* mutant as compared to the NaCl pre-treated wild-type *Anabaena* cells (Fig. 3.7A and Fig. 3.7 B). Similarly, the *katB* mutant also showed considerably higher levels of lipid peroxidation than the wild-type *Anabaena* under the conditions specified above (Fig. 3.7 C). H<sub>2</sub>O<sub>2</sub> has been shown to damage cellular RNA pool in *Anabaena* when the culture lacks sufficient catalase activity [200]. In the NaCl pre-treated *katB* mutant, complete degradation of the cellular RNA was observed after 24 hours of H<sub>2</sub>O<sub>2</sub> exposure. Whereas, in contrast, the NaCl pre-treated wild-type *Anabaena* showed remarkable protection of RNA even after 24 hours of exposure to H<sub>2</sub>O<sub>2</sub> (Fig. 3.7 D). Similarly, severe reduction in  $F_v/F_m$  was noted in the *katB* mutant upon exposure to H<sub>2</sub>O<sub>2</sub> (Fig. 3.7 E).

Unlike the wild-type *Anabaena* culture (Fig. 3.2.1 A) the NaCl pre-treated *katB* mutant was severely bleached within a day of H<sub>2</sub>O<sub>2</sub> exposure (Fig. 3.7 F). All the results presented in this section confirm the vital role played by the *katB* gene in combating the detrimental effects of H<sub>2</sub>O<sub>2</sub> in the salt pre-treated *Anabaena* culture.

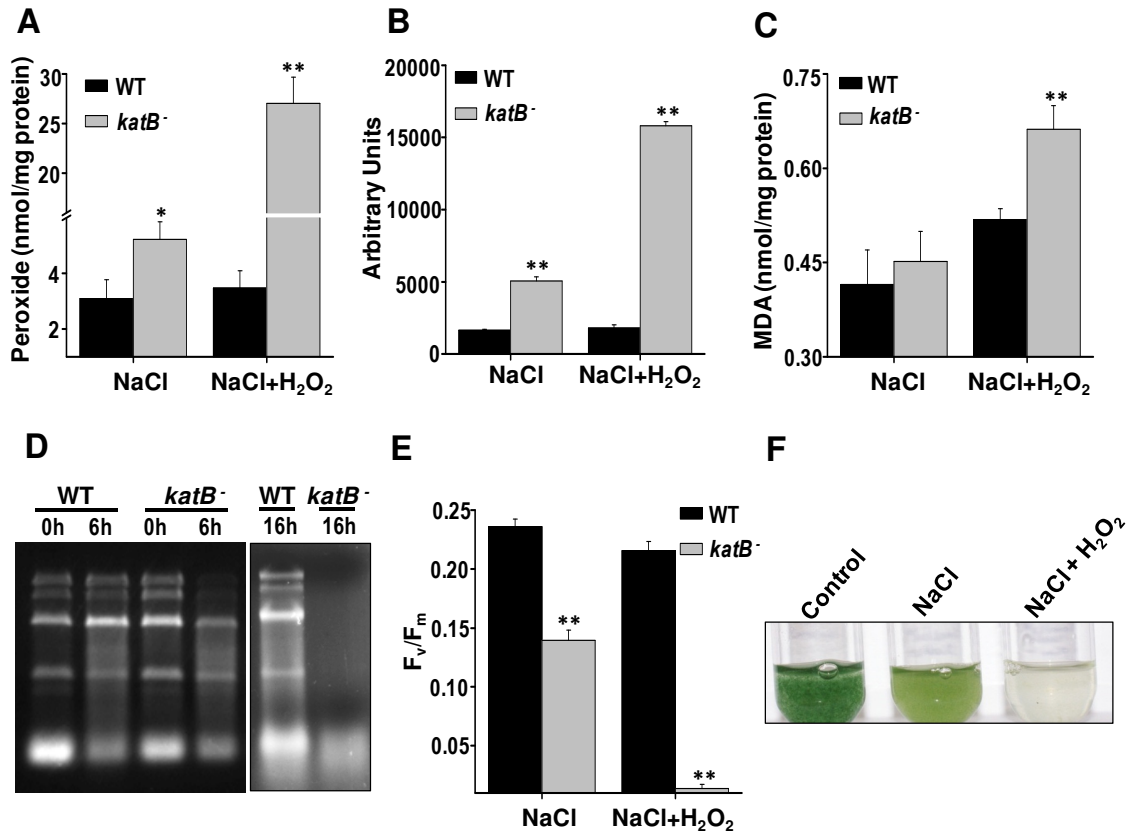


**Fig. 3.7 Exposure of the NaCl pre-treated *katB* mutant *Anabaena* to H<sub>2</sub>O<sub>2</sub>.** The wild-type *Anabaena* (WT) or the *katB* mutant (*katB*<sup>-</sup>) was subjected to pre-treatment with 100 mM NaCl (NaCl) for 16 hours followed by exposure to 1mM H<sub>2</sub>O<sub>2</sub> (NaCl+H<sub>2</sub>O<sub>2</sub>). **(A)** Production of total ROS after 6 hours of H<sub>2</sub>O<sub>2</sub> treatment was measured with DCHFDA probe. Error bars represent SE (n = 3) and \*\* indicates significant differences at P<0.01 compared to the corresponding wild type. **(B)** Production of total peroxides after 16 hours of H<sub>2</sub>O<sub>2</sub> exposure. Error bars represent SE (n = 3) while the asterisks indicate significant differences (\*P<0.05 and \*\*P<0.01) compared with the corresponding wild type. **(C)** Lipid peroxidation. The MDA equivalent produced in the above-mentioned cell types is depicted as bar diagram. Error bars show SE (n = 3). \*\* indicates significant differences at P<0.01 compared with the corresponding wild type. **(D)** RNA damage in response to NaCl stress. Total RNA (5 μg), isolated from the NaCl pre-treated cells that were exposed to H<sub>2</sub>O<sub>2</sub> for duration as indicated, was resolved on formaldehyde-agarose gels and photographed under UV illumination. The experiment was repeated at least three times and a representative image is shown. **(E)** F<sub>v</sub>/F<sub>m</sub> of the NaCl pre-treated wild-type (WT) or the *katB* mutant (*katB*<sup>-</sup>) after 16 hours of exposure to 1 mM H<sub>2</sub>O<sub>2</sub>. Error bars represent SE (n = 5) and \*\* indicates significant differences at P<0.01 compared with the respective wild type. **(F)** The NaCl pre-treated *katB* mutant *Anabaena* strain was exposed to 1 mM H<sub>2</sub>O<sub>2</sub> for 2 days and photographed.

### 3.8 Ultra-structural changes associated with H<sub>2</sub>O<sub>2</sub> stress in salt pre-treated *katB* mutant

Transmission Electron Microscope (TEM) analyses were carried out to visualize the ultra-structural changes in response to H<sub>2</sub>O<sub>2</sub> stress in the NaCl pre-treated *katB* mutant (Fig. 3.8). The *katB* mutant showed loss of typical thylakoid ultrastructure and loss of cellular content, indicating cell lysis was observed in some cases. In contrast, the wild-type cells were found to be intact with proper thylakoid membrane integrity even after treatment with H<sub>2</sub>O<sub>2</sub>. The wild-type cells also showed the presence of carboxysomes whereas absence of these structural features was noted in the *katB* mutant.

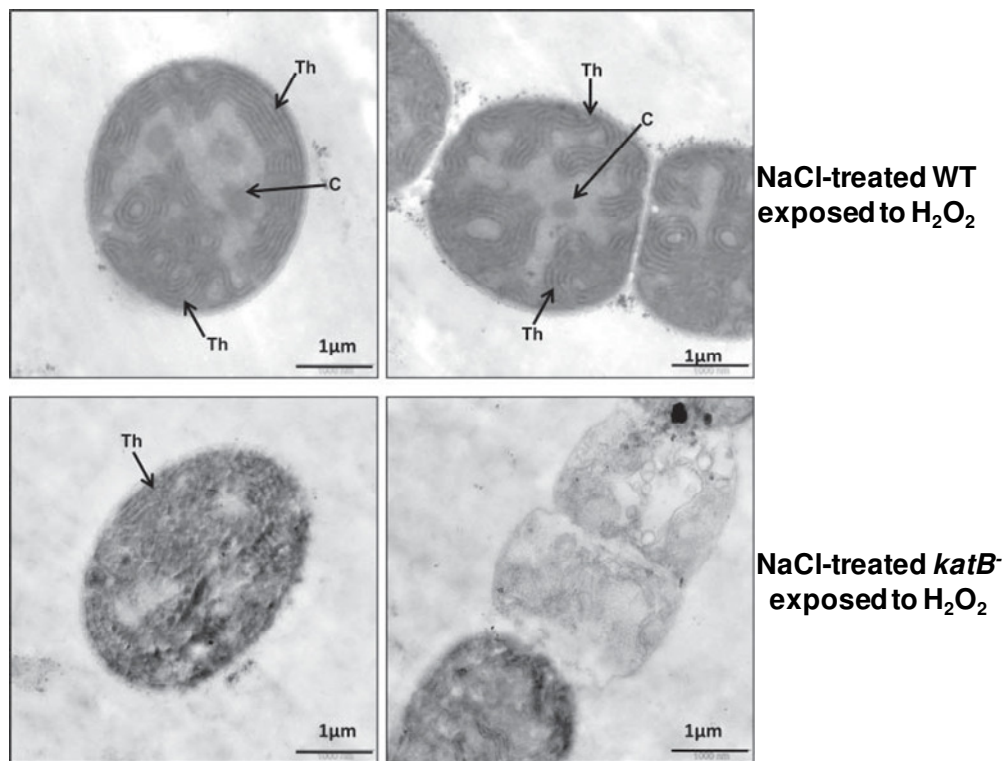


**Fig. 3.8 Ultrastructural changes associated with NaCl and H<sub>2</sub>O<sub>2</sub> treatment.** Transmission electron micrograph of the NaCl pre-treated wild-type (upper panel) or *katB* mutant (lower panel) after 24 hours of H<sub>2</sub>O<sub>2</sub> exposure. Thylakoid membranes (Th) and carboxysomes (C) are indicated by arrows.

### 3.9 Expression analyses of *katB*/KatB under various abiotic stresses

Expression of the *katB* gene in *Anabaena* PCC 7120 was monitored both at RNA and protein level under various stresses.

#### 3.9.1 Detection of *katB* transcript by Northern blotting-hybridization

The wild-type *Anabaena* PCC 7120 cells were exposed to NaCl, sucrose or direct oxidative stress causing agents such as hydrogen peroxide (H<sub>2</sub>O<sub>2</sub>) or methyl viologen (MV) for 16 hours. The total RNA was subsequently isolated from these stressed cultures, blotted onto a nylon membrane and hybridized to the DIG-labeled *katB* probe.

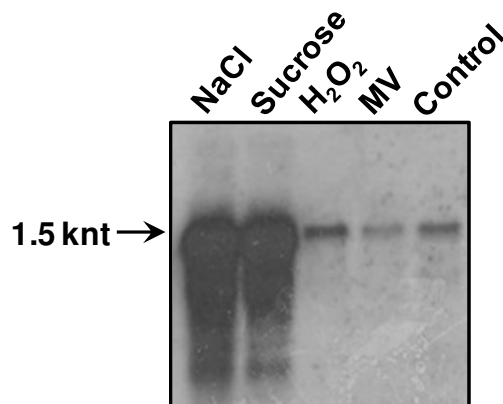


**Fig. 3.9.1 Detection of *katB* transcript in *Anabaena* in response to various abiotic stresses.** Total cellular RNA was isolated from untreated *Anabaena* PCC 7120 (control) or from cells treated with various stressors viz. 150 mM NaCl, 300 mM Sucrose, 1 mM H<sub>2</sub>O<sub>2</sub>, or 2  $\mu$ M Methyl Viologen (MV) for 16 hours. The RNA (5  $\mu$ g/lane) was run on formaldehyde-agarose gels, blotted onto nylon membrane and probed with the DIG-labeled *katB* DNA. The *katB* transcript (approximately 1.5 kilo-nucleotide long) is indicated by an arrow. The northern blot-hybridization experiment was repeated four times with consistent results and a representative blot is shown.

The result indicated that, in comparison to the control cells, many-fold induction of the *katB* transcript (~1.5 knt) was observed in response to salt or sucrose stress. Surprisingly, no induction of *katB* was observed in response to MV or in particular, H<sub>2</sub>O<sub>2</sub>, which is the direct substrate of the KatB enzyme (Fig. 3.9.1).

### 3.9.2 Assessment of KatB protein content in *Anabaena* by Western blot analyses

In agreement with the transcriptional analysis, Western blot analyses also revealed the 26 kDa KatB protein to be accumulate in *Anabaena* cells stressed with salt or sucrose, but not in the H<sub>2</sub>O<sub>2</sub>/MV-treated cells (Fig. 3.9.2 A). In natural environment, cyanobacteria are often exposed to desiccation, an extreme form of osmotic stress. Therefore, level of KatB protein in *Anabaena* after exposure to desiccation stress was monitored. The protein could not be detected in the control cells, however, accumulation of KatB protein was clearly observed after day 1 of desiccation and beyond (Fig. 3.9.2 B).

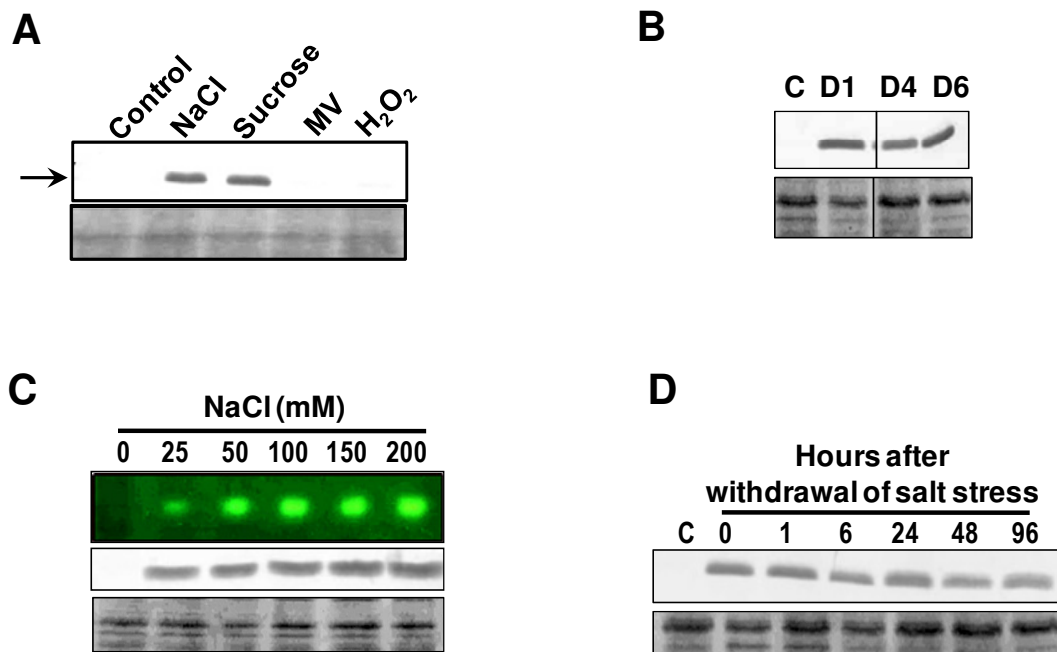


**Fig. 3.9.2 Expression of KatB protein under various abiotic stresses.** (A) Induction of the KatB protein in *Anabaena*. Cell free extracts were prepared from *Anabaena* cells treated with 150 mM NaCl (NaCl) or 300 mM sucrose (Suc) or 2  $\mu$ M methyl viologen (MV) or 1 mM H<sub>2</sub>O<sub>2</sub> (H<sub>2</sub>O<sub>2</sub>) and resolved on 14% SDS-PAGE (20  $\mu$ g/lane), transferred onto nitrocellulose membrane and probed with the KatB antiserum (1:10,000 dilution). The 26 kD KatB protein is shown by an arrow. (B) Expression of KatB in response to desiccation. Extracts of the control *Anabaena* (C) and desiccated *Anabaena* after 1 day (D1), 4 days (D4) or 6 days (D6) were probed with KatB antiserum on Western blots. A Ponceau S-stained part of the blot is shown as loading control. (C) *Anabaena* cultures were treated with various concentrations of NaCl as indicated in the figure for 20 h and cell extracts were prepared. Subsequently, the extracts

were used for zymographic analysis (top) or probed with the KatB antiserum (middle). Part of the Ponceau S-stained nitrocellulose membrane is shown as loading control (bottom). **(D)** Stability of KatB protein after synthesis. *Anabaena* cells were subjected to 150 mM NaCl treatment for 16 hours, washed thoroughly with fresh BG11N+ medium, reinoculated in fresh medium devoid of NaCl, and the content of KatB protein was assessed by Western blots probing with the KatB antiserum at different time points as indicated. Part of the Ponceau S-stained blot is shown as loading control at the bottom.

As the concentration of NaCl was increased from 0 to 200 mM, a concomitant rise in the KatB activity was observed on zymograms, which correlated well with the rise in the content of the KatB protein as observed on Western blots (Fig. 3.9.2 C, upper and middle panel respectively). To assess the stability of the KatB protein in *Anabaena*, cells were stressed with NaCl for 16 hours, washed thoroughly with plain BG11 medium and re-inoculated in fresh BG11N+ medium lacking NaCl. KatB was distinctly visualized even after 96 hours of the withdrawal of NaCl treatment (Fig. 3.9.2 D). This observation suggested that once synthesized, the KatB protein was relatively stable *in vivo*. It is important to mention here that expression of KatB could also be observed the wild-type 'control' *Anabaena* when higher concentration of antiserum (1: 5000) was employed while performing the Western blot analysis (Fig. 3.5.2 C). However, this basal level of expression in untreated cells (i.e. control) was inadequate to form a zone of clearance on zymograms (Fig. 3.5.2 C) [200].

### **3.10 Nitrogen status-dependent expression of *katB*/KatB**

The wild-type *Anabaena* PCC 7120 cells were grown in nitrogen supplemented medium (BG11N+) or in nitrogen free medium (BG11N-) and subjected to NaCl treatment. Under these growth conditions the production of the *katB* transcript or the KatB protein was monitored. Under control condition (without NaCl treatment), *katB* transcript or the KatB protein could not be detected in *Anabaena* grown in BG11N-

medium whereas, very low level of the same was observed in cells grown on BG11N+ medium (Fig. 3.10 A and B). Although NaCl treatment caused an increase in the *katB*/KatB levels in cells grown in BG11N+ or BG11N- medium, the NaCl-induced *katB*/KatB content in *Anabaena* grown in BG11N- medium was several fold lower than that observed in the corresponding cells grown in BG11N+ medium (Fig. 3.10 A and B).

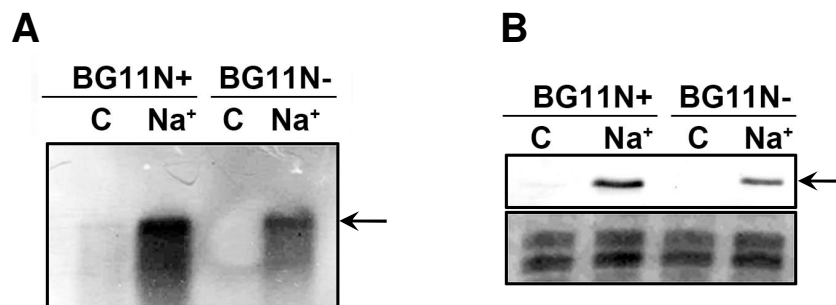


**Fig. 3.10 Nitrogen status dependent expression of *katB*/KatB in *Anabaena*.** (A) The wild-type *Anabaena* cultures were grown in BG11 medium with (BG11N+) or without combined nitrogen (BG11N-) and subjected to treatment with 150 mM NaCl (Na<sup>+</sup>) for 16 hours. Cells grown in absence NaCl i.e. untreated cells were served as control (C) in both types of media. From the above-mentioned cultures RNA was isolated, resolved on formaldehyde agarose gel, blotted onto nylon membrane and probed with the DIG-labeled *katB* DNA as probe. (B) Cell free extracts (corresponding to 60 µg/lane protein content) from the control (C) or the NaCl treated (Na<sup>+</sup>) *Anabaena* cells grown in BG11N+ or BG11N- medium were resolved by 14% SDS-PAGE and probed with the KatB antiserum on Western blots. The 26-kDa KatB protein is shown by an arrow.

### 3.11 Identification of *katB* promoter region by 5' RACE analysis

Osmotic stress caused by NaCl or sucrose resulted in distinct induction of the *katB* transcript in *Anabaena* (Fig. 3.9.2 A). From the Northern blot, the size of the transcript was estimated to be around 1.5 knt whereas the size of *katB* ORF is much smaller (693 bp). Hence, it was desired to identify the transcription start site and the promoter of the *katB* gene (Fig. 3.11). The total RNA was isolated from the control or the NaCl-treated

wild-type *Anabaena* PCC7120 cells and subjected to 5' RACE procedure. A ~450 bp fragment was detected when the RACE product was resolved on agarose gel (Fig. 3.11 A). This DNA product was sequenced to identify the transcription start site.

The transcriptional start point was identified to be 410 nucleotides upstream of the translational start of the *katB* ORF (Fig. 3.11 B). Also, bioinformatic analysis identified the probable -10 and -35 like promoter sequences to be present upstream of the transcriptional start site (Fig. 3.11 B).

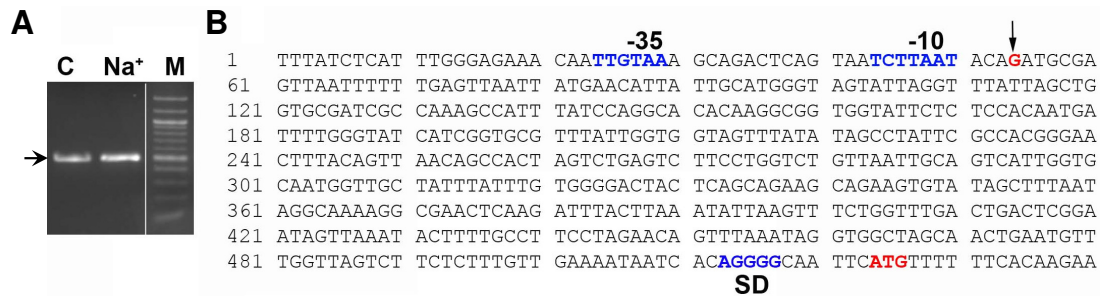


**Fig. 3.11 RACE analysis and identification of *katB* promoter.** (A) RNA was isolated from the wild-type control *Anabaena* cells (C) or cells exposed to 150 mM NaCl (Na<sup>+</sup>) for 16 hours and RACE was performed. 20  $\mu$ l and 5  $\mu$ l of the PCR reaction products were loaded in the C and Na<sup>+</sup> lane respectively. The approximately 450 bp DNA product is shown by an arrow. M, 100 bp DNA marker. (B) Analysis of the RACE product after sequencing. The transcriptional start site (G) is marked in red color and is shown by an arrow. Translational start codon (ATG) is depicted in red color. The ribosome binding site (SD) and the nucleotide sequence corresponding to the -10 and -35 region of the *katB* promoter are also denoted.

### 3.12 Generation of *katB* promoter-GFP fusion *Anabaena* strain and analysis of the *katB* promoter activity under various stresses

To monitor its promoter activity, it was desired to generate *katB* promoter-*gfp* fusion *Anabaena* strain.

#### 3.12.1 Cloning of *katB* promoter upstream of *gfp* reporter in pAM1956 vector and generation of *katB* promoter-*gfp* fusion *Anabaena* strain

The putative *katB* promoter region (as identified by RACE analysis) along with and its adjacent DNA were cloned in pAM1956 vector just upstream of the *gfp* (green fluorescent protein) reporter gene (*gfp mut2*). The resultant vector, named as pAM3090prom (Fig. 3.12.1 A), was eventually transferred into *Anabaena* PCC 7120 through triparental mating to yield *An3090prom* strain.

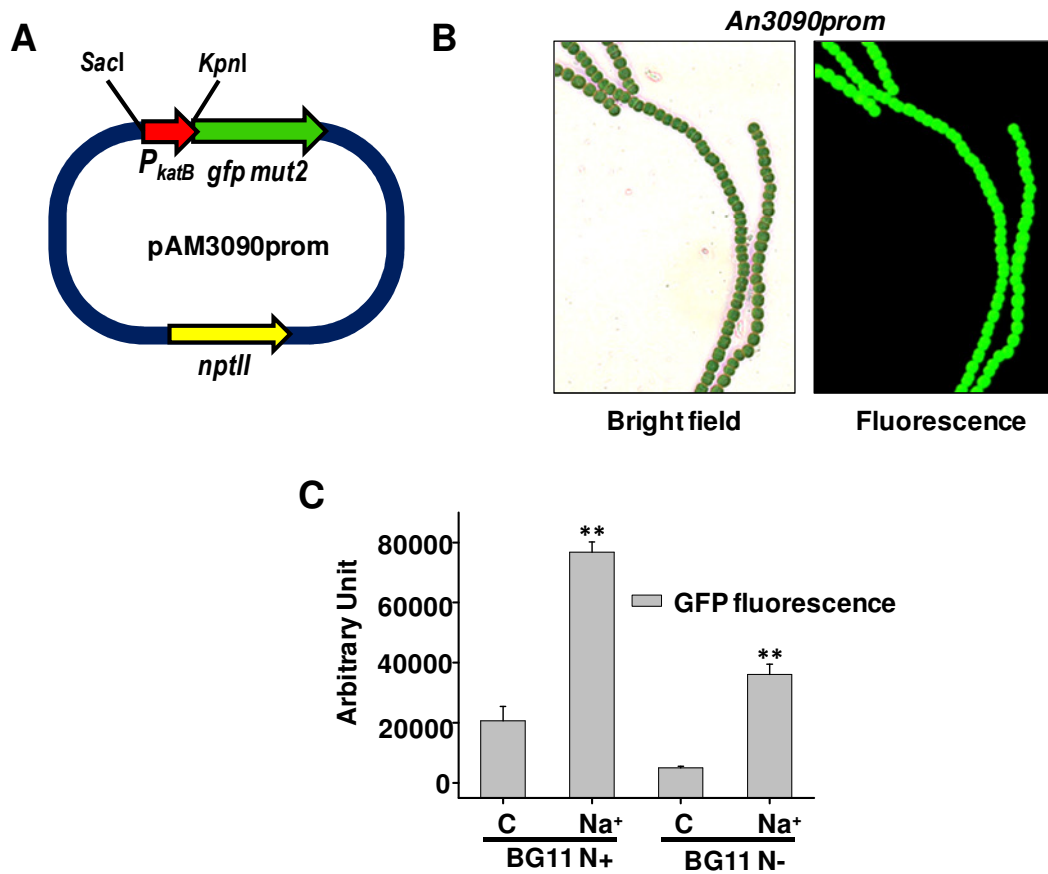


**Fig. 3.12.1** Generation of *katB* promoter-*gfp* fusion *Anabaena* strain. (A) Schematic representation of the pAM3090prom vector. *SacI* and *KpnI* sites were used to clone *katB* promoter (*P<sub>katB</sub>*) upstream of *gfp mut2* coding sequence in pAM1956 vector. (B) Bright field (left) and fluorescence (right) micrograph of *An3090prom* strain grown in BG11N+ strain after treatment with 100 mM NaCl for 16 hours. (C) The *An3090prom* strain was grown in the presence (BG11N+) or in the absence of combined nitrogen (BG11N-), treated with 100 mM NaCl (Na<sup>+</sup>) for 16 hours and GFP fluorescence was monitored with a spectrofluorimeter. Relative fluorescence values measured in arbitrary units is represented. Error bars represent SE and \*\* indicates significant difference at P<0.01 compared to the respective control.

This strain was used to assess the expression of *katB* promoter by monitoring GFP fluorescence. For *in vivo* validation, the *An3090prom* strain was subjected to NaCl treatment and the GFP fluorescence was observed under fluorescence microscope. Strong GFP fluorescence was detected in filaments of *An3090prom* strain (Fig. 3.12.1 B) suggesting that the cloned *katB* promoter was indeed functional in the *An3090prom* strain.

Fluorimetric quantification of GFP fluorescence showed that under control condition (i.e. in absence of NaCl), cells grown in BG11N- exhibited ~6-fold lower fluorescence compared to those grown in BG11N+ medium. There was 6-7 fold increase in GFP fluorescence after NaCl treatment in the *An3090prom* cells grown in BG11N-. However, even then, this elevated level was still 3-4 fold less than the GFP fluorescence observed in the corresponding cells grown in BG11N+ after exposure to NaCl (Fig. 3.12.1 C).

### **3.12.2 Assessment of *katB* promoter activity in response to various stresses by monitoring GFP fluorescence**

The *An3090prom* strain was further subjected to various types of osmotic stimuli that could activate *katB* expression in *Anabaena*. Enhanced GFP expression compared to the control was observed on treatment with all the osmolytes tested, i.e. NaCl, manitol, sucrose, sorbitol, glycerol and PEG indicating that all these osmolytes were able to activate the *katB* promoter in *Anabaena* (Fig. 3.12.2). Induction of *katB* promoter with non-ionic as well as ionic osmolytes (NaCl) suggested that *katB* was indeed a genuine osmo-inducible gene.

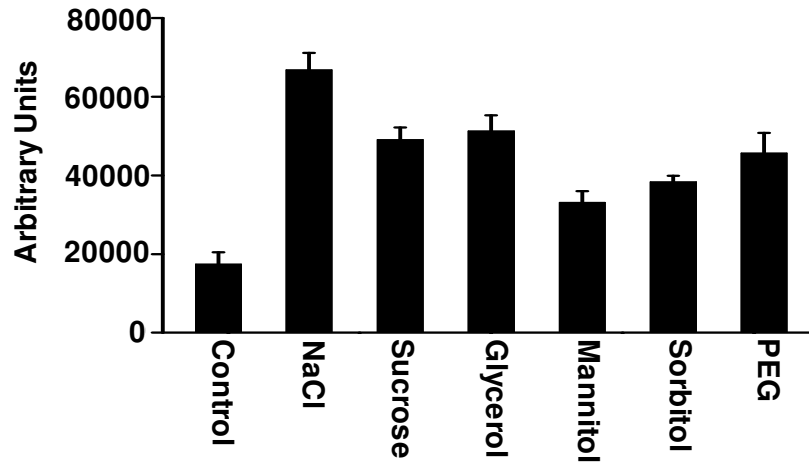


**Fig. 3.12.2 Expression of *katB* promoter in response to different osmotic stimuli.** The *An3090prom* strain was treated with NaCl (150 mM), sucrose (300 mM), glycerol (300 mM), manitol (300 mM), sorbitol (300 mM) and PEG (100 mM) for 18 hours and the green fluorescence ( $\lambda_{ex} = 490$  nm,  $\lambda_{em} = 520$  nm) of the cells was monitored with spectrofluorimeter and the values were plotted as arbitrary unit in the form of bar diagram. Error bars represent the standard deviation for 5 independent experiments.

### 3.13 Vegetative cell-specific expression *katB* promoter

Microscopic analysis with the *An3090prom* strain grown in BG11N- Medium (i.e. without nitrogen supplementation) showed the presence of strong GFP fluorescence in the vegetative cells while there was hardly any fluorescence in the heterocysts. These images clearly demonstrated that the *katB* promoter was active only in vegetative cells but not in the heterocysts (Fig. 3.13).

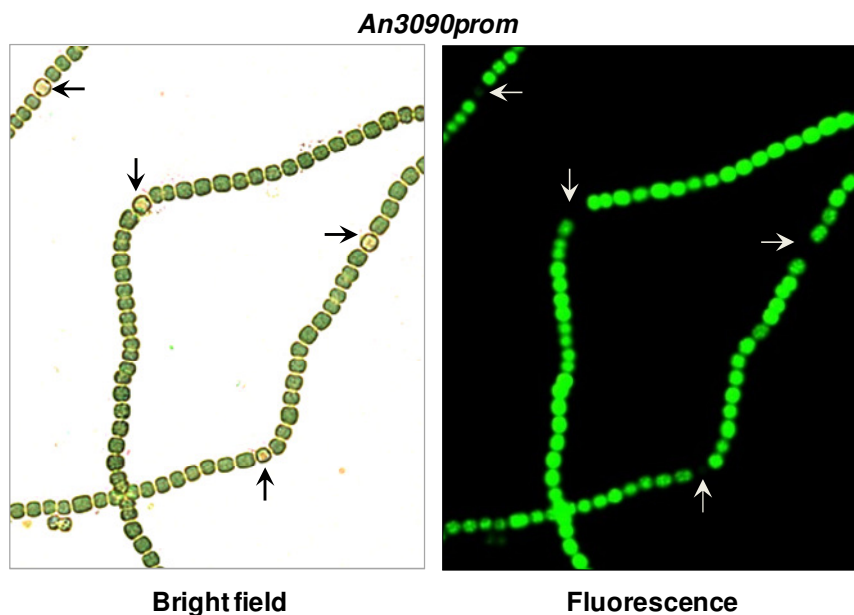


**Fig. 3.13 Lack of  $P_{katB}$ -*gfp* expression in heterocysts.** The *An3090prom* strain grown in BG11N-medium was treated with 100 mM NaCl for 16 hours and observed under a fluorescence microscope. Left panel shows the bright field micrograph, while, the right panel is the same microscopic field viewed under fluorescence mode using GFP filter (excitation BP, 450–490 nm and emission LP, 515 nm). The heterocysts are marked with arrows.

### 3.14 Discussion

Catalases are the highly active, ubiquitous enzymes, which play a major role in detoxification of  $H_2O_2$  in cellular environment. Although, in cyanobacteria, Mn-catalases represent a minor gene family but, interestingly, genome analyses reveal the presence of at least one ORF corresponding to Mn-catalase remarkably in all nitrogen-fixing cyanobacteria [148]. In this chapter, physiological characterization of a Manganese containing catalase (KatB) from the nitrogen-fixing cyanobacterium, *Anabaena* PCC7120, is reported.

In spite of presence of two genes corresponding to Mn-catalases, *Anabaena* under control condition (unstressed) exhibit very low inherent catalase activity. In contrast, cyanobacteria like *Synechocystis* PCC 6803 and *Synechococcus* PCC 7942 show profuse catalase activity, which could be easily detected by zymographic analysis [200,

228]. Higher level of inherent catalase activity is well correlated with the fact that both *Synechococcus* PCC 7942 and *Synechocystis* PCC 6803 are more tolerant to H<sub>2</sub>O<sub>2</sub> than *Anabaena* [202]. Both *Synechococcus* PCC 7942 and *Synechocystis* PCC 6803 do not possess genes for Mn-catalase, but instead, the bi-functional catalase peroxidase (KatG) appears to be the principal H<sub>2</sub>O<sub>2</sub> degrading enzyme. Deletion of *katG* in *Synechococcus* and *Synechocystis* resulted in marked sensitivity to exogenous addition of H<sub>2</sub>O<sub>2</sub>. However, under control condition (in the absence of any stress) these mutants did not have any obvious phenotype [229, 230]. This study also revealed the *Anabaena katB* mutant to grow akin to the wild-type under normal (i.e. control) conditions of growth. However, in contrast to the two above-mentioned cyanobacteria, the *Anabaena katB* mutant showed no difference in sensitivity to H<sub>2</sub>O<sub>2</sub> when compared to the control wild-type cells. Possibly, due to the inherently low catalase activity, both the wild-type and the *katB* mutant exhibit similar sensitivity to H<sub>2</sub>O<sub>2</sub>. Similar to *Anabaena* PCC 7120, disruption of *npun\_R4582ORF* that encodes a *katB* homolog in another heterocystous cyanobacterium, *Nostoc punctiforme* PCC 73102, did not alter the growth profile of this organism under control conditions. However, growth of the mutant strain was compromised when treated with heavy metals (Cu, Ni, Co, Mn) and H<sub>2</sub>O<sub>2</sub> [231]. It should be noted that in this organism, the *R4582* ORF was also found to be induced in response to the above-mentioned heavy metals.

*Anabaena* PCC 7120 encodes rubrerythrin, several peroxiredoxins (Prxs) that, like the catalase enzyme, also decompose cellular H<sub>2</sub>O<sub>2</sub>. In *Anabaena*, Prxs like All1541 or Alr4641 are induced in response to H<sub>2</sub>O<sub>2</sub> stress [159, 200], suggesting an important role of these Prxs in detoxifying H<sub>2</sub>O<sub>2</sub> under normal conditions or on exposure to H<sub>2</sub>O<sub>2</sub>. However, role of KatB becomes evident when the organism is stressed with NaCl, a

stressor that activates synthesis of KatB (Fig. 3.3; Fig. 3.9.1; Fig. 3.9.2). Increased accumulation of KatB in the NaCl pre-treated *Anabaena* cells confers enhanced H<sub>2</sub>O<sub>2</sub> tolerance (Fig. 3.2.1 and Fig. 3.2.2). This NaCl induced cross-protection to H<sub>2</sub>O<sub>2</sub> was totally absent in the salt pre-treated *katB* mutant *Anabaena*, which was found hypersensitive to combined salt and H<sub>2</sub>O<sub>2</sub> stress (Fig. 3.7 and Fig. 3.8). This result clearly demonstrated that KatB was responsible for the above-mentioned cross-protection of the salt pre-treated wild-type *Anabaena* cells from H<sub>2</sub>O<sub>2</sub> toxicity. This was further substantiated from the result that over-expression of KatB in *Anabaena* through genetic manipulation also protected the organism from oxidative stress mediated by H<sub>2</sub>O<sub>2</sub> (Fig. 3.4).

As mentioned earlier, there are two genes encoding Mn-catalase in *Anabaena* PCC 7120. Previous studies showed that over-production of the other Mn-catalase, KatA, resulted in reduced ROS burden and consequently, no significant increase in the expression of Alr4641 protein (2-Cys-Prx) after exposure to H<sub>2</sub>O<sub>2</sub> was observed [200]. In this study too, reduced levels of ROS and no increase the content of 2-Cys-Prx were observed when the NaCl pre-treated cells were exposed to H<sub>2</sub>O<sub>2</sub> (Fig. 3.2.2 A and Fig. 3.3 C). Put together, over-production of Mn-catalases in *Anabaena* resulted in enhanced survival and reduced ROS burden in this organism when challenged with exogenous addition of H<sub>2</sub>O<sub>2</sub>. This protective effect was found irrespective of the mode of over-production of the Mn-catalase. When adequately present in the cell, either by salt pre-treatment or by plasmid based over-expression, KatB can offer protection to *Anabaena* from H<sub>2</sub>O<sub>2</sub>-induced oxidative stress.

Although a weak oxidant by itself, H<sub>2</sub>O<sub>2</sub> in the presence of Fe<sup>2+</sup> give rise to hydroxyl radicals, which can damage virtually all types of cellular macro molecules directly or

indirectly (via formation of proteinradicals or sustaining chain of lipid peroxidation etc.), leading to cell death. Bleaching of the photosynthetic pigments due to H<sub>2</sub>O<sub>2</sub> toxicity is very common in photosynthetic bacteria. In *Microcystis aeruginosa*, impaired pigment synthesis and loss of membrane integrity due to higher ROS accumulation after treatment with H<sub>2</sub>O<sub>2</sub> has been reported [232]. In cyanobacteria, protein synthesis is also specifically targeted by H<sub>2</sub>O<sub>2</sub> [233]. Efficient and timely repair of the photosystems following photodamage was not possible due to inhibition of protein synthesis. This led to severe pigment loss and eventual impairment of photosynthetic activity [233, 234]. In *Anabaena* too, treatment with H<sub>2</sub>O<sub>2</sub> was found to be associated with marked bleaching of the culture [95, 159]. However, when the culture was pre-treated with common salt, cells could decompose externally added H<sub>2</sub>O<sub>2</sub> very efficiently due to elevated levels of KatB. As a result, overall ROS burden was reduced and deleterious processes like protein oxidation or lipid peroxidation were also drastically reduced. All these beneficial effects culminated into better survival of the cells as evidenced by better photosynthetic efficiency, protection of pigments or RNA etc. It is important to note here that this protective effect of NaCl was absent in the *Anabaena katB* mutant. This underscores the importance of KatB for protection of the salt pre-treated cells from the deleterious effects of H<sub>2</sub>O<sub>2</sub>. The damaging effects of H<sub>2</sub>O<sub>2</sub> that are countered by pre-treatment with NaCl via induction of KatB, consequently leading to protection of *Anabaena* cells is schematically depicted in Fig. 3.14.1.

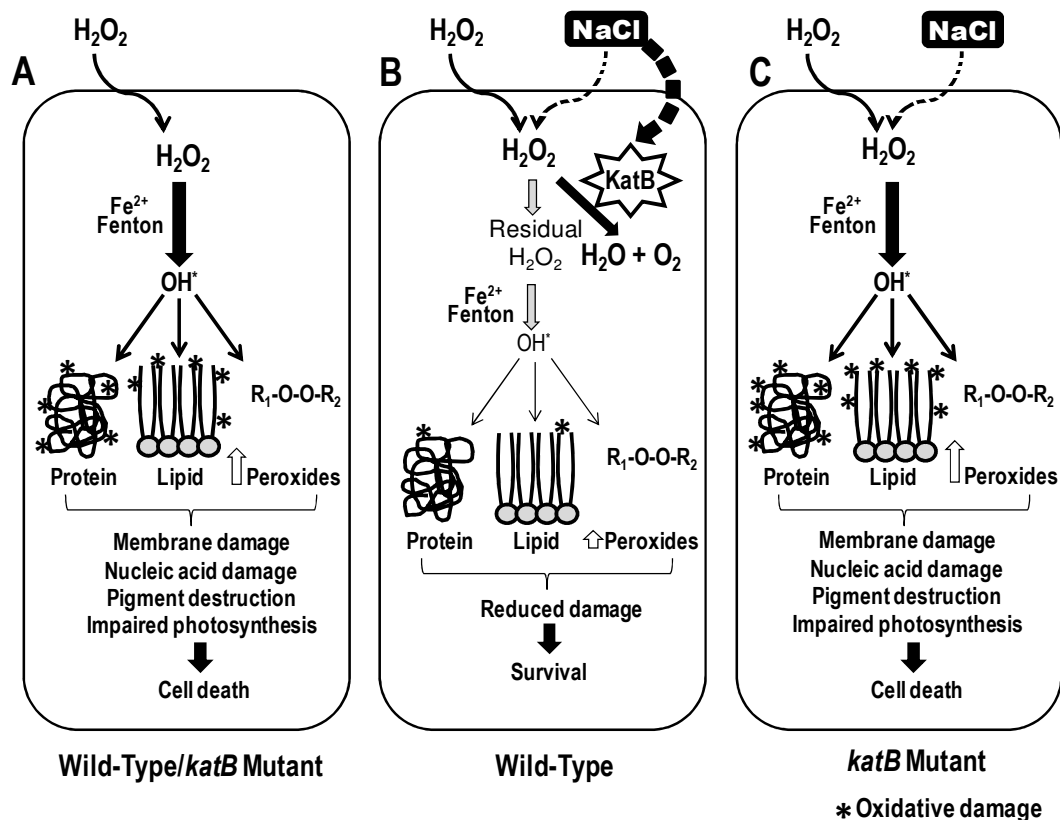


**Fig. 3.14.1** Schematic representation showing the NaCl mediated *KatB* induction and consequent protection of the organism against oxidative damage.

*Anabaena* fixes atmospheric nitrogen in the specialized cells called heterocysts. Heterocysts harbor the nitrogenase enzyme which converts inorganic nitrogen into bio-available form. Nitrogenase enzyme is extremely sensitive to  $O_2$  and heterocysts have evolved multiple strategies to protect this enzyme from  $O_2$ -induced damage, [235, 236]. Like vegetative cells, reactive oxygen species including  $H_2O_2$  are generated in heterocysts [204] and effective scavenging of these is needed, particularly for protection of the nitrogenase enzyme. Our result showed that the heterocysts lacked GFP fluorescence in the *AnKatBProm* strain indicating that the *katB* promoter was inactive in heterocysts (Fig. 3.13). In contrast, the vegetative cells showed abundant green fluorescence, demonstrating high activity of the *katB* promoter in the vegetative cells. In heterocysts, absence of oxygen is absolutely essential. In this context, lack of

KatB enzyme in heterocysts is particularly important as oxygen itself is a by-product of the catalase reaction. In the context of reduced O<sub>2</sub> environment required in heterocysts, the absence of KatB may confer a distinct advantage as oxygen, one of the products of catalase activity, is not produced. It should be noted that peroxiredoxins like Alr2375 (PrxQ) or Alr4641 (2 Cys-Prx) and the ruberythrin protein (RbrA, a FNR-dependent peroxidase) are expressed in both heterocysts and vegetative cells [95, 148]. These proteins too detoxify H<sub>2</sub>O<sub>2</sub> but they do not generate O<sub>2</sub> as by-product. The burden of H<sub>2</sub>O<sub>2</sub> decomposition in heterocyst rests on these enzymes rather than catalase. In fact, elevated level of H<sub>2</sub>O<sub>2</sub> was detected in heterocysts in *Anabaena* strain lacking the RbrA protein, indicating its strong role in scavenging of H<sub>2</sub>O<sub>2</sub> [204]. As opposed to catalase, possibly, Prxs are better suited for H<sub>2</sub>O<sub>2</sub> decomposition in heterocysts thereby protecting the nitrogenase enzyme from O<sub>2</sub> toxicity. A schematic representation depicting the differential strategy employed for H<sub>2</sub>O<sub>2</sub> detoxification in heterocyst or vegetative cell is shown in Fig. 3.14.2.

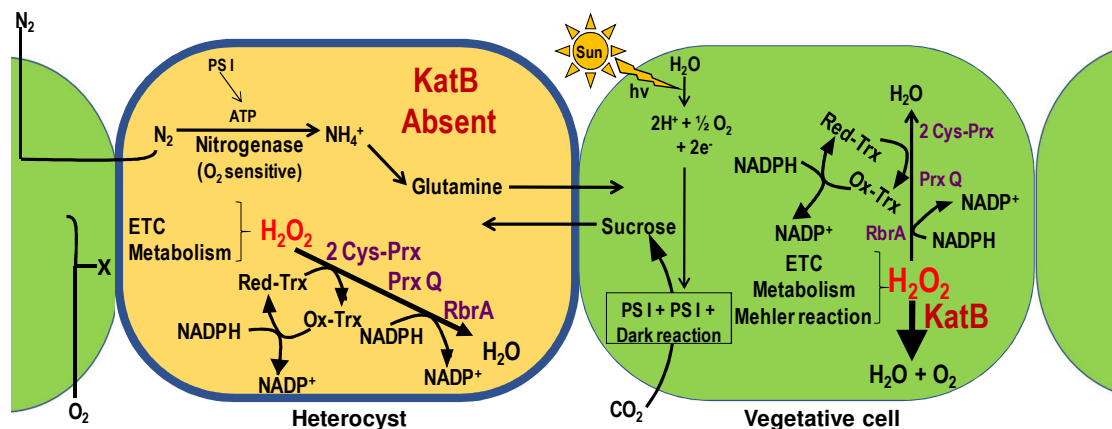


**Fig. 3.14.2 Schematic representation of H<sub>2</sub>O<sub>2</sub> detoxification pathways in vegetative cells and heterocysts.** The thick-walled heterocysts express the oxygen-sensitive nitrogenase enzyme that fixes atmospheric nitrogen. Both PSI and PSII are present in vegetative cells whereas, only PSI is present in heterocysts. H<sub>2</sub>O<sub>2</sub> is generated in vegetative cells and heterocysts by electron transport chains (ETC), cellular metabolism or Mehler reaction. In vegetative cells, H<sub>2</sub>O<sub>2</sub> is primarily neutralized by KatB, which

is induced by stresses like salinity or desiccation. Other H<sub>2</sub>O<sub>2</sub> decomposing enzymes like rubrerythrin (RbrA), peroxiredoxins (PrxQ/ 2 Cys-Prx) play a relatively minor role under these conditions. In heterocysts, KatB is not expressed. Here, PrxQ, 2 Cys-Prx and RbrA majorly perform the task of H<sub>2</sub>O<sub>2</sub> decomposition. Peroxiredoxins use reduced thioredoxin (Red-Trx) as electron donor which gets oxidized (Ox-Trx) during the reaction. Red-Trx is eventually regenerated by NADPH. RbrA, on the other hand, use NADPH directly for catalysis. As opposed to KatB, Reaction of Prx or RbrA does not yield oxygen as by-product. Hence, nitrogenase enzyme remains protected in heterocysts.

Salinity and desiccation are known to cause severe oxidative stress in several organisms [158, 237]. Compared to the control cells, significant production of H<sub>2</sub>O<sub>2</sub> was observed in *Microcystis aeruginosa* in response to salinity stress [238]. Similarly, increased H<sub>2</sub>O<sub>2</sub> content was reported under desiccation stress in *Nostoc flagelliforme*, a nitrogen-fixing cyanobacterium like *Anabaena* PCC 7120 [239]. As described in this chapter, contrary to the wild-type cells, treatment with NaCl leads to a substantial increase in ROS/total peroxides/oxidized protein/lipid peroxides in the *Anabaena* strain that lacks KatB (Fig. 3.6.1 and Fig. 3.6.2).

*Anabaena* often encounters stresses like salinity or desiccation in its natural habitat. These stresses are responsible for eventual rise in intracellular H<sub>2</sub>O<sub>2</sub> levels. Efficient removal of these endogenously produced ROS is essential for reducing the burden of oxidative stress. Our results show that both salinity and desiccation result in marked induction of KatB in *Anabaena* (Fig. 3.9.2). Under these natural stresses, the elevated level of KatB effectively decomposes the H<sub>2</sub>O<sub>2</sub> that is produced during these stresses, which in turn results in better cell survival. Naturally, the *katB* mutant *Anabaena* strain was susceptible to not only to salinity stress (Fig. 3.6.1 and Fig. 3.6.2) but also to desiccation [205].

As revealed by proteomic screens, certain stresses like arsenic, iron limitation or treatment with herbicide butachlor resulted in induction of the KatB protein [206, 207, 187]. However, expression of the other Mn-catalase, KatA, could not be detected in any of these conditions. Surprisingly, in spite of being substrate of the catalase enzyme, exposure to H<sub>2</sub>O<sub>2</sub> did not result in KatB induction suggesting that the regulation of *katB* gene is independent of H<sub>2</sub>O<sub>2</sub> in *Anabaena* (Fig. 3.9.1 and Fig. 3.9.2 A). In *N. punctiforme* too H<sub>2</sub>O<sub>2</sub> failed to induce the *katB*-homolog, indicating that Mn-catalases from filamentous cyanobacteria do not appear to be induced by H<sub>2</sub>O<sub>2</sub> per se [231]. So, it is indeed perplexing that *katB* is induced by salinity or desiccation but not by its actual substrate (H<sub>2</sub>O<sub>2</sub>). Results stated in this chapter (Fig. 3.9.1; Fig. 3.9.2 and Fig. 3.10) show careful regulation of *katB* expression wherein certain environmental stimuli (e.g. salinity, desiccation, presence of combined nitrogen etc.) activate expression. Moreover, heterocysts (the seat of nitrogen-fixation) show a distinct lack of *katB* expression. All these observations imply that the transcriptional regulation of *katB* is complicated and various environmental cues contribute to it. Also, the relatively long (>450-bp) 5' un-translated region of *katB* gene may have important functional significance in its regulation. Recent studies indicated that over-expression of LexA regulator in *Anabaena* resulted in repression of KatB expression and putative LexA binding box was detected in the *katB* promoter region [240]. However, involvement of this classical SOS-response regulator protein in regulating *katB* expression in the wild-type strain remains to be elucidated. Histidine kinases are known to regulate a good number of the osmotically induced genes in the unicellular cyanobacterium *Synechocystis* PCC 6803 [241, 242]. Homologues of some of these kinases are present in *Anabaena*. Plausibly, in *Anabaena* too, the osmo-inducible *katB* gene may be

regulated by histidine kinases. These, or other as of now unidentified regulators may perceive environmental conditions like salinity or desiccation (but not H<sub>2</sub>O<sub>2</sub> itself) and activate the signal cascade necessary for KatB synthesis.

To summarize, the results described in this chapter not only emphasize the crucial role played by KatB in surmounting different stresses in *Anabaena* but also reveal the ability of a simple molecule (NaCl) to modulate the general oxidative stress response of an organism by inducing a ROS scavenging enzyme

## **CHAPTER 4**

# **Biochemical, Biophysical & Structural Characterization of the KatB Protein**



## 4.1 Introduction

Although not present in eukaryotes, Mn-catalases are present in several bacteria and archaea. Presence of Mn-catalase in anaerobes has also been documented. In spite of wide distribution in prokaryotes and archaea, Mn-catalases have been relatively poorly studied as compared to the widely characterized heme-containing catalases [243]. Only a few Mn-catalases have been actually biochemically characterized so far. As far as structural biology of Mn-catalase is concerned, crystal structure of only two Mn-catalases, from *Thermus thermophilus* (TTC) and *Lactobacillus plantarum* (LPC), was reported when this work was initiated [130, 131]. A search with the keyword catalases in Protein Database (PDB) shows about 3350 results whereas, with keyword “Mn-catalase”, shows only 7 entries in total. This underscores the lacunae present in structural information related to an important class of ROS detoxifying enzyme from prokaryotic domain.

Heterocystous, nitrogen-fixing cyanobacterium *Anabaena* is resistant to stresses like desiccation, radiation etc. These stresses are known to generate different kinds of ROS including H<sub>2</sub>O<sub>2</sub>. Between the two Mn-catalases, KatA and KatB, results described in the previous chapter showed that the *katB* gene was massively induced in response to osmotic stress. Subsequently, the *katB* gene was found to play a key role in adaptation to salinity or oxidative stress. Considering the importance of this gene in combating salinity in *Anabaena*, it was desired to decipher the biochemical and physical nature of the *katB* gene product. Pairwise alignment showed that Mn-catalase KatB to show poor sequence similarity with LPC (31% identity) or TTC (26% identity). Another important feature of KatB was its relatively shorter length (230 amino acids) as compared to that of LPC (266 amino acids) or TTC (302 amino acids). Hence, it was also pertinent to

decipher how this protein was structurally different from TTC or LPC. In the current chapter, heterologous over-expression, purification and biochemical/biophysical characterization of KatB from *Anabaena* are reported. The important structural features of the KatB protein are explained with the crystal structure and structural similarities and dissimilarities with the other two available Mn-catalases are expounded here. Uniqueness of the KatB active site and phylogenetic analyses which categorize Mn-catalases on basis of their active site configuration is also discussed in this chapter.

#### 4.2 Cloning of *alr3090* ORF (*katB* gene) from *Anabaena* in pET21a expression vector and over-expression in *E. coli*

For the heterologous over-expression of KatB in *E. coli* and subsequent purification of the over-produced protein, the *katB* ORF was ligated to pET21a expression vector.

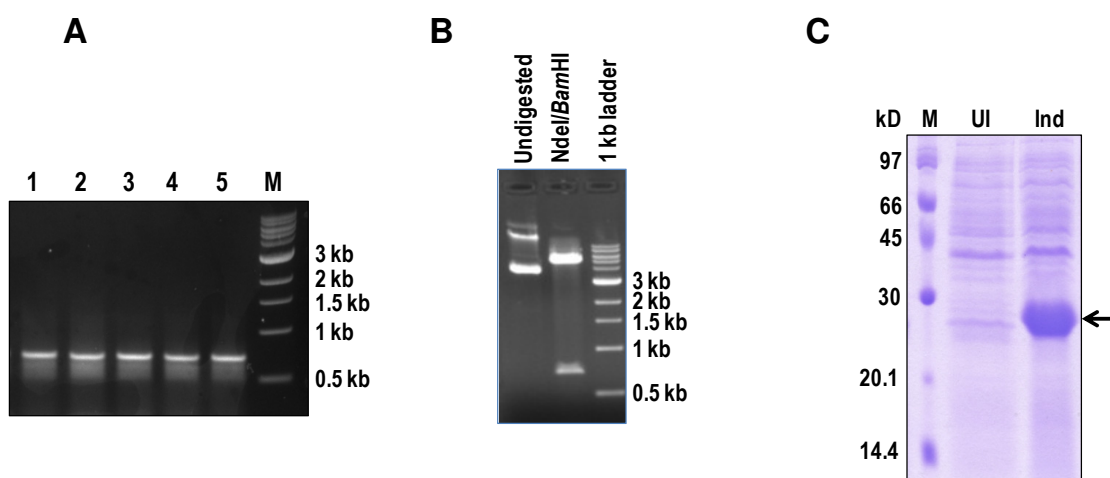


**Fig. 4.2 Cloning of *katB* ORF in pET21a expression vector and heterologous over expression of the recombinant KatB in *E. coli*.** (A) Agarose gel electrophoresis of the product of colony PCR performed with the putative *E. coli* DH5 $\alpha$  strains transformed with pETkatB plasmid. Number 1 to 5 denotes the colony number; M, 1 kb DNA ladder. (B) Restriction digestion of pETkatB plasmid. Plasmid was isolated from one of the colony PCR-positive clones and subjected to restriction digestion with *Nde*I and *Bam*HI. M, 1 kb DNA ladder. (C) Heterologous over-expression of recombinant KatB in *E. coli* BL21 (DE3) pLysS strain transformed with pETKatB. Cell extracts of the recombinant strain was resolved by 14% SDS-PAGE and subsequently stained with Coomassie blue. UI, un-induced sample (without IPTG); Ind, Induced sample (with IPTG); M, protein molecular weight marker. Over-produced protein is shown by an arrow.

The *katB* ORF was PCR amplified from *Anabaena* genomic DNA using KatB\_Nde\_Fwd and KatB\_BamHis\_Rev primers (Table 2.2). The reverse primer also contained six in-frame codons for histidine to facilitate production of a C-terminal his-tagged protein for NiNTA affinity-based purification. The PCR amplified product was ligated into pET21a expression vector employing *NdeI* and *BamHI* restriction sites (resultant plasmid was named as pETkatB). The presence of the appropriate plasmid was confirmed by colony PCR (Fig. 4.2 A), restriction digestion (Fig. 4.2 B) and by sequencing of the pETkatB plasmid. pETkatB plasmid thus generated was transformed into *E. coli* BL21(DE3) pLysS expression host and the production of the KatB protein was observed on induction with 1 mM IPTG (Fig. 4.2 C).

#### **4.3 Purification of KatB protein from KatB over-producing *E. coli* strain**

For over-producing the KatB protein, the *E. coli* BL21(DE3) pLysS strain carrying the pETkatB plasmid was grown in LB medium and induced with IPTG as described in the 'Materials & Methods' chapter. Cells were harvested, lysed and the soluble fraction was separated from the inclusion bodies by centrifugation. When analyzed by SDS-PAGE, majority of the over-produced protein was found to be present in the inclusion body fraction. As low temperature is known to promote production of soluble protein in *E. coli*, culture was incubated at 20°C for 16 hours after addition of IPTG. At this temperature, solubility of the over-produced KatB protein improved considerably (Fig. 4.3 A) and the over-produced KatB protein could be purified to near homogeneity employing the NiNTA matrix (Fig. 4.3 B). The identity of the protein was confirmed with the monoclonal penta-His antiserum on Western blots (Fig. 4.3 C). The KatB protein thus purified was used to generate polyclonal antiserum in rabbits at a commercial facility.

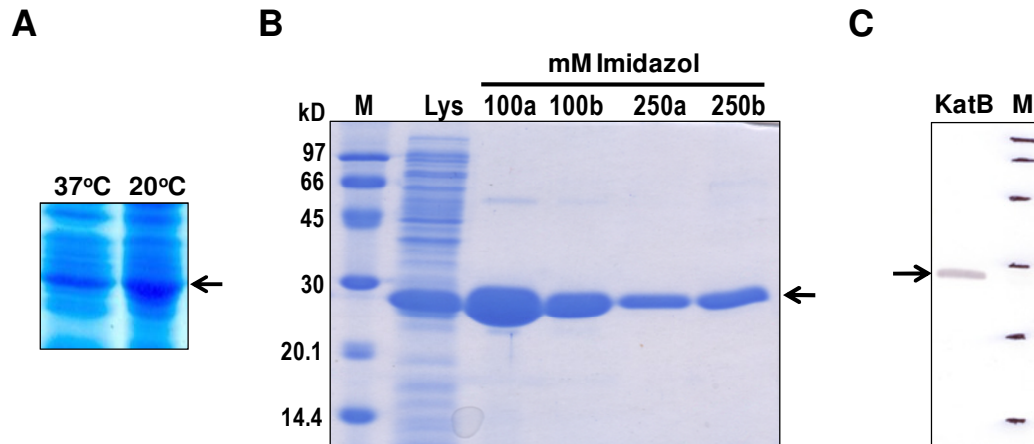


**Fig. 4.3 Effect of low temperature on solubility of the over-produced KatB protein and its subsequent purification.** (A) Solubility of over-produced KatB protein. *E. coli* cells were induced with 1 mM IPTG at 37°C or at 20°C, as indicated in the figure, and cell extracts were resolved by 14% SDS-PAGE. KatB protein band is depicted by an arrow. (B) NiNTA affinity purification of the over-expressed KatB protein. The soluble fraction obtained from the KatB over-expression cells was bound to NiNTA slurry, washed thoroughly with lysis buffer and the bound protein was eluted by increasing imidazole concentration (indicated in the figure) in the lysis buffer. All the fractions were resolved by 14% SDS-PAGE and stained with Coomassie Brilliant Blue (CBB) stain. Purified protein band is indicated by an arrow. (C) The purified protein (0.2 µg) was resolved by SDS-PAGE, transferred onto nitrocellulose membrane and probed with monoclonal anti-his antibody.

#### 4.4 Effect of Manganese supplementation the *E. coli* growth medium

As the KatB protein is a Mn-catalase (i.e. Mn is present at the active site), it was desired to verify if exogenous addition of Mn to the growth medium would increase production of the soluble KatB protein.

##### 4.4.1 Solubility of the over-produced protein in recombinant *E. coli* grown on Mn-supplemented medium

*E. coli* BL21(DE3) pLysS cells carrying the pET21katB plasmid was induced with IPTG in the presence of 100 µM MnCl<sub>2</sub> (at 20°C) and subsequently tested for production of the soluble KatB protein. SDS-PAGE analysis revealed a considerable improvement in the solubility of the KatB protein on addition of Mn. Approximately

10-fold increase in solubility was observed with 100  $\mu\text{M}$   $\text{MnCl}_2$  compared to the un-supplemented cultures (Fig. 4.4 A). The higher solubility also improved the overall purification yield of the KatB protein i.e. considerably higher amount of protein could be purified from Mn-supplemented cultures (Fig. 4.4 B).

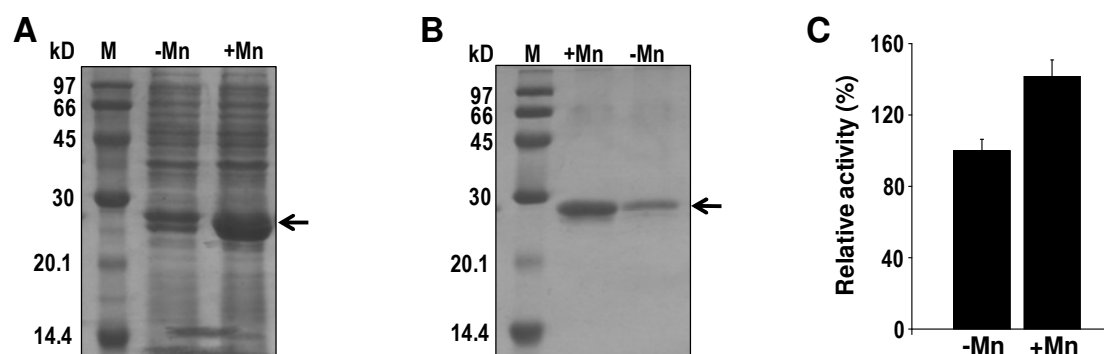


**Fig. 4.4 Effect of  $\text{Mn}^{2+}$  supplementation on solubility and activity of the over-produced KatB protein.** (A) *E. coli* BL21 (DE3) pLysS/pETkatB strain was grown in the absence (-Mn) or in the presence of 100  $\mu\text{M}$   $\text{MnCl}_2$  in LB medium, induced by 1 mM IPTG for 16 hours at 20°C, soluble fraction was prepared and resolved by SDS-PAGE (14%) followed by staining with CBB. Protein band corresponding to over-produced KatB protein is indicated by an arrow. (B) Purification of over-produced KatB protein from recombinant *E. coli* cultures grown in absence (-Mn) or in presence (+Mn) of  $\text{MnCl}_2$ . Equal volume of purified proteins (20  $\mu\text{l}$ ) were resolved by SDS-PAGE (12%) and visualized by CBB staining. Purified KatB protein is indicated by an arrow. (C) Spectrophotometer based catalase activity of KatB protein purified from *E. coli* cultures grown in the absence (-Mn) or in the presence (+Mn) of 100  $\mu\text{M}$   $\text{MnCl}_2$ . Error bars denotes the SE.

#### 4.4.2 Enzymatic activity of KatB purified from Mn-supplemented or Mn-lacking *E. coli* cultures

The  $\text{H}_2\text{O}_2$  decomposition activity of the KatB protein purified from Mn-supplemented culture medium or medium lacking externally added Mn was compared. Results showed KatB purified from Mn-supplemented cells to decompose  $\text{H}_2\text{O}_2$  with a rate that was 40% higher than KatB isolated from non Mn-supplemented cells. Thus, addition of Mn to the growth medium not only increased the solubility of KatB, but also increased

its activity (Fig. 4.4 C). The KatB protein, purified from Mn-supplemented *E. coli* culture grown at 20°C after addition of 1 mM IPTG, was used for all the biochemical as well as biophysical experiments.

#### 4.5 Biophysical properties of the purified KatB protein

The purified KatB protein was used for deciphering its biophysical properties.

##### 4.5.1 Gel filtration and native PAGE analyses of purified KatB protein

To get an insight into its oligomerization status, the purified KatB protein was subjected to gel filtration analysis. The elution profile showed only a single peak, corresponding to a molecular weight of ~109 kDa (Fig. 4.5.1 A), which corresponded to a tetramer.

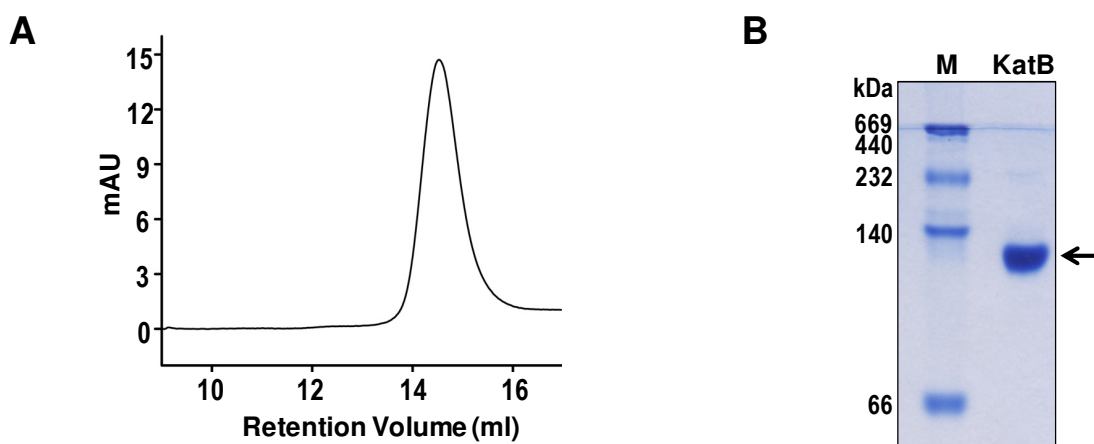


**Fig. 4.5.1 Gel filtration and native PAGE analysis of purified KatB protein.** (A) Gel filtration profile of the purified KatB protein. 200  $\mu$ g of KatB protein was injected into Superdex 200 10/300 GL column pre-equilibrated with buffer containing 20 mM Tris and 50 mM NaCl, pH 7.2. (B) Purified KatB protein (1  $\mu$ g) was resolved by non-denaturing native polyacrylamide gel electrophoresis (PAGE; 10%) and visualized by CBB staining. The KatB protein band is indicated by an arrow.

Presence of a single peak also showed that the purified protein was indeed pure. Similar result was obtained when the purified protein was resolved on native PAGE (Fig. 4.5.1

B) wherein, a single band corresponding to ~110 kDa was visualized on the Coomassie-stained native gel.

#### 4.5.2 Determination of secondary structure of KatB protein by CD spectropolarimetry

The prevalent secondary structure of the purified protein was evaluated by CD spectropolarimetry (Fig. 4.5.2). Results revealed that the KatB protein was largely alpha helical and contained ~56%  $\alpha$ -helix along with ~33%  $\beta$ -sheets.

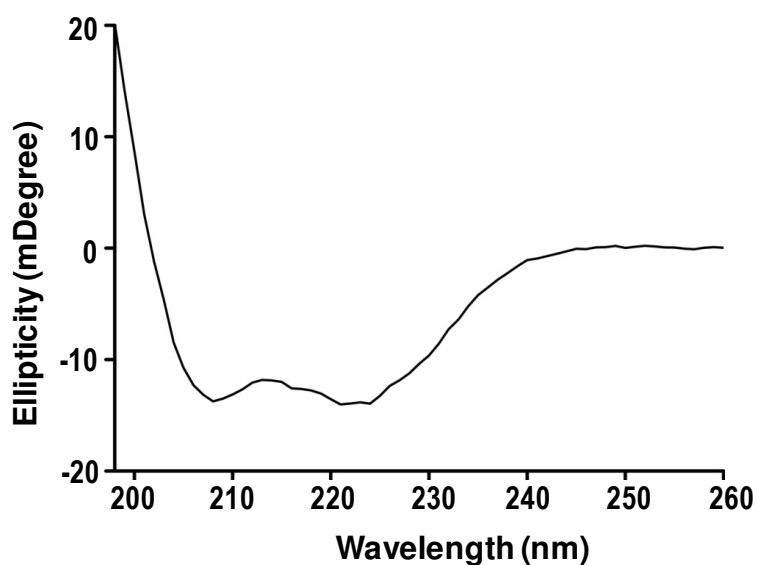


**Fig. 4.5.2 CD spectra of the KatB protein.** Purified KatB protein (0.1 mg/ml) in 20 mM Tris buffer pH 8.0 was taken in a quartz cuvette of 1 mm path length and dichroic intensity was measured in a CD spectropolarimeter.

#### 4.5.3 DLS spectroscopy of KatB protein

Dynamic Light Scattering was performed in order to determine the hydrodynamic volume of the KatB protein. The result suggested that the KatB protein is monodisperse in nature, i.e., only a single oligomeric species was present in the KatB

solution (Fig. 4.5.3). The hydrodynamic volume of the KatB oligomer was found to be around 9 nm.

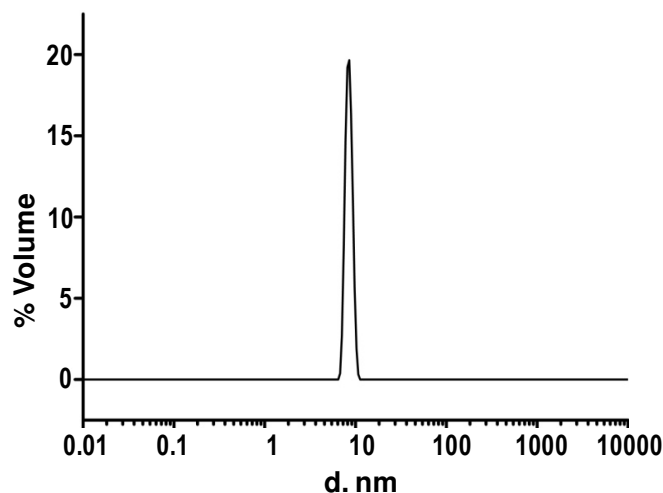


**Fig. 4.5.3 Dynamic Light Scattering (DLS) profile of KatB protein in 20 M Tris buffer, pH 8.0.**

#### **4.6 Biochemical characterization of the purified KatB protein**

After deciphering the biophysical properties of the KatB protein, biochemical properties of this enzyme were determined.

##### **4.6.1 Zymographic and spectrophotometric H<sub>2</sub>O<sub>2</sub> decomposition assay**

Once purified, the protein was subjected to in-gel catalase activity (zymogram) assay. On zymographic analysis, a distinct zone of clearance (indicating catalase activity) was observed with the purified protein on native gels (Fig. 4.6.1 A, upper panel). The same protein was resolved on SDS-PAGE and probed with KatB antisera (Fig. 4.6.1 A, lower panel). A strong cross-reaction with the specific antiserum indicated that the protein was indeed KatB. H<sub>2</sub>O<sub>2</sub> shows a characteristic absorbance peak at 240 nm. So activity of catalase enzyme can be monitored by measuring the decrease in absorbance (due to decomposition of H<sub>2</sub>O<sub>2</sub>) at this wavelength. Spectroscopic H<sub>2</sub>O<sub>2</sub> decomposition assay also showed a time-dependent reduction in the absorbance of H<sub>2</sub>O<sub>2</sub> in the presence of the KatB protein (Fig. 4.6.1 B), thus demonstrating its catalase activity.

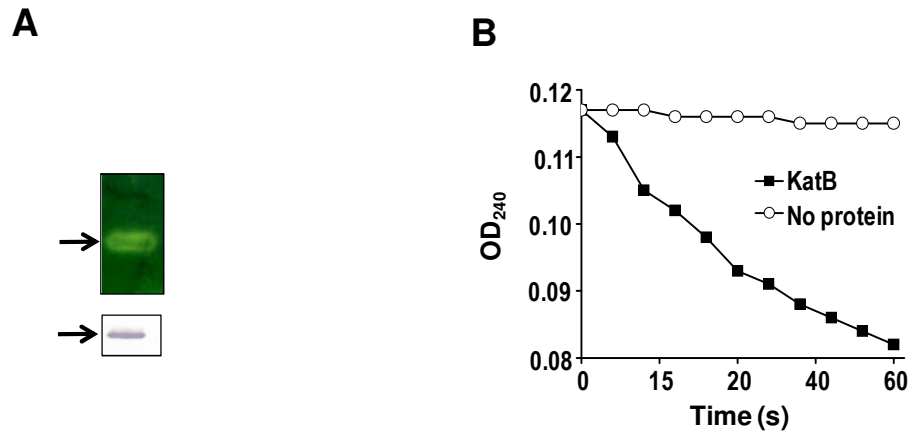


**Fig. 4.6.1 Activity of the purified KatB protein.** (A) The KatB protein (1  $\mu$ g) was resolved on native 10% PAGE and subjected to zymographic staining for in-gel catalase activity (top). Colourless zone of catalase activity is indicated by an arrow. The same protein preparation was resolved on SDS-PAGE (14%), transferred onto nitrocellulose membrane and probed with KatB antisera (bottom). (B) Spectrophotometer based H<sub>2</sub>O<sub>2</sub> decomposition assay. 1  $\mu$ g of purified KatB protein was added to a quartz cuvette containing H<sub>2</sub>O<sub>2</sub> substrate (2 mM) in 1 ml reaction buffer (20 mM Tris, pH 8.0), mixed thoroughly and immediately put into spectrophotometer for measuring absorbance. Decrease in absorbance at 240 nm with time was monitored.

#### 4.6.2 Determination of the kinetic parameters of KatB enzyme

The purified KatB protein was incubated with various concentrations of H<sub>2</sub>O<sub>2</sub> in 20 mM Tris buffer pH 8.5 and decomposition of H<sub>2</sub>O<sub>2</sub> with time was monitored by following the decrease in A<sub>240</sub>. Velocity of the reaction was plotted against the substrate concentration and a rectangular hyperbolic curve was obtained, which indicated that the enzymatic reaction followed Michaelis-Menten kinetics (Fig. 4.6.2 A). For K<sub>m</sub> and V<sub>max</sub> determination, inverse of velocity of reaction was plotted with respect to inverse of substrate concentration to obtain the Lineweaver-Burk plot (Fig. 4.6.2 B).

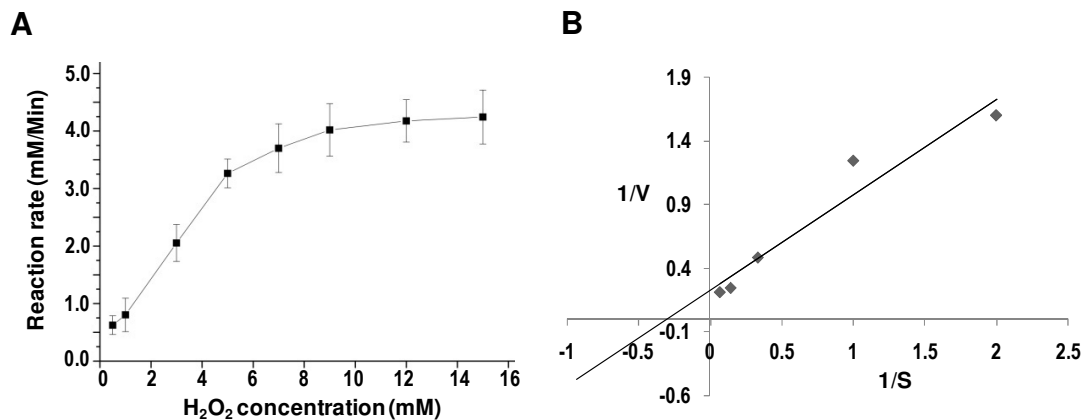


**Fig. 4.6.2 Kinetic properties of KatB enzyme.** (A) Michaelis-Menten curve showing rate of H<sub>2</sub>O<sub>2</sub> decomposition by KatB protein at various substrate concentration as indicated in the figure. Error bars represent the SE. (B) Lineweaver-Burk plot. Inverse of the reaction rate was plotted as a function of inverse of the substrate concentration.

As per the Lineweaver-Burk plot, the  $K_m$  value for the KatB enzyme was calculated to be  $3.29 \pm 0.95$  mM. The  $V_{max}$  for the enzyme was calculated to be  $263 \pm 71.54$  mM<sup>-1</sup>min<sup>-1</sup>μg<sup>-1</sup> of protein. The catalytic efficiency ( $k_{cat}$ ) of the KatB enzyme was worked out to be  $1.15 \times 10^5$  s<sup>-1</sup>subunit<sup>-1</sup>.

#### 4.6.3 Determination of the pH optima of KatB

H<sub>2</sub>O<sub>2</sub> decomposition activity of the purified KatB protein was tested at different pH, ranging from 4.0 to 10.5. Almost no activity was found at pH 4.0 or 5.0 (sodium acetate buffer) whereas minor activity was observed between pH 6.0 and 7.0 (potassium phosphate buffer). A considerable increase in activity was observed in the pH range 7.0-9.0 (Tris buffer), and the pH optima was found to be around pH 8.5, however subsequently, there was a severe drop in activity between pH 9.0 and 10.0 (Glycine-NaOH buffer) (Fig. 4.6.3).

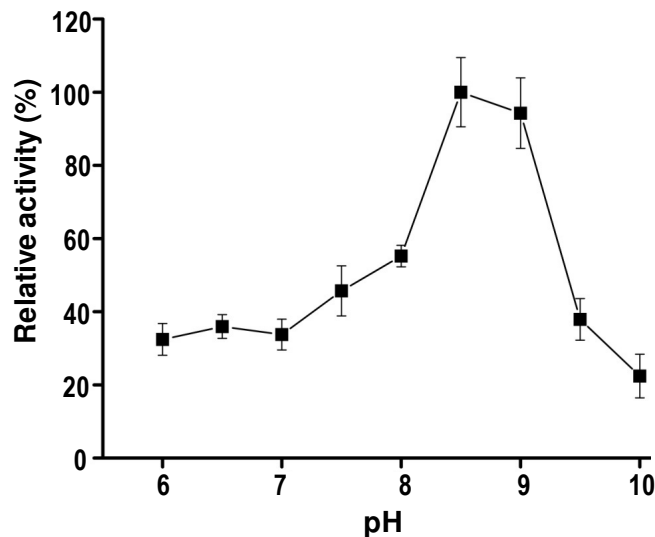


**Fig. 4.6.3 pH dependent activity of KatB.** H<sub>2</sub>O<sub>2</sub> decomposition activity of KatB protein was measured at different pH using various buffer systems as mentioned in the ‘Materials and Methods’ section. Maximum measured activity (at pH 8.5) was considered to be 100% and other rates were calculated accordingly. Error bars indicate the SE.

#### 4.6.4 Enzyme inhibition studies

Mn-catalases are known to be inactivated by hydroxylamine but relatively insensitive to azide. Inhibition studies showed KatB to be significantly inhibited in presence of hydroxylamine. About 50% of the KatB activity was lost on treatment with as low as 50  $\mu$ M hydroxylamine (Fig. 4.6.4 A).

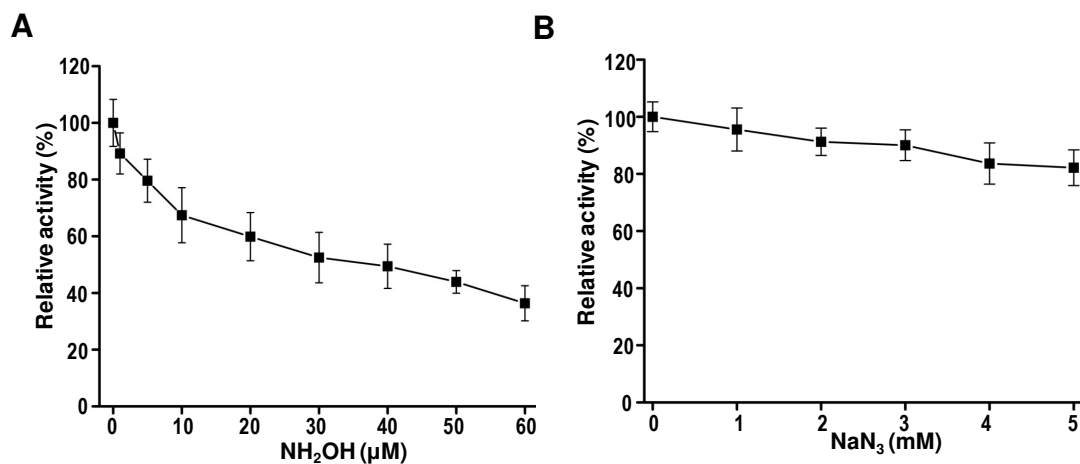


**Fig. 4.6.4 Inhibition of KatB activity by hydroxylamine or sodium azide.** (A) H<sub>2</sub>O<sub>2</sub> decomposition activity of the purified KatB protein in presence of various concentration of hydroxylamine (indicated in

the figure) was measured and plotted. Activity in absence of hydroxylamine was considered to be 100% and other activities were calculated accordingly. (B) KatB activity in the presence of sodium azide. Activity in absence of sodium azide was considered to be 100% and other activities were calculated accordingly. Error bars represent the SE.

On the other hand, as expected, the KatB protein was found to be relatively insensitive to sodium azide. The enzyme retained almost 90% of its original activity in presence of a relatively high (5 mM) concentration of sodium azide (**Fig. 4.6.4 B**).

#### 4.6.5 Effect of NaCl on KatB function

H<sub>2</sub>O<sub>2</sub> decomposition by the purified KatB protein, in the presence of different concentrations of NaCl, was assayed spectrophotometrically. Results showed that with the increase in salt concentration, KatB activity increased initially and peaked in presence of 200 mM NaCl. With further increase in salt concentration, KatB activity decreased marginally, but even in the presence of 2.5 M NaCl, KatB could retain 77% of its activity (Fig. 4.6.5), indicating that KatB can function under conditions of high ionic strength.

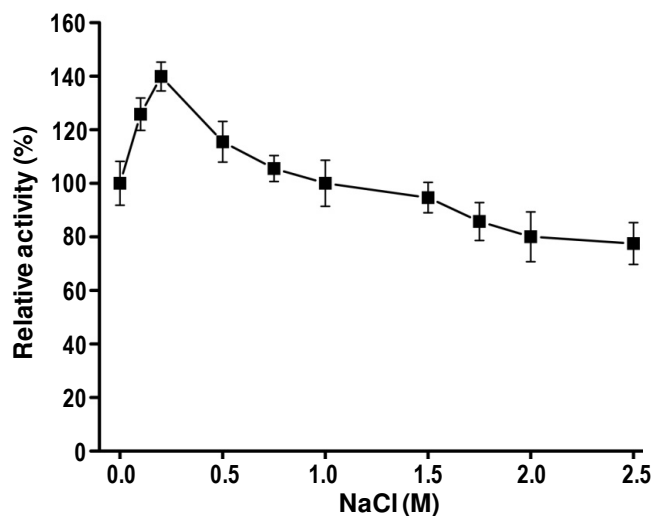


**Fig. 4.6.5 Effect of NaCl on KatB activity.** H<sub>2</sub>O<sub>2</sub> decomposition activity of the KatB protein in presence of various concentrations of NaCl (as indicated in the figure). Activity in absence of NaCl was considered to be 100% and all other activities were calculated accordingly. Error bars represent the SE.

#### 4.7 Thermostability of the KatB protein

Mn-catalases are known to be thermostable in nature. Since KatB is also a Mn-catalase, it was desired to assess the thermostability of this enzyme. Circular Dichroism (CD) spectropolarimetry was used to determine the  $T_m$  of the purified KatB protein. The CD spectra of KatB protein showed a characteristic peak at 222 nm wavelength (Fig. 4.5.2). To monitor the loss of secondary structure with increase in temperature, CD signal was monitored continuously at 222 nm while increasing the temperature of the protein sample. The melting analyses revealed that the KatB protein could retain its secondary structure even after applying temperature above 90°C. This suggested that the protein is highly thermostable, and from the CD melting curve the  $T_m$  of KatB was found to be around 97°C (Fig. 4.7 A).

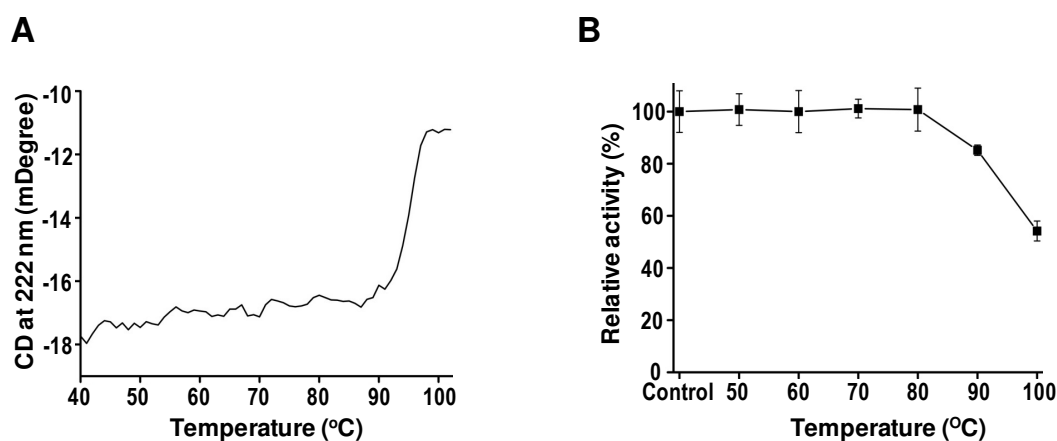


**Fig. 4.7 Thermostability of KatB.** (A) Dichroic intensity (in milli degree) of the purified KatB protein at 222 nm during thermal denaturation (40-101°C). (B) The KatB protein was incubated at the indicated temperatures for 10 minutes and the catalase activity was measured subsequently at room temperature. Activity of the protein incubated at room temperature (control) was taken as 100% and the other rates were calculated accordingly. Error bars represent the SE.

To test activity after exposure to high temperature, the purified KatB protein was incubated at different temperatures for 10 minutes, cooled down to room temperature and subsequently assayed for catalase activity. Almost no loss in activity was observed

till about 80°C but at 90°C, a marginal drop in activity was observed. The KatB protein could retain almost 50% of its original activity even after incubation at 100°C for 10 minutes (Fig. 4.7 B). Thus, like the previously characterized Mn-catalase (Alr0998) from *Anabaena*, KatB was also found to be a thermostable catalase.

#### 4.8 Sensitivity of the KatB protein to chemical denaturant (GuHCl)

Guanidium hydrochloride (GuHCl) is a strong chemical denaturant. The purified KatB protein was assayed for GuHCl sensitivity.

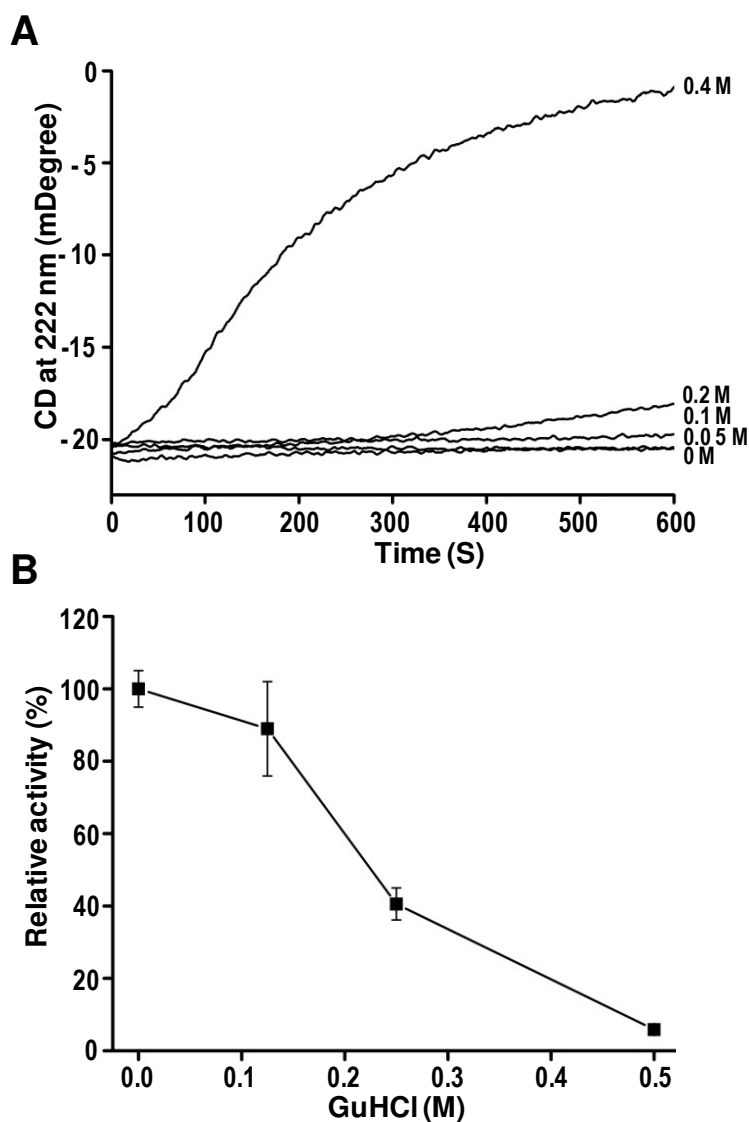


**Fig. 4.8 Sensitivity of the KatB protein to guanidium hydrochloride (GuHCl).** (A) Loss of secondary structure in the presence of GuHCl. Purified KatB protein (0.1 mg/ml) was mixed with different

concentration of GuHCl as indicated, in quartz cuvette and change in ellipticity (at 222 nm) with time was monitored at 25°C with a CD spectropolarimeter. Increase in CD signal at 222 nm indicated loss of secondary structures. **(B)** Effect of GuHCl on KatB activity. Purified KatB protein (0.5 µg) was subjected to treatment with different concentration of GuHCl as indicated in the figure for 30 minutes at room temperature and subsequently its activity was measured. Activity in absence GuHCl was considered as 100% to calculate the relative rate of the rests. Error bars represent SE.

The loss of secondary structure in presence of various concentration of GuHCl was monitored by CD spectropolarimetry (Fig. 4.8 A). KatB could withstand upto 0.2 M of GuHCl without any marked loss of secondary structure during the assay period (600 seconds). However as the GuHCl concentration was raised to 0.4 M, loss of secondary structure was evident almost immediately. The KatB protein was also exposed to different concentrations of GuHCl for 30 min at room temperature and analysed for catalase activity on a spectrophotometer. The protein could retain 40% of its original activity after treatment with 0.25 M GuHCl. However, it became inactive when incubated with 0.5 M GuHCl (Fig. 4.8).

#### **4.9 Crystal structure of the KatB protein**

As mentioned in the introduction part, the structural aspects Mn-catalases are poorly explored. Crystal structure of only two Mn-catalases (LPC, Mn-catalase from *Lactobacillus plantarum* and TTC, Mn-catalase from *Thermus thermophilus*) have been solved to date. Keeping this in mind, the KatB protein was crystallized and its molecular structure was determined. Crystallography and structural analyses were carried out by our collaborator, Dr. Subhash C. Bihani, RBHSD, BARC. The crystallization conditions, X-ray diffraction, data collection, determination of the crystal structure etc were done as described [215, 244].

#### 4.9.1 Four-helix bundle type architecture of KatB

Similar to the other two Mn-catalases with available crystal structure (LPC and TTC), the KatB protein was arranged as four helix bundle-fold type architecture specific to ferritin super-family (Fig. 4.9.1). The four helices were labelled as helix-A, helix-B, helix-C and helix-D. These helices were arranged as a pair of anti-parallel helices. There was a long BC loop which connected helix-B and the helix-C in reverse orientation. The active site contained two Mn atoms. The bi-metallocore was buried in the central region of the four-helix core which was flanked by a long C-terminal tail and a relatively short N-terminal region.

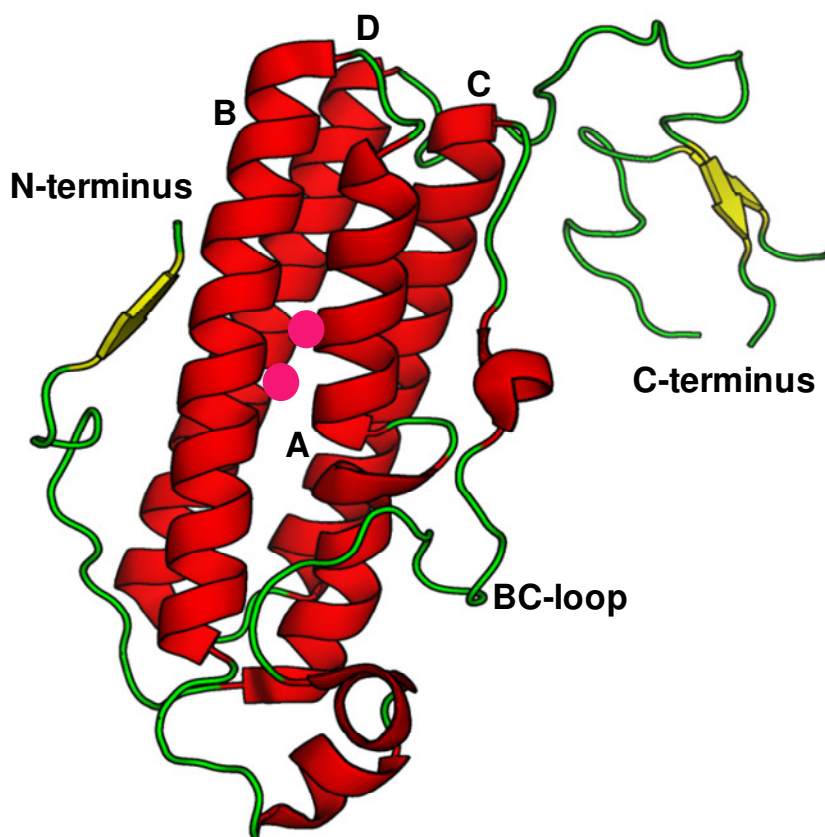


**Fig. 4.9.2 Structure of an individual KatB monomer.** The 4-helix bundle architecture of the KatB monomer with bimetallocore positioned at the centre. Mn ions are depicted by magenta spheres. The helices are labeled as 'A', 'B', 'C' and 'D'.

### 4.9.2 Hexameric assembly of the KatB protein

Overall, the KatB monomers were arranged in a triangular hexamer where the N- and C-terminal regions were involved extensively in the oligomerization of the individual monomers. Hexamer of KatB was arranged as trimer of dimers with dimer forming the core of the assembly (Fig. 4.9.2 A & Fig. 4.9.2 B). The space filling model of KatB hexamer indicated the compact nature of the oligomer (Fig. 4.9.2 B).

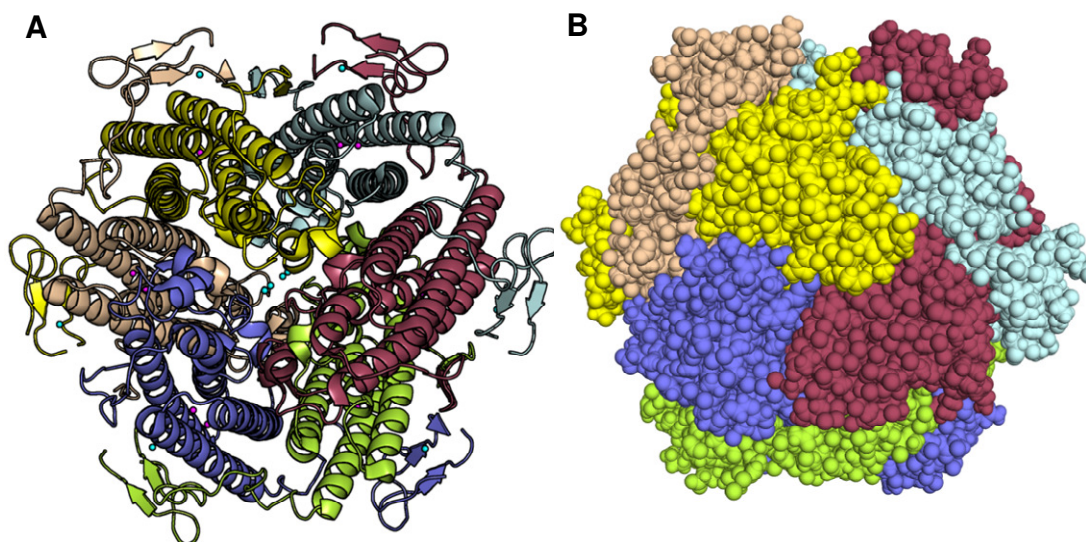


**Fig. 4.9.2 Crystal structure of KatB.** (A) Cartoon representation of the KatB protein showing hexameric organization (trimer of dimer) with dimer as core of the unit. The Ca<sup>2+</sup> atoms are represented by cyan sphere while, the Mn atoms at the active site is represented by magenta spheres. (B) Space filling model of KatB showing a very compact hexameric assembly.

### 4.9.3 Bi-manganese core structure of KatB

Each of the two Mn<sup>2+</sup> atoms in the active site was found to be coordinated with 3 glutamates, 1 histidine and 1 solvent molecule in an octahedral geometry (Fig. 4.9.3). Thus the arrangement of the bimetallo core is typical to the canonical Glu<sub>4</sub>His<sub>2</sub> coordination with two terminal water molecules. The Glu-65 from helix B and Glu-163 from helix D simultaneously coordinated both the Mn<sup>2+</sup> ions in monodentate binding mode. On the other hand Glu-35 from helix A and Glu-133 from helix C interacted

individually with Mn1 and Mn2 respectively in a bidentate chelating mode. The Mn1 and Mn2 are also coordinated by His-68 and His-166 respectively. However, the sixth coordination site of Mn1 or Mn2 was not occupied by any amino acid. These two sites, *trans* to the His-68 or His-166, were found to be occupied by two terminal water molecules (Fig. 4.9.3).

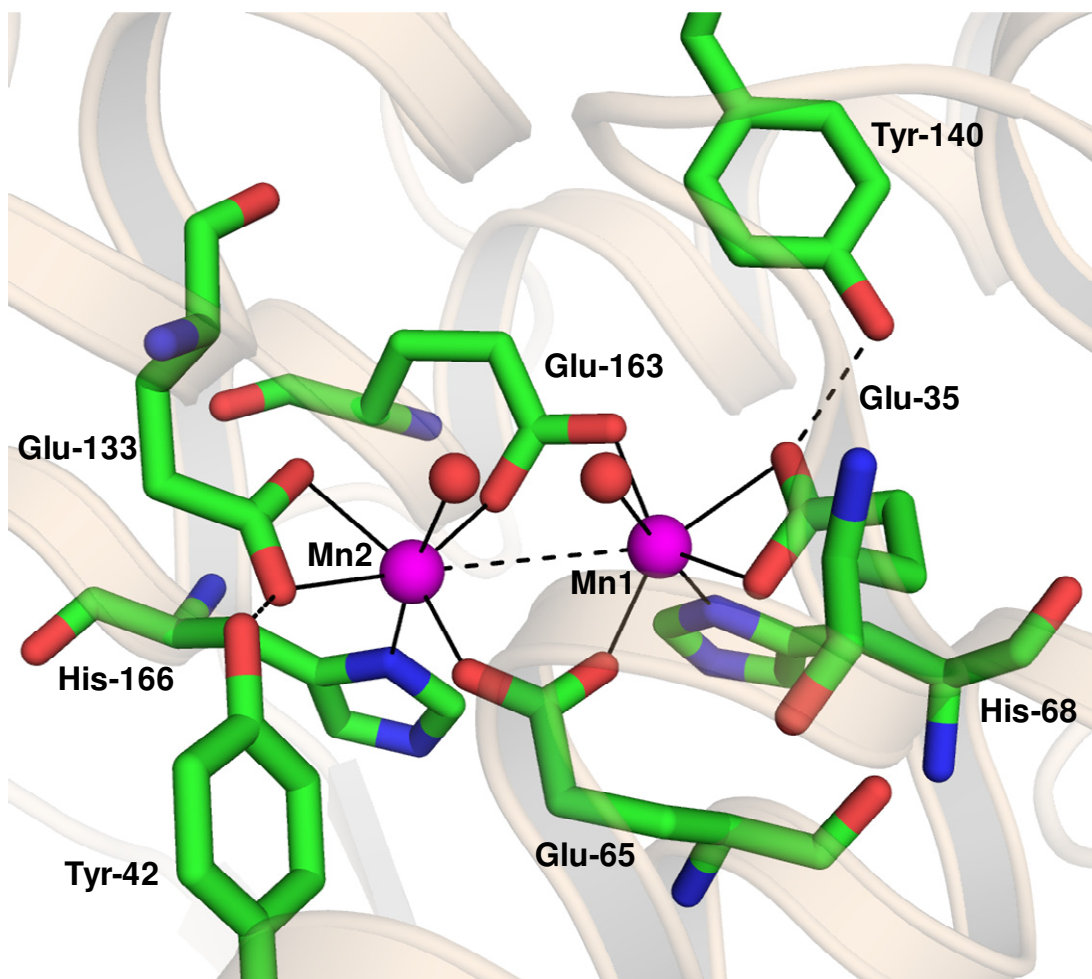


**Fig. 4.9.3 Active site configuration of KatB.** The two Mn ions (magenta spheres) are held with canonical Glu<sub>4</sub>His<sub>2</sub> coordination geometry. The two terminal water molecules (W1 and W2) are depicted as cyan spheres.

#### 4.9.4 Comparison of KatB active site with that of LPC or TTC

Structural superposition of KatB active site and that of LPC or TTC indicated that there were few unique features in the KatB active site.

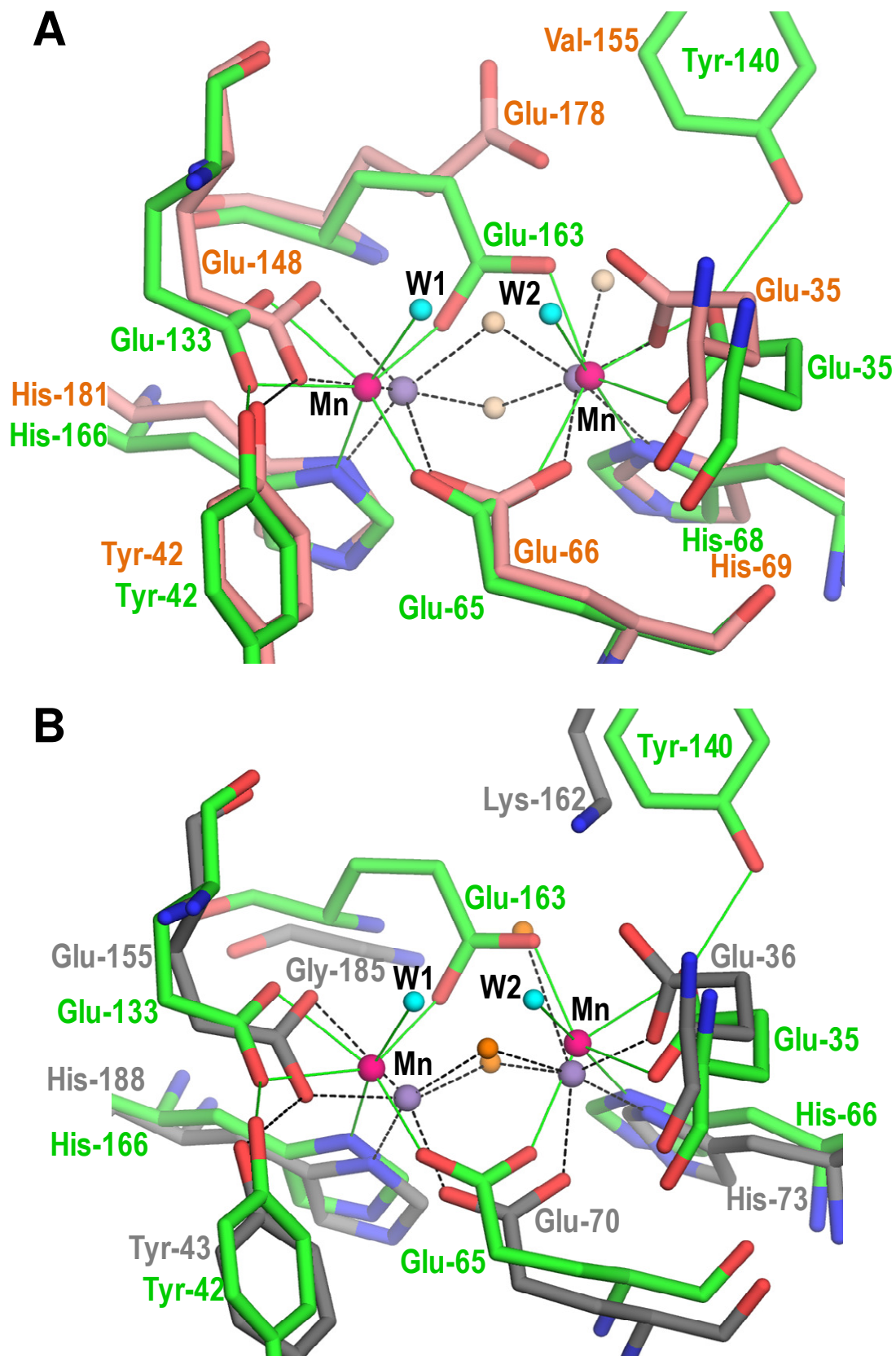


**Fig. 4.9.4 Active site comparison.** The KatB structure is shown in green color with active site water molecules as cyan spheres. Mn atoms in KatB are shown as magenta sphere. Mn atoms in LPC or TTC

are shown as grayish sphere. (A) Superposition of KatB active site with that of LPC (PDB Id 1JKU). LPC active site structure is shown in red color. The water molecules of LPC are shown as whitish spheres. Presence of Tyr-140 in KatB and its strong hydrogen bonding with Glu-35 affects the configuration of Glu-35 and Glu-163 as compared to LPC's Glu-35 and equivalent Glu-178. (B) Comparison of active site of KatB with that of TTC (PDB Id 2V8U). The TTC structure is shown in grey color Lys-162 and Gly-185 in TTC are the equivalent residues of Tyr-140 and Glu-163 respectively in KatB.

There were two bridging glutamate residues (Glu-65 and Glu-163) in KatB, which interacted with both the Mn atoms simultaneously (Fig. 4.9.3). Unlike KatB, LPC and TTC had only one bridging glutamate. The non-bridging glutamates (Glu-35 and Glu-133) in KatB interacted with the Mn atoms in bidentate fashion. But in LPC and TTC one of these two glutamates interacted in a monodentate mode (Fig. 4.9.4 A and Fig. 4.9.4 B) [122].

Unlike LPC and TTC, the Tyr-140 residue made second shell hydrogen-bonded interactions with the non-bridging glutamates, Glu-35 and Glu-133 in KatB (Fig. 4.9.4 A and B). Thus the KatB active site region was characterized by the presence of two unique residues, Glu-163 and Tyr-140. It is important to note here that the Tyr-42 residue is conserved in all the structures that were compared in this study. But the other second shell interacting residue (Tyr-140) is a unique feature of KatB and other proteins that have canonical  $\text{Glu}_4\text{His}_2$  coordination.

#### **4.10 Site directed mutagenesis of the important second shell interacting residues**

As per the crystal structure of KatB active site, the Tyr-42 and the Tyr-140 residues were the important second shell interacting, hence site directed mutagenesis was performed to assess their role in KatB structure-function.

#### 4.10.1 Substitution of Tyr-42 by phenyl alanine

The Tyr-42 residue of the KatB protein was replaced by Phe residue employing a suitable set of custom made primers (Table 2.2). This variant ORF was cloned into pET21a expression vector and the recombinant plasmid was transformed into *E. coli* BL21 (DE3) pLysS expression host. Following induction by IPTG the protein could be purified to near homogeneity by NiNTA-based affinity chromatography (protein named as KatBY42F) (Fig. 4.10.1 A).

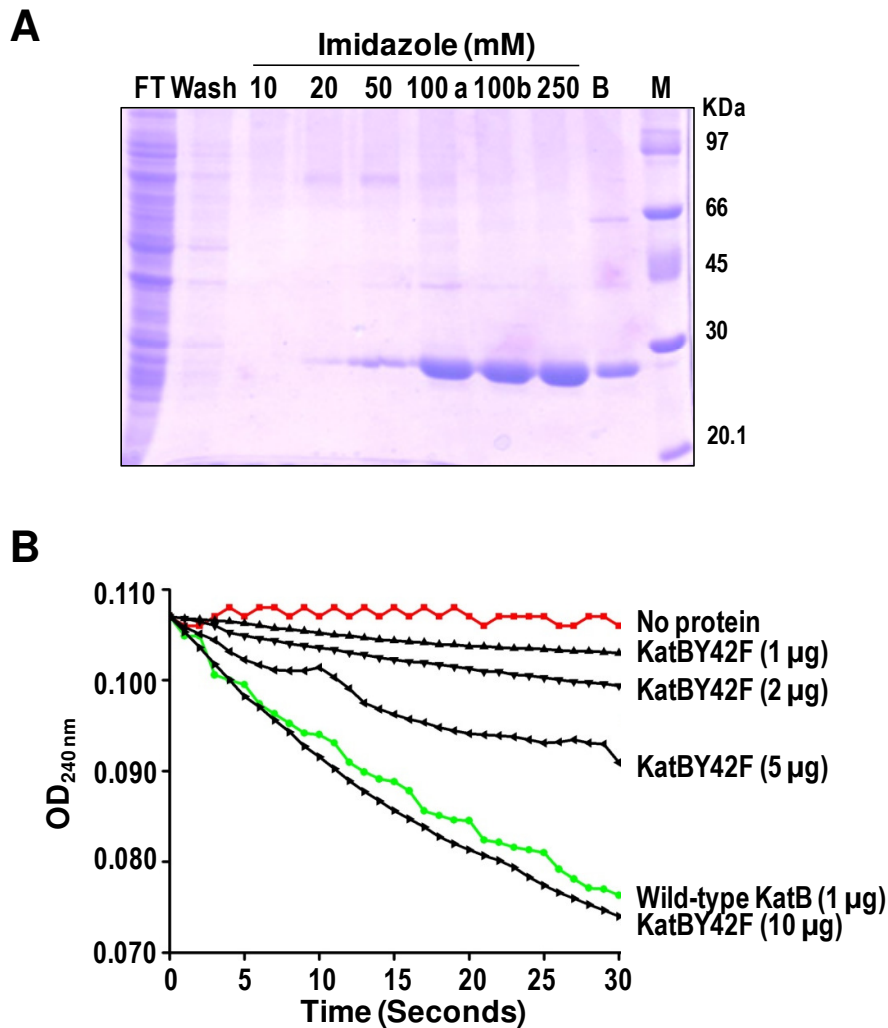


**Fig. 4.10.1 Site directed mutagenesis of Tyr-42 in KatB.** (A) Purification of KatBY42F. Cell extract of *E. coli* strain over-expressing KatBY42F was allowed to bind to NiNTA, washed thoroughly and the bound protein was eluted by increasing the imidazole concentration in the buffer as indicated. FT, flow-

through. **(B)** Spectrophotometric determination of H<sub>2</sub>O<sub>2</sub> decomposition activity by wild-type KatB or by KatBY42F. Reaction was performed with 2 mM H<sub>2</sub>O<sub>2</sub> substrate in 1 ml of 20 mM tris buffer, pH 8.0.

Subsequent spectrophotometric H<sub>2</sub>O<sub>2</sub> decomposition assay showed this mutation to severely affect the catalase activity. 10 times more of the KatBY42F variant protein had to be added in the reaction mixture to obtain activity comparable to that of the wild-type protein (Fig. 4.10.1 B).

#### 4.10.2 Substitution of Tyr-140 by phenyl alanine

The Tyr-140 is unique to KatB and not present in LPC or TTC. Tyr-140 residue of KatB was replaced by phenyl alanine by site directed mutagenesis and the variant ORF was ligated into pET21a expression vector. The resultant plasmid was transformed into *E. coli* BL21 (DE3) pLysS expression host. The recombinant variant KatB protein (named as KatBY140F) was purified from the *E. coli* cells following IPTG induction. The purified protein showed mobility that was similar to that of the wild-type KatB protein on native PAGE (10%), indicating no alteration in the compactness of the KatBY140F oligomer (Fig. 4.10.2 A).

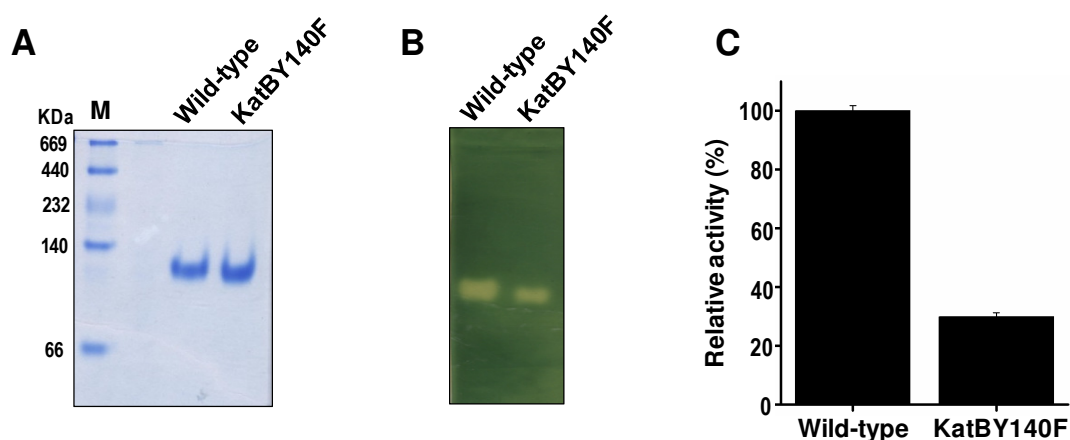


**Fig. 4.10.2 Site directed mutagenesis of Tyr-140 in KatB.** The purified wild-type KatB protein or KatBY140F (1  $\mu$ g each) was resolved on native polyacrylamide gels (10%) and visualized by staining with CBB **(A)** or zymographic analysis **(B)**. **(C)** Spectrophotometric H<sub>2</sub>O<sub>2</sub> decomposition activity shown

by the wild-type KatB protein or the KatBY140F variant. Activity of the wild-type protein was considered to be 100% and the activity of KatBY140F was calculated accordingly. Error bars represent SE.

On zymographic analysis, a distinct reduction in zone of clearance compared to the wild-type protein was observed (Fig. 4.10.2 B). Spectrophotometric  $H_2O_2$  decomposition assay also indicated the KatBY140F variant to be almost 3-fold less active than the wild-type KatB protein (Fig. 4.10.2 C). These results showed that both these second shell interacting residues were important for KatB activity, however, the compactness of the enzyme was independent of these residues.

#### **4.11 Discussion**

Catalases being highly active enzymes play an important role in detoxifying  $H_2O_2$  in all the three phylogenetic domains viz. Eukaryota, Bacteria and Archaea. Mn-catalases form a minor gene family in cyanobacteria, but remarkably, all nitrogen-fixing cyanobacteria have at least one ORF that encodes a Mn-catalase. In this chapter, a comprehensive biochemical and structural characterization of the Mn-catalase, KatB, from the nitrogen-fixing cyanobacterium, *Anabaena* PCC 7120, was performed.

When overproduced in *E. coli*, a substantial portion of the over-produced protein was found to be present in the insoluble fraction. Although, solubility of this over-expressed protein was enhanced to some extent by lowering the temperature post induction, a marked improvement in production of the soluble protein was observed when  $MnCl_2$  was added to the *E. coli* growth medium (Fig. 4.4 A and Fig. 4.4 B). Supplementation of  $Mn^{2+}$  also enhanced activity of the purified protein by 40% compared to the same protein purified from *E. coli* grown on LB medium without  $Mn^{2+}$  supplementation (Fig. 4.4 C). Similar to KatB, the Mn-catalase from *Geobacillus* sp.WCH70 also showed

improved solubility when  $Mn^{2+}$  was added to the *E. coli* growth medium during induction [245]. In few cases, supplementation of exogenous Mn to the growth medium has enhanced activity of the heterologously over-expressed Mn-catalase. For example, when Mn-catalase from *Metallosphaera hakonensis* (an alkali tolerant, thermophilic bacterium) was expressed in *E. coli*, addition of  $Mn^{2+}$  led to production of active enzyme, while in the absence of  $Mn^{2+}$ , the enzyme remained inactive in spite of being present in the soluble fraction [246]. Presumably,  $Mn^{2+}$  incorporation of into the active site region of KatB aids in proper folding of the enzyme in *E. coli* which consequently leads to substantial increase in solubility and the production of active KatB protein.

In contrast to these observations, Mn-catalase from *Thermus thermophilus* and *Thermus* sp. YS 8-13 did not show any catalase activity in spite of being partitioned in the soluble fraction when overproduced (with exogenously added  $Mn^{2+}$ ) in *E. coli* [247, 248]. In contrast to these Mn-catalases, KatA, the other Mn-catalase from *Anabaena* or the Mn-catalase from *Geobacillus thermopakistaniensis* were found to be completely in the inclusion bodies when over-produced in recombinant *E. coli* strains [200, 124]. Unlike KatB or the other above-mentioned Mn-catalases, exogenous addition of  $Mn^{2+}$  in the *E. coli* growth medium did not improve their solubility, indicating the inability of *E. coli* to fold these proteins appropriately.

Mn-catalases are relatively insensitive to inhibition by azide but are rapidly inactivated by hydroxylamine [121, 163]. Although, large scale genome sequencing projects have shown the presence of Mn-catalases in several bacteria, it is possible that some of these assignments may not be correct [122]. The Z1921P (Mn-catalase) protein from *E. coli* O157:H7 was purified as a soluble hexameric protein, but surprisingly, the protein neither showed any catalase activity nor did bind to  $Mn^{2+}$ . The KatB protein from

*Anabaena* PCC7120, which was annotated as a hypothetical Mn-catalase in “Cyanobase”, showed classical hallmark of Mn-catalases, i.e., insensitivity to azide (Fig. 4.6.4 B) indicating that it is indeed a bona fide Mn-catalase.

Mn-catalases are generally hexameric in nature [130, 131]. However, as per gel filtration analysis and native PAGE analysis KatB appeared to be tetrameric (Fig. 4.5.1). Similarly, Mn-catalase from *Pyrobaculum calidifontis* VA1 was reported to be homotetrameric based on gel filtration analysis [108]. However, subsequent X-ray crystallography-based structural analysis has shown KatB to be homohexameric (Fig. 4.9.2 A). Incidentally, the monomers of KatB are arranged very compactly in the hexameric assembly (Fig. 4.9.2 B). Thus causes slower migration, resulting in delayed elution in gel filtration analysis or faster movement in native PAGE, hence appearing as an (apparent) tetramer.

Unlike the peroxiredoxins, which have  $K_m$  values for  $H_2O_2$  in  $\mu M$  range [95], all the reported Mn-catalases have  $K_m$  values in mM range. In case of KatB, the  $K_m$  value was worked out to be  $3.29 \pm 0.95$  mM which was comparable to that of other biochemically characterized Mn-catalases (Table 4.1).

**Table 4.1 Kinetic parameters of biochemically characterized Mn-catalases**

Mn-catalase	$K_m$	$k_{cat}$	Reference
	mM	$s^{-1}subunit^{-1}$	
<i>L. plantarum</i>	350	$3.3 \times 10^4$	[121]
<i>T. thermophilus</i>	83	$2.6 \times 10^5$	[123]
<i>T. album</i>	15	$6.2 \times 10^3$	[249]
<i>P. calidifontis</i>	170	$2.9 \times 10^4$	[108]
<i>Geobacillus</i> sp. WCH70	67.26	$2.9 \times 10^4$	[245]
<i>G. thermopakistansis</i>	260	$1.04 \times 10^4$	[124]
<i>T. roseum</i>	20	$2.02 \times 10^4$	[250]
KatB	3.29	$1.15 \times 10^5$	This study

Like other Mn-catalases [108, 245], KatB also showed maximal activity at alkaline pH (i.e. pH 8.5) (Fig. 4.6.3). In previous chapter, the role of KatB protein in combating the salinity stress was discussed in details. In this regard, the effect of addition of NaCl on activity of this enzyme was also tested. Surprisingly, KatB showed substantial activity in the presence of high concentrations of NaCl (Fig. 4.6.5), demonstrating the ability of this enzyme to withstand extreme saline environments.

As discussed earlier, bi-functional catalase-peroxidases (KatGs) are prevalent in cyanobacteria. Compared to KatGs, Mn-catalases are relatively more thermostable in nature. Mn-catalases from the extremophilic bacteria are known to be thermostable [108, 124, 245]. Earlier studies showed that the other Mn-catalase from *Anabaena* PCC 7120 (KatA, Alr0998) was a thermostable enzyme, while KatG from *Synechococcus* PCC 7942 was found to be thermolabile, losing activity at temperatures beyond 50°C [200]. Similarly, Mn-catalase from another mesophilic bacteria *Lactobacillus plantarum* was also thermostable. CD spectropolarimetric analysis revealed that the secondary structure of the purified KatB protein was intact even after exposure to around 90°C (Fig. 4.7), suggesting that like KatA, KatB too was a thermostable protein. Put together, these reports show that thermostability is a general property of Mn-catalase and not restricted to thermophiles. Presence of thermostable Mn-catalases in mesophilic organisms like *Anabaena* is perplexing, but suggests the possible inheritance of this protein from thermophilic bacteria by lateral transfer.

Sequence comparison of KatB with TTC and LPC showed crucial differences between these proteins. Crystal structure of KatB, which is in fact the first manganese catalase to be structurally characterized from any photosynthetic organism, has helped in understanding the structural alterations due to these differences. Comparison with TTC

and LPC structures provided useful information about the uniqueness of the KatB protein within the overall architectural similarity shown by Mn-catalases. General comparison of the three structures (LPC, TTC and KatB) showed that residues forming primary coordination sphere of  $Mn^{2+}$  ions were well conserved. Other conserved residues either were in the secondary coordination sphere or were involved in crucial interactions. All three manganese catalases with available crystal structure showed similar four-helix core arranged in the form of complex hexameric assembly.

The KatB active site contains two Mn atoms. The atoms are coordinated by Glutamate and histidine residues. The crystal structure of KatB protein showed that the active site had canonical  $Glu_4His_2$  coordination [137], while the active sites of TTC or LPC had a modified  $Glu_3His_2$  coordination [130, 131]. In KatB, two glutamates, Glu-65 and Glu-133 coordinated  $Mn^{2+}$  ions in bridging mode. However, LPC and TTC active site showed only one glutamate in bridging mode. While residue equivalent to Glu-65 is present in LPC and TTC, there are differences at residue corresponding to Glu-163. In LPC, equivalent glutamate, Glu-178 does not ligate metal ions and in TTC a glycine, Gly-185, replaces glutamate at this position (Fig. 4.9.4). Therefore, LPC and TTC active site has only one as opposed to two bridging glutamates as in KatB. Based on the uniqueness of the KatB active site compared to LPC or TTC, an alternate mode of  $H_2O_2$  binding was proposed [244]. Recently, modern computational approaches were employed to decipher the mechanism of  $H_2O_2$  decomposition by KatB based on the high-resolution structure of this protein. Due to presence of  $Glu_4His_2$  conformation, considerable differences were found between the reaction mechanism of KatB and TTC [251].

Interestingly, the KatB active site was found almost identical to the active site of *Desulfovibrio* bacterioferritin [252] except for the nature of metal ions [244]. Higher structural similarity of KatB with bacterioferritin, together with the presence of an identical bimetallocentre, strongly supports an evolutionary link between Mn-catalases and bacterioferritins. Structure of KatB active site suggests that nature has successfully recruited an ancient bacterioferritin protein for H<sub>2</sub>O<sub>2</sub> decomposition without having to change the core of the active site.

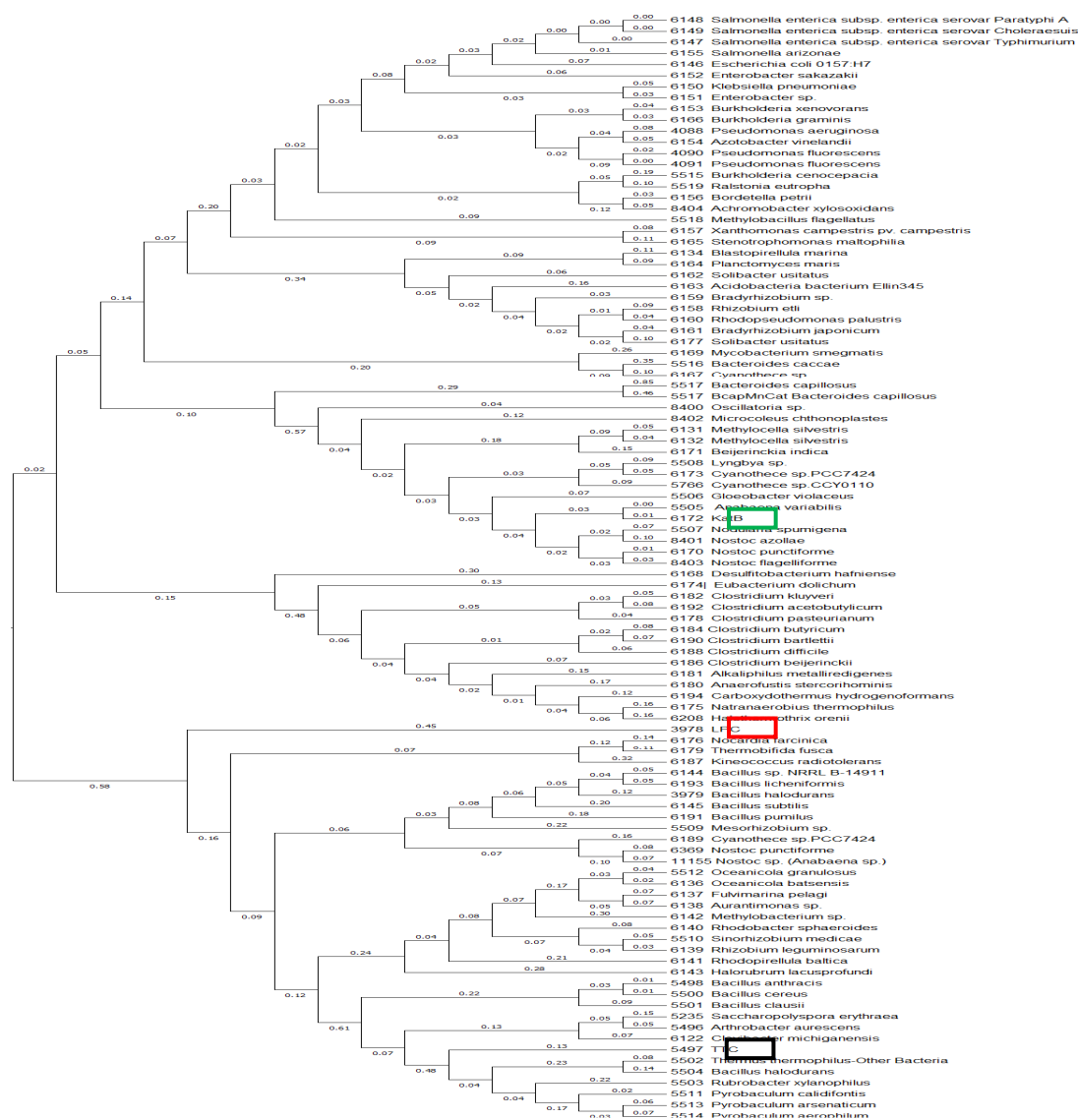


Fig. 4.11 Phylogenetic analysis of catalases present among various taxa. KatB, LPC and TTC are indicated in green, red and black box respectively.

Phylogenetic analysis (Fig. 4.11) with Mn-catalase sequences from various genera indicated that there are two broad groups among Mn-catalases [244]. Interestingly, all the Mn-catalases in the group in which KatB belongs, shows the combined presence of the two unique active site residues, Glu-163 and Tyr-140. Mn-catalase from *Halothermothrix orenii*, considered to be at the origin of ferritin superfamily [253], is in the same group with KatB and shows identical residues at location corresponding to Glu-163 and Tyr-140 of KatB. Therefore, it was argued that the active site configuration of KatB is more basic compared to the other two Mn-catalases with available crystal structure (LPC and TTC) [244]. Simple mutation of Glu163/Tyr140 allowed KatB configuration to change to that of LPC and TTC. Both these mutations effectively removed the steric hindrance for the water molecules to occupy the positions as seen in LPC and TTC.

Structural analysis suggests that interactions of secondary coordination sphere are considerably different in KatB as compared to that LPC or TTC. Both non-bridging glutamates in KatB, Glu-35 and Glu-133 make second shell hydrogen bond interaction with Tyr-140 and Tyr-42 respectively (Fig. 4.9.3 & Fig. 4.9.4). These inter-helix hydrogen bond interactions may provide stability to the bimetallocore and play important functional role. Of these two important second shell interactions, the interaction between Tyr-42 and one of the non-bridging glutamate is conserved in other related proteins too. However, Tyr-140, which interacts with the other non-bridging glutamate, is unique to KatB and not present in TTC or LPC wherein only one of the glutamates has tyrosine as hydrogen bonding partner (Fig. 4.9.4). The interaction between Tyr-42 and Glu-133 in KatB is equivalent to the one found in LPC [Glu-148---Tyr-42] or TTC [Tyr-43---Glu-155]. Interestingly, this glutamate binds Mn<sup>2+</sup> in

bidentate ligating mode. Evidences from other studies show that this conserved tyrosine residue forms a phenoxyl free radical that serves as the hydrogen abstraction site during catalysis [254]. In LPC, the role of this residue (Tyr-42) in maintenance of structural integrity was established by site directed mutagenesis [254]. In our study too, site directed mutagenesis of Tyr-42 resulted in severe drop in catalase activity in KatB, suggesting its important role in maintaining the active site architecture (Fig. 4.10.1).

The other tyrosine residue that strongly interacts with the other non-bridging glutamate is Tyr-140 and this interaction is unique to KatB (i.e. not present in LPC or TTC). The Tyr-140 is replaced by Val-155 in LPC and by Lys-162 in TTC (Fig. 4.9.4). Substitution of bulky and rigid Tyr-140 with Val, allows the non-bridging Glu-33 to be more flexible in LPC. Due to the increased flexibility and space created by this substitution, Glu-33 rotates and adopts monodentate interaction with Mn1. Similarly, TTC has flexible lysine in place of rigid tyrosine allowing Glu-36 to have both monodentate and bidentate interactions with Mn1. Site directed mutagenesis was performed to establish the role played by Tyr-140 in KatB. The result suggested that upon substitution of Tyr-140 with Phe (which has the aromatic ring structure but lacks the hydroxyl group) the activity of the enzyme dropped by 60% (Fig. 4.10.2). This indicates the crucial role played by this important second shell interacting residue.

To summarize, KatB, the first Mn-catalase to be biochemically/structurally characterized from any photosynthetic organism, was shown to be robust protein with ability to withstand high temperature/ionic strength. Structural analysis showed the KatB monomers to have a four-helix bundle fold and a compact hexameric assembly. The active site of KatB was quite distinct from that of the other characterized Mn-

catalases and resembled that of ferritin, indicating that nature has fruitfully enlisted a primeval bacterioferritin/ruberythrin like protein for  $H_2O_2$  detoxification without altering the main structure of the active site.



## **CHAPTER 5**

# **Role of N-Terminal Region in Maintenance of KatB Structure- Function**



## 5.1 Introduction

Cyanobacteria, the ancient photosynthetic organisms, were the first microbes to combine both the photosystems, PSI and PSII, which eventually lead to the release of oxygen as a by-product during photosynthesis [144, 255]. Given their intimate association with oxygen, cyanobacteria have evolved an elaborate network of proteins for management of oxidative stress [148, 256]. Among the two Mn-catalases present in *Anabaena*, the KatB protein was shown to be important in adaptation to salinity stress and the detailed biochemistry and structural analysis this protein was performed (discussed in previous chapters).

Compared to the heme catalases, Mn-catalases have been poorly characterized. Apart from KatB, crystal structures of only two other Mn-catalases i.e. *Thermus thermophilus* (TTC) and *Lactobacillus plantarum* (LPC) are known [130, 131]. Active site of the KatB was found to be distinctly different from the other two Mn-catalases with available crystal structure. Instead of  $\text{Glu}_3\text{His}_2$  coordination, a canonical  $\text{Glu}_4\text{His}_2$  coordination was observed at the bi-metallocore active site of KatB, suggesting an alternative mode of substrate binding. The crystal structure of LPC indicated that the short N-terminal region formed a  $\beta$ -strand, which interacted with the same  $\beta$ -strand from the neighbouring subunit. This antiparallel  $\beta$  assembly was very likely to be involved in the proper maintenance of the oligomeric structure [122]. Multiple sequence alignments also suggested that the first few N-terminal residues to be relatively conserved in Mn-catalases. These aspects suggested the relatively short N-terminal region to play a crucial role in KatB structure/function. The detailed structural and mutational analysis of the N-terminal region of the KatB protein is described in this chapter. Subsequently, the important role played the 2<sup>nd</sup> amino acid (Phe-2) in KatB

structure-function, which was elucidated by biochemical as well as structural analysis of the KatB variant, KatBF2V, is also elaborated in this chapter.

## **5.2 Localization and importance of the N-terminal residues at the subunit interface**

Careful observation of the crystal structure of KatB (described in Chapter 4) revealed that the first few N-terminal residues were arranged as short  $\beta$ -strand. This  $\beta$ -strand interacted with the same strand from the other subunit of the core dimer in an antiparallel fashion to form a  $\beta$ -sheet (Fig. 5.2 A).

The N-terminal residues were found to be extensively involved in oligomerization of the KatB subunits and the core dimer (i.e. subunit A and B) was held together by extensive hydrogen bonding along with hydrophobic interactions. The network of hydrogen bonds in this antiparallel  $\beta$ -sheet is shown in the Fig. 5.2 B. As per the crystal structure, the residues from this antiparallel  $\beta$  sheet participated in hydrophobic interactions with residues from both the subunits including Lys-40, Trp-43, Ile-63, Phe-66 (Fig. 5.2 B). The bulky and highly hydrophobic second amino acid residue (Phe-2) was found to be involved in strong hydrophobic inter and intra subunit interactions.

Presence of extensive interactions involving the N-terminal residues suggested that although not present in the active site region, these residues are likely to play major role in maintaining the structural integrity of this protein.

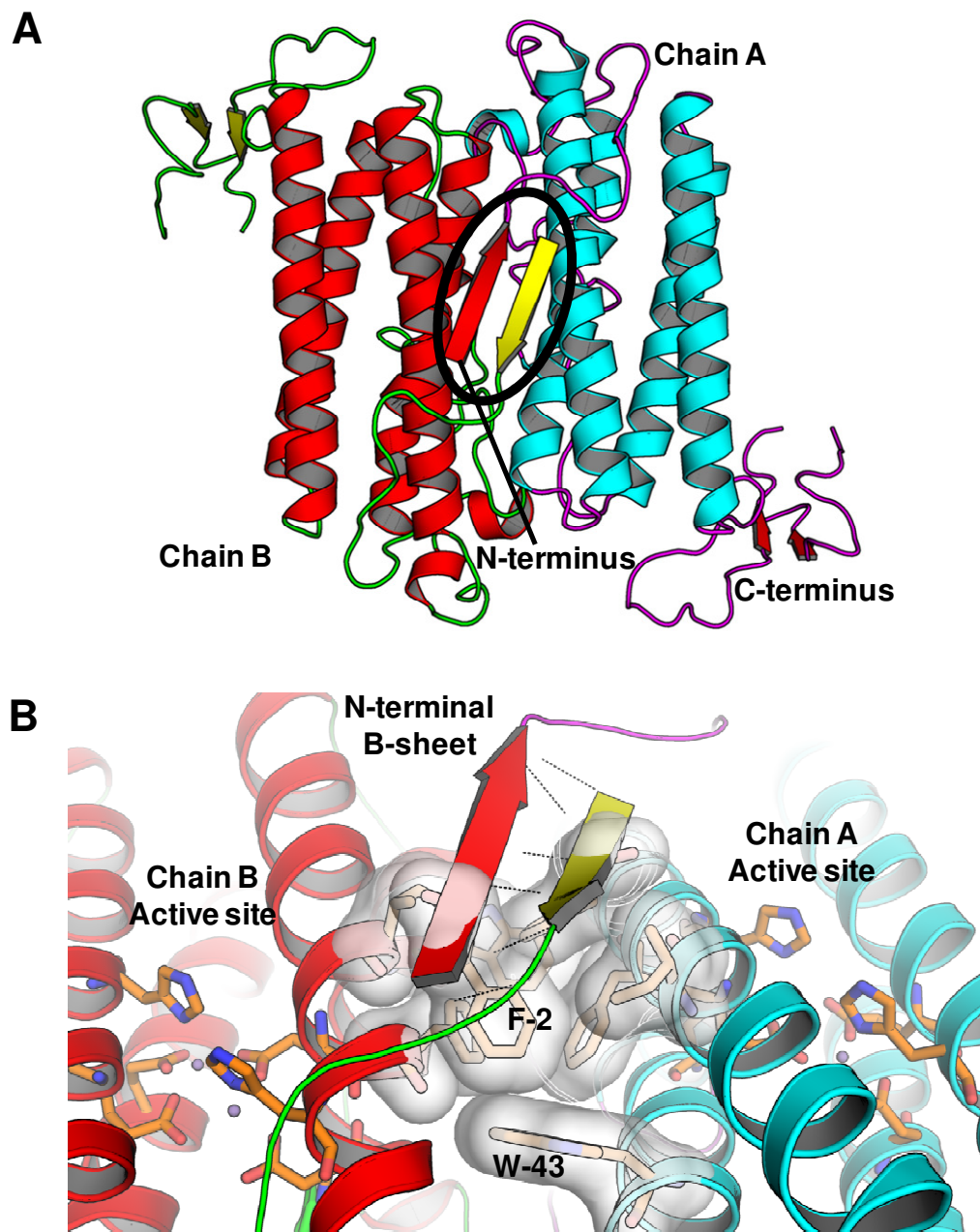


**Fig. 5.2 The N-terminal  $\beta$ -sheet and hydrophobic interactions of the relevant residues.** (A) Cartoon representation of the core dimer of KatB structure. Antiparallel  $\beta$ -sheet involving the N-terminal residues is circled. (B) Cartoon representation of interface region at dimer core in KatB crystal structure. Hydrogen bonds forming the N-terminal  $\beta$ -sheet are shown as dotted lines. The hydrophobic patch interconnecting chain A and chain B from both the subunits and the N-terminal  $\beta$ -sheet is shown .

### 5.3 Sequence conservation of the N-terminal region

To analyze N-terminal sequence similarity of Mn-catalases in general, the amino acid sequences of Mn-catalases from the RedoxiBase database [210] were downloaded and

aligned using ClustalW. A representative alignment file is shown in Fig. 5.3 A. All the cyanobacterial Mn-catalase sequences were also aligned and compiled to generate a sequence logo (Fig. 5.3 B).

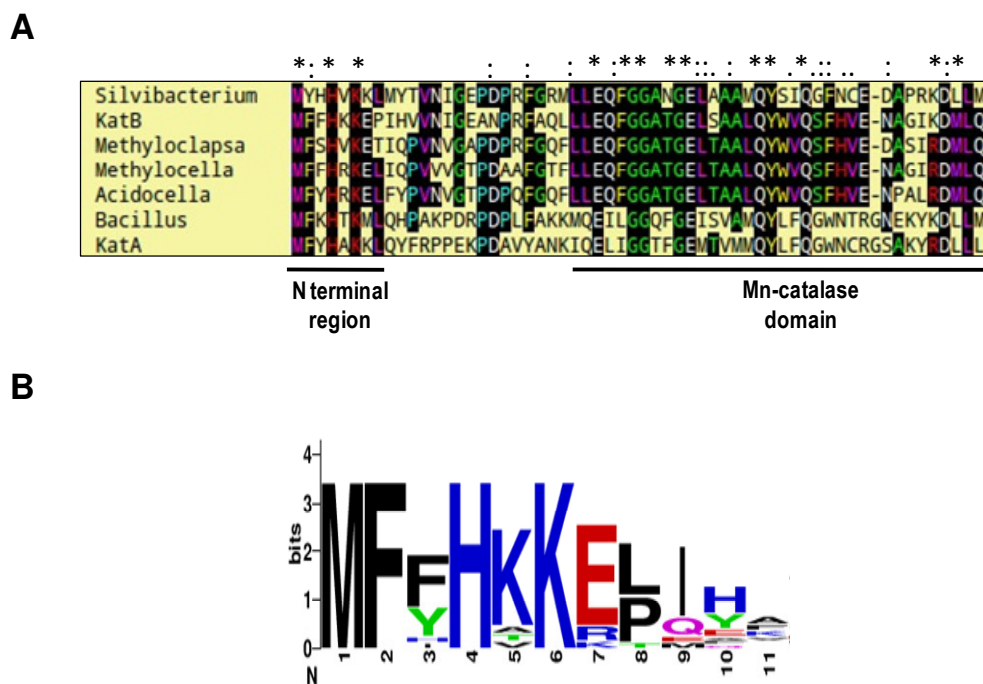


**Fig. 5.3 Sequence analysis of the N-terminal region of Mn-catalases.** (A) A representative multiple sequence alignment file depicting Mn-catalases from various organism as mentioned in the figure. KatA or KatB are the two Mn-catalases from *Anabaena* PCC 7120. Conserved and similar residues are marked by ‘\*’ and ‘.’ respectively. (B) Sequence logo generated after alignment of all the cyanobacterial Mn-catalases.

This analysis suggested that the N-terminal residues are relatively conserved in all cyanobacteria. The conservation of these residues in Mn-catalases indirectly indicated the importance of these in maintenance of KatB structure-function.

#### 5.4 Site directed mutagenesis of the N-terminal amino acid residues

To identify which of the N-terminal amino acids were more critical for function, site directed mutagenesis was employed to individually alter each residue (i.e residue number 2 to 7) in this stretch to alanine. By using forward primer with the desired mutation (Table 2.2) and the common reverse primer (KatB\_BamHis\_Rev, Table 2.2),

the different *katB* variants were PCR-amplified individually from the *Anabaena* genomic DNA. To facilitate purification by affinity chromatography, the reverse primer also contained six in-frame histidine codons for production of a his-tagged protein.

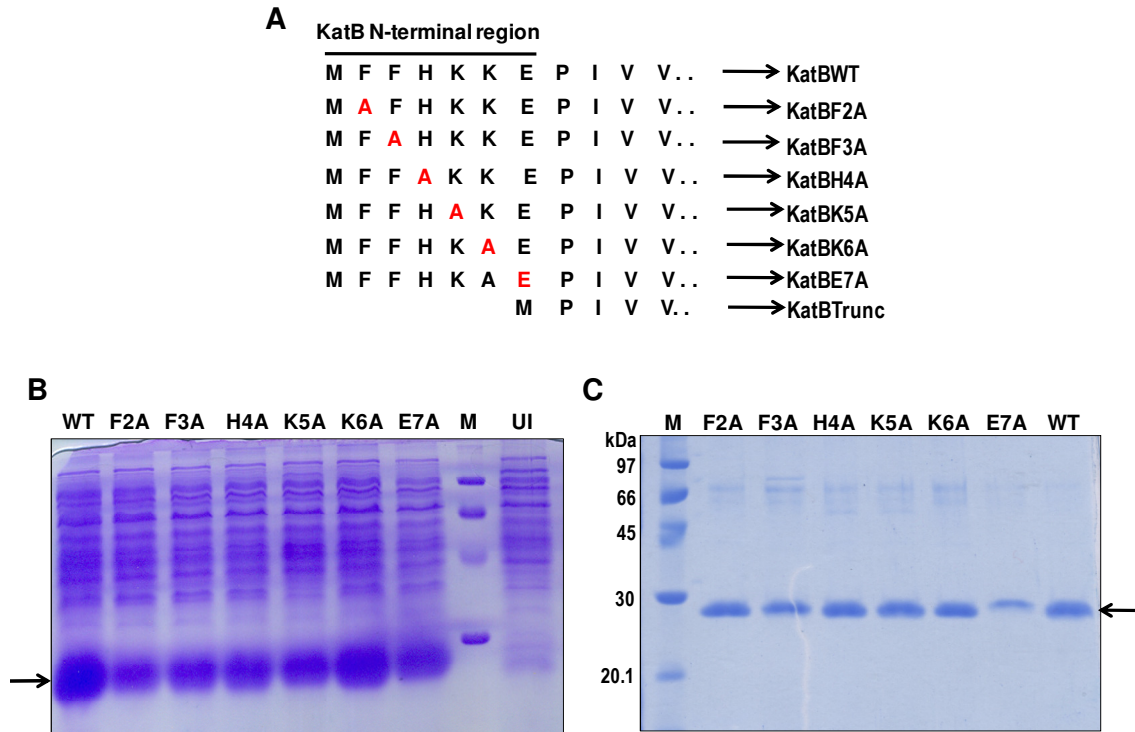


**Fig. 5.4 Site directed mutagenesis to generate N-terminal variants of KatB.** (A) Diagrammatic representation of all the N-terminal variants generated for the study. The first few amino acids are shown. Except for KatBTrunc, the substituted alanine residue is shown in red font. (B) Presence of over-expressed protein in the soluble fraction. The cell extracts from the N-terminal variant KatB over-producing *E. coli* strains were resolved by SDS-PAGE (14% acrylamide) and visualized by staining with CBB. WT, wild-type KatB protein (KatBWT); F2A, KatBF2A; F3A, KatBF3A; H4A, KatBH4A; K5A, KatBK5A; K6A, KatBK6A and E7A, KatBE7A; UI, un-induced sample from KatBWT over-expressing *E. coli* strain. The over-expressed protein band is indicated by an arrow (C) Purification of the N-terminal variants. All the purified proteins were resolved by SDS-PAGE and stained with CBB. The purified protein is indicated by an arrow.

All the mutated ORFs were individually ligated to pET21a as *NdeI*–*BamHI* digested fragments, and the corresponding plasmids (after sequencing to confirm the presence of the desired mutation) were transformed into *E. coli* BL21(DE3) pLysS for over-production and subsequent purification of the mutant KatB proteins. Along with these,

a KatB variant ORF, lacking 6 codons (i.e. from 2<sup>nd</sup> codon to 7<sup>th</sup> codon), was also generated by performing PCR with suitable forward primer (Table 2.2) and the same reverse primer (KatB\_BamHis\_Rev, Table 2.2). The variants thus generated were named as KatBF2A (Phe at 2<sup>nd</sup> position replaced with Ala), KatBF3A (Phe at 3<sup>rd</sup> position replaced by Ala), KatBH4A (His at 4<sup>th</sup> position replaced with Ala), KatBK5A (Lys at 5<sup>th</sup> position replaced with Ala), KatBK6A (Lys at 6<sup>th</sup> position replaced with Ala), KatBE7A (Glu at 7<sup>th</sup> position replaced with Ala) and KatBTrunc (wherein the original 2<sup>nd</sup> to 7<sup>th</sup> N-terminal residues were deleted) (Fig. 5.4 A). All the mutant proteins when over-expressed in *E. coli* were found to be present in the soluble fraction (Fig. 5.4 B) and could be purified to near homogeneity through NiNTA column chromatography (Fig. 5.4 C). The purified KatB variants were employed for biochemical and biophysical analyses along with the wild-type KatB protein (hereafter referred to as KatBWT).

### 5.5 Effect of the N-terminal residues on compactness of the KatB protein

All the N-terminal KatB variants (KatBF2A, KatBF3A, KatBH4A, KatBK5E, KatBK6A, KatBE7A and KatBTrunc) and the KatBWT protein were resolved on native polyacrylamide gels to ascertain the differences in their mobilities (Fig. 5.5 A).

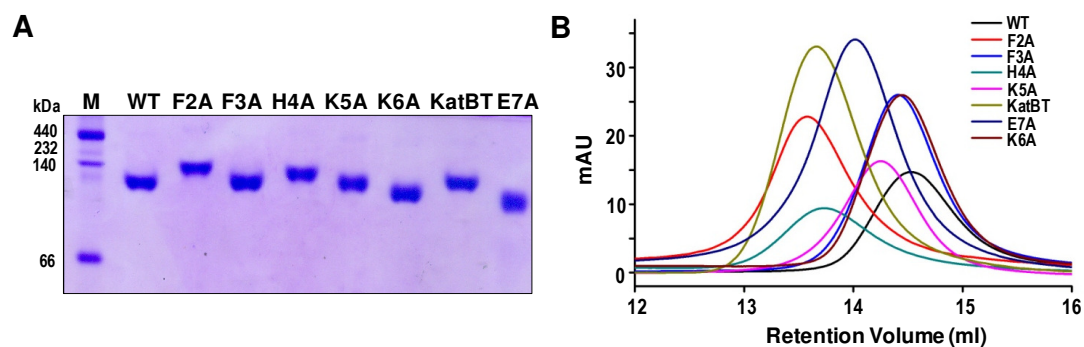


**Fig. 5.5 Compactness of the N-terminal variants of KatB.** (A) Native PAGE analysis. All the N-terminal variants along with the KatBWT (WT) were resolved (1  $\mu$ g each) by native 10% PAGE and visualized by CBB staining (KatBTrunc is depicted by KatBT) (B) Size exclusion chromatography

profile of the N-terminal variants. 200 µg of purified protein was injected into Superdex 200 10/300 GL column pre-equilibrated with buffer containing 20 mM Tris and 50 mM NaCl, pH 7.2.

KatBWT along KatBF3A, KatBK5A, KatBK6A and KatBE7A showed higher mobility on native PAGE than KatBF2A, KatBH4A or KatBTrunc, indicating that the former set of KatB proteins was more compact than the later. Gel filtration analysis revealed KatBWT, KatBF3A, KatBK6A or KatBK7A to be more compact as they eluted later than KatBE5A, which in turn eluted after KatBF2A, KatBH4A or KatBTrunc (Fig. 5.5 B). These results suggested that the N-terminal region was important for the structural compactness of the KatB enzyme, and within that region, few residues (Phe-2, His-4) played a more critical role in the structural integrity of this protein.

#### **5.6 Activity of KatB N-terminal amino acid substitution mutants**

To assess the effect of the above-mentioned N-terminal substitutions or truncation on activity, all the variants were subjected to spectrophotometric H<sub>2</sub>O<sub>2</sub> decomposition assays. The result suggested that KatBWT, KatBF3A, KatBK6A or KatBE7A were catalytically more active compared to the other variants. These variants showed appreciable catalase activity while, the KatBK5A showed considerably reduced activity. Other three N-terminal variants, KatBTrunc, KatBF2A or KatBH4A hardly showed any activity at all (Fig. 5.6). It should be noted that only the variants which were compact in nature as discussed in the previous section, showed appreciable catalase activity, whereas, the less compact variants (i.e KatBF2A, KatBH4A or KatBTrunc) were found to be inactive. These results suggested a good correlation between the compactness and activity of the KatB enzyme i.e. only compact enzyme showed activity.

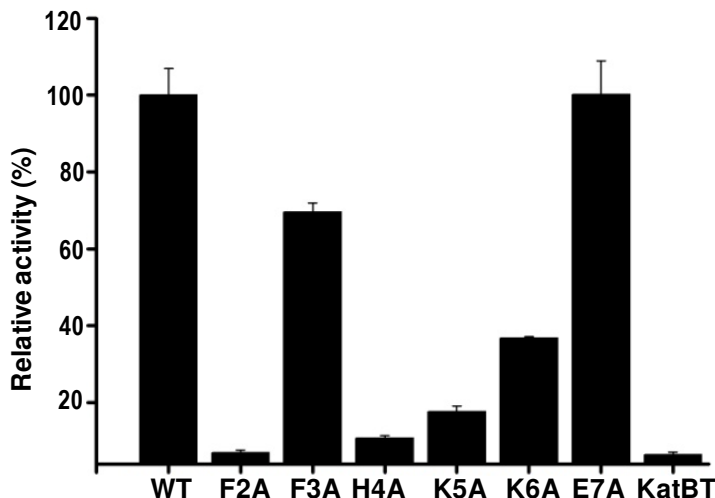


**Fig. 5.6 Catalase activity of the N-terminal variants.** H<sub>2</sub>O<sub>2</sub> decomposition activity exhibited by the different N-terminal variants was measured spectrophotometrically. Activity shown by the KatBWT was considered to be 100% and rests were calculated accordingly. Error bars represent SE.

### 5.7 Sensitivity of KatB mutants to chemical denaturation

Gel filtration and the native PAGE analysis indicated differential compactness of the KatB oligomer in the N-terminal KatB variants. The ability of these variants to withstand the effect chemical denaturant was evaluated. In the previous chapter, it was shown that the wild-type KatB protein (KatBWT) could tolerate up to 0.2 M GuHCl (Fig. 4.8). Hence, to assess the differential response to GuHCl-induced chemical denaturation, all the mutant proteins were treated with 0.2 M GuHCl and monitored for loss of secondary structure or activity. The secondary structure of the KatBWT or KatBE7A was found to be unaffected in the presence of the GuHCl used for this experiment (0.2 M), but in contrast, all other N-terminal variants showed a loss in secondary structure to various degrees as shown in Fig. 5.7 A. The catalytically active mutants were treated with various concentration of GuHCl for 30 min and assayed for catalase activity. As expected, the KatBWT and the KatBE7A were found to be most resistant to GuHCl while others (KatBF3A, KatBK5A and KatBK6A) were sensitive (Fig. 5.7 B).

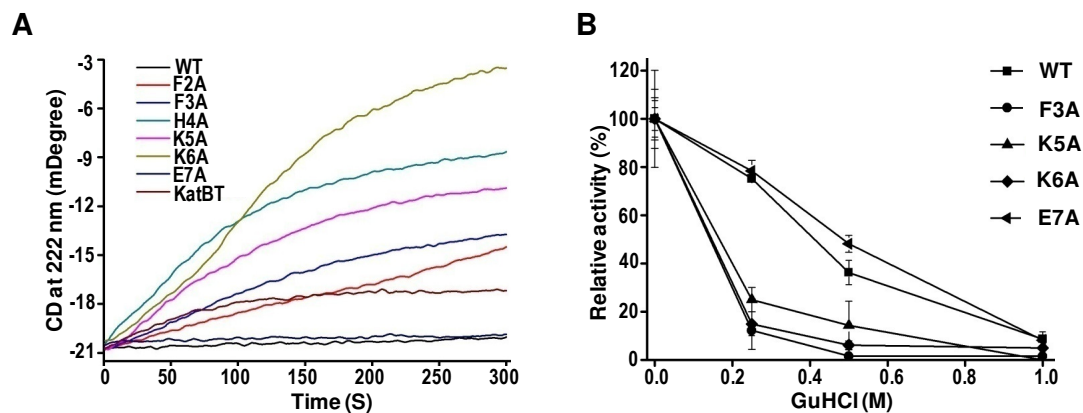


**Fig. 5.7 Sensitivity of the N-terminal variants towards GuHCl mediated chemical denaturation.** (A) Loss of secondary structure in presence of GuHCl. Purified proteins were mixed with 0.2 M GuHCl in quartz cuvette and change in ellipticity (mDegree) at 222 nm with time was monitored in a CD spectropolarimeter. (B) Each purified protein was treated with different concentration of GuHCl (as indicated) for 30 minutes at room temperature and assayed for H<sub>2</sub>O<sub>2</sub> decomposition activity. Activities of the variants without GuHCl treatment were considered to be 100% and others were calculated accordingly. Error bars represent SE.

All the above-mentioned results indicated that the amino acid residues present in the N-terminal  $\beta$ -strand were important for the stability of the KatB protein. Interestingly, as the Glu-7 residue is not the part of the  $\beta$ -strand, its substitution with Ala did not affect the stability of the protein, which again emphasized the important structural role played by the short N-terminal  $\beta$ -strand.

### 5.8 Detailed analysis of the N-terminal second amino acid

The study with the N-terminal KatB variants revealed the N-terminal  $\beta$ -strand to be important for both for activity as well as the structural integrity. Deletion of this strand led to the formation of a protein that was inactive. Moreover, within this  $\beta$ -strand, the second (Phe-2), fourth (His-4) and the fifth (Lys-5) amino acid appeared to be the major determinants in maintaining the KatB structure-function. Among these residues, alteration in the 2<sup>nd</sup> residue impacted the activity of the KatB enzyme the most. Hence

this residue (i.e. Phe-2) was evaluated in greater detail for its role played in governing the structure-function of this protein.

### 5.8.1 Sequence analysis

Interestingly, multiple sequence analyses revealed the second amino acid present in all Mn-catalases across the genera to always be an aromatic bulky amino acid (i.e. Phe, Tyr or Trp) (Fig. 5.8.1 A). In all the Mn-catalases analysed, the occurrence of Phe, Tyr or Trp as the second amino acid residue was 82.95%, 15.91% or 1.14% respectively (Fig. 5.8.1 B). To get an insight into the role played by this non-active site residue in Mn-catalase function, 2<sup>nd</sup> residue was replaced with different amino acids and the resulting (mutant) KatB proteins were thoroughly characterised.

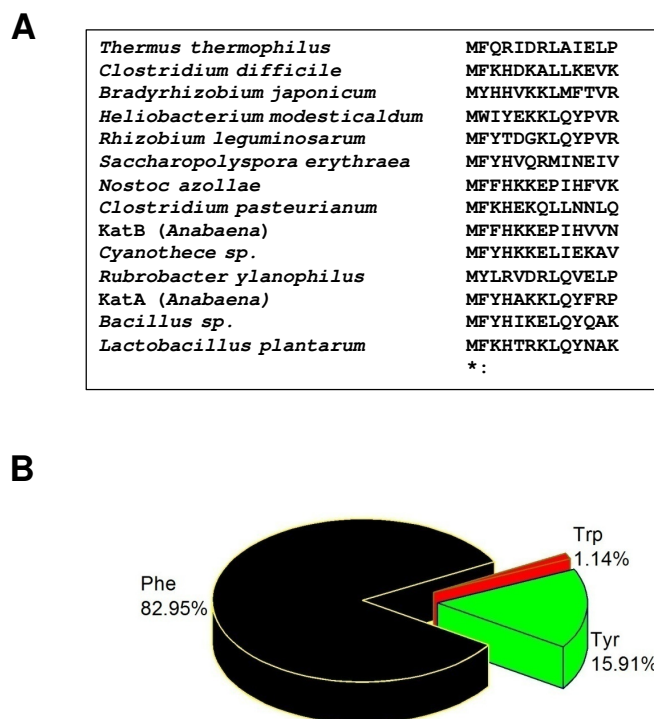


**Fig. 5.8.1 Conservation of the second amino acid in Mn-catalases.** (A) A representative multiple sequence alignment file showing high degree of conservation of the N-terminal second amino acid residue in Mn-catalases. (B) Pie chart indicating the occurrence of an aromatic amino acid as the N-terminal second residue in the Mn-catalase sequences available in the RedoxiBase database.

### 5.8.2 Substitution of the second amino acid with amino acid of different sizes by site directed mutagenesis and purification of the corresponding proteins

As described earlier in this chapter (Section 5.2), the second amino acid (i.e. Phe-2) played an important role in hydrophobic interactions. Sequence analysis also revealed a preferential presence of Phe residue at the second position in majority of Mn-catalases. To assess its role more thoroughly, it was desired to replace Phe-2 with amino acids of varying sizes. Therefore, the Phe-2 residue was replaced by site directed mutagenesis (as described in the methods section) with smaller residue (G/V) or bulkier hydrophobic residue (Y/W) to give rise to KatBF2G, KatBF2V, KatBF2Y or KatBF2W respectively (Fig. 5.8.2 A). The intended mutations were introduced into the forward primers and in all cases KatB\_BamHis\_Rev was used as the reverse primer (Table 2.2).

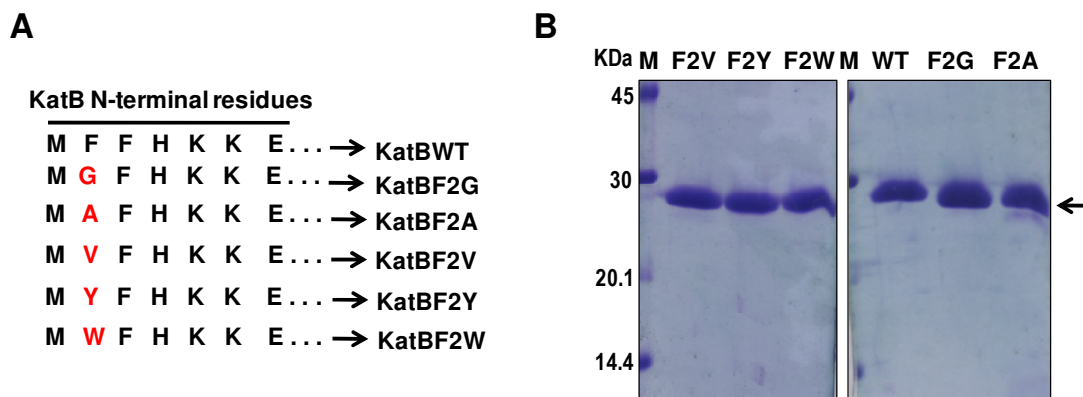


**Fig. 5.8.2 Purification of the second amino acid variants of KatB.** (A) Diagrammatic representation of all the N-terminal second amino acid variants generated for the study. The substituted residue is indicated by red font. (B) Purification of the second amino acid variants. The purified proteins (1 µg each) were resolved by SDS-PAGE (14%) and visualized by staining with CBB. F2V, KatBF2V; F2Y, KatBF2Y; F2W, KatBF2W, WT, KatBWT; F2G, KatBF2G, F2A, KatBF2A; M, protein marker. Position of the purified protein is indicated by an arrow.

The different PCR-amplified fragments of the *katB* gene variants were inserted into pET21a expression vector employing *NdeI* and *BamHI* restriction endonucleases. Resultant plasmids (pETKatF2G, pETKatF2A, pETKatF2V, pETKatF2Y and pETKatF2W) were eventually transformed into *E. coli* BL21 (DE3) pLysS expression host and production of the recombinant protein was obtained by induction with IPTG. The KatBF2G/KatBF2A/KatBF2Y/KatBF2W protein was expressed in the soluble fraction of *E. coli*. All these second amino acid variants of KatB protein were purified to near homogeneity by affinity chromatography employing NiNTA matrix (Fig. 5.8.2 B).

### 5.8.3 Effect of second amino acid mutation on compactness of KatB

The hydrodynamic size of the various 2<sup>nd</sup> amino acid variants were ascertained by performing gel filtration chromatography (Fig. 5.8.3 A). The gel filtration chromatogram suggested a clear 2<sup>nd</sup> amino acid residue-dependent elution pattern. Bulkier the second amino acid, more was the retention time. The KatBF2G variant, the one with the smallest residue at 2<sup>nd</sup> position, exhibited lowest retention volume (i.e. fastest elution).

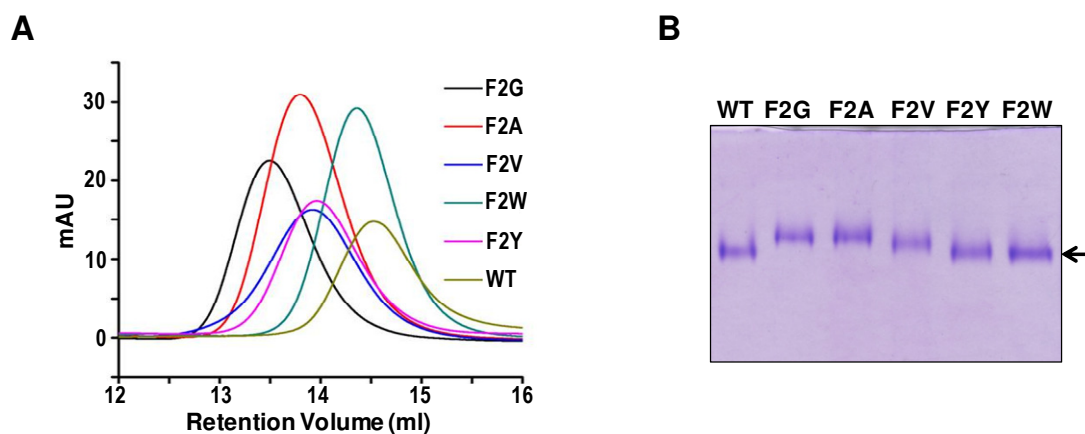


**Fig. 5.8.3 Effect of the N-terminal second amino acid on compactness of the KatB oligomer.** (A) Gel filtration profile of the purified KatB variants. 200  $\mu$ g of the purified protein was injected into Superdex

200 10/300 GL column pre-equilibrated with buffer containing 20 mM Tris and 50 mM NaCl, pH 7.2. **(B)** Native PAGE analysis of the second amino acid variants. Purified proteins (0.5 µg each) were resolved on native polyacrylamide gels and stained with CBB. Position of the proteins is indicated by an arrow.

In contrast, the KatBWT or KatBF2W (that contained bulky residues at the N-terminal 2<sup>nd</sup> position) required maximum time to elute out of the column, indicating that these were more compact than the other variants with smaller second amino acid (KatBF2G, KatBF2A, KatBF2V) (Fig. 5.8.3 A). The order of elution was KatBF2G first, followed by KatBF2A, KatBF2V, KatBF2Y, KatBF2W and KatBWT at last.

In agreement with the gel filtration data, native polyacrylamide gel electrophoresis too indicated a similar difference in mobility among the KatB variants. The KatBWT, KatBF2W and KatBF2Y showed higher mobility than KatBF2G, KatBF2A or KatBF2V (Fig. 5.8.3 B). These results clearly demonstrated that the second amino acid determined the overall compactness of the KatB protein and a bulky aromatic amino acid was required at the second position for optimal compaction.

#### **5.8.4 Catalase activity of the KatB variants at different pH**

All the second amino acid variants were subjected to catalase activity assay along with the KatBWT protein. Distinct zone of catalase activity was detected with KatBWT, KatBF2W and KatBF2Y on in-gel catalase activity assay (zymogram). However, other KatB variants did not show any catalase activity on zymograms (Fig. 5.8.4 A).

In the more sensitive spectrophotometric assays, the KatBF2V variant did show some catalase activity, but KatBF2G or KatBF2A were completely inactive. On the other hand, KatBWT, KatBF2W or KatBF2Y showed an appreciable degree of H<sub>2</sub>O<sub>2</sub> decomposition, and their activity was found significantly higher than that of KatBF2V (Fig. 5.8.4 B).

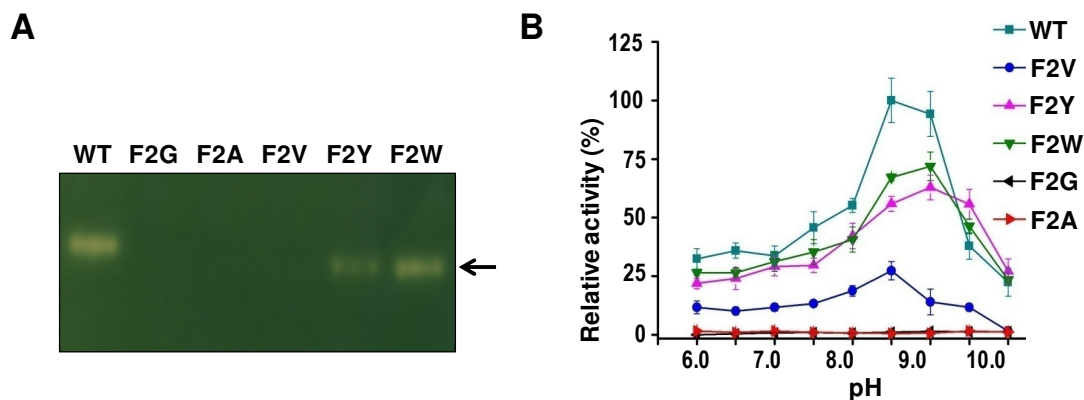


**Fig. 5.8.4 H<sub>2</sub>O<sub>2</sub> decomposition activity of the N-terminal second amino acid variants of KatB.** (A) Purified proteins (0.5 µg each) were resolved on native 10% PAGE and stained for catalase activity (zymogram). (B) H<sub>2</sub>O<sub>2</sub> decomposition activity of the different KatB variants was measured spectrophotometrically at different pH (as indicated in the figure). The maximum activity exhibited by the KatBWT protein (obtained at pH 8.5) was considered to be 100%, and the other rates were calculated accordingly. Error bars represent SE.

Activity measurement at different pH indicated that KatBWT and KatBF2V had maximal activity at pH 8.5 whereas, surprisingly, KatBF2W and KatBF2Y showed maximum activity at pH 9.0. However, at their respective optimal pH, activity of KatBF2W/KatBF2Y was 25-30% less than that of the KatBWT protein (Fig. 5.8.4 B).

### 5.8.5 Kinetic properties of the 2<sup>nd</sup> residue variants of KatB

The catalytically active second amino acid variants (KatBF2V, KatBF2Y and KatBF2W) were subjected to catalase assays to calculate their kinetic properties. Rate of reaction was calculated at various substrate concentrations and the data were compiled to generate the Lineweaver-Burk plot for all the variants individually (Fig. 5.8.5).

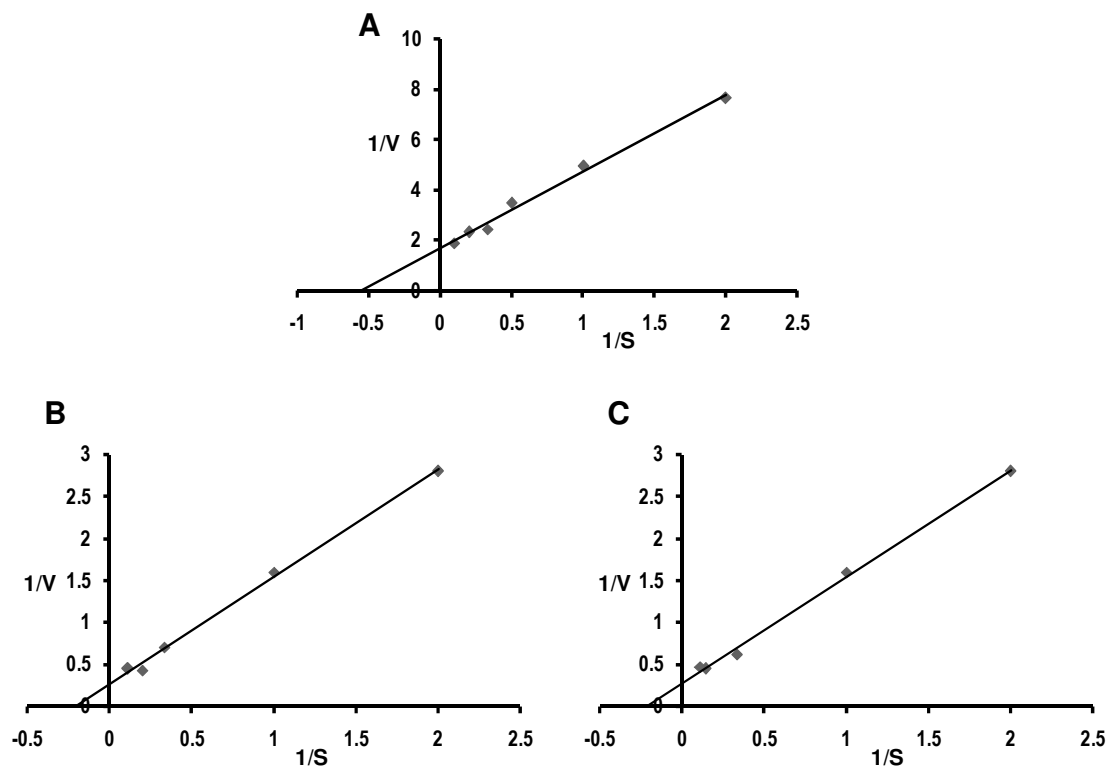


**Fig. 5.8.5** Lineweaver-Burk plot for the catalytically active second amino acid variants, KatBF2V (A), KatBF2Y (B) or KatBF2W (C).

The  $K_m$  values were determined from these plots, and subsequently the turn-over numbers ( $k_{cat}$ ) was also calculated (Table 5.1).

**Table 5.1** Kinetic paramets of the catalytically active KatB mutants.

Variants	$K_m$ (mM)	$V_{max}$ (mM min <sup>-1</sup> μg <sup>-1</sup> )	$k_{cat}$ (s <sup>-1</sup> Subunit <sup>-1</sup> )
KatBWT	3.29 ± 0.95	263 ± 71.54	1.15 x 10 <sup>5</sup>
KatBF2V	2.21 ± 1.82	31 ± 6.28	1.36 x 10 <sup>4</sup>
KatBF2Y	4.60 ± 1.19	217 ± 45.21	9.52 x 10 <sup>4</sup>
KatBF2W	4.88 ± 1.06	236 ± 67.32	1.04 x 10 <sup>5</sup>

Although the  $K_m$  values of the variants were in the same range (between 2.2-4.9 mM of  $H_2O_2$ ), the  $k_{cat}$  values differed significantly between KatBF2V and others. As shown in the Table 5.1, the KatBF2V variant (which had a small non-aromatic amino acid Val at 2<sup>nd</sup> position) exhibited a  $k_{cat}$  value that was almost 10 times less than that of the KatBWT/KatBF2Y/ KatBF2W i.e. variants with bulky aromatic amino acid at the second position.

### 5.8.6 Sensitivity of the KatB variants to thermal or chemical denaturation

Since the second amino acid was found to affect compactness of KatB, it was desired to verify if this residue also impacted the thermal or chemical stability of this protein. The basic CD profile indicated that alteration of the second amino acid did not cause any obvious change in the overall secondary structure of the protein (Fig. 5.8.6 A).

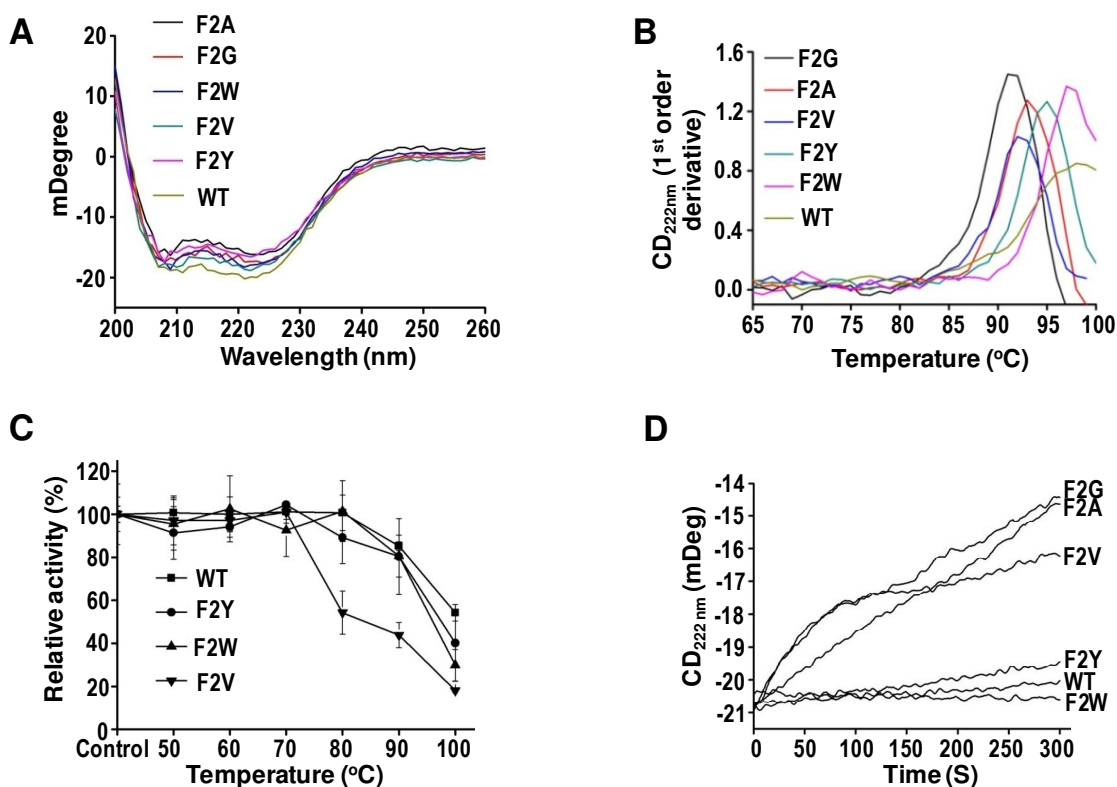


**Fig. 5.8.6 Sensitivity of the KatB variants to thermal or chemical denaturation.** (A) CD spectra of the N-terminal second amino acid variants. (B) Thermal denaturation of N-terminal second amino acid

variants of KatB. Dichroic intensities (at 222 nm) of the variants were monitored in the temperature range mentioned in the figure. Melting points were obtained from the first order differential plot generated from the melting curve. **(C)** Thermostability of the KatB variants. The purified proteins were exposed for 10 minutes at different temperatures, as indicated in the figure, followed by catalase activity measurement at room temperature. Activity of the protein kept at room temperature was considered to be 100% and other rates were calculated accordingly. Error bars represent SE. **(D)** Loss of secondary structure in presence of GuHCl. Purified proteins were mixed with 0.2 M GuHCl in quartz cuvette and change in ellipticity (mDegree) at 222 nm with time was monitored in a CD spectropolarimeter.

However, these KatB variants showed a different thermal denaturation profile, indicating differences in their melting temperatures ( $T_m$ ) (Fig. 5.8.6 B; Table 5.2). KatBWT and KatBF2W showed high  $T_m$  (around 98.0°C respectively) while KatBF2Y showed  $T_m$  of  $95.3 \pm 0.58^\circ\text{C}$ . Interestingly, the other KatB variants (KatBF2G, KatBF2A or KatBF2V) showed reduced  $T_m$  ranging from 91-93°C (Table 5.2). This result was further substantiated by performing catalase activity assay with all the catalytically active KatB variants (KatBWT, KatBF2W, KatBF2Y and KatBF2V) after subjecting these to elevated temperatures. KatBF2W, KatBF2Y or the KatBWT did not show any loss in their activity even after exposure to about 80°C (Fig. 5.8.6 C). In contrast, the KatBF2V protein began to lose its activity when incubated at temperature above 70°C, indicating reduced stability.

**Table 5.2:  $T_m$  of the second amino acid variants**

<b>Variants</b>	<b><math>T_m</math> (°C)</b>
KatBWT	$97.6 \pm 1.14$
KatBF2G	$92.7 \pm 1.51$
KatBF2A	$91.3 \pm 0.58$
KatBF2V	$92.7 \pm 1.8$
KatBF2Y	$95.3 \pm 0.58$
KatBF2W	$98.0 \pm 1.0$

The ability of these second amino acid variants to withstand chemical denaturation (i.e. loss in secondary structure) caused by guanidium hydrochloride (GuHCl) was assessed with the help of CD spectropolarimetry. The variants with smaller amino acids at the second position, namely, KatBF2G, KatBF2A and KatBF2V lost their secondary structure in the presence of guanidium chloride (0.2 M), while the KatBWT, KatBF2W and KatBF2Y showed relatively intact secondary structure throughout the assay time (Fig. 5.8.6 D). The above-mentioned results clearly demonstrated that presence of a bulky amino acid at the second position of the KatB polypeptide enhanced its thermostability and ability to resist chemical denaturation.

### **5.9 Over-expression of an N-terminal second amino acid variant (KatBF2V) of KatB in *Anabaena***

Earlier, induction of the KatBWT protein in response to NaCl stress was shown to protect *Anabaena* from a subsequent challenge with H<sub>2</sub>O<sub>2</sub>. Similarly, over-expression of KatBWT (from a plasmid-based construct) also reduced the ROS burden caused by addition of H<sub>2</sub>O<sub>2</sub> (described in Chapter 3). The *in vitro* assays described earlier clearly showed that the second amino acid residue of the KatB protein affected the biochemical and the biophysical properties of this enzyme. To determine whether these *in vitro* observations had any physiological consequences, the variant that showed substantially reduced activity, KatBF2V, was over-expressed in *Anabaena* and the ability this strain detoxify the exogenously added H<sub>2</sub>O<sub>2</sub> was assessed.

#### **5.9.1 Cloning of *katBF2V* ORF into *E. coli*/*Anabaena* shuttle vector pAM1956 and transfer to *Anabaena***

To accomplish the above-mentioned objective, The *katBF2V* DNA fragment (693 bp) was PCR amplified employing *Anabaena* PCC 7120 genomic DNA using primers

(KatB\_F2V\_Fwd & KatB\_Bam\_Rev; Table 2.2) and the corresponding product was ligated downstream of the strong light-inducible  $P_{psbA1}$  promoter in pFPN vector [195] using *NdeI* and *BamHI* restriction endonucleases (plasmid called pFPNKatBF2V). Subsequently, the *katBF2V* gene along with the  $P_{psbA1}$  promoter was excised out as a *SalI*–*XmaI* fragment from pFPNKatBF2V and subcloned into *E. coli/Anabaena* shuttle vector pAM1956 [212] to generate pAMKatBF2V, which was confirmed by restriction digestion (Fig. 5.9.1 A). The pAMKatBF2V plasmid is schematically depicted in Fig. 5.9.1 B.

The pAMKatBF2V plasmid was conjugally transferred into *Anabaena* PCC 7120 and exconjugants selected on BG11N+ plates (containing neomycin) were repeatedly subcultured. The transformed *Anabaena* strain thus obtained (designated *AnKatBF2V*<sup>+</sup>) was maintained on BG11N+ medium under neomycin selection pressure.

In the *AnKatBF2V*<sup>+</sup> strain, both *katBF2V* and *gfp* (driven by the  $P_{psbA1}$  promoter) are co-transcribed together, but the proteins are translated separately, resulting in synthesis of both the proteins. As a result, the expression of the transgene of interest (here *katBF2V*) can be indirectly monitored by observing the GFP fluorescence in the transformants. Abundant fluorescence of GFP was observed in the *AnKatBF2V*<sup>+</sup> strain, indicating expression of the transgene (Fig. 5.9.1 C).

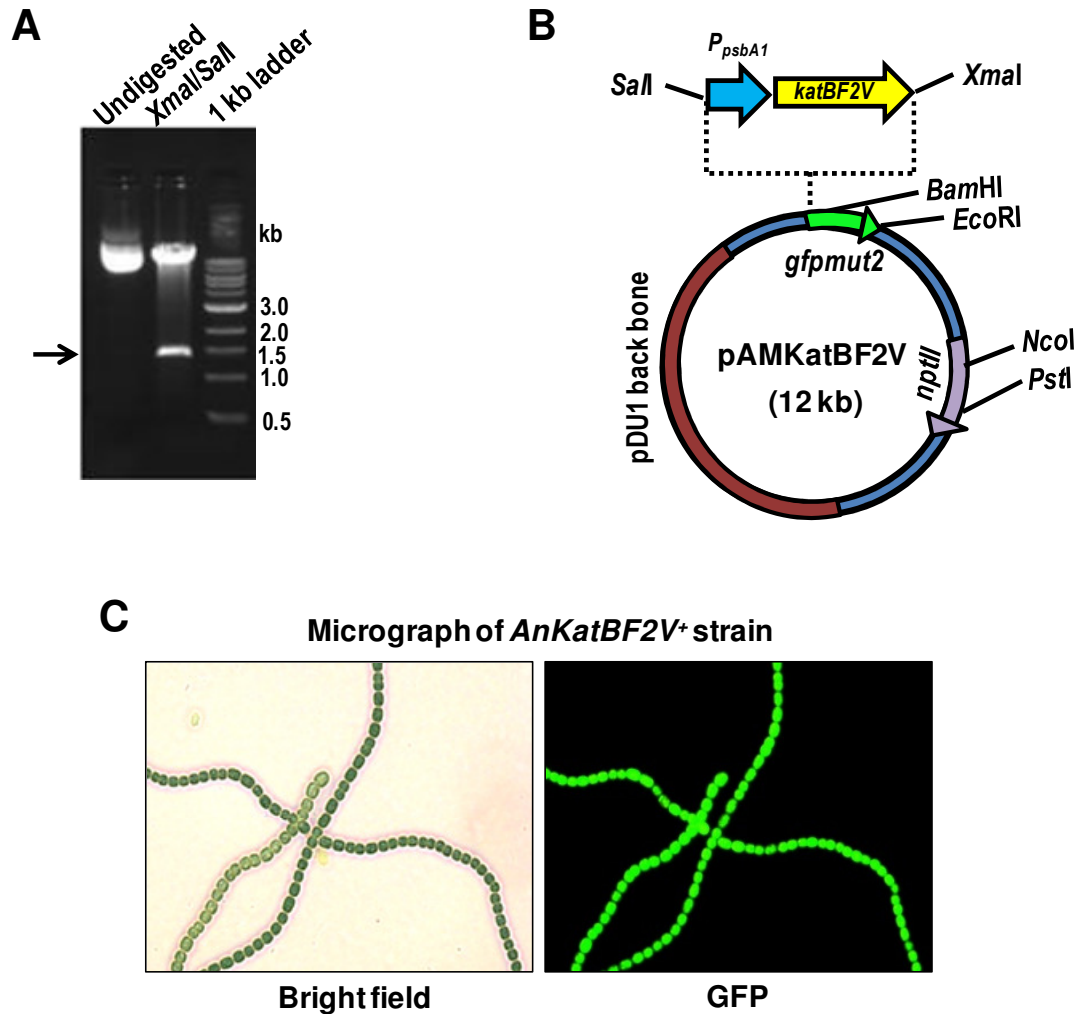


**Fig. 5.9.1 Over-expression of KatBF2V variant in *Anabaena*.** (A) Verification of pAMKatBF2V plasmid by restriction digestion. The plasmid was digested with *Xma*I and *Sal*I restriction endonucleases. Release of approximately 1.5 kb insert (*katBF2V*-*P<sub>psbA1</sub>*-F1 region) is indicated by an arrow. (B) Schematic vector map of pAMKatBF2V showing the site of the *katBF2V* ORF. (C) Bright field and green fluorescence (GFP) micrograph (400X) of *Anabaena* strain over-expressing the KatBF2V protein (*AnKatBF2V*<sup>+</sup>).

### 5.9.2 Production of KatB in the *AnKatBF2V*<sup>+</sup> strain

Production of the KatB protein in the recombinant *Anabaena* strain (*AnKatBF2V*<sup>+</sup>) was monitored on Western blots (with KatB-specific antiserum) while its activity was assayed on zymograms. Cell extracts from *AnKatBF2V*<sup>+</sup> or *AnKatB*<sup>+</sup> (recombinant *Anabaena* strain expressing the wild-type *katB* gene from *P<sub>psbA1</sub>* promoter, described in CHAPTER 3) or the wild-type *Anabaena* PCC 7120 were resolved on SDS-PAGE,

transferred onto nitrocellulose membrane and probed with the KatB antiserum (1:15000 diluted). Abundant production of the KatBF2V protein was observed in the recombinant *AnKatBF2V<sup>+</sup>* strain. Similar level of the KatBWT protein was also detected in the *AnKatB<sup>+</sup>* strain. However, hardly any KatB expression could be detected in the wild-type strain, again demonstrating the lack of noticeable KatB production in unstressed *Anabaena* cells (Fig. 5.9.2, upper panel).

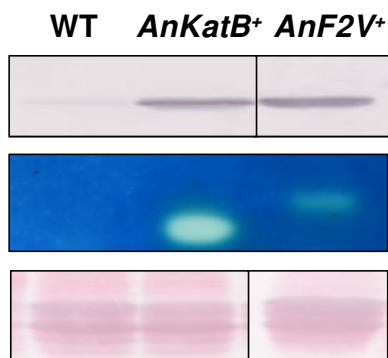


**Fig. 5.9.2 Expression of KatB in *Anabaena* strain over-expressing KatBWT or KatBF2V.** Cell-free extracts of the control wild-type *Anabaena* (WT), *AnKatB<sup>+</sup>* (*Anabaena* over-expressing KatBWT), or *AnKatBF2V<sup>+</sup>* strain (*AnF2V<sup>+</sup>*) were solublized in Laemmli's sample buffer, resolved on SDS-PAGE, transferred on to nitrocellulose membrane, and probed with the KatB antiserum (top). A Ponceau-S-stained part of the blot is shown as the loading control (bottom). The same samples were resolved by non-denaturing PAGE (10%) and employed for zymographic analysis (middle).

Although the Western blot indicated similar level of KatB expression in both the recombinant cells, profuse catalase activity was detected in only in *AnKatB<sup>+</sup>* extracts on zymograms. In contrast, only a marginal catalase activity was observed in *AnKatBF2V<sup>+</sup>* (Fig. 5.9.2, middle panel). The zymogram also revealed that the zone of clearance shown by KatBWT was at a lower position in the gel than the activity zone formed by KatBF2V. In good agreement with the earlier *in vitro* observations (Fig. 5.8.4), when expressed in *Anabaena* too, the KatBWT protein showed higher mobility and activity (in zymograms) than KatBF2V.

### 5.9.3 Ability of *KatBF2V* over-producing *Anabaena* strain to decompose externally added $H_2O_2$

The efficiency of the *AnKatBF2V*<sup>+</sup> culture to detoxify the externally added  $H_2O_2$  was monitored and compared with that of *AnKatB*<sup>+</sup> strain (that expresses the KatBWT protein) or the wild-type *Anabaena*. 1 mM  $H_2O_2$  was added to the cultures (in exponential phase) and the culture medium was removed at various time points to measure the level of residual  $H_2O_2$  (Fig. 5.9.3 A).

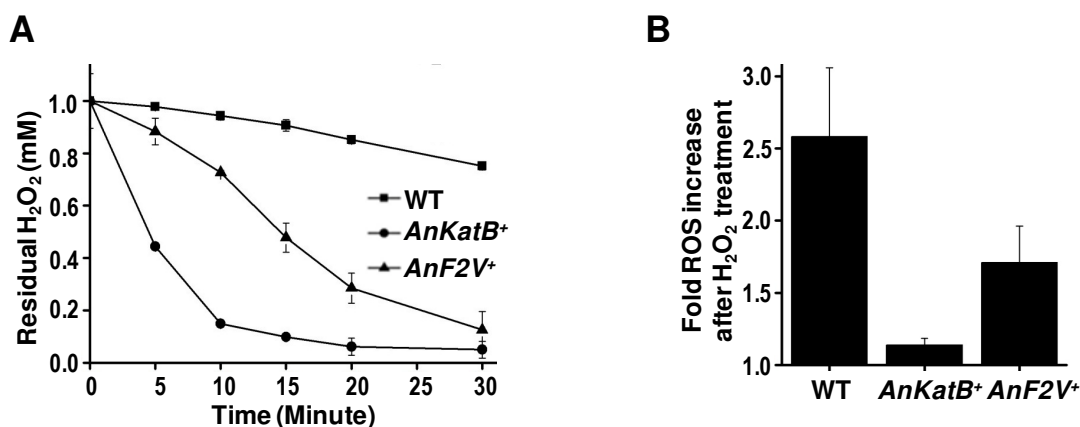


**Fig. 5.9.3** Decomposition of externally added  $H_2O_2$  by *AnKatBF2V*<sup>+</sup>, *AnKatB*<sup>+</sup> or the wild-type *Anabaena* strain. (A) 1 mM  $H_2O_2$  was added to the *AnKatB*<sup>+</sup>, *AnKatBF2V*<sup>+</sup> (*AnF2V*<sup>+</sup>) or wild-type *Anabaena* PCC 7120 (WT) cultures and the residual  $H_2O_2$  remaining in the medium was measured at time points as indicated. Error bars represent SE. (B) Fold change in ROS production in response to externally added  $H_2O_2$  (1mM) with respect to their corresponding untreated control cultures. The wild-type *Anabaena* PCC 7120 (WT), *AnKatB*<sup>+</sup> or *AnKatBF2V*<sup>+</sup> (*AnF2V*<sup>+</sup>) cells were incubated with 10  $\mu$ M DCHFDA for 20 minutes in dark and fluorescence emission ( $\lambda_{ex}$  = 490 nm,  $\lambda_{em}$  = 520 nm) from cells was measured immediately on a spectrofluorimeter.

The *AnKatBF2V*<sup>+</sup> strain could decompose around 25% of added  $H_2O_2$  within 10 minutes. In contrast, the *AnKatB*<sup>+</sup> strain decomposed more than 90% of the added  $H_2O_2$  within 10 minutes, indicating that the KatBWT protein was more efficient compared to KatBF2V. The wild-type, on the other hand, could detoxify only 5% of the added  $H_2O_2$  during the period of study. Clearly, among the 3 strains tested, *AnKatB*<sup>+</sup> decomposed

H<sub>2</sub>O<sub>2</sub> most competently. Accumulation of ROS in response to H<sub>2</sub>O<sub>2</sub> treatment in those cultures was tested by DCHFDA assay. A 2.6-fold or a 1.7-fold increased levels of ROS was detected in the wild-type *Anabaena* or the *AnKatBF2V*<sup>+</sup> strain, respectively. But, the *AnKatB*<sup>+</sup> strain exhibited only a marginal increase in ROS generation under the same conditions (Fig. 5.9.3 B), largely due to the efficient decomposition of the added H<sub>2</sub>O<sub>2</sub>.

To visualize the structural perturbations resulting from altering the second amino acid residue, it was desired to compare the structure of KatBF2V with that of the KatBWT protein. Crystallization and subsequent analysis of the KatBF2V protein was performed by our collaborator Dr. Subhash C. Bihani, Radiation Biology & Health Sciences Division, BARC.

### **5.10 Crystal structure of the KatBF2V protein**

The KatBF2V protein (with C-terminal hexa-histidine tag), over-produced in *E. coli* (and purified there from) was used to determine its crystal structure (PDB Id: 4R42) [215, 244]. Like other Mn-catalases whose structures are available (LPC and TTC, discussed in details in Chapter 4), the KatBF2V protein was also found to adopt a four-helix bundle type architecture, which is the characteristic of the Ferritin-like superfamily (Fig. 5.10 A).

Similar to KatBWT, the KatBF2V molecules are arranged as triangular hexamer in the crystal (Fig. 5.10 B). Both the N and the C-terminal regions are extensively involved in the oligomerization of the individual monomers. As expected, the crystal structure of the KatBF2V and the KatBWT are largely similar.

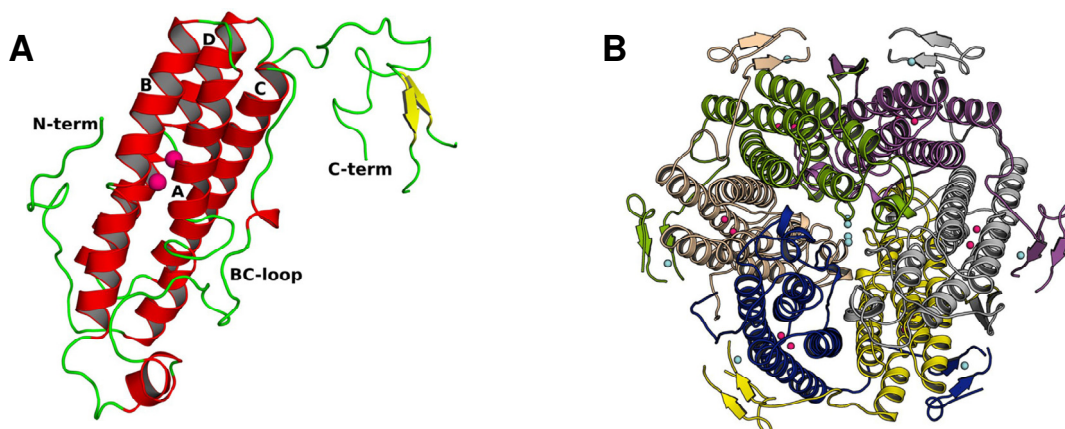


**Fig. 5.10 Crystal structure of the KatBF2V protein.** (A) The four-helix bundle architecture of KatB monomer with bimetallocore at the middle of helices. Mn ions are shown as magenta spheres. (B) Hexameric assembly of KatBF2V. The Mn ions are depicted as magenta sphere. The N and C-terminal residues are extensively involved in oligomerisation.  $\text{Ca}^{2+}$  ions at the oligomer interfaces are shown by cyan spheres.

## 5.11 Comparison of KatBWT and KatBF2V structures

### 5.11.1 Involvement of second residue in hydrophobic interactions at the oligomer interface

As mentioned in the Section 5.2, the second amino acid (Phe-2) is an integral part of the hydrophobic pocket in the subunit interface (Fig. 5.2 B). Comparison of the crystal structure of the KatBWT and the KatBF2V protein revealed that hydrophobic residues Phe-2, Lys-40, Trp-43, Ile-63 and Phe-66 were closely packed in the KatBWT protein (Fig. 5.11.1 A). In contrast to this, due to shorter chain length of Val-2, tight packing was not possible in KatBF2V. As a result a big gap was observed in that hydrophobic patch (Fig. 5.11.1 B). To get a clear idea about the differences between KatBWT and KatBF2V, the hydrophobic region involving the second amino acid from both the structures were superimposed (Fig. 5.11.1 C). In KatBF2V, Phe-2 to Val-2 mutation caused the otherwise compactly-arranged residues to fit loosely now, which was clearly visible from the superimposed structures (Fig. 5.11.1 C).

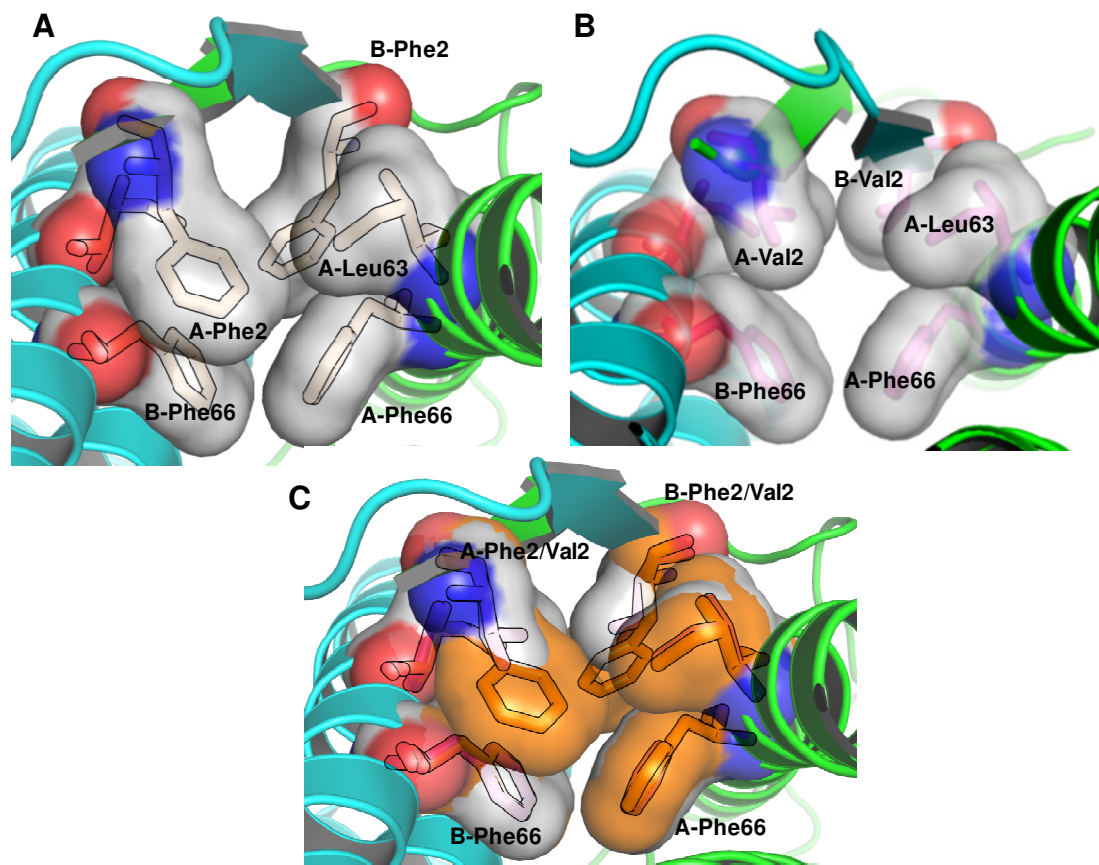


**Fig. 5.11.1 Hydrophobic interactions at the dimer interface.** (A) Hydrophobic patch between the N-terminal  $\beta$ -sheet and helix A from the neighbouring subunit in KatBWT. (B) Hydrophobic patch between helix A and N-terminal  $\beta$ -sheet from neighbouring subunits in KatBF2V. A gap in the middle of the hydrophobic patch is seen. (C) Superimposition of KatBF2V and KatBWT showing the impact of the Phe-2 to Val-2 mutation on packing of the hydrophobic residues at the dimer interface.

### 5.11.2 Interaction between the second amino acid and Phe-66

The N-terminal second residue was found to be located just above the Phe-66 residue, which is located in the vicinity of the catalytic site (Fig. 5.2 B). This residue in helix A held the active site residues His-68 and Glu-65, which coordinated the Mn ions. The Phe-66 residue made extensive interactions and fit perfectly in a hydrophobic pocket created by Phe-2, Lys-36, Lys-40, Trp-43, Ile-63 and Lys-69 of the same chain and Phe-2, Trp-43 and Phe-66 of the neighbouring subunit (Fig. 5.11.3 B and Fig. 5.2 B). Phe-66 made direct interactions with the second residue (Phe-2) of both the subunits

(Fig. 5.11.2 A) in KatBWT. However, in the KatBF2V structure, these interactions were compromised due short side chain length of Val-2 (Fig. 5.11.2 B).

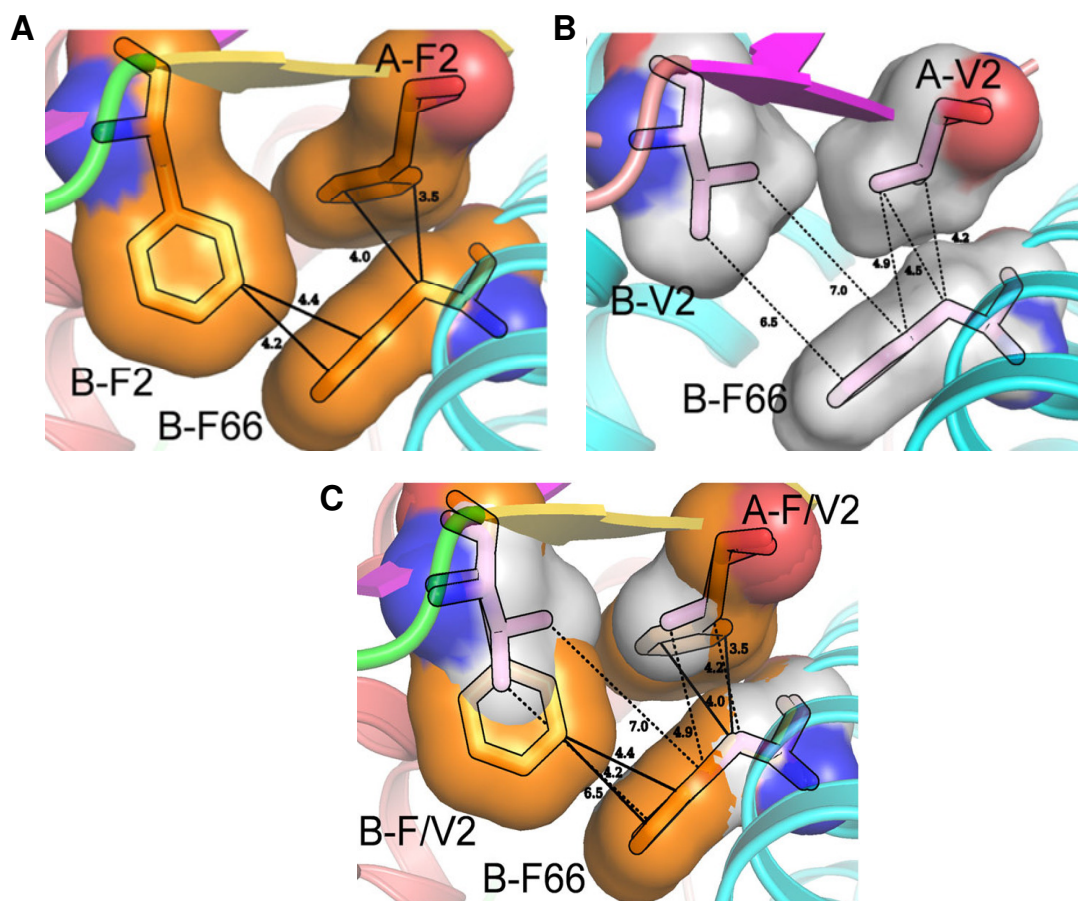


**Fig. 5.11.2 Interaction between the second amino acid and Phe-66.** (A) van der Waals interactions of Phe-66 with the N-terminal second amino acid (Phe-2) from the neighbouring chains in KatBWT. (B) Interactions of Val-2 from one chain with Phe-66 from the neighboring Chain. (C) Superposition of KatBF2V with KatBWT showing reduced interactions between Val-2 and Phe-66 in KatBF2V in contrast to those observed between Phe-2 and Phe-66 in KatBWT.

Superposition of the two structures clearly demonstrated that, unlike in KatBWT, the distance between Val-2 and Phe-66 from the same chain was too large for possible van der Waals interactions (Fig. 5.11. 3 C).

### 5.11.3 Interaction of Phe-2 with structurally important residue Trp-43

In KatBWT, Phe-2 also interacted strongly with Trp-43 that was located next to the Tyr-42, which is one of the important second shell-interacting residue in the active site region (discussed in Chapter 4) (Fig. 5.11.3 A).

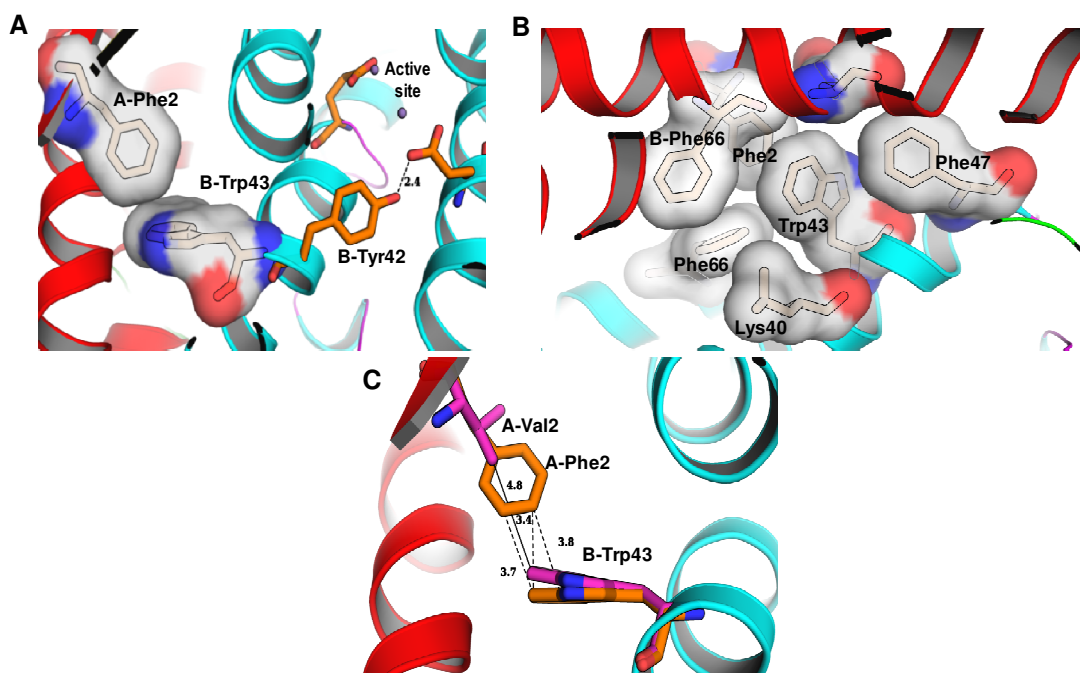


**Fig. 5.11.3 Interaction of the N-terminal second residue with Trp-43. (B)** Non-bonded interactions between Phe-2 and Trp-43. Trp-43 is near to Tyr-42, an important second shell interacting residue close to the active site. **(B)** Close packing of Trp-43 with extensive non-bonded interactions in KatBWT. **(C)** Loss of direct interaction of Val-2 with Trp-43 in KatBF2V. Considerable displacement of the Trp-43 in absence of close packing with the second residue was found in KatBF2V. The KatBF2V and the KatBWT structures are shown in magenta and dark orange color respectively.

In the KatBWT, Trp-43 made strong hydrophobic interactions with several residues from neighboring subunits (Fig. 5.11.3 B). Such extensive interactions suggested that the structural stability of Trp-43 is important for KatB. In KatBF2V, the interactions between Val-2 and Trp-43 were completely lost, leading to a shift in the position of the indole ring of Trp-43 (Fig. 5.11.3 C).

#### 5.11.4 Calculation of interaction energies

Comparison of the crystal structures of KatBWT and KatBF2V indicated that Phe to Val mutation at the second position of KatB polypeptide resulted in marked alteration of few crucial residue-to-residue interactions. The INTAA web server [224] was used to quantify some those interactions to assess the importance of the second amino acid in maintaining the structural integrity in KatB protein. The KatBWT protein showed a stabilizing interaction between Phe-2 and Phe-66 of the same subunit with interaction energy of  $-3.4 \text{ kJ mol}^{-1}$ . Whereas, in KatBF2V, this interaction reduced substantially to  $-0.7 \text{ kJ mol}^{-1}$ , indicating a destabilizing effect of the mutation. Similarly, in KatBWT, the Phe-2 and the Phe-66 from the other subunit displayed interaction energy of  $-16.6 \text{ kJ mol}^{-1}$ . However in KatBF2V this energy (among Val-2 and Phe-66 present in separate subunits) was found to be  $-8.8 \text{ kJ mol}^{-1}$ . In similar line, the interaction energy between the second amino acid residue and Trp-43 was altered from  $-9.2 \text{ kJ mol}^{-1}$  in KatBWT to  $-2.2 \text{ kJ mol}^{-1}$  in KatBF2V, in spite of shifting of position of the indole ring of Trp-43 (Fig. 5.11.3 C).

#### 5.12 Discussion

Multiple sequence analyses revealed the N-terminal residues to be relatively conserved in all cyanobacterial Mn-catalases. To get an insight into the role played by these residues, detailed mutational analysis of this short stretch was performed. To further understand their importance, KatB mutants wherein the individual amino acids (from 2<sup>nd</sup> amino acid to 7<sup>th</sup> amino acid) were replaced with Ala were synthesized along with an N-terminal deletion mutant of KatB (i.e. lacking 2<sup>nd</sup> -7<sup>th</sup> amino acid).

Results showed the N-terminal residues to affect activity as well as the compactness of the protein. Mutational analysis of individual amino acids indicated that all residues in this stretch were not equally important. The variants KatBF3A, KatBK6A and KatBE7A showed appreciable catalase activity while KatBF2A and KatBH4A did not show any catalase activity whereas the KatBK5A variant showed marginal activity. These results suggested that the Phe-2, His-4 and the Lys-5 residues were crucial for optimal catalase activity.

N-terminal region of the protein is known to play an important role in protein folding [257], biochemistry and structure. Site directed mutagenesis has shown the extreme N-terminal residues to play a variable role in a particular protein's activity. For example, enhanced thermostability and increased activity was reported on deletion of the N-terminal of the alkaline  $\alpha$ -amylase (from *Bacillus*) [258]. But, in contrast to this example, deletion of the N-terminal residues reduced stability (Fig. 5.7) and completely abolished the activity of KatB (Fig. 5.6).

In some cases, The N-terminal residues apparently do not play a significant role in maintenance of structure-function of a protein. In the case of *E. coli* lactose permease, deletion of amino acids 2-9 from the N-terminus did not affect the ability of this permease to catalyze lactose transport [259]. In spite of having several conserved residues in the N-terminal region of mature cardiolipin synthase, the first 60 residues were found to be dispensable [260]. Similarly, the mutant palmitoyl carnitine transferase (from rat liver) lacking the conserved 18 N-terminal amino acids showed kinetic properties identical to the wild-type protein [261]. Unlike these enzymes, N-terminus of KatB was undoubtedly required for function as alteration of few key residues or deletion of the 6 residues from the N-terminal end influenced its overall

enzymatic activity, making it more prone to chemical denaturation. Similarly, change in the N-terminus of luciferase (i.e. deletion of the first 7 residues) reduced the activity of that enzyme to about 30% of the wild-type and increased its sensitivity to guanidine unfolding [262].

The *Candida tropicalis* catalase (CTC, a tetrameric heme catalase) showed 80% decrease in activity when the first 4 amino acids were deleted. Along with the catalytically active tetrameric form, the mutant CTC also showed the presence the smaller oligomers which were found to be inactive [263]. Although the deletion of N-terminal region of KatB did not change its oligomeric form, the protein (i.e. KatBTrunc) was completely inactive. Similar to KatB, the N-terminally deleted luciferase or CTC proteins too showed considerably reduced activity and moreover their overall secondary structure was very similar to that of their respective wild-type protein.

Interestingly, the second amino acid was always found to be an aromatic amino acid in Mn-catalases across the genera (Fig. 5.8.1). Initial results showed the replacement of this residue (Phe-2) with alanine to markedly reduce its activity, compactness and stability of KatB. Keeping this in mind, it was desired to delve deeper into the role played by this amino acid so that the reason for conservation of 2<sup>nd</sup> residue in Mn-catalases could be understood. Detailed analyses were carried out wherein the second amino acid of KatB (Phe in the wild-type KatB) was replaced with smaller (Ala/Gly) or intermediate (Val) or relatively bulkier (Trp/Tyr) amino acids. The size of 2<sup>nd</sup> residue affected activity as well as the structural compactness of the protein.

While not many studies have focused exclusively on the role played by the second amino acid of a polypeptide, few reports have shown a correlation between the amount of protein synthesized and the amino acid located at the second position. One

bioinformatic study has shown lysine to be the preferred second amino acid in prokaryotes, whereas serine or alanine were the favored second amino acid in lower eukaryotes and higher eukaryotes respectively [264]. Another analysis showed that highly expressed proteins in prokaryotes to have an enhanced frequency of alanine in the second amino acid position [265]. In fact, Bivona and group have recommended replacement of the second amino acid with alanine or serine as a general method to enhance production of recombinant proteins in *E. coli* [266]. However, this approach should be treated with caution if biological activity of protein is desired, as in our study, the KatBF2A was completely inactive.

In cyanobacteria, exposure to H<sub>2</sub>O<sub>2</sub> causes increase in intracellular ROS level which eventually damages the photosynthetic pigments leading to bleaching of cultures [232]. Heterocystous, filamentous cyanobacterium *Anabaena* is particularly sensitive to H<sub>2</sub>O<sub>2</sub> mediated oxidative stress [148, 190, 267]. The reason for this sensitivity can partly be attributed to the lack of basal catalase expression under control (unstressed) conditions in this organism. *In vitro* studies of KatB variants with non-aromatic amino acid at second position (i.e. KatBF2A/G/V) showed complete or substantial loss of catalase activity. Similarly, the KatBF2V-expressing *Anabaena* (*AnKatBF2V*<sup>+</sup>) strain also could not detoxify the externally added H<sub>2</sub>O<sub>2</sub> as efficiently as the *Anabaena* strain expressing KatBWT (*AnKatB*<sup>+</sup>). Consequently, *AnKatBF2V*<sup>+</sup> showed considerably higher ROS burden (Fig. 5.9.3). Thus an excellent correlation was obtained between *in vitro* activity and the *in vivo* ability of the protein to carry out its physiological role i.e. detoxification of H<sub>2</sub>O<sub>2</sub>.

To explain the underlying reason for the vital role played by the 2<sup>nd</sup> amino acid, the crystal structure of KatBF2V variant was compared with that of KatBWT. Like other

Mn-catalases, KatB/KatBF2V too was hexameric, suggesting that the conserved hexameric oligomeric assembly was important for their biological function. The conserved N-terminal  $\beta$  sheet was shown to be an important structural element for stabilization of the oligomeric assembly in LPC and TTC [122, 131]. In case of LPC, this  $\beta$  sheet shielded and stabilized the catalytic core by restricting access to the catalytic regions [131]. Both in KatBWT and KatBF2V, the first five residues from the N-terminal end participate in formation of antiparallel  $\beta$  sheet which stabilizes the core dimer and capping the entry to the active site (Fig. 5.2; Fig. 5.11.1).

Crystal structure of the KatBWT showed the second amino acid (Phe-2) to participate in extensive interactions within a hydrophobic patch created by residues Lys-36, Lys-40, Trp-43, Phe-66 and Lys-69 between helix A and helix B from both the subunits in core dimer (Fig. 5.2; Fig. 5.11.3). This arrangement was similar to the other two Mn-catalases whose structure is available (i.e. LPC and TTC). The hydrophobic patch plays a crucial role in stabilizing the core by forming interactions between four-helix bundle and the N-terminal  $\beta$ -strand residues (Fig. 5.2). As per the INTAA server analysis, the Phe-2 residue provides stabilizing interaction energy of more than  $-120 \text{ kJ mol}^{-1}$  through these interactions. The Phe-2 residue plays a pivotal role in connecting the N-terminal  $\beta$ -sheet with helix A and helix B from both the subunits. However, these interactions were compromised in KatBF2V, due to shorter side chain length of Val-2, which is unable to fit properly in this hydrophobic patch (Fig. 5.11.1). INTAA server analysis showed that the stabilizing interaction energy reduced to  $-85 \text{ kJ mol}^{-1}$  in KatBF2V. Therefore, mutation of Phe-2 to Val-2 reduced the strength of these interactions which affected the dimer interface and consequently destabilized the hexameric assembly of the protein. This destabilization manifested in reduced

thermal/chemical stability (Fig. 5.8.6) and decreased mobility of the KatBF2V protein than KatBWT, Fig. 5.8.3 and Fig. 5.9.2). Naturally, substitution of Phe-2 with even smaller amino acids like Ala or Gly would diminish these interactions further. This is indeed reflected from the lower  $T_m$  and reduced compactness observed in KatBF2G or KatBF2A as compared to KatBF2V (Table 5.2; Fig. 5.8.6). It is important to mention here that the KatBTrunc variant, wherein the entire  $\beta$ -strand is absent, the above mentioned interactions are not possible. Consequently, this protein also showed reduced compactness, decreased thermostability and complete loss in activity.

What is the probable reason for the reduced activity of the KatBF2V protein? Structural analysis shows the Phe-2 to interact with Phe-66 and Trp-43, both of which are present in the active site region. Hence, mutation of Phe to Val at the second position may affect this interaction, contributing to the reduced activity observed in KatBF2V. Phe-66 is very close to the active site residues, His-68 and Glu-65 (that coordinate the Mn ions), whereas, Trp-43 is positioned next to catalytically important Tyr-42 (Fig. 5.11.3). In LPC, mutation of Tyr-42 resulted in marked perturbation of the active site, leading to severe drop in catalytic activity [122] and in KatB too, reduced activity of Tyr-42 mutant was observed (Chapter 4). In the KatBWT protein, both Phe-66 and Trp-43 are strongly held at their respective position by extensive interactions with a group of hydrophobic residues from both the subunits (Fig. 5.2 B and Fig. 5.11.3 B). These extensive interactions appear to be crucial for maintenance of the stability in the active site residues. However, in KatBF2V, due to absence of the aromatic ring and short side chain length of Val-2, the interaction with Phe-66 and Trp-43 is severely reduced, which apparently affects rigidity and stability of the active site, leading to drop in catalytic activity. On the other hand, substitution of Phe-2 with Trp or Tyr is well

tolerated with no major effect on activity or stability (Fig. 5.8.3; Fig. 5.8.4; Fig. 5.8.6) indicating that these residues are able to maintain the required hydrophobic interactions. Multiple sequence alignment analysis shows that the second residue of Mn-catalases is an aromatic large hydrophobic amino acid (either Phe, Tyr, or Trp) (Fig. 5.8.1 A and B). This study has shed light on the reason for selection of these amino acids during evolution. Clearly, replacement of the second residue with a smaller amino acid results in a drastic reduction in activity whereas variants with Phe, Tyr or Trp show considerable activity. As discussed above, the presence of these amino acids at 2<sup>nd</sup> position ensures proper inter-subunit interaction, which provides stability to the KatB hexamer. These residues also form the proper hydrophobic pocket which holds the active site in perfect geometry. Hence, only Phe or Tyr or Trp is found at the second position in all Mn-catalases and other residues are not tolerated. In summary, the results presented in this study suggest that a bulky amino acid is required at the second position of Mn-catalases for optimal activity and stability, justifying the selection these amino acids during evolution.

## **CHAPTER 6**

### **Facile Production of the Thermostable Catalase KatB using *Anabaena* as a Production Platform: Biotechnological Implications**



## 6.1 Introduction

Cyanobacteria, the ancient photosynthetic bacteria, are believed to be the progenitors of plant chloroplasts. Their ability to convert CO<sub>2</sub> into organic compounds by oxygenic photosynthesis is particularly important as it reduces the global levels of this notorious greenhouse gas. Few cyanobacteria are endowed with the ability to convert atmospheric nitrogen into bio-available form and some strains of the heterocystous, filamentous, nitrogen-fixing cyanobacterium *Anabaena* are traditionally used as natural biofertilizers in rice fields of South-East Asia [268]. Due to their photoautotrophic nature and rapid rate of biomass accumulation, cyanobacteria are not only good candidates for biofuel production, but can also be a potential source of high quality protein [269]. Moreover, because of their minimal nutrient requirement and largely non-pathogenic nature, cyanobacteria are desirable hosts for over-production of commercially relevant proteins [270].

There are plenty of reports wherein heterotrophic microorganisms like bacteria, yeast, fungi etc. are used in industrial scale for the bio-production of commercially relevant products [271]. However, all these microbes require carbon sources which are expensive thereby increasing the production cost. In view of this, photoautotrophs like cyanobacteria or plants offer advantage as they can harness solar energy and atmospheric CO<sub>2</sub> which is cheap, abundant form of carbon, thus reducing consumption of organic carbon derived from crops [272, 273]. However, cyanobacteria have distinct advantages over plants for bioproduction of high value compounds as they have faster growth rates, greater salt tolerance, better ability to grow on marginal lands, and can also use waste water as nutrients [273]. Some cyanobacteria such as *Synechococcus elongates* PCC 7942, *Synechocystis* sp. PCC 6803, *Synchococcus* sp. PCC 7002 and

*Anabaena* sp. PCC 7120 are amenable to genetic manipulation thereby making them potential candidate for bioengineering. Cyanobacterial hosts have been genetically modified for generation of bio-products like ethanol, butanol, squalene etc. or for higher biomass production [274, 275, 195].

H<sub>2</sub>O<sub>2</sub> is widely used as a bleaching agent or microbial disinfectant in industries [275]. The primary industrial applications of H<sub>2</sub>O<sub>2</sub> are bleaching of raw fibres in textile processing [277, 278]; delignification and bleaching of paper pulp [279]; disinfection of microbes in food and pharmaceutical industries [276]; bleaching of hides to obtain uniform tanning in the leather industry [280] etc. Being an efficient H<sub>2</sub>O<sub>2</sub> detoxifying enzyme, catalases are extensively used to detoxify residual H<sub>2</sub>O<sub>2</sub> in industrial processes [276]. In fact, catalases are one the most commercially exploited enzymes today [281].

As described in earlier chapters, the purified KatB protein was found to be a robust, thermostable Mn-catalase functional at high pH and high ionic strength. The unique biochemical and biophysical attributes of KatB made it an appealing prospect for use in industry. In this chapter, the feasibility of using the cyanobacterium *Anabaena* as a platform for production of KatB is explored and the properties of the KatB protein purified from *Anabaena* are compared with those from a commercially available heme catalase

## **6.2 Over-expression of the his tagged KatB protein in *Anabaena* PCC 7120**

To assess the prospect of using *Anabaena* as the production platform for expression of recombinant proteins, over-expression of his-tagged KatB protein in this organism was attempted.

### 6.2.1 Cloning of *katB* ORF with 6 in-frame *His* codons into *E. coli/Anabaena* shuttle vector pAM1956

For the purpose of over-expression of KatB protein in *Anabaena*, the *katB* ORF along with strong light-inducible promoter was cloned into *E. coli/Anabaena* shuttle vector pAM1956. As the N-terminal region of KatB is important for crucial inter-subunit interactions and enzymatic activity (Chapter 5), the his-tag was included at the C-terminal end of the protein. For that, 6 *in-frame* histidine codons were introduced into the reverse primer. The forward and the reverse primer (Table 2.2) also contained *NdeI* and *BamHI* site respectively, to facilitate directional cloning into the pFPN vector [195]. The PCR fragment (*katB<sub>6His</sub>*) obtained after PCR amplification (with *Anabaena* PCC 7120 chromosomal DNA as template) was ligated into pFPN vector downstream of strong light inducible promoter  $P_{psbA1}$  using the two above-mentioned restriction sites (Fig. 6.2.1 A).

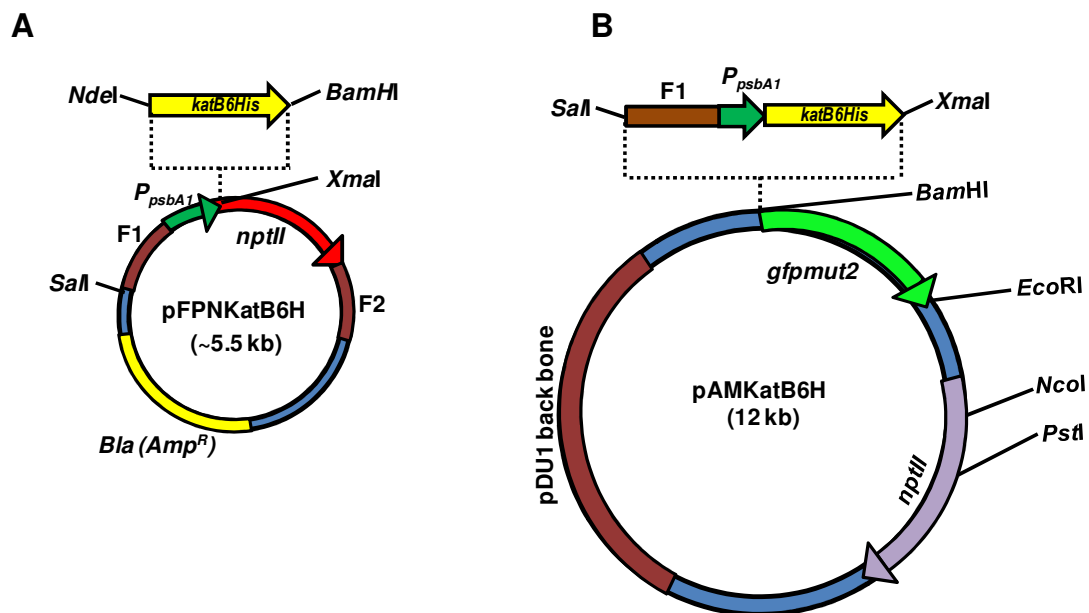


**Fig. 6.2.1** Schematic diagram of the vectors generated for KatB over-expression in *Anabaena*. (A) Schematic diagram of pFPNKatB6H. The *katB<sub>6His</sub>* DNA fragment was cloned employing *NdeI* and

*Bam*HI restriction site. **(B)** Schematic diagram of pAMKatB6H plasmid. The *katB<sub>6His</sub>* DNA fragment along with P<sub>*psbA1*</sub> promoter and F1 region was excised from pFPNKatB6H vector using *Sal*I and *Xma*I restriction endonucleases and cloned into pAM1956 employing the same restriction enzymes.

The resultant vector (pFPNKatB6H) was digested with *Sal*I and *Xma*I restriction endonucleases to excise out the *katB<sub>6his</sub>* fragment along with the P<sub>*psbA1*</sub> sequence upstream of it. The fragment (F1-P<sub>*psbA1*</sub>-*katB<sub>6his</sub>*) was then cloned just upstream of *gfp* reporter (*gfpmut2*) into *Anabaena* PCC 7120-*E. coli* shuttle vector pAM1956 to obtain pAMKatB6H (Fig. 6.2.1 B).

### **6.2.2 Generation of *Anabaena* strain over-producing his-tagged KatB protein**

The pAMKatB6His was conjugally transferred by into *Anabaena* PCC 7120 using a conjugal *E. coli* donor [HB101 (pRL623 + pRL443)] [194]. The exconjugants (*AnKatB6H<sup>+</sup>*) were selected on BG11N+ plates containing neomycin (25 µg/ml) and repeatedly subcultured. In *AnKatB6H<sup>+</sup>* strain, *katB<sub>6his</sub>* and *gfpmut2* genes are co-transcribed via the P<sub>*psbA1*</sub> promoter, yielding a bicistronic mRNA, which eventually leads to independent translation of both An-KatB (i.e. C-terminally His tagged KatB produced in *Anabaena*) and GFP protein. When the *AnKatB6H<sup>+</sup>* cells were observed under fluorescence microscope, abundant expression of GFP was observed indicating expression of transgenes (Fig. 6.2.2). The transformed *Anabaena* strain thus obtained (designated *AnKatB6H<sup>+</sup>*) was maintained on BG11N+ media supplemented with neomycin.

### ***AnKatB6H<sup>+</sup>* strain**

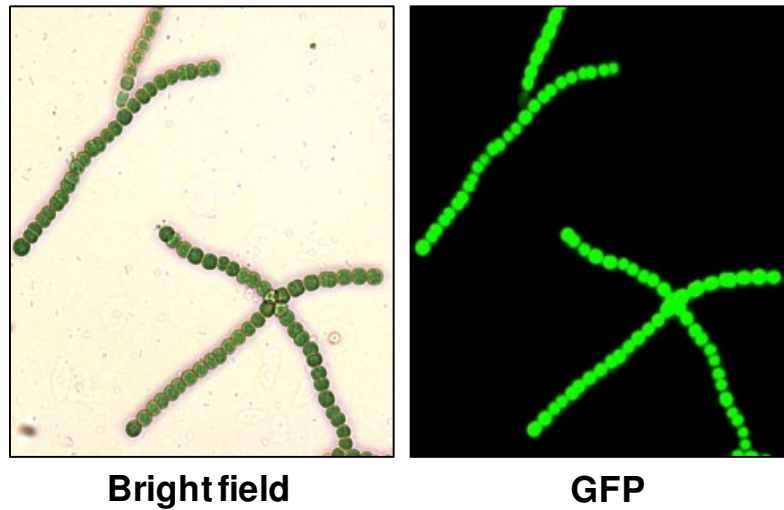


**Fig. 6.2.2** Micrograph of recombinant *AnKatB6H<sup>+</sup>* strain (400 X). Left panel, bright field micrograph; right panel, fluorescence micrograph of the same microscopic field observed under GFP filter.

### **6.2.3 Confirmation of recombinant protein production by SDS-PAGE and Western blot analysis**

The *AnKatB6H<sup>+</sup>* culture thus obtained was analyzed for the production of the recombinant An-KatB protein. The SDS-PAGE profile clearly showed the presence of the ~26 kDa protein in the crude extracts of *AnKatB6H<sup>+</sup>* strain but not in the extract of the wild-type *Anabaena* (Fig. 6.2.3 A). This protein cross-reacted with the anti-His as well as the KatB antisera, suggesting that the over-produced protein was indeed his-tagged KatB (Fig. 6.2.3 B and 6.2.3 C). Unlike the wild-type *Anabaena*, extracts from *AnKatB6H<sup>+</sup>* strain showed a copious zone of catalase activity on zymogram, indicating that the over-produced An-KatB protein was indeed an active catalase (Fig. 6.2.3 D).

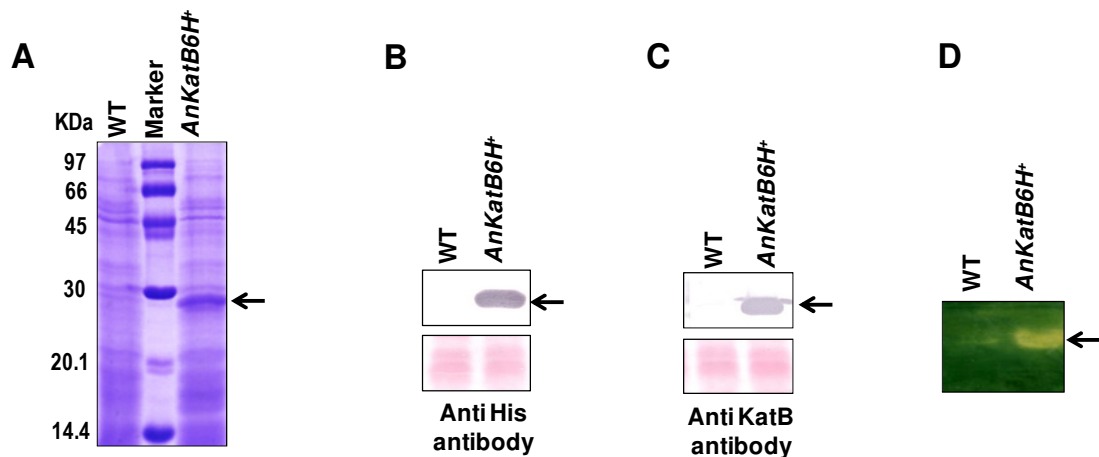


**Fig. 6.2.3 Expression of recombinant his-tagged An-KatB protein in *AnKatB6H<sup>+</sup>* strain.** (A) Cell-free extracts were prepared from the wild-type *Anabaena* PCC 7120 (WT) or the *AnKatB6H<sup>+</sup>* strain, resolved on SDS-polyacrylamide gel (14%) and visualized by staining with Coomassie brilliant blue (CBB). Over-produced protein band of approximately 26 kDa is indicated by an arrow. (B) The cell-free extracts of the wild-type *Anabaena* PCC 7120 (WT) or *AnKatB6H<sup>+</sup>* were resolved by SDS-PAGE, transferred onto nitrocellulose membrane and probed with anti-Histidine antibody or the KatB antiserum (C). Parts of Ponceau S-stained blots are shown at the bottom as loading controls. (D) *In-gel* catalase activity assay (zymogram). Cell-free extracts of the wild-type *Anabaena* PCC 7120 (WT) or *AnKatB6H<sup>+</sup>* were resolved by native 10% PAGE and stained for catalase activity. Positions of the proteins are indicated by arrows.

#### 6.2.4 Localization of the over-expressed An-KatB protein

In *E. coli*, due to improper folding, many a times the over-expressed protein is partitioned into the inclusion body fraction. In the present study, the degree of distribution of An-KaB in soluble or the insoluble fraction was assessed. The crude extracts of the *AnKatB6H<sup>+</sup>* cells were subjected to high-speed centrifugation (20000xg) to separate the soluble fraction from inclusion bodies, cell membranes, etc. As seen in Fig. 6.2.4 A, the over-expressed An-KatB protein was observed mostly in the soluble fraction, while hardly any protein could be detected in the membrane/inclusion fraction.

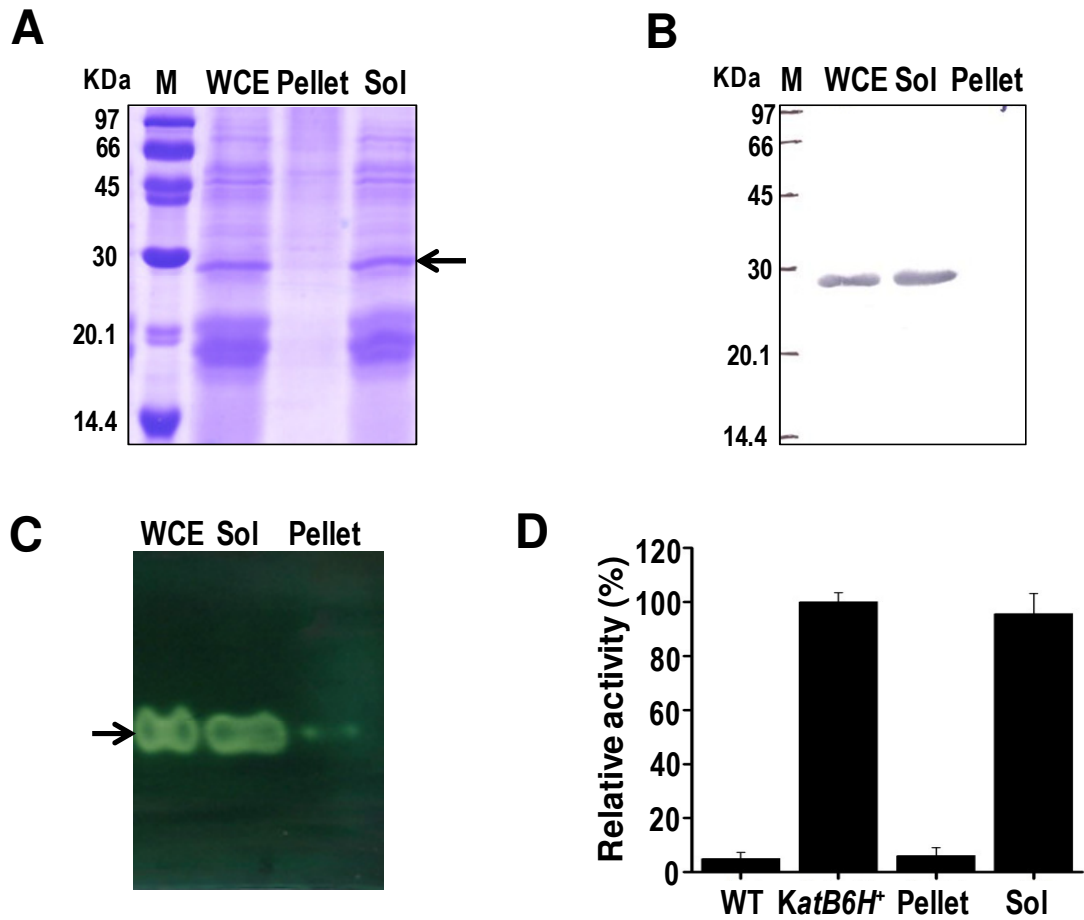


**Fig. 6.2.4 Localization of over-produced An-KatB protein in the soluble fraction.** (A) The whole cell extract (WCE) of *AnKatB6H<sup>+</sup>* strain was separated into soluble (sol) or insoluble (pellet) fractions by centrifugation, resolved on denaturing acrylamide gels and visualized by staining with CBB. Protein band corresponding to An-KatB is indicated by an arrow. (B) The above-mentioned fractions were resolved by SDS-PAGE, electro-blotted onto nitrocellulose membrane and probed with KatB antisera. (C) *In-gel* catalase activity assay (zymogram) of whole cell extracts (WCE), soluble (sol) and insoluble (pellet) fractions of *AnKatB6H<sup>+</sup>* strain. The zone of clearance representing KatB activity is depicted by an arrow. (D) Spectrophotometric H<sub>2</sub>O<sub>2</sub> decomposition assay with cell extracts of wild-type *Anabaena* (WT); *AnKatB6H<sup>+</sup>* (*KatB6H<sup>+</sup>*) and the inclusion body (Pellet) or the soluble (Sol) fraction of the *AnKatB6H<sup>+</sup>* strain. Activity exhibited by the whole cell extract of *AnKatB6H<sup>+</sup>* was considered to be 100% and other rates were calculated accordingly. Error bars represent SE.

The SDS-PAGE result was well supported by the immunoblotting experiments wherein the KatB protein could be detected only in the soluble fraction (Fig. 6.2.4 B). These fractions were resolved by native PAGE and subjected to zymographic staining. The

soluble fraction and the crude extract showed almost similar zones of clearance, suggesting that the over-expressed protein was mostly present in the soluble fraction (Fig. 6.2.4 C). These results were also corroborated with spectrophotometric catalase activity assay wherein too most of the activity was observed in the soluble fraction (Fig. 6.2.4 D).

### 6.3 Purification of his-tagged An-KatB protein using affinity chromatography

After confirming the presence of the over-produced An-KatB protein in the soluble fraction, attempts were made to purify this protein employing NiNTA resin-based affinity chromatography (as described in the methods section).

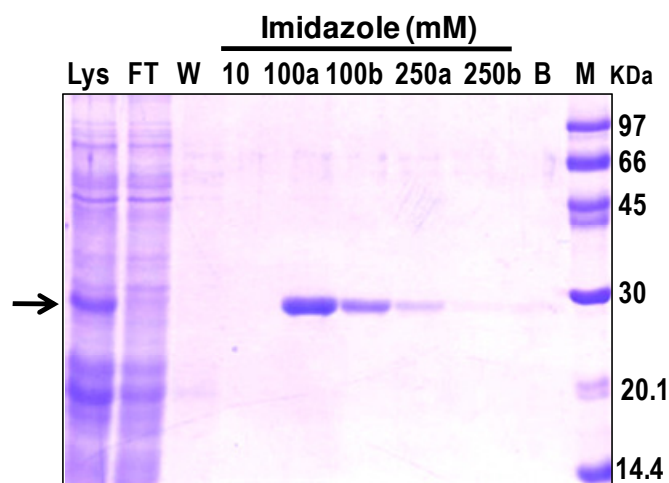


**Fig. 6.3 Purification of An-KatB protein by NiNTA affinity chromatography.** The NiNTA bound An-KatB protein was eluted by raising imidazole concentration as indicated in the figure. Lys, cell lysate; FT, flow-through, W, wash fraction; 10, 10 mM imidazole elution fraction; 100a and 100b, 1st and 2nd 100 mM imidazole elution fraction respectively; 250a and 250b; 1st and 2nd 250 mM imidazole elution fraction respectively; B, NiNTA beads fraction after protein was eluted with 250 mM imidazole; M, molecular weight marker. Position corresponding to the KatB protein is indicated by an arrow.

When all the wash and elution fractions were analyzed on denaturing polyacrylamide gels, a fairly pure band corresponding to the An-KatB protein was visualized in the elution fraction with 100 mM imidazole (Fig. 6.3). The purified protein was dialyzed against 20 mM Tris and subsequently used for biochemical and biophysical analyses.

#### 6.4 Facile purification of the overproduced KatB by simple physical downstream processes involving heat treatment and ammonium sulphate precipitation

Many proteins get unfolded/denatured at elevated temperature, resulting in their aggregation. The heat labile proteins generally aggregate, but the heat stable proteins remain soluble at high temperatures. Since, KatB is a thermostable protein; it was desired to use this property to purify An-KatB from *AnKatB6H<sup>+</sup>* extracts.

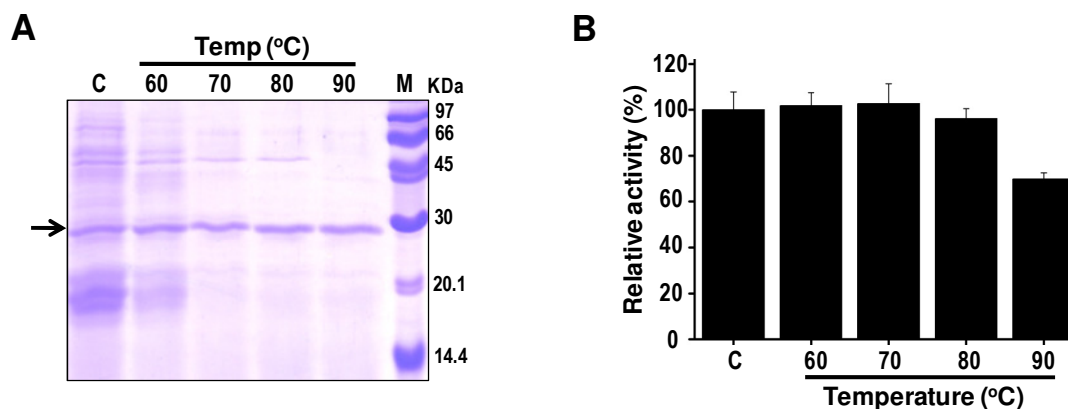


**Fig. 6.4.1 Partial purification of An-KatB with elevated temperature.** (A) High temperature treatment of *AnKatB6H<sup>+</sup>* cell extracts. Cell extracts were exposed to temperatures as indicated for 15 minutes, the soluble protein fractions were separated by centrifugation and resolved by SDS-PAGE (15%). C, soluble protein fraction obtained from the control cell extract (kept at 4 °C). The An-KatB protein is shown by an arrow. (B) Spectrophotometric H<sub>2</sub>O<sub>2</sub> decomposition activity of the above-mentioned soluble protein fractions. Activity of soluble fraction of control cell extract (C) (i.e. not exposed to elevated temperature) was considered to be 100% and the other rates were calculated accordingly. Error bars represent the SE.

Cell extracts from *AnKatB6H<sup>+</sup>* cultures were exposed to temperatures as mentioned in Fig. 6.4.1 A for 15 min. Subsequently, the soluble proteins were separated from the aggregated proteins by centrifugation and were analyzed on denaturing polyacrylamide gels. Even at 90°C, the intensity of the band corresponding to KatB remained virtually

unchanged, indicating that the KatB protein did not aggregate at this temperature and remained soluble. On the other hand, distinct decrease in the content of the other cytosolic proteins was observed at temperatures above 70°C (Fig. 6.4.1 A). An-KatB obtained from the supernatant of the above-mentioned treatments was also assayed for the catalase activity. Up to 80°C there was no loss in catalase activity. However, at 90°C, a 22% drop in enzyme activity was noticed (Fig. 6.4.1 B). Hence, to achieve the best possible heat-mediated purification, 80°C i.e. the temperature at which no enzyme activity was lost, was chosen and the incubation time was optimized at this temperature. The cell extract (green in colour) was exposed to 80°C for various time points and the soluble fractions were obtained by centrifugation. Within 10 minutes of incubation at 80°C, the green cell extract turned colourless (Fig. 6.4.2 A). When the fractions were assayed for catalase activity, it was found that the activity remained unaffected for up to 20 minutes of incubation at 80°C. However, at the end of 30 minutes incubation, a small decrease in activity was noticed (Fig. 6.4.2 B).

On SDS-PAGE, the soluble fraction of the cell extract incubated at 80°C for 20 minutes showed the efficient removal of other cytosolic proteins, while virtually intact An-KatB protein was detected (Fig. 6.4.2 C). Spectrophotometric H<sub>2</sub>O<sub>2</sub> decomposition assay indicated that there was no loss in catalase activity after exposure to 80°C for 20 minutes and the entire activity was essentially confined only to the supernatant (Fig. 6.4.2 D).

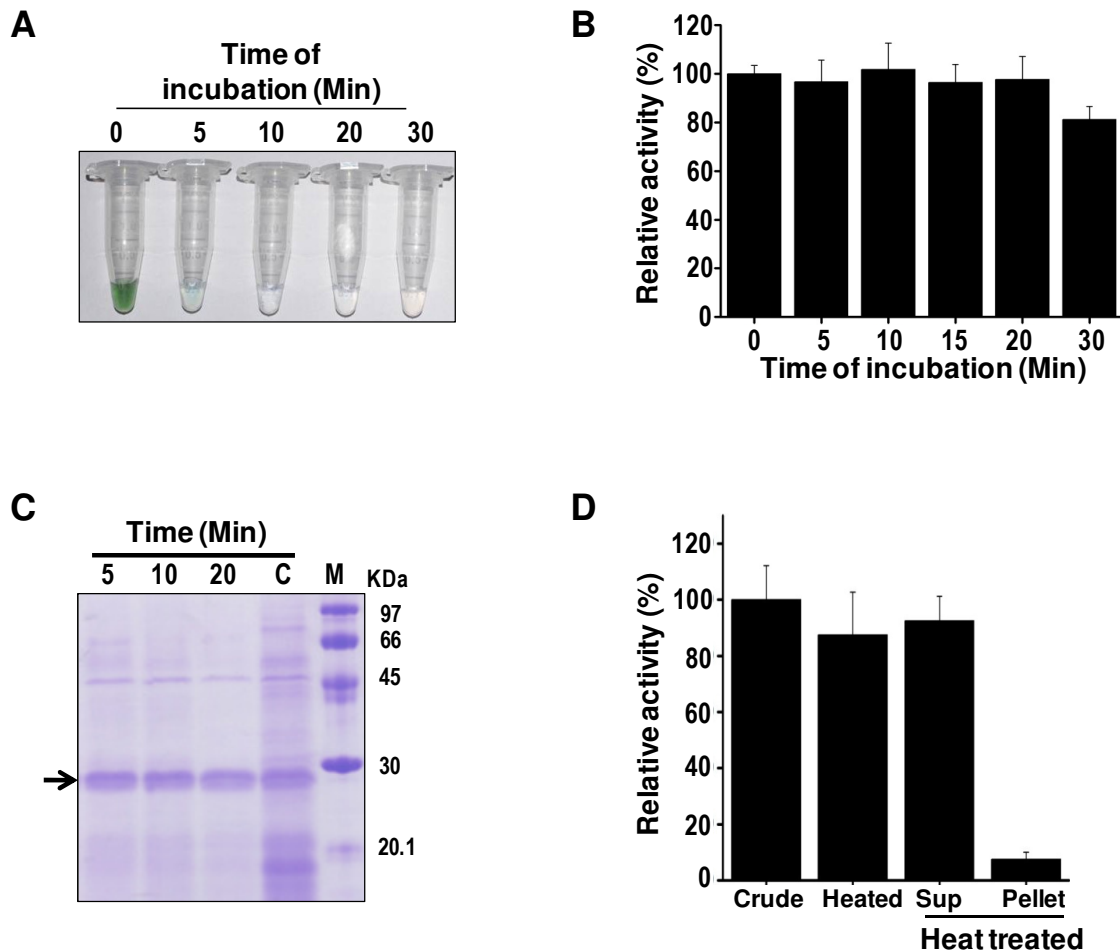


**Fig. 6.4.2 Optimization of incubation time at 80°C.** (A) Decolorization of the *AnKatB6H<sup>+</sup>* soluble fraction at 80°C. The cell extract was kept at 80°C for time point as indicated in the figure. Soluble fraction was then separated by centrifugation and photographed. (B) H<sub>2</sub>O<sub>2</sub> decomposition activity of the cell extract heated at 80°C for time points as indicated. Activity shown by control sample (0 minute) was considered to be 100% and other rates were calculated accordingly. Error bars depict the SE. (C) SDS-PAGE profile showing the partial purification of An-KatB after exposure to 80°C at various time points. C, the cell-free extract (without heat treatment) from the *AnKatB6H<sup>+</sup>* strain loaded as a control. (D) The cell-free extracts of *AnKatB6H<sup>+</sup>* strain (Crude) was exposed to 80°C for 20 minutes (Heated) followed by separation of the soluble (Sup) and insoluble fraction (Pellet) by centrifugation. Sample from each step was aliquoted and employed for H<sub>2</sub>O<sub>2</sub> decomposition assay. Activity exhibited by crude extract was considered to be 100% and other rates were calculated accordingly. Error bars represent SE.

After heating the *AnKatB6H<sup>+</sup>* extract at 80°C for 20 min, selective precipitation of An-KatB was carried out with ammonium sulphate. On treatment with 30% ammonium sulphate, most of the contaminating proteins were precipitated while the An-KatB

protein remained in the soluble fraction. When the ammonium sulphate concentration was raised to 60%, a fairly pure form of the KatB protein precipitated (Fig. 6.4.3 A). Most the An-KatB protein precipitated with 60% ammonium sulphate and no protein was detected when ammonium sulphate concentration was raised further to 90%. The identity of the protein precipitated with 60% ammonium sulphate was ascertained with the *Anabaena* KatB antiserum (Fig. 6.4.3 B). The immunoblot also showed the protein band of ~50 kDa which co-purified with An-KatB to cross-react with the KatB antiserum, indicating that it may be a higher (dimeric?) form of KatB that remains undissociated even when subjected to denaturing PAGE (Fig. 6.4.3 B).

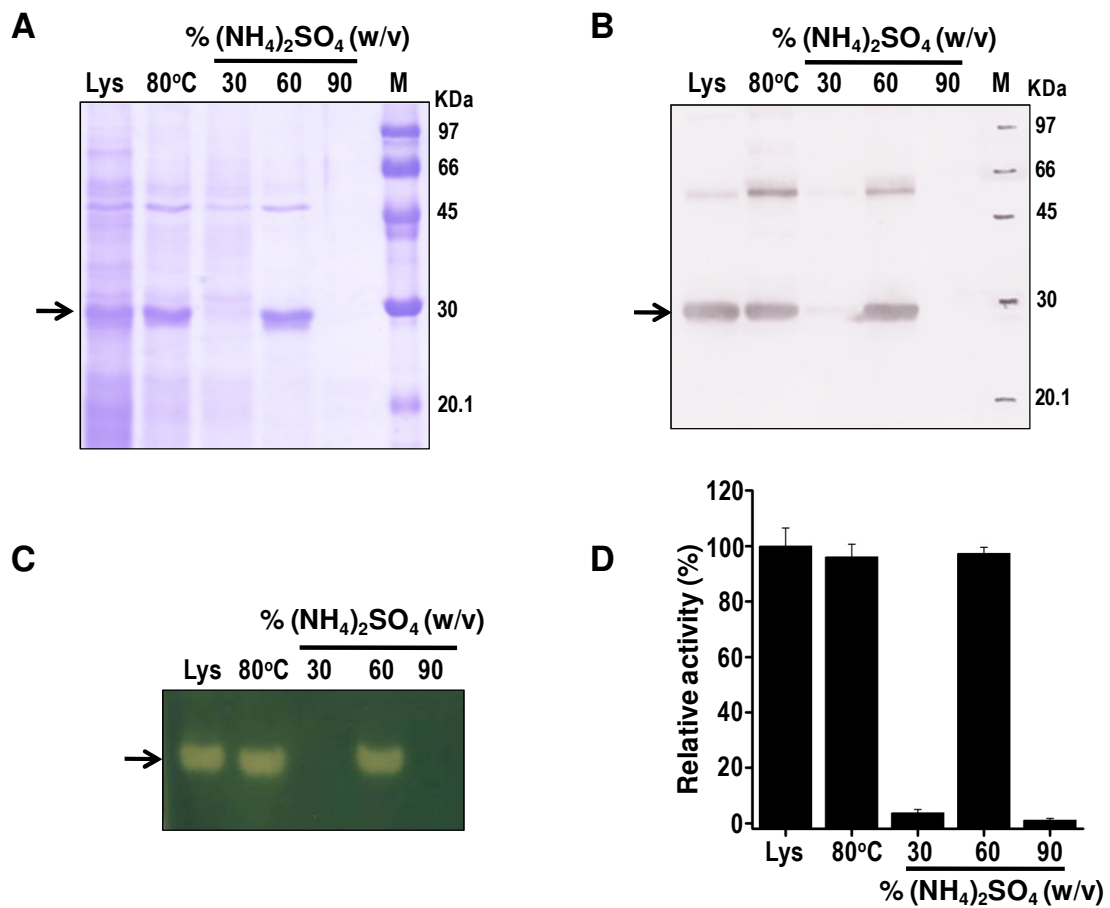


**Fig. 6.4.3. Purification of An-KatB by ammonium sulphate precipitation.** (A) Ammonium sulphate precipitation for purification of An-KatB from *AnKatB6H<sup>+</sup>* extracts. Cell-free extract of *AnKatB6H<sup>+</sup>*

culture was exposed to 80°C for 20 min and the soluble fraction, separated by centrifugation, was subjected to (NH<sub>4</sub>)<sub>2</sub>SO<sub>4</sub> precipitation. The precipitate obtained from different (NH<sub>4</sub>)<sub>2</sub>SO<sub>4</sub> fractions (30%, 60% and 90%, as indicated in the figure) was dissolved in buffer and equal volume (25 µl) from each sample was resolved by SDS-PAGE. Lys, cell lysate of *AnKatB6H*<sup>+</sup>; 80 °C, heat-treated *AnKatB6H*<sup>+</sup> cell lysate; M, molecular weight marker. **(B)** Western blotting and immunodetection. The above mentioned samples were resolved by SDS-PAGE, transferred onto nitrocellulose membrane and probed with KatB antibody. **(C)** Zymogram showing the catalase activity of the samples described in (A). **(D)** Spectrophotometer-based H<sub>2</sub>O<sub>2</sub> decomposition activity shown by the samples described in (A). Activity shown by the *AnKatB6H*<sup>+</sup> cell lysate (Lys) was considered to be 100% and the other rates were calculated accordingly. Error bars represent SE.

All the fractions were assayed for catalase activity (Fig. 6.4.3 C and Fig. 6.4.3 D) and almost the entire activity (as exhibited by the *AnKatB6H*<sup>+</sup> cell lysate) was retained in the 60% ammonium sulphate fraction, indicating that no activity was lost during this process.

### **6.5 Biophysical and biochemical characteristics of the purified An-KatB**

The An-KatB protein, purified through heat treatment followed by ammonium sulphate precipitation or through NiNTA affinity chromatography, was thoroughly analyzed to make sure that its biophysical or biochemical characteristics were not adversely affected by the mode of purification performed. The protein purified through heat treatment followed by ammonium sulphate precipitation was named as An-KatB-H-A, while, the protein purified by NiNTA chromatography was named as An-KatB-N. When assayed, both the preparations showed almost the same level of catalase activity (Fig. 6.5.1 A).

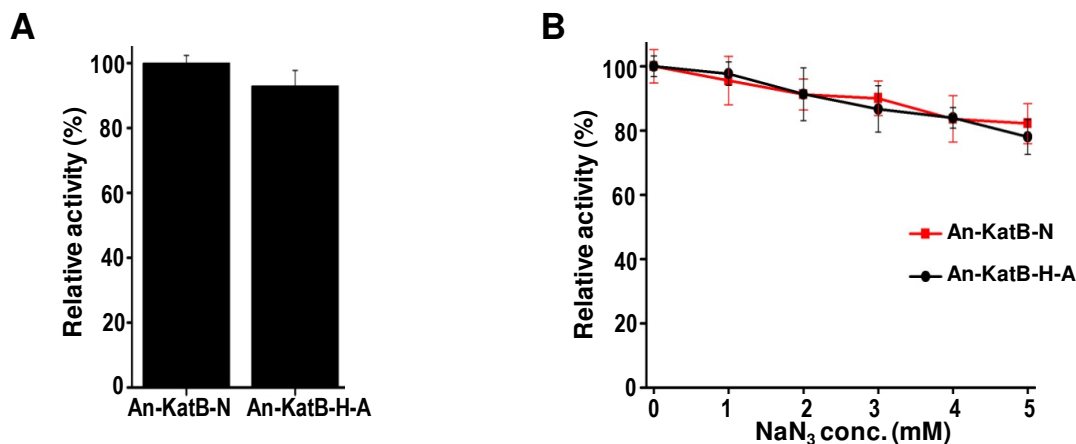


**Fig. 6.5.1. Activity of An-KatB-H-A and An-KatB-N.** (A) H<sub>2</sub>O<sub>2</sub> decomposition activity of An-KatB purified by affinity chromatography (An-KatB-N) or by heat treatment (80°C for 20 minutes) followed by 60% (NH<sub>4</sub>)<sub>2</sub>SO<sub>4</sub> precipitation (An-KatB-H-A). For the assay, equal amount of both the protein (5 μg) was taken and activity of the An-KatB-N protein was considered as 100% while activity of An-KatB-H-A was calculated accordingly. Error bars represent SE. (B) Sensitivity to sodium azide. Catalase activity of An-KatB-N or An-KatB-H-A was measured in the presence of sodium azide as indicated in the figure. Activity in the absence of sodium azide was taken as 100% and other rates were calculated accordingly. Error bars depict the SE.

As mentioned in the previous chapter, insensitivity to azide is one of the hallmarks of Mn-catalases. Both the protein preparations showed similar (lack of) sensitivity to inhibition by sodium azide (Fig. 6.5.1 B). CD spectropolarimetry showed both An-KatB-N and An-KatB-H-A to have practically the same secondary structure (Fig. 6.5.2 A). CD based melting curve analysis further suggested that both the preparations were equally resistant to thermal denaturation. The T<sub>m</sub> of both the proteins was determined to be 98 ± 1°C (Fig. 6.5.2 B). Thus, in conclusion, the chemical or physical properties of the An-KatB protein were unaffected by the mode of purification.

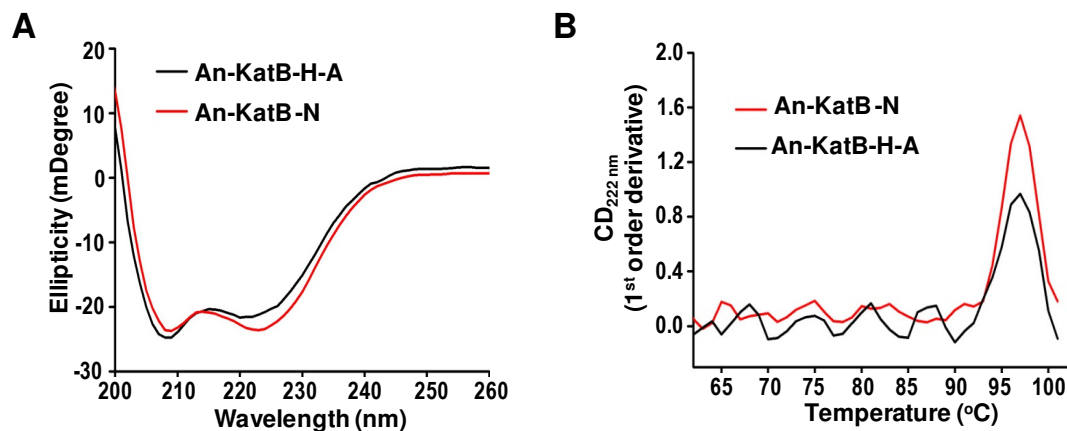


**Fig. 6.5.2 Secondary structure and melting curve analysis.** (A) CD spectra of An-KatB-H-A and An-KatB-N. (B) Thermal denaturation of An-KatB-N or An-KatB-H-A. Dichroic intensities at 222 nm of the proteins were monitored in the temperature range mentioned in the figure. Melting points were obtained from the first order differential plot generated from the melting curve.

## 6.6 Comparison of biophysical properties of An-KatB and KatB purified from *E. coli* (Ec-KatB)

In most laboratories, *E. coli* is usually preferred as the expression host for recombinant protein expression and purification. As elaborated in the earlier chapters, the KatB protein was over-expressed in *E. coli* and purified via affinity chromatography for characterization whereas in this chapter, purification of the KatB protein after over-expression in *Anabaena* PCC 7120 is detailed. To study the effect of the expression-host on the over-produced protein, a comparative analysis of the KatB protein purified from *Anabaena* PCC 7120 (An-KatB) or *E. coli* (Ec-KatB), was performed.

### 6.6.1 Compactness of An-KatB and Ec-KatB

Surprisingly, on native PAGE analysis, Ec-KatB showed reduced mobility as compared to the An-KatB protein, suggesting that the later was more compact in nature (Fig. 6.6.1 A). In size exclusion chromatography too the Ec-KatB protein eluted earlier than An-

KatB (Fig. 6.6.1 B), indicating that An-KatB was more compact, with a lower hydrodynamic radius than Ec-KatB.

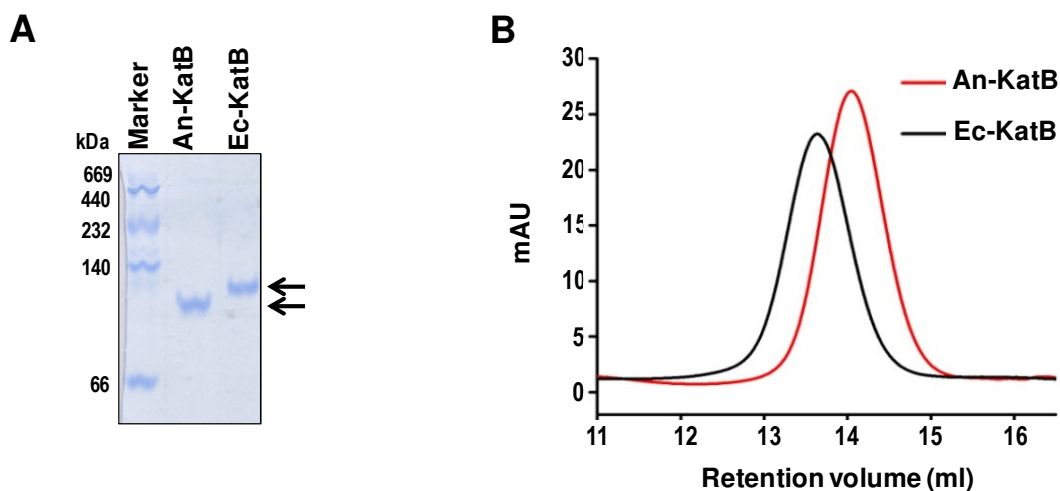


**Fig. 6.6.1 Oligomeric compactness of An-KatB or Ec-KatB.** (A) Native PAGE. The An-KatB or Ec-KatB proteins were resolved by non-denaturing polyacrylamide gels and stained with CBB. (B) Gel filtration chromatographic profile of An-KatB or Ec-KatB. 200  $\mu$ g of the purified protein was injected into Superdex 200 10/300 GL column pre-equilibrated with buffer containing 20 mM Tris and 50 mM NaCl, pH 7.2.

### 6.6.2 Secondary structure and thermostability

Both the protein preparations were subjected to CD analysis to evaluate their secondary structures. An-KatB and Ec-KatB showed nearly identical secondary structure (Fig. 6.6.2A). Melting curve analysis showed both the proteins to be equally thermostable with  $T_m$  of  $\sim 98^\circ\text{C}$  (Fig. 6.6.2 B).

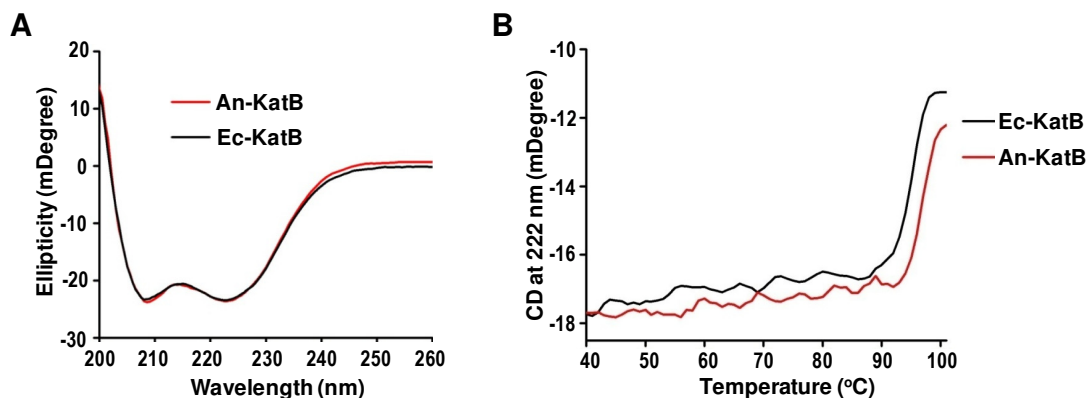


**Fig. 6.6.2 Circular dichroism spectropolarimetry of An-KatB or Ec-KatB.** (A) CD spectra of An-KatB or Ec-KatB. (B) Thermal denaturation of An-KatB or Ec-KatB. Dichroic intensities at 222 nm of the proteins were monitored in the temperature range mentioned in the figure.

### 6.7 Comparison of the biochemical properties of An-KatB and Ec-KatB

The An-KatB and Ec-KatB protein were compared for their ability to decompose  $H_2O_2$ . Surprisingly, on zymographic analysis, the An-KatB protein showed a distinctly larger zone of catalase activity as compared to Ec-KatB (Fig. 6.7 A). The result suggested that An-KatB was catalytically more active than Ec-KatB. This evidence was further supported by spectrophotometric  $H_2O_2$  decomposition assays wherein the An-KatB protein showed about four fold higher specific activity than Ec-KatB (Fig. 6.7 B).

$H_2O_2$  decomposition activity of both the proteins was tested at different pH (ranging from 5.0 to 10.0). An-KatB exhibited good catalase activity over a wide range starting from pH 5.5 to 9.0. On the other hand, the Ec-KatB protein showed appreciable catalase only activity between pH 7.5 and pH 9.0. Both the proteins were also assayed for their sensitivity towards guanidine hydrochloride-mediated denaturation. Although the two types of KatB protein differed in their compactness and catalytic activity, both of them showed similar level of susceptibility to this chemical denaturant (Fig. 6.7 D).

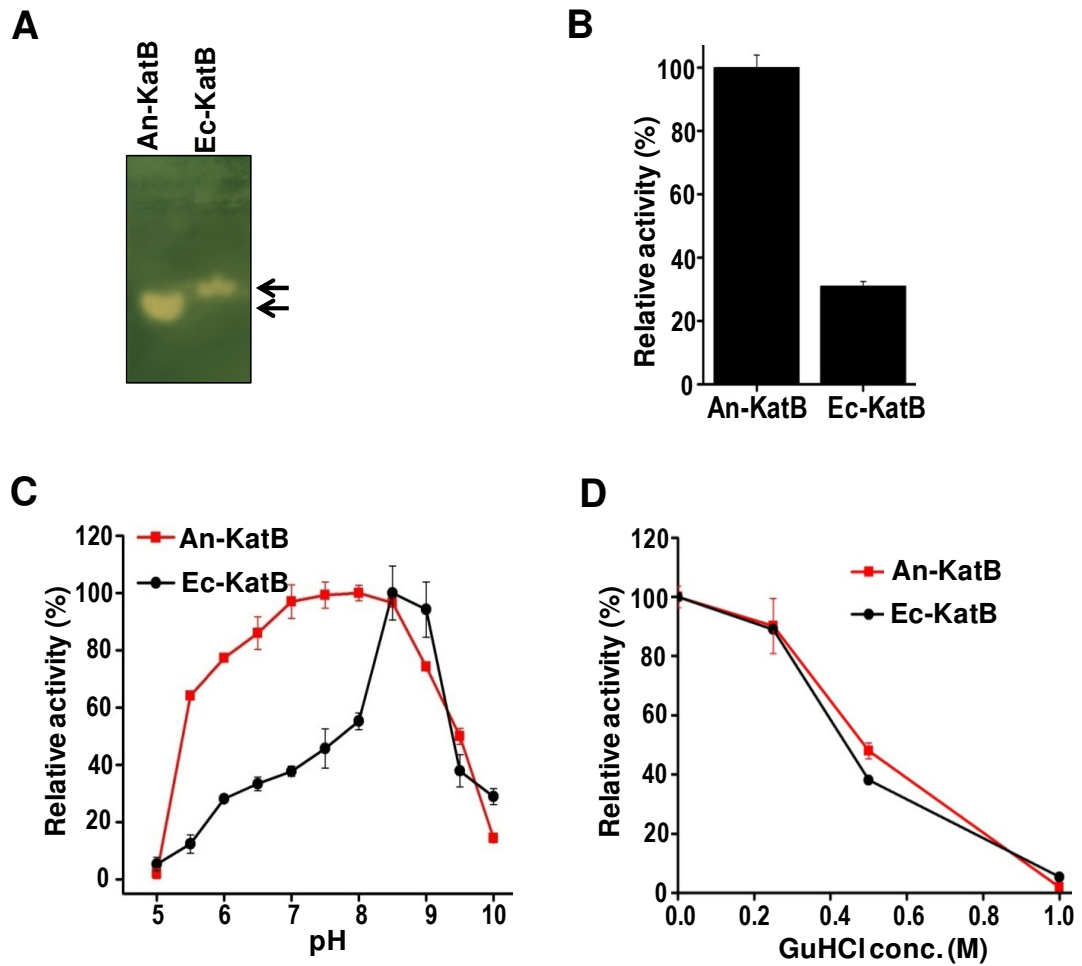


**Fig. 6.7 Comparison of KatB purified from *Anabaena* (An-KatB) or from *E. coli* (Ec-KatB).** (A) *In-gel* catalase activity assay (zymogram) An-KatB or Ec-KatB. (B) Spectrophotometric  $\text{H}_2\text{O}_2$  decomposition activity of An-KatB or Ec-KatB. Activity shown by An-KatB was considered as 100% and activity of Ec-KatB was calculated accordingly. Error bars represent SE. (C) pH dependent catalase activity of An-KatB or Ec-KatB. Rate of  $\text{H}_2\text{O}_2$  decomposition was measured at various pH for both the proteins and plotted as relative activity. Maximum measured activity of An-KatB (recorded at pH8.0) was considered as 100% whereas maximum activity of Ec-KatB (recorded at pH 8.5) was considered as 100%. Error bars depict the SE. (D) Effect of GuHCl on activity. The An-KatB or the Ec-KatB protein was incubated with different concentration of GuHCl as indicated and their catalase activity was measured with spectrophotometer. Activity of each protein in the absence of GuHCl was considered to be 100% and other rates were calculated accordingly. Error bars represent SE.

## **6.8 Comparison of the total KatB protein yield obtained from *Anabaena* or *E. coli* expression host**

One of the most important factors for recombinant protein production is the yield of over-produced protein per unit biomass of the expression host. The total amount of the purified KatB recovered after over-expression in *Anabaena* or *E. coli* was calculated and compared. The yield of KatB was measured on the basis of per unit fresh weight of the expression host.  $10.5 \pm 0.8$  mg of Ec-KatB protein was recovered per gram (fresh weight) of *E. coli* biomass. On the other hand  $7.1 \pm 0.6$  mg An-KatB protein was obtained from equivalent amount of *Anabaena* biomass (i.e. 1 g fresh weight). It is important to note here that 30% lower yield of An-KatB compared to Ec-KatB was adequately compensated by the four fold higher activity of the An-KatB protein.

## **6.9 Comparison of An-KatB with a commercially procured heme-catalase**

A commercially available heme-catalase enzyme (named as Comm Cat) was procured for comparing its physical and biochemical attributes with that of the An-KatB protein.

### **6.9.1 Biochemical properties**

In spectrophotometric H<sub>2</sub>O<sub>2</sub> decomposition assays, the specific activity of the An-KatB protein was slightly lower as compared to that of the Comm Cat (Fig. 6.9.1 A). Activity of the Comm Cat and the An-KatB protein was compared at different pH. The Comm Cat protein was found to be most active at neutral pH (7.0) but thereafter at higher pH the catalase activity of this protein declined rapidly (Fig. 6.9.1 B). In contrast to Comm Cat, the An-KatB protein showed appreciable catalase activity even at pH 9.0 (Fig. 6.9.1 B).

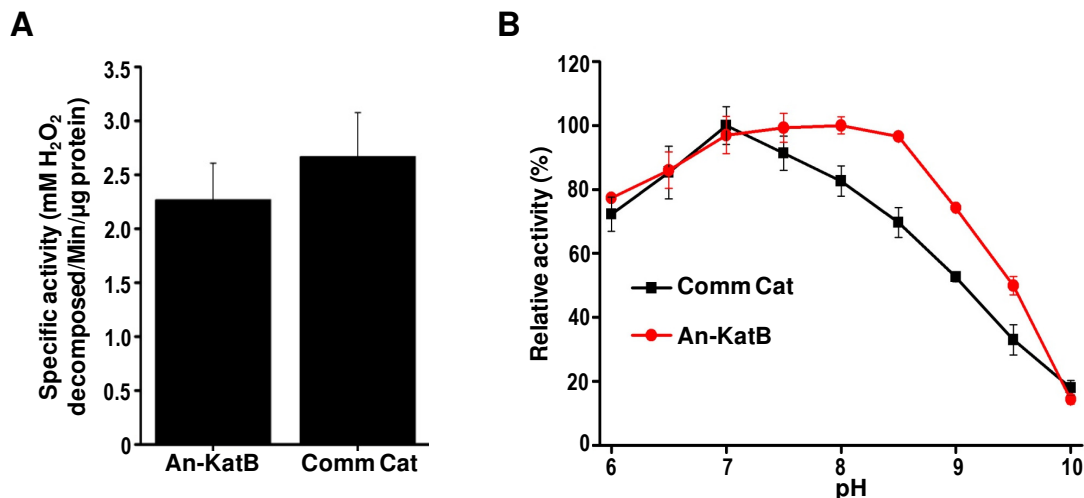


**Fig. 6.9.1** Comparison of specific activity and effect of pH on An-KatB and Comm Cat. **(A)** H<sub>2</sub>O<sub>2</sub> decomposition activity exhibited by An-KatB or Comm Cat. Error bars represent SE. **(B)** The catalase activity of An-KatB or Com Cat was measured at different pH as indicated in the figure. Maximum activity of the proteins (obtained at pH 7.0) was considered to be 100% and the rest were calculated accordingly. Error bars represent the SE.

### 6.9.2 CD spectropolarimetric analyses

CD spectropolarimetric analysis with the commercial catalase (Comm Cat) indicated that the commercial catalase (Comm Cat), like An-KatB, was also a largely  $\alpha$ -helical protein (Fig. 6.9.2 A). However, during thermal denaturation Comm Cat showed a loss in secondary structure when temperature was raised above 40°C (Fig. 6.9.2 B). In contrast, there was no loss of secondary structure of An-KatB even at 90°C. The melting curve analysis suggested that unlike An-KatB, Comm Cat was a heat labile protein.

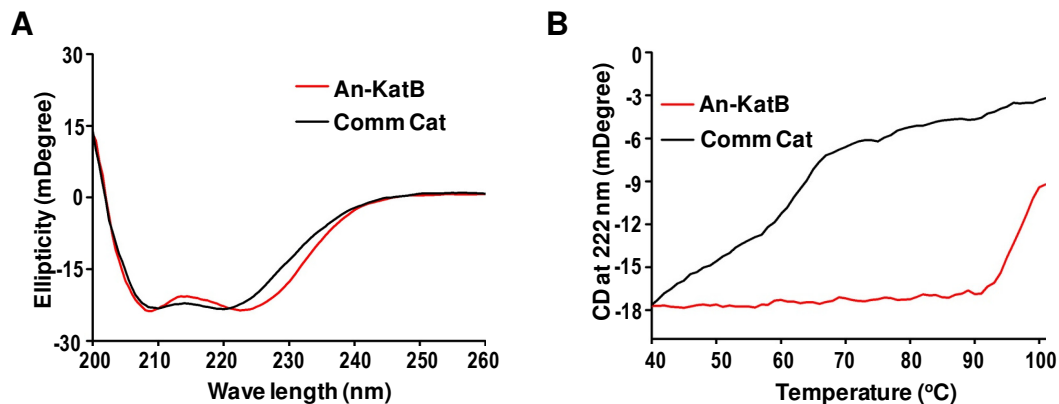


**Fig. 6.9.2 CD spectropolarimetric analysis of An-KatB or Comm Cat.** (A) CD spectra of An-KatB or Comm Cat. (B) Thermal denaturation of An-KatB or Comm Cat. Dichroic intensities at 222 nm was measured at the temperature range mentioned in the figure

### 6.9.3 Effect of high temperature on catalase activity

To assess their ability to withstand exposure to elevated temperatures, both the enzyme preparations (An-KatB and Comm Cat) were exposed to various temperatures for 10 minutes and subsequently assayed for their ability to decompose  $H_2O_2$  (at room temperature) (Fig. 6.9.3 A). The activity of An-KatB was found fairly stable even after exposure to 90°C, whereas the Comm Cat protein showed a distinct drop in activity when the incubation temperature was over 50°C. This result correlated well with the CD melting curve analysis of Comm Cat (Fig. 6.9.2 B) wherein loss of secondary structure was observed at temperature beyond 40°C. This enzyme preparation lost over 40% of its original activity when exposed at 60°C and it became completely inactive at temperature above 80°C (Fig. 6.9.3 A).

Both the enzyme preparations were incubated at 85°C for various time points to determine their thermostability at this temperature. The An-KatB protein could withstand 85°C for 30 minutes with minor loss in activity (Fig. 6.9.3 B). In fact it retained around 70% of its original activity at the end of 1 hour of incubation at 85°C.

On the other hand, the commercial catalase lost all of its activity within 10 minutes of incubation at that temperature (Fig. 6.9.3 B).

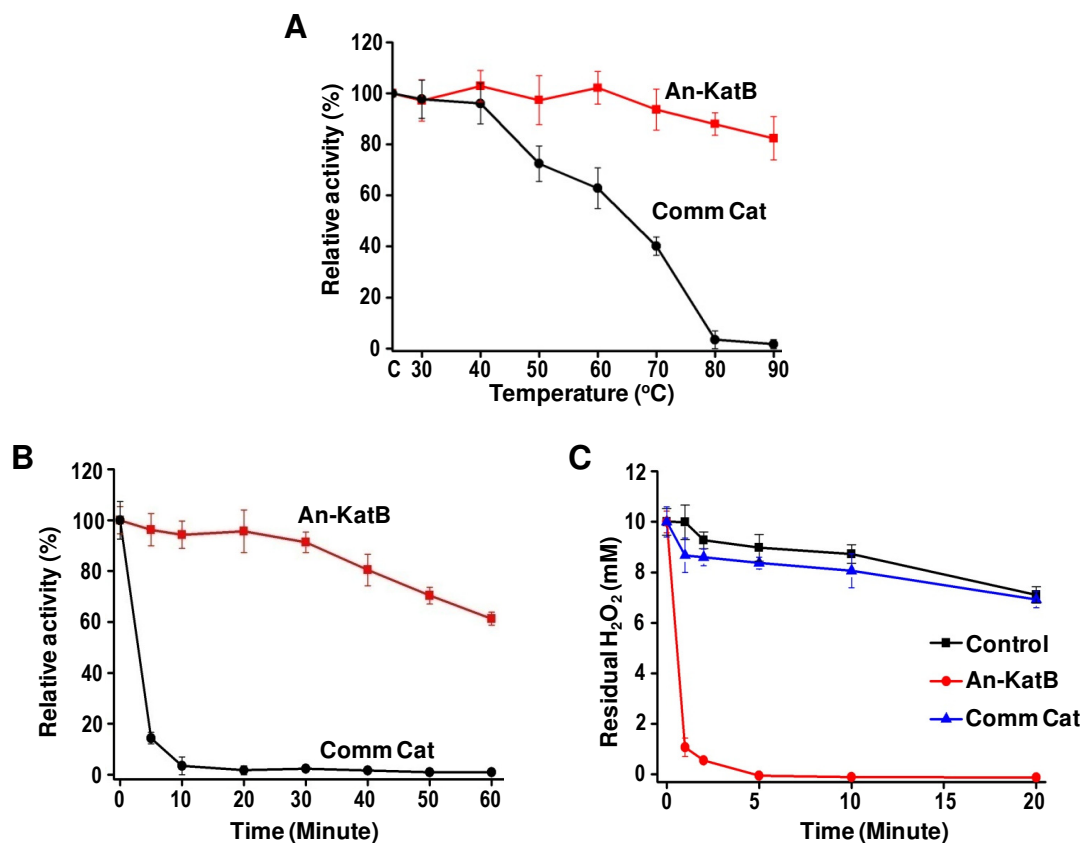


**Fig. 6.9.3 Comparison of thermostability.** (A) Ability of An-KatB or Comm Cat to withstand elevated temperature. Both the proteins were incubated at different temperatures (as indicated) followed by measurement of catalase activity at room temperature. Activity of the sample kept at room temperature was considered to be 100% and other rates were calculated accordingly. Error bars show SE. (B) The An-KatB or Comm Cat protein was incubated at 85°C and catalase activity was measured at the time points indicated. Relative activity of the respective enzymes kept at room temperature was taken as 100% and other rates were calculated accordingly. Error bars represent SE. (C) Activity An-KatB or Comm Cat at 85°C. 10 mM H<sub>2</sub>O<sub>2</sub> substrate was added to the reaction mixture containing proteins at 85°C and aliquots were taken at time points as indicated for determination of residual H<sub>2</sub>O<sub>2</sub> in the reaction mixture. Control, no enzyme added (negative control); An-KatB (20 μg); Comm Cat, Commercial catalase (20 μg). Error bars represent SE.

Ability of these two enzymes to function at high temperature was also assayed. At 85°C, An-KatB could decompose H<sub>2</sub>O<sub>2</sub> efficiently, but the Comm Cat was unable to function

at this temperature (Fig. 6.9.3 C). All these results show that unlike the commercial heme-catalase, An-KatB protein is not only thermostable but also functional at elevated temperatures.

## 6.10 Discussion

In spite of the distinct advantage of photoautotrophy, cyanobacteria are still under exploited as production platforms for generation of high-value products [282]. In most of the cases, heterotrophic micro organisms have been used in bio-industrial processes for the production of variety of commercial products like amino acids, vitamins, recombinant peptides etc. These platforms, including the common ones that utilize *E. coli*, require expensive carbohydrates as nutritional inputs. On the other hand, due to their photosynthetic nature, cyanobacteria can grow on minimal medium containing few salts by harnessing the abundantly available solar energy [283, 284]. As cyanobacteria are more efficient in photosynthesis than plants, they can effectively use solar energy for fixation of atmospheric carbon (CO<sub>2</sub>) into organic matter [285]. As a result, using cyanobacterial biomass for bio-production of high-value compounds also leads to reduction in the atmospheric load of CO<sub>2</sub>, which is a major contributor to global warming [286]. Additionally, nitrogen-fixing strains of cyanobacteria like *Anabaena* can convert the atmospheric N<sub>2</sub> into bio-available form, thereby, circumventing the requirement of nitrogenous compounds for their growth. Moreover, specialized bioreactors are needed for the growth of heterotrophic bacteria, while, for growing cyanobacteria these type of bioreactors are not needed. They can be grown in tanks, pits, raceway ponds etc [287]. For many cyanobacteria, genetic manipulation techniques are well established. Cyanobacteria such as *Synechocystis* sp. PCC 6803,

*Synchococcus* sp. PCC 7002, *Synechococcus elongates* PCC 7942 and *Anabaena* sp. PCC 7120 etc have been genetically modified for expression of transgenes.

Recombinant proteins have been over-expressed in various cyanobacterial hosts in the past. However, most of these reports are confined to unicellular, non-nitrogen fixing strains such as *Synechocystis* or *Synechococcus*. Several proteins have been over-expressed in these cyanobacteria for enhancing their stress tolerance or for production of biofuels/hydrocarbons [288, 289, 290, 291]. Proteins like mosquito larvicidal protein, human superoxide dismutase, metallothionein or lactate dehydrogenase have been successfully over-produced employing cyanobacterial expression systems [292, 293, 294, 270].

More recently, several endogenous proteins (superoxide dismutase A/B; peroxiredoxins All1541, Alr3183 or Alr4641; Mn-catalase KatA etc.) involved in oxidative stress management were overexpressed in *Anabaena* PCC 7120 with an aim to enhance its stress tolerance [198, 159, 95, 191]. Although the above-mentioned proteins were over-produced in good amounts, attempts were not made to purify these from the recombinant *Anabaena* strains. In the present study, we have not only overproduced the KatB protein, but have also demonstrated that the over-expressed protein can be easily purified in its form from *Anabaena* (Fig. 6.3 and Fig. 6.4.3).

For over-expression of a recombinant protein in certain expression host, the choice of promoter element is very crucial. Native or heterologous promoters like  $P_{tac}$  (IPTG-inducible),  $P_{trc}$  (IPTG-inducible),  $P_{psbA1}$  (light-dependent),  $P_{smtA}$  (zinc-inducible),  $P_{petE}$  (copper-inducible) and  $P_{nir}$  (nitrate-inducible) promoters have been used to drive the expression of genes in *Anabaena* [274, 195, 295]. As the  $P_{psbA1}$  is driven by light, this promoter offers a distinct advantage over others as no other chemical inducer is

additionally needed for its induction in *Anabaena*. Since light is the basic requirement for growth of this photosynthetic cyanobacterium, the  $P_{psbAI}$  promoter functions as a strong promoter under the normal conditions of growth. But, it should be noted that this promoter is not stringently regulated. However, this lack of tight regulation can be of distinct advantage when constitutive expression of protein is desired. In current study too, use of  $P_{psbAI}$  promoter resulted in copious production of the recombinant KatB protein in *Anabaena* (Fig. 6.2.3).

One major concern associated with over-expression of proteins in *E. coli* is the partitioning of the over-expressed protein into the insoluble inclusion bodies due to improper folding of the recombinant protein [296]. Results described in the previous chapter (Chapter 4) showed that, when overproduced in *E. coli*, the KatB protein was present in the inclusion body fraction when cells were grown at 37°C. The protein was partly obtained in the soluble fraction only when the incubation temperature was reduced to 20°C. Interestingly, when over-expressed in *Anabaena*, almost the entire amount of over-produced KatB protein was found to be present in the soluble fraction (Fig. 6.2.4). The solubility of the protein was not affected in spite of the fact that the *AnKatB6H<sup>+</sup>* cells were grown at ambient temperature ( $27 \pm 2^\circ\text{C}$ ). Earlier, few proteins like KatA (the other Mn-catalase in *Anabaena*) or Alr4642 (a peroxiredoxin) were over-produced in *E. coli*, but could not be purified as they were completely insoluble in this host. However, these proteins were found to be expressed in their soluble and catalytically active forms when over-expressed in *Anabaena* [200, 190]. It is definitely worthwhile to explore *Anabaena* as an expression system for over-production of proteins that remain completely insoluble when expressed in *E. coli*.

Notably, depending on the expression platform used, distinct differences were observed in the biophysical and biochemical properties of KatB. The *Anabaena* derived KatB (An-KatB) was several-fold more active than the Ec-KatB i.e. the *E. coli*-derived KatB protein (Fig. 6.7 A and Fig. 6.7 B). The An-KatB protein was active in a broader pH range compared to the Ec-KatB protein (Fig. 6.7 C). The exact reason for this phenomenon is not known yet. Results from the previous chapter established that there is a positive correlation between the compactness of KatB oligomer and its catalase activity. Although, An-KatB and Ec-KatB showed similar secondary structure, gel filtration and native PAGE analysis showed An-KatB to be more compact compared to Ec-KatB (Fig. 6.6.1). Another reason for differences in enzyme properties could be the post translational modifications, which are specific to the expression hosts. To shed light on this phenomenon, attempts to crystallize the An-KatB protein for structural characterization are underway.

Although, An-KatB and Ec-KatB showed notable differences in compactness and activity, both the proteins were found to be equally thermostable. Like all Mn-catalases, including KatA from *Anabaena*, An-KatB or Ec-KatB was found to be thermostable. Heme-catalases, on the other hand, are generally heat labile in nature. Heme-catalase, KatG from unicellular cyanobacteria *Synechococcus* PCC 7942 was inactivated when incubated temperature above 50°C [200]. The commercial heme-catalase used in this study too showed a distinct drop in activity above 50°C (Fig. 6.9.4).

Hydrogen peroxide (H<sub>2</sub>O<sub>2</sub>) has widespread use as disinfectant in food or pharmaceutical industries [110]. It is also extensively utilized in textile and paper-pulp industry as universal bleaching agent to increase the whiteness of the substrate [297].

After the process is over, the residual  $\text{H}_2\text{O}_2$  has to be effectively eliminated because the presence of  $\text{H}_2\text{O}_2$  has undesirable effects in the downstream processes. Earlier, repeated washing of the material with water was performed to remove the residual  $\text{H}_2\text{O}_2$ . However, this is not preferred now a days as this is a highly water consuming process. Moreover, direct release of left-over  $\text{H}_2\text{O}_2$  into the environment not acceptable as [111] as  $\text{H}_2\text{O}_2$  *per se* is a toxic reactive oxygen species (ROS), which easily diffuses across cell membranes [298] and threatens cell survival. Therefore, it is essential to detoxify the residual  $\text{H}_2\text{O}_2$  to prevent toxicity to aquatic life and for smooth downstream processing. Hence, in industries, heme-catalases from bovine, fungal or microbial origin are widely used to remove residual  $\text{H}_2\text{O}_2$  after the bleaching process is over [299, 276]. In textile industries, the bleaching process is carried out at high temperature and at alkaline pH. Therefore, the use of heme-catalases poses a major drawback as these enzymes show a steep drop in their activity over  $50^\circ\text{C}$  or at alkaline pH [299]. Hence, a thermostable and alkali tolerant enzyme can offer distinct advantage over currently available heme-catalases in textile industry. Results described in this chapter clearly show that KatB is a robust catalase that can withstand high temperatures and function at alkaline pH (Fig. 6.7 and Fig. 6.9.4). Therefore, thermostable and alkali tolerant catalases such as KatB may prove to be better substitutes for heme-catalases in applications such as bleaching of textiles where  $\text{H}_2\text{O}_2$  is to be decomposed at higher temperatures (over  $60^\circ\text{C}$ ) and alkaline pH [300].

To summarize, the thermostable Mn-catalase KatB, successfully overproduced in *Anabaena* was purified by a simple physical processes. The KatB protein obtained from *Anabaena* had better-quality characteristics than the similar KatB protein purified from *E. coli*. KatB was more thermo-stable than a commercially procured heme catalase.

Thus, *Anabaena* can be an ideal platform for overexpression/purification of proteins, and furthermore, the Mn-catalase KatB may be advantageous over heme-catalases in processes where hydrogen peroxide has to be eliminated at elevated temperatures.

## SUMMARY

Of the two Mn-catalases (KatA and KatB) present in the cyanobacterium *Anabaena* PCC 7210, KatB was found to be induced under NaCl stress. Interestingly, pre-treatment with NaCl provided enhanced resistance to *Anabaena* cells to externally added H<sub>2</sub>O<sub>2</sub>. Analysis with the KatB deficient *Anabaena* strain showed that *katB* was indeed responsible for NaCl-induced cross-protection. Moreover, the *katB* mutant was found susceptible to the oxidative effect of NaCl stress. Conversely, addition of NaCl sharply increased the ROS levels in the *Anabaena katB* mutant as compared to the corresponding wild-type strain.

Northern-blotting hybridization or Western blotting and immunodetection techniques along with the promoter-*gfp* analyses demonstrated that the *katB* gene was indeed a genuine osmo-inducible gene. The *katB* promoter was active only in vegetative cells but not in the heterocysts. These results demonstrate the role of Mn-catalase KatB in overcoming salt/oxidative stress and furthermore show that the oxidative stress resistance of an organism can be modulated by a simple molecule such as NaCl.

The KatB protein, purified after over-expression in *E. coli*, was found to be a thermostable robust Mn-catalase that functioned at high ionic strength and at alkaline pH. Crystal structure of the protein showed the protein to adopt a hexameric assembly with four-helix bundle type architecture which was specific to ferritin-like super family. With a different Mn-coordination environment, the active site was found to be distinctly different from other Mn-catalases with available crystal structures. Surprisingly, the active site was almost identical to that of bacterioferritin, which contains iron in its active site.

The N-terminal region of KatB, which is involved in oligomerization, was shown to be important for structure-function. Within this  $\beta$ -strand, 2<sup>nd</sup> and 4<sup>th</sup> amino acids were the most crucial residues. Systematic mutagenesis studies revealed that a bulky aromatic acid (Phe, Tyr or Trp) was necessary at the second position for optimal compactness, stability and activity under *in vitro* or *in vivo* conditions. Crystal structure revealed that only a bulky second amino acid could form optimal hydrophobic interactions at the oligomer interface or the proper active site configuration. As these interactions are critical, nature has selected only bulky hydrophobic amino acids (Phe, Tyr, Trp) at the second position in all Mn-catalases.

The photoautotrophic, nitrogen-fixing cyanobacterium *Anabaena* PCC 7120 was used as an expression platform for production of recombinant proteins. The KatB protein could be purified by simple physical processes after over-production in *Anabaena*. The KatB protein purified from *Anabaena* was more compact with better enzymatic characteristics than the KatB protein purified after over-expression in *E. coli*. Unlike a commercially procured heme-catalase, the KatB from *Anabaena* was stable and active at high temperature and alkaline pH, thus demonstrating its use in applications where H<sub>2</sub>O<sub>2</sub> is to be degraded at elevated temperature or pH.

## **CHAPTER 6**

# **Facile Production of the Thermostable Catalase KatB using *Anabaena* as a Production Platform: Biotechnological Implications**



## 6.1 Introduction

Cyanobacteria, the ancient photosynthetic bacteria, are believed to be the progenitors of plant chloroplasts. Their ability to convert CO<sub>2</sub> into organic compounds by oxygenic photosynthesis is particularly important as it reduces the global levels of this notorious greenhouse gas. Few cyanobacteria are endowed with the ability to convert atmospheric nitrogen into bio-available form and some strains of the heterocystous, filamentous, nitrogen-fixing cyanobacterium *Anabaena* are traditionally used as natural biofertilizers in rice fields of South-East Asia [268]. Due to their photoautotrophic nature and rapid rate of biomass accumulation, cyanobacteria are not only good candidates for biofuel production, but can also be a potential source of high quality protein [269]. Moreover, because of their minimal nutrient requirement and largely non-pathogenic nature, cyanobacteria are desirable hosts for over-production of commercially relevant proteins [270].

There are plenty of reports wherein heterotrophic microorganisms like bacteria, yeast, fungi etc. are used in industrial scale for the bio-production of commercially relevant products [271]. However, all these microbes require carbon sources which are expensive thereby increasing the production cost. In view of this, photoautotrophs like cyanobacteria or plants offer advantage as they can harness solar energy and atmospheric CO<sub>2</sub> which is cheap, abundant form of carbon, thus reducing consumption of organic carbon derived from crops [272, 273]. However, cyanobacteria have distinct advantages over plants for bioproduction of high value compounds as they have faster growth rates, greater salt tolerance, better ability to grow on marginal lands, and can also use waste water as nutrients [273]. Some cyanobacteria such as *Synechococcus elongates* PCC 7942, *Synechocystis* sp. PCC 6803, *Synchococcus* sp. PCC 7002 and

*Anabaena* sp. PCC 7120 are amenable to genetic manipulation thereby making them potential candidate for bioengineering. Cyanobacterial hosts have been genetically modified for generation of bio-products like ethanol, butanol, squalene etc. or for higher biomass production [274, 275, 195].

H<sub>2</sub>O<sub>2</sub> is widely used as a bleaching agent or microbial disinfectant in industries [275]. The primary industrial applications of H<sub>2</sub>O<sub>2</sub> are bleaching of raw fibres in textile processing [277, 278]; delignification and bleaching of paper pulp [279]; disinfection of microbes in food and pharmaceutical industries [276]; bleaching of hides to obtain uniform tanning in the leather industry [280] etc. Being an efficient H<sub>2</sub>O<sub>2</sub> detoxifying enzyme, catalases are extensively used to detoxify residual H<sub>2</sub>O<sub>2</sub> in industrial processes [276]. In fact, catalases are one the most commercially exploited enzymes today [281].

As described in earlier chapters, the purified KatB protein was found to be a robust, thermostable Mn-catalase functional at high pH and high ionic strength. The unique biochemical and biophysical attributes of KatB made it an appealing prospect for use in industry. In this chapter, the feasibility of using the cyanobacterium *Anabaena* as a platform for production of KatB is explored and the properties of the KatB protein purified from *Anabaena* are compared with those from a commercially available heme catalase

## **6.2 Over-expression of the his tagged KatB protein in *Anabaena* PCC 7120**

To assess the prospect of using *Anabaena* as the production platform for expression of recombinant proteins, over-expression of his-tagged KatB protein in this organism was attempted.

### 6.2.1 Cloning of *katB* ORF with 6 in-frame *His* codons into *E. coli/Anabaena* shuttle vector pAM1956

For the purpose of over-expression of KatB protein in *Anabaena*, the *katB* ORF along with strong light-inducible promoter was cloned into *E. coli/Anabaena* shuttle vector pAM1956. As the N-terminal region of KatB is important for crucial inter-subunit interactions and enzymatic activity (Chapter 5), the his-tag was included at the C-terminal end of the protein. For that, 6 *in-frame* histidine codons were introduced into the reverse primer. The forward and the reverse primer (Table 2.2) also contained *NdeI* and *BamHI* site respectively, to facilitate directional cloning into the pFPN vector [195]. The PCR fragment (*katB<sub>6His</sub>*) obtained after PCR amplification (with *Anabaena* PCC 7120 chromosomal DNA as template) was ligated into pFPN vector downstream of strong light inducible promoter  $P_{psbA1}$  using the two above-mentioned restriction sites (Fig. 6.2.1 A).

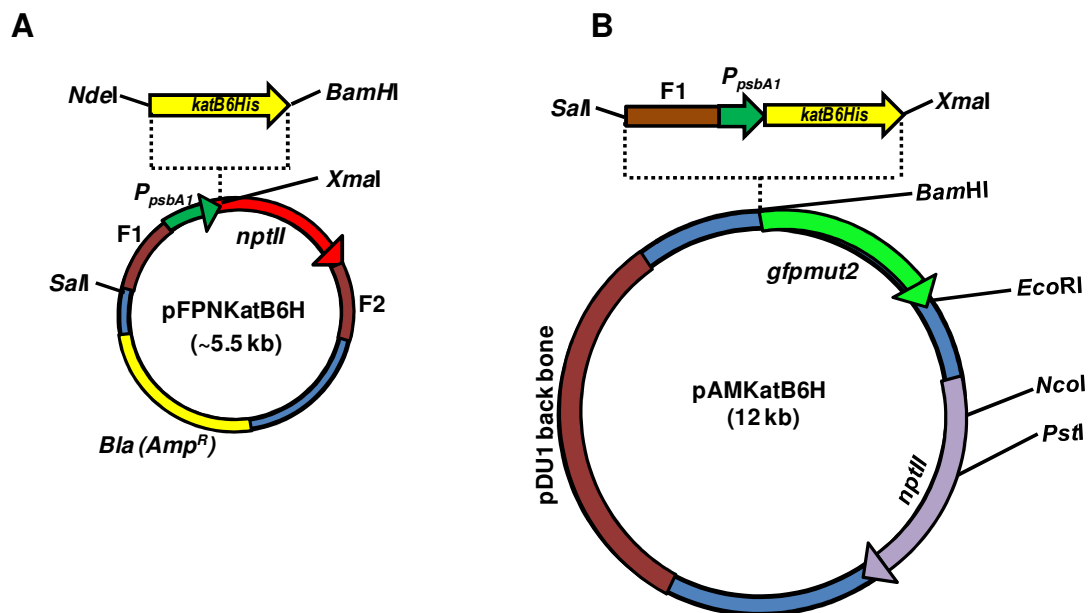


**Fig. 6.2.1** Schematic diagram of the vectors generated for KatB over-expression in *Anabaena*. (A) Schematic diagram of pFPNKatB6H. The *katB<sub>6His</sub>* DNA fragment was cloned employing *NdeI* and

*Bam*HI restriction site. **(B)** Schematic diagram of pAMKatB6H plasmid. The *katB<sub>6His</sub>* DNA fragment along with P<sub>*psbA1*</sub> promoter and F1 region was excised from pFPNKatB6H vector using *Sal*I and *Xma*I restriction endonucleases and cloned into pAM1956 employing the same restriction enzymes.

The resultant vector (pFPNKatB6H) was digested with *Sal*I and *Xma*I restriction endonucleases to excise out the *katB<sub>6his</sub>* fragment along with the P<sub>*psbA1*</sub> sequence upstream of it. The fragment (F1-P<sub>*psbA1*</sub>-*katB<sub>6his</sub>*) was then cloned just upstream of *gfp* reporter (*gfpmut2*) into *Anabaena* PCC 7120-*E. coli* shuttle vector pAM1956 to obtain pAMKatB6H (Fig. 6.2.1 B).

### **6.2.2 Generation of *Anabaena* strain over-producing his-tagged KatB protein**

The pAMKatB6His was conjugally transferred by into *Anabaena* PCC 7120 using a conjugal *E. coli* donor [HB101 (pRL623 + pRL443)] [194]. The exconjugants (*AnKatB6H<sup>+</sup>*) were selected on BG11N+ plates containing neomycin (25 µg/ml) and repeatedly subcultured. In *AnKatB6H<sup>+</sup>* strain, *katB<sub>6his</sub>* and *gfpmut2* genes are co-transcribed via the P<sub>*psbA1*</sub> promoter, yielding a bicistronic mRNA, which eventually leads to independent translation of both An-KatB (i.e. C-terminally His tagged KatB produced in *Anabaena*) and GFP protein. When the *AnKatB6H<sup>+</sup>* cells were observed under fluorescence microscope, abundant expression of GFP was observed indicating expression of transgenes (Fig. 6.2.2). The transformed *Anabaena* strain thus obtained (designated *AnKatB6H<sup>+</sup>*) was maintained on BG11N+ media supplemented with neomycin.

### *AnKatB6H<sup>+</sup>* strain

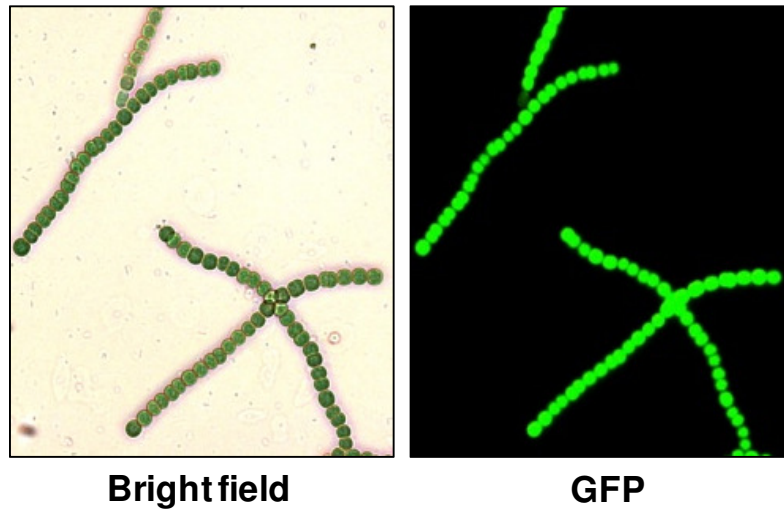


**Fig. 6.2.2** Micrograph of recombinant *AnKatB6H<sup>+</sup>* strain (400 X). Left panel, bright field micrograph; right panel, fluorescence micrograph of the same microscopic field observed under GFP filter.

### **6.2.3 Confirmation of recombinant protein production by SDS-PAGE and Western blot analysis**

The *AnKatB6H<sup>+</sup>* culture thus obtained was analyzed for the production of the recombinant An-KatB protein. The SDS-PAGE profile clearly showed the presence of the ~26 kDa protein in the crude extracts of *AnKatB6H<sup>+</sup>* strain but not in the extract of the wild-type *Anabaena* (Fig. 6.2.3 A). This protein cross-reacted with the anti-His as well as the KatB antisera, suggesting that the over-produced protein was indeed his-tagged KatB (Fig. 6.2.3 B and 6.2.3 C). Unlike the wild-type *Anabaena*, extracts from *AnKatB6H<sup>+</sup>* strain showed a copious zone of catalase activity on zymogram, indicating that the over-produced An-KatB protein was indeed an active catalase (Fig. 6.2.3 D).

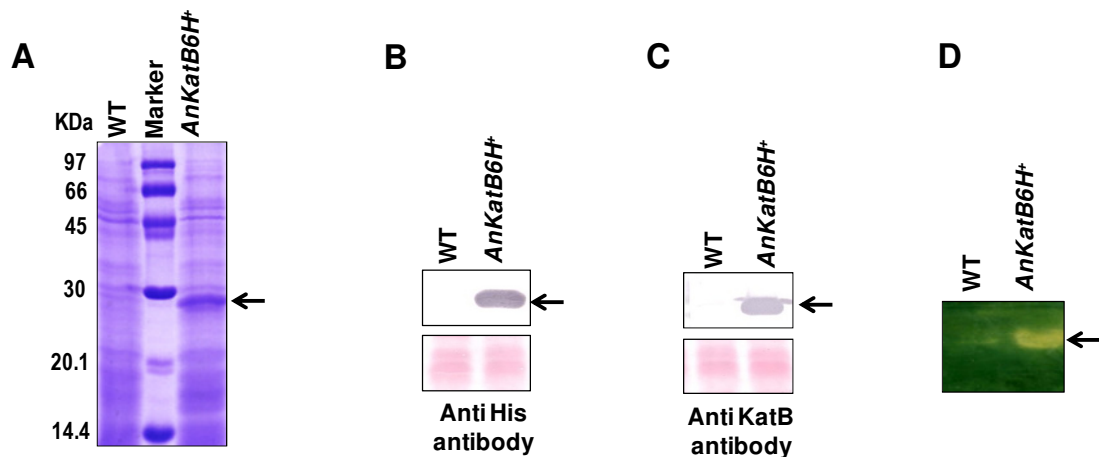


**Fig. 6.2.3 Expression of recombinant his-tagged An-KatB protein in *AnKatB6H*<sup>+</sup> strain.** (A) Cell-free extracts were prepared from the wild-type *Anabaena* PCC 7120 (WT) or the *AnKatB6H*<sup>+</sup> strain, resolved on SDS-polyacrylamide gel (14%) and visualized by staining with Coomassie brilliant blue (CBB). Over-produced protein band of approximately 26 kDa is indicated by an arrow. (B) The cell-free extracts of the wild-type *Anabaena* PCC 7120 (WT) or *AnKatB6H*<sup>+</sup> were resolved by SDS-PAGE, transferred onto nitrocellulose membrane and probed with anti-Histidine antibody or the KatB antiserum (C). Parts of Ponceau S-stained blots are shown at the bottom as loading controls. (D) *In-gel* catalase activity assay (zymogram). Cell-free extracts of the wild-type *Anabaena* PCC 7120 (WT) or *AnKatB6H*<sup>+</sup> were resolved by native 10% PAGE and stained for catalase activity. Positions of the proteins are indicated by arrows.

#### 6.2.4 Localization of the over-expressed An-KatB protein

In *E. coli*, due to improper folding, many a times the over-expressed protein is partitioned into the inclusion body fraction. In the present study, the degree of distribution of An-KaB in soluble or the insoluble fraction was assessed. The crude extracts of the *AnKatB6H*<sup>+</sup> cells were subjected to high-speed centrifugation (20000xg) to separate the soluble fraction from inclusion bodies, cell membranes, etc. As seen in Fig. 6.2.4 A, the over-expressed An-KatB protein was observed mostly in the soluble fraction, while hardly any protein could be detected in the membrane/inclusion fraction.

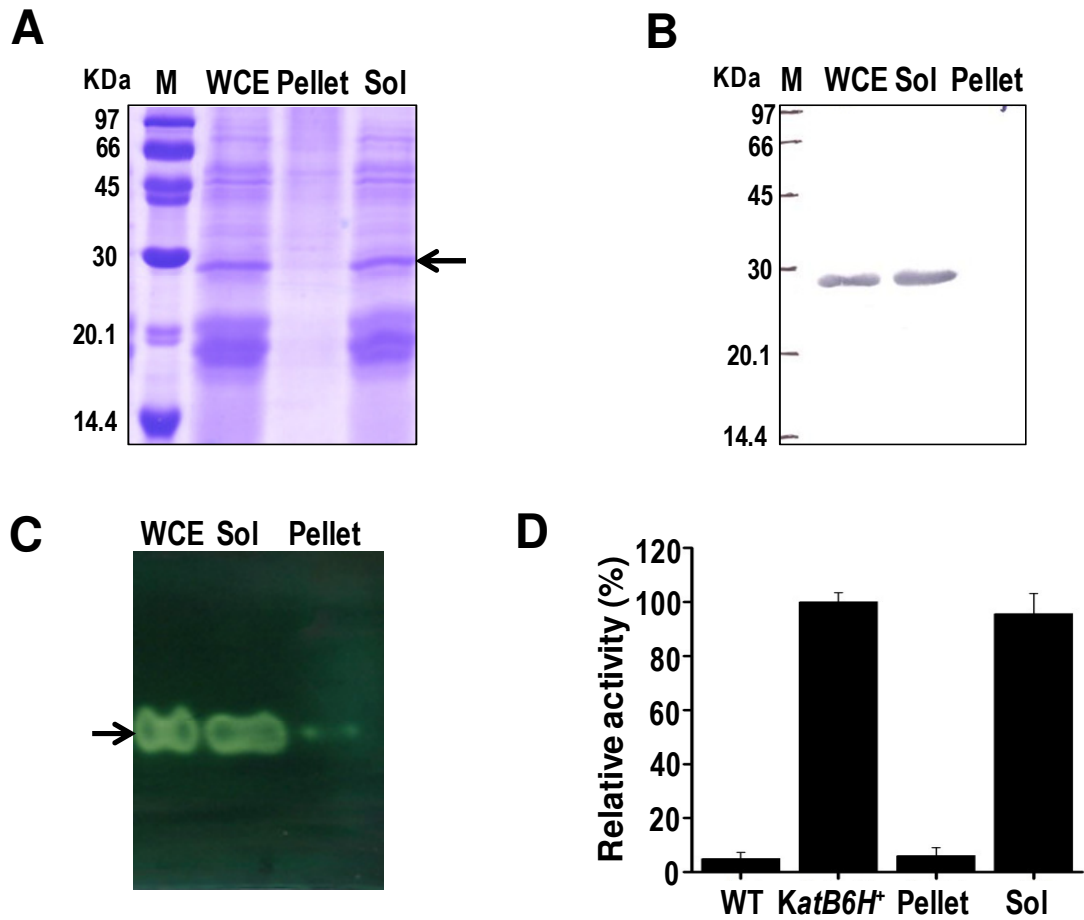


**Fig. 6.2.4 Localization of over-produced An-KatB protein in the soluble fraction.** (A) The whole cell extract (WCE) of *AnKatB6H<sup>+</sup>* strain was separated into soluble (sol) or insoluble (pellet) fractions by centrifugation, resolved on denaturing acrylamide gels and visualized by staining with CBB. Protein band corresponding to An-KatB is indicated by an arrow. (B) The above-mentioned fractions were resolved by SDS-PAGE, electro-blotted onto nitrocellulose membrane and probed with KatB antisera. (C) *In-gel* catalase activity assay (zymogram) of whole cell extracts (WCE), soluble (sol) and insoluble (pellet) fractions of *AnKatB6H<sup>+</sup>* strain. The zone of clearance representing KatB activity is depicted by an arrow. (D) Spectrophotometric H<sub>2</sub>O<sub>2</sub> decomposition assay with cell extracts of wild-type *Anabaena* (WT); *AnKatB6H<sup>+</sup>* (*KatB6H<sup>+</sup>*) and the inclusion body (Pellet) or the soluble (Sol) fraction of the *AnKatB6H<sup>+</sup>* strain. Activity exhibited by the whole cell extract of *AnKatB6H<sup>+</sup>* was considered to be 100% and other rates were calculated accordingly. Error bars represent SE.

The SDS-PAGE result was well supported by the immunoblotting experiments wherein the KatB protein could be detected only in the soluble fraction (Fig. 6.2.4 B). These fractions were resolved by native PAGE and subjected to zymographic staining. The

soluble fraction and the crude extract showed almost similar zones of clearance, suggesting that the over-expressed protein was mostly present in the soluble fraction (Fig. 6.2.4 C). These results were also corroborated with spectrophotometric catalase activity assay wherein too most of the activity was observed in the soluble fraction (Fig. 6.2.4 D).

### 6.3 Purification of his-tagged An-KatB protein using affinity chromatography

After confirming the presence of the over-produced An-KatB protein in the soluble fraction, attempts were made to purify this protein employing NiNTA resin-based affinity chromatography (as described in the methods section).

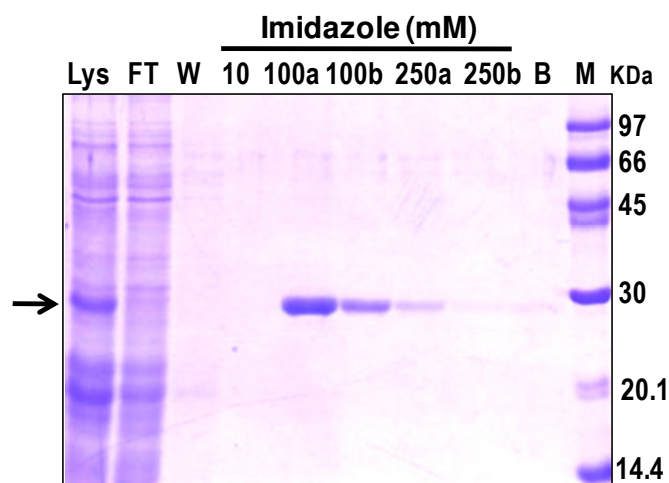


**Fig. 6.3 Purification of An-KatB protein by NiNTA affinity chromatography.** The NiNTA bound An-KatB protein was eluted by raising imidazole concentration as indicated in the figure. Lys, cell lysate; FT, flow-through, W, wash fraction; 10, 10 mM imidazole elution fraction; 100a and 100b, 1st and 2nd 100 mM imidazole elution fraction respectively; 250a and 250b; 1st and 2nd 250 mM imidazole elution fraction respectively; B, NiNTA beads fraction after protein was eluted with 250 mM imidazole; M, molecular weight marker. Position corresponding to the KatB protein is indicated by an arrow.

When all the wash and elution fractions were analyzed on denaturing polyacrylamide gels, a fairly pure band corresponding to the An-KatB protein was visualized in the elution fraction with 100 mM imidazole (Fig. 6.3). The purified protein was dialyzed against 20 mM Tris and subsequently used for biochemical and biophysical analyses.

#### 6.4 Facile purification of the overproduced KatB by simple physical downstream processes involving heat treatment and ammonium sulphate precipitation

Many proteins get unfolded/denatured at elevated temperature, resulting in their aggregation. The heat labile proteins generally aggregate, but the heat stable proteins remain soluble at high temperatures. Since, KatB is a thermostable protein; it was desired to use this property to purify An-KatB from *AnKatB6H<sup>+</sup>* extracts.

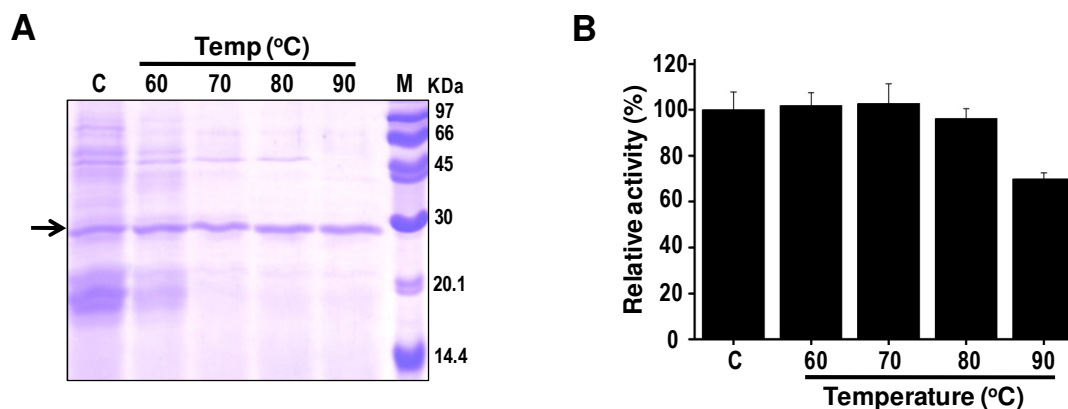


**Fig. 6.4.1 Partial purification of An-KatB with elevated temperature.** (A) High temperature treatment of *AnKatB6H<sup>+</sup>* cell extracts. Cell extracts were exposed to temperatures as indicated for 15 minutes, the soluble protein fractions were separated by centrifugation and resolved by SDS-PAGE (15%). C, soluble protein fraction obtained from the control cell extract (kept at 4 °C). The An-KatB protein is shown by an arrow. (B) Spectrophotometric H<sub>2</sub>O<sub>2</sub> decomposition activity of the above-mentioned soluble protein fractions. Activity of soluble fraction of control cell extract (C) (i.e. not exposed to elevated temperature) was considered to be 100% and the other rates were calculated accordingly. Error bars represent the SE.

Cell extracts from *AnKatB6H<sup>+</sup>* cultures were exposed to temperatures as mentioned in Fig. 6.4.1 A for 15 min. Subsequently, the soluble proteins were separated from the aggregated proteins by centrifugation and were analyzed on denaturing polyacrylamide gels. Even at 90°C, the intensity of the band corresponding to KatB remained virtually

unchanged, indicating that the KatB protein did not aggregate at this temperature and remained soluble. On the other hand, distinct decrease in the content of the other cytosolic proteins was observed at temperatures above 70°C (Fig. 6.4.1 A). An-KatB obtained from the supernatant of the above-mentioned treatments was also assayed for the catalase activity. Up to 80°C there was no loss in catalase activity. However, at 90°C, a 22% drop in enzyme activity was noticed (Fig. 6.4.1 B). Hence, to achieve the best possible heat-mediated purification, 80°C i.e. the temperature at which no enzyme activity was lost, was chosen and the incubation time was optimized at this temperature. The cell extract (green in colour) was exposed to 80°C for various time points and the soluble fractions were obtained by centrifugation. Within 10 minutes of incubation at 80°C, the green cell extract turned colourless (Fig. 6.4.2 A). When the fractions were assayed for catalase activity, it was found that the activity remained unaffected for up to 20 minutes of incubation at 80°C. However, at the end of 30 minutes incubation, a small decrease in activity was noticed (Fig. 6.4.2 B).

On SDS-PAGE, the soluble fraction of the cell extract incubated at 80°C for 20 minutes showed the efficient removal of other cytosolic proteins, while virtually intact An-KatB protein was detected (Fig. 6.4.2 C). Spectrophotometric H<sub>2</sub>O<sub>2</sub> decomposition assay indicated that there was no loss in catalase activity after exposure to 80°C for 20 minutes and the entire activity was essentially confined only to the supernatant (Fig. 6.4.2 D).

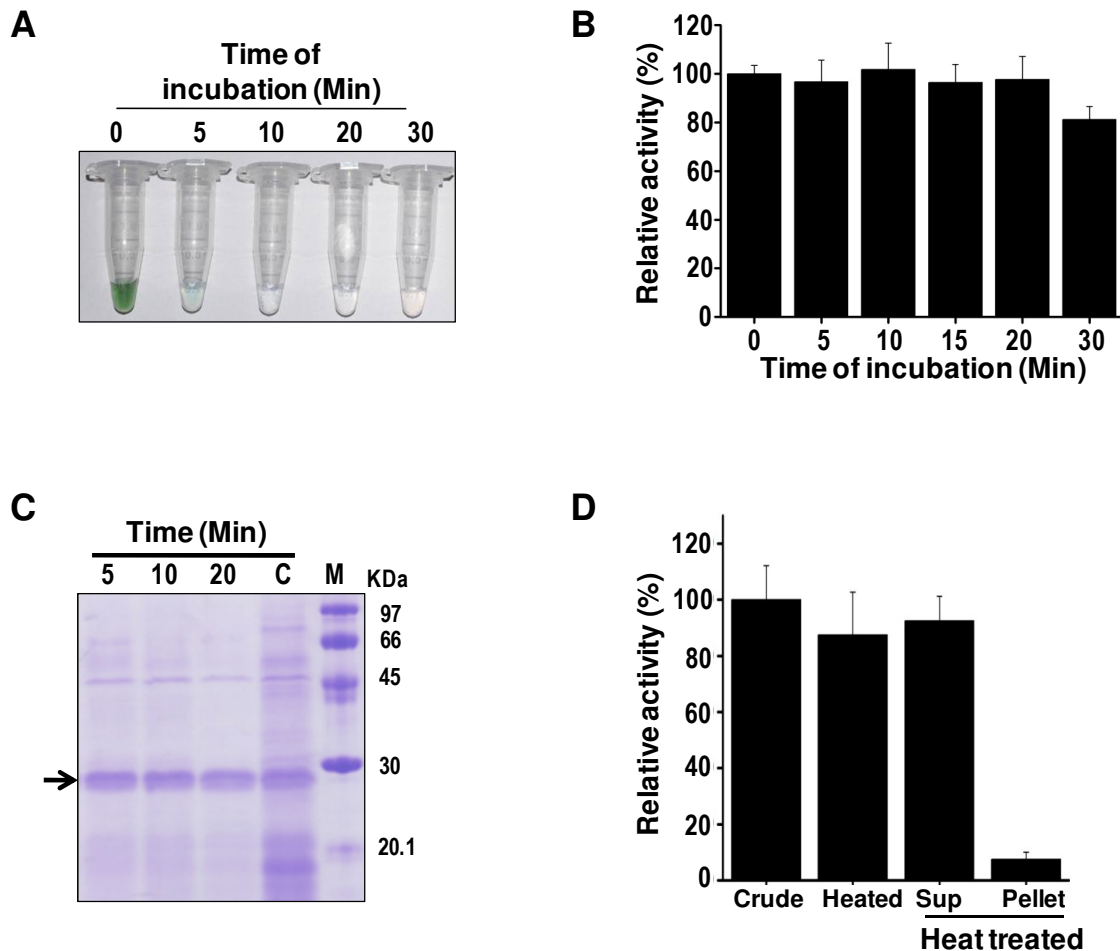


**Fig. 6.4.2 Optimization of incubation time at 80°C.** (A) Decolorization of the *AnKatB6H<sup>+</sup>* soluble fraction at 80°C. The cell extract was kept at 80°C for time point as indicated in the figure. Soluble fraction was then separated by centrifugation and photographed. (B) H<sub>2</sub>O<sub>2</sub> decomposition activity of the cell extract heated at 80°C for time points as indicated. Activity shown by control sample (0 minute) was considered to be 100% and other rates were calculated accordingly. Error bars depict the SE. (C) SDS-PAGE profile showing the partial purification of An-KatB after exposure to 80°C at various time points. C, the cell-free extract (without heat treatment) from the *AnKatB6H<sup>+</sup>* strain loaded as a control. (D) The cell-free extracts of *AnKatB6H<sup>+</sup>* strain (Crude) was exposed to 80°C for 20 minutes (Heated) followed by separation of the soluble (Sup) and insoluble fraction (Pellet) by centrifugation. Sample from each step was aliquoted and employed for H<sub>2</sub>O<sub>2</sub> decomposition assay. Activity exhibited by crude extract was considered to be 100% and other rates were calculated accordingly. Error bars represent SE.

After heating the *AnKatB6H<sup>+</sup>* extract at 80°C for 20 min, selective precipitation of An-KatB was carried out with ammonium sulphate. On treatment with 30% ammonium sulphate, most of the contaminating proteins were precipitated while the An-KatB

protein remained in the soluble fraction. When the ammonium sulphate concentration was raised to 60%, a fairly pure form of the KatB protein precipitated (Fig. 6.4.3 A). Most the An-KatB protein precipitated with 60% ammonium sulphate and no protein was detected when ammonium sulphate concentration was raised further to 90%. The identity of the protein precipitated with 60% ammonium sulphate was ascertained with the *Anabaena* KatB antiserum (Fig. 6.4.3 B). The immunoblot also showed the protein band of ~50 kDa which co-purified with An-KatB to cross-react with the KatB antiserum, indicating that it may be a higher (dimeric?) form of KatB that remains undissociated even when subjected to denaturing PAGE (Fig. 6.4.3 B).

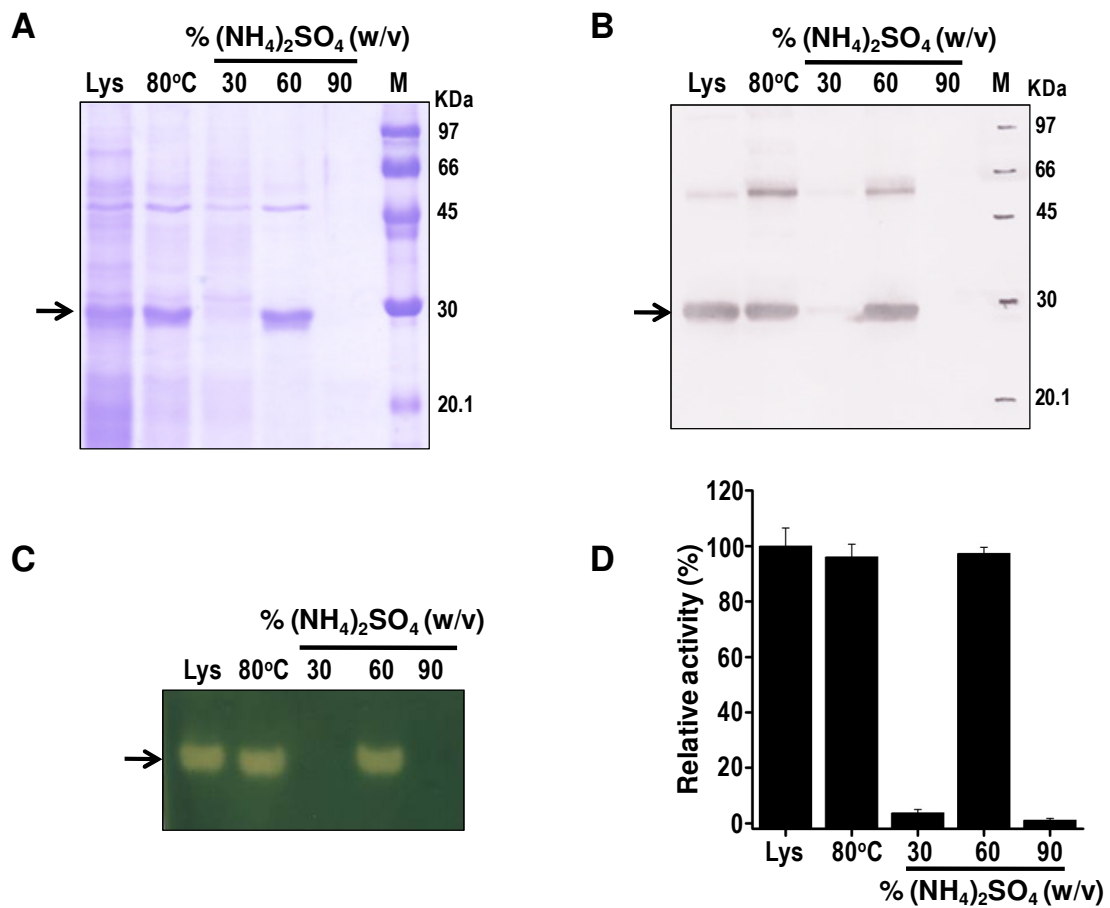


**Fig. 6.4.3. Purification of An-KatB by ammonium sulphate precipitation.** (A) Ammonium sulphate precipitation for purification of An-KatB from *AnKatB6H<sup>+</sup>* extracts. Cell-free extract of *AnKatB6H<sup>+</sup>*

culture was exposed to 80°C for 20 min and the soluble fraction, separated by centrifugation, was subjected to (NH<sub>4</sub>)<sub>2</sub>SO<sub>4</sub> precipitation. The precipitate obtained from different (NH<sub>4</sub>)<sub>2</sub>SO<sub>4</sub> fractions (30%, 60% and 90%, as indicated in the figure) was dissolved in buffer and equal volume (25 µl) from each sample was resolved by SDS-PAGE. Lys, cell lysate of *AnKatB6H*<sup>+</sup>; 80 °C, heat-treated *AnKatB6H*<sup>+</sup> cell lysate; M, molecular weight marker. **(B)** Western blotting and immunodetection. The above mentioned samples were resolved by SDS-PAGE, transferred onto nitrocellulose membrane and probed with KatB antibody. **(C)** Zymogram showing the catalase activity of the samples described in (A). **(D)** Spectrophotometer-based H<sub>2</sub>O<sub>2</sub> decomposition activity shown by the samples described in (A). Activity shown by the *AnKatB6H*<sup>+</sup> cell lysate (Lys) was considered to be 100% and the other rates were calculated accordingly. Error bars represent SE.

All the fractions were assayed for catalase activity (Fig. 6.4.3 C and Fig. 6.4.3 D) and almost the entire activity (as exhibited by the *AnKatB6H*<sup>+</sup> cell lysate) was retained in the 60% ammonium sulphate fraction, indicating that no activity was lost during this process.

### **6.5 Biophysical and biochemical characteristics of the purified An-KatB**

The An-KatB protein, purified through heat treatment followed by ammonium sulphate precipitation or through NiNTA affinity chromatography, was thoroughly analyzed to make sure that its biophysical or biochemical characteristics were not adversely affected by the mode of purification performed. The protein purified through heat treatment followed by ammonium sulphate precipitation was named as An-KatB-H-A, while, the protein purified by NiNTA chromatography was named as An-KatB-N. When assayed, both the preparations showed almost the same level of catalase activity (Fig. 6.5.1 A).

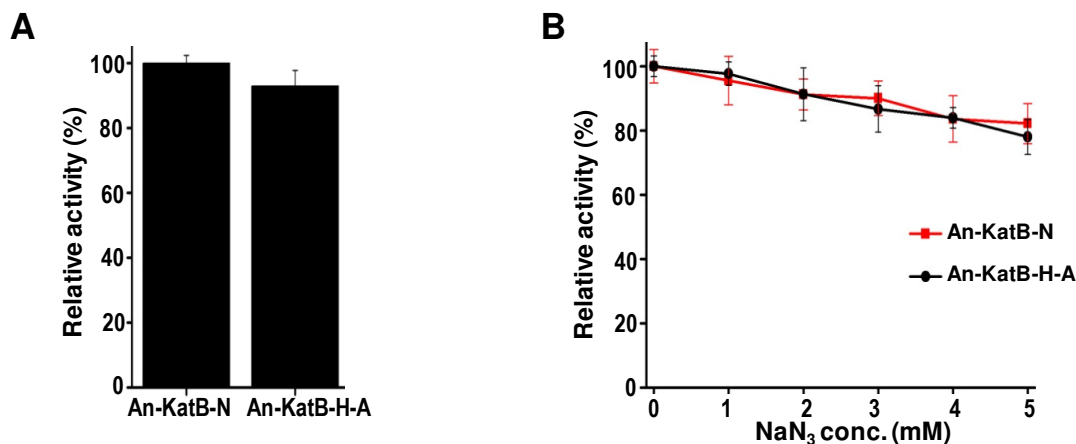


**Fig. 6.5.1. Activity of An-KatB-H-A and An-KatB-N.** (A) H<sub>2</sub>O<sub>2</sub> decomposition activity of An-KatB purified by affinity chromatography (An-KatB-N) or by heat treatment (80°C for 20 minutes) followed by 60% (NH<sub>4</sub>)<sub>2</sub>SO<sub>4</sub> precipitation (An-KatB-H-A). For the assay, equal amount of both the protein (5 μg) was taken and activity of the An-KatB-N protein was considered as 100% while activity of An-KatB-H-A was calculated accordingly. Error bars represent SE. (B) Sensitivity to sodium azide. Catalase activity of An-KatB-N or An-KatB-H-A was measured in the presence of sodium azide as indicated in the figure. Activity in the absence of sodium azide was taken as 100% and other rates were calculated accordingly. Error bars depict the SE.

As mentioned in the previous chapter, insensitivity to azide is one of the hallmarks of Mn-catalases. Both the protein preparations showed similar (lack of) sensitivity to inhibition by sodium azide (Fig. 6.5.1 B). CD spectropolarimetry showed both An-KatB-N and An-KatB-H-A to have practically the same secondary structure (Fig. 6.5.2 A). CD based melting curve analysis further suggested that both the preparations were equally resistant to thermal denaturation. The T<sub>m</sub> of both the proteins was determined to be 98 ± 1°C (Fig. 6.5.2 B). Thus, in conclusion, the chemical or physical properties of the An-KatB protein were unaffected by the mode of purification.

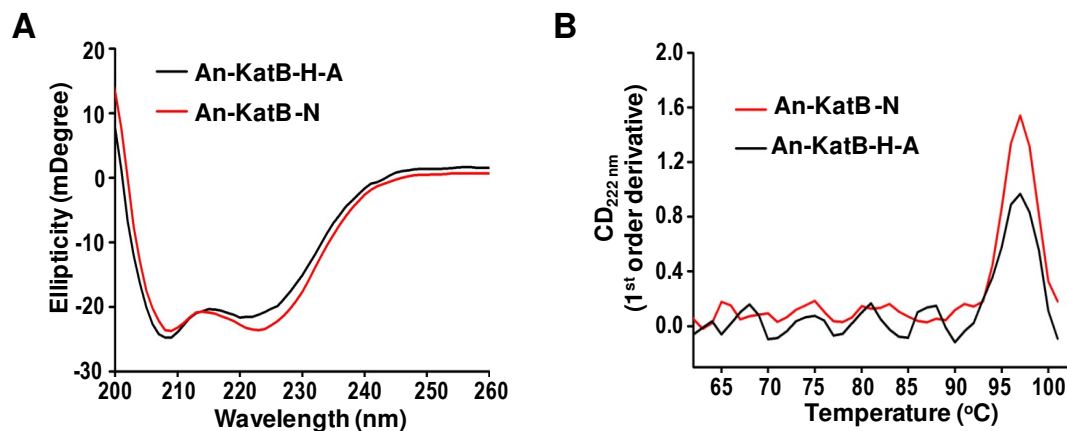


**Fig. 6.5.2 Secondary structure and melting curve analysis.** (A) CD spectra of An-KatB-H-A and An-KatB-N. (B) Thermal denaturation of An-KatB-N or An-KatB-H-A. Dichroic intensities at 222 nm of the proteins were monitored in the temperature range mentioned in the figure. Melting points were obtained from the first order differential plot generated from the melting curve.

## 6.6 Comparison of biophysical properties of An-KatB and KatB purified from *E. coli* (Ec-KatB)

In most laboratories, *E. coli* is usually preferred as the expression host for recombinant protein expression and purification. As elaborated in the earlier chapters, the KatB protein was over-expressed in *E. coli* and purified via affinity chromatography for characterization whereas in this chapter, purification of the KatB protein after over-expression in *Anabaena* PCC 7120 is detailed. To study the effect of the expression-host on the over-produced protein, a comparative analysis of the KatB protein purified from *Anabaena* PCC 7120 (An-KatB) or *E. coli* (Ec-KatB), was performed.

### 6.6.1 Compactness of An-KatB and Ec-KatB

Surprisingly, on native PAGE analysis, Ec-KatB showed reduced mobility as compared to the An-KatB protein, suggesting that the later was more compact in nature (Fig. 6.6.1 A). In size exclusion chromatography too the Ec-KatB protein eluted earlier than An-

KatB (Fig. 6.6.1 B), indicating that An-KatB was more compact, with a lower hydrodynamic radius than Ec-KatB.

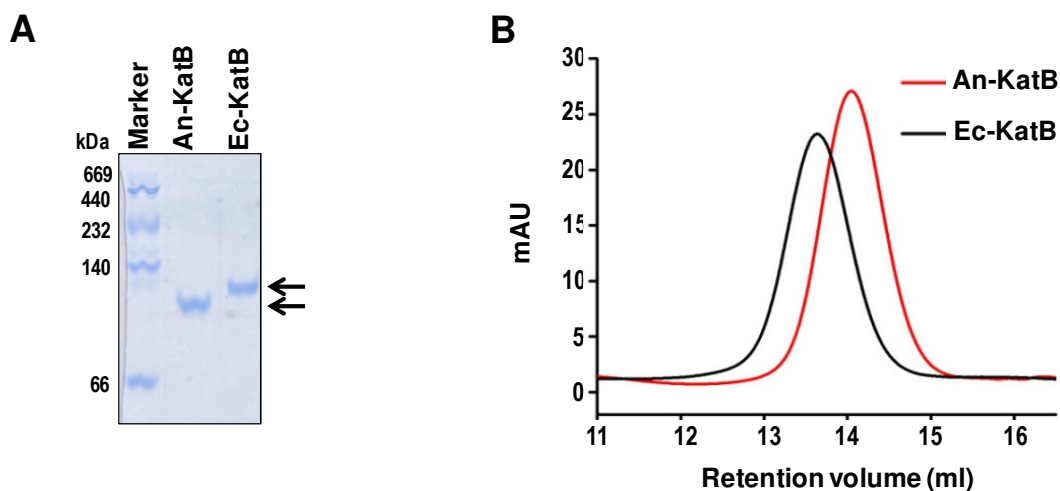


**Fig. 6.6.1 Oligomeric compactness of An-KatB or Ec-KatB.** (A) Native PAGE. The An-KatB or Ec-KatB proteins were resolved by non-denaturing polyacrylamide gels and stained with CBB. (B) Gel filtration chromatographic profile of An-KatB or Ec-KatB. 200  $\mu$ g of the purified protein was injected into Superdex 200 10/300 GL column pre-equilibrated with buffer containing 20 mM Tris and 50 mM NaCl, pH 7.2.

### 6.6.2 Secondary structure and thermostability

Both the protein preparations were subjected to CD analysis to evaluate their secondary structures. An-KatB and Ec-KatB showed nearly identical secondary structure (Fig. 6.6.2A). Melting curve analysis showed both the proteins to be equally thermostable with  $T_m$  of  $\sim 98^\circ\text{C}$  (Fig. 6.6.2 B).

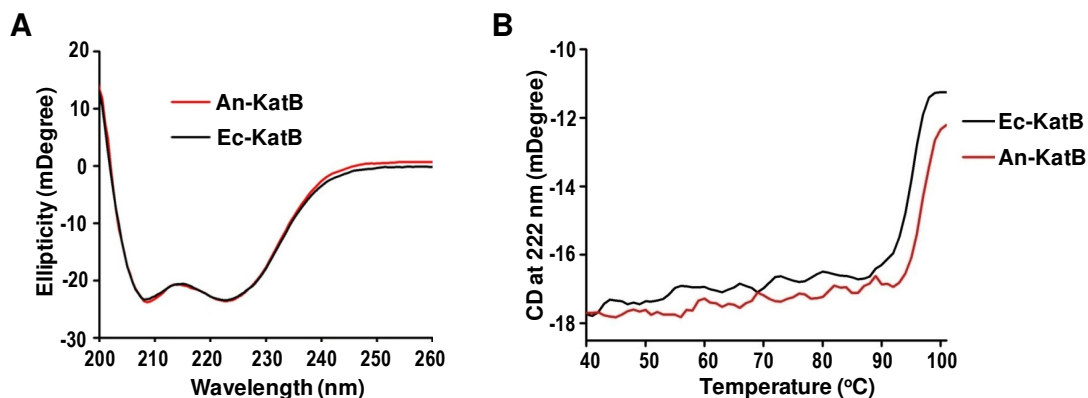


**Fig. 6.6.2 Circular dichroism spectropolarimetry of An-KatB or Ec-KatB.** (A) CD spectra of An-KatB or Ec-KatB. (B) Thermal denaturation of An-KatB or Ec-KatB. Dichroic intensities at 222 nm of the proteins were monitored in the temperature range mentioned in the figure.

### 6.7 Comparison of the biochemical properties of An-KatB and Ec-KatB

The An-KatB and Ec-KatB protein were compared for their ability to decompose  $H_2O_2$ . Surprisingly, on zymographic analysis, the An-KatB protein showed a distinctly larger zone of catalase activity as compared to Ec-KatB (Fig. 6.7 A). The result suggested that An-KatB was catalytically more active than Ec-KatB. This evidence was further supported by spectrophotometric  $H_2O_2$  decomposition assays wherein the An-KatB protein showed about four fold higher specific activity than Ec-KatB (Fig. 6.7 B).

$H_2O_2$  decomposition activity of both the proteins was tested at different pH (ranging from 5.0 to 10.0). An-KatB exhibited good catalase activity over a wide range starting from pH 5.5 to 9.0. On the other hand, the Ec-KatB protein showed appreciable catalase only activity between pH 7.5 and pH 9.0. Both the proteins were also assayed for their sensitivity towards guanidine hydrochloride-mediated denaturation. Although the two types of KatB protein differed in their compactness and catalytic activity, both of them showed similar level of susceptibility to this chemical denaturant (Fig. 6.7 D).

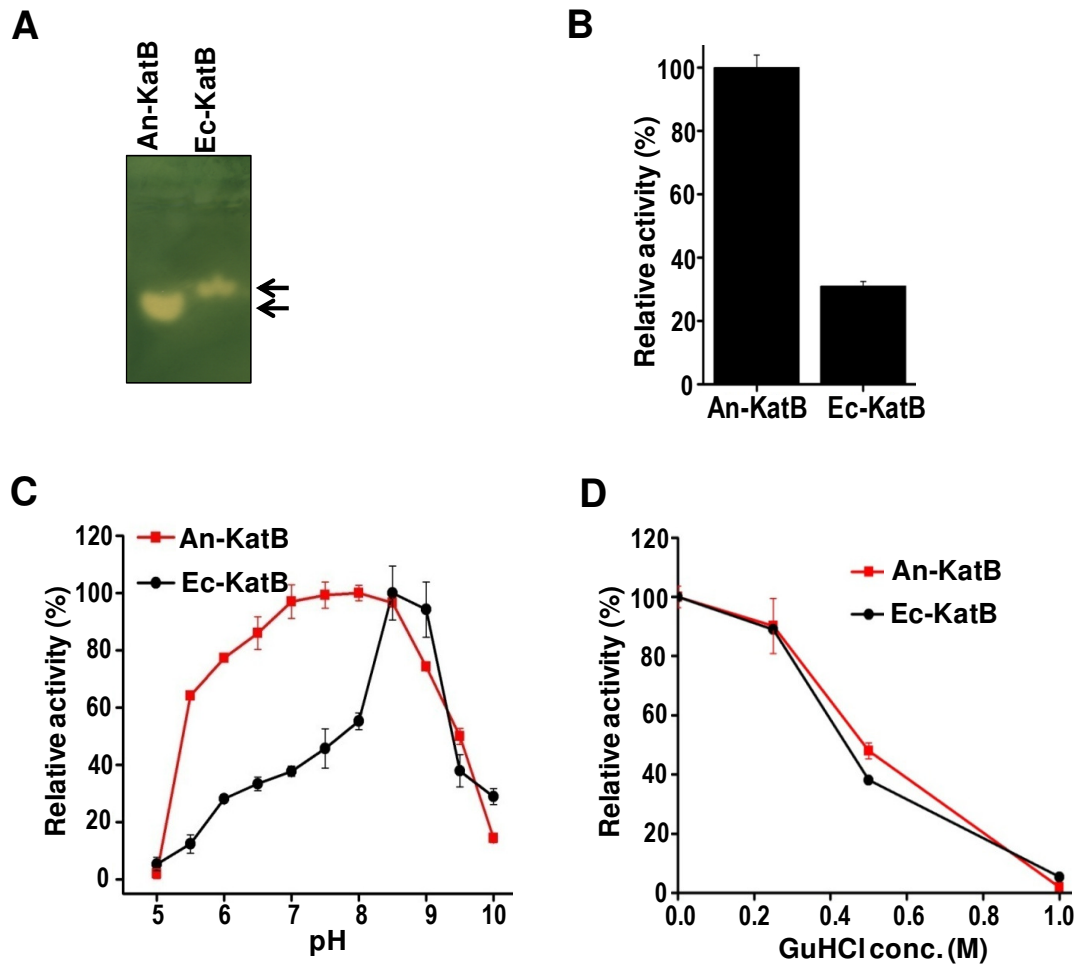


**Fig. 6.7 Comparison of KatB purified from *Anabaena* (An-KatB) or from *E. coli* (Ec-KatB).** (A) *In-gel* catalase activity assay (zymogram) An-KatB or Ec-KatB. (B) Spectrophotometric  $H_2O_2$  decomposition activity of An-KatB or Ec-KatB. Activity shown by An-KatB was considered as 100% and activity of Ec-KatB was calculated accordingly. Error bars represent SE. (C) pH dependent catalase activity of An-KatB or Ec-KatB. Rate of  $H_2O_2$  decomposition was measured at various pH for both the proteins and plotted as relative activity. Maximum measured activity of An-KatB (recorded at pH8.0) was considered as 100% whereas maximum activity of Ec-KatB (recorded at pH 8.5) was considered as 100%. Error bars depict the SE. (D) Effect of GuHCl on activity. The An-KatB or the Ec-KatB protein was incubated with different concentration of GuHCl as indicated and their catalase activity was measured with spectrophotometer. Activity of each protein in the absence of GuHCl was considered to be 100% and other rates were calculated accordingly. Error bars represent SE.

## **6.8 Comparison of the total KatB protein yield obtained from *Anabaena* or *E. coli* expression host**

One of the most important factors for recombinant protein production is the yield of over-produced protein per unit biomass of the expression host. The total amount of the purified KatB recovered after over-expression in *Anabaena* or *E. coli* was calculated and compared. The yield of KatB was measured on the basis of per unit fresh weight of the expression host.  $10.5 \pm 0.8$  mg of Ec-KatB protein was recovered per gram (fresh weight) of *E. coli* biomass. On the other hand  $7.1 \pm 0.6$  mg An-KatB protein was obtained from equivalent amount of *Anabaena* biomass (i.e. 1 g fresh weight). It is important to note here that 30% lower yield of An-KatB compared to Ec-KatB was adequately compensated by the four fold higher activity of the An-KatB protein.

## **6.9 Comparison of An-KatB with a commercially procured heme-catalase**

A commercially available heme-catalase enzyme (named as Comm Cat) was procured for comparing its physical and biochemical attributes with that of the An-KatB protein.

### **6.9.1 Biochemical properties**

In spectrophotometric H<sub>2</sub>O<sub>2</sub> decomposition assays, the specific activity of the An-KatB protein was slightly lower as compared to that of the Comm Cat (Fig. 6.9.1 A). Activity of the Comm Cat and the An-KatB protein was compared at different pH. The Comm Cat protein was found to be most active at neutral pH (7.0) but thereafter at higher pH the catalase activity of this protein declined rapidly (Fig. 6.9.1 B). In contrast to Comm Cat, the An-KatB protein showed appreciable catalase activity even at pH 9.0 (Fig. 6.9.1 B).

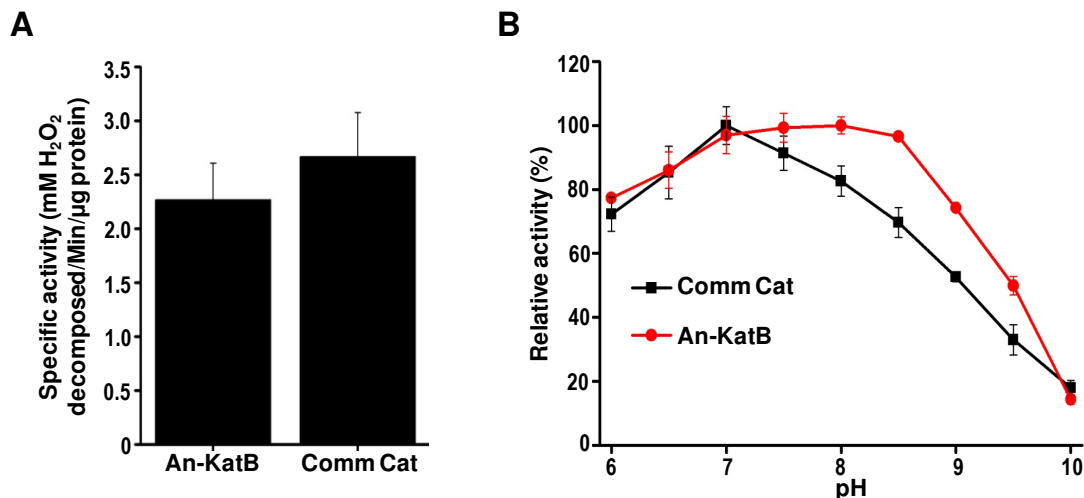


**Fig. 6.9.1** Comparison of specific activity and effect of pH on An-KatB and Comm Cat. **(A)** H<sub>2</sub>O<sub>2</sub> decomposition activity exhibited by An-KatB or Comm Cat. Error bars represent SE. **(B)** The catalase activity of An-KatB or Com Cat was measured at different pH as indicated in the figure. Maximum activity of the proteins (obtained at pH 7.0) was considered to be 100% and the rest were calculated accordingly. Error bars represent the SE.

### 6.9.2 CD spectropolarimetric analyses

CD spectropolarimetric analysis with the commercial catalase (Comm Cat) indicated that the commercial catalase (Comm Cat), like An-KatB, was also a largely  $\alpha$ -helical protein (Fig. 6.9.2 A). However, during thermal denaturation Comm Cat showed a loss in secondary structure when temperature was raised above 40°C (Fig. 6.9.2 B). In contrast, there was no loss of secondary structure of An-KatB even at 90°C. The melting curve analysis suggested that unlike An-KatB, Comm Cat was a heat labile protein.

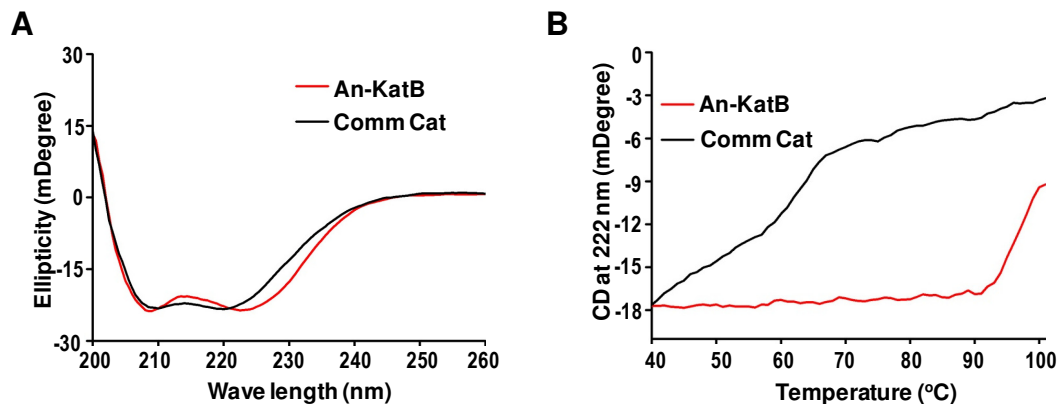


**Fig. 6.9.2 CD spectropolarimetric analysis of An-KatB or Comm Cat.** (A) CD spectra of An-KatB or Comm Cat. (B) Thermal denaturation of An-KatB or Comm Cat. Dichroic intensities at 222 nm was measured at the temperature range mentioned in the figure

### 6.9.3 Effect of high temperature on catalase activity

To assess their ability to withstand exposure to elevated temperatures, both the enzyme preparations (An-KatB and Comm Cat) were exposed to various temperatures for 10 minutes and subsequently assayed for their ability to decompose  $H_2O_2$  (at room temperature) (Fig. 6.9.3 A). The activity of An-KatB was found fairly stable even after exposure to 90°C, whereas the Comm Cat protein showed a distinct drop in activity when the incubation temperature was over 50°C. This result correlated well with the CD melting curve analysis of Comm Cat (Fig. 6.9.2 B) wherein loss of secondary structure was observed at temperature beyond 40°C. This enzyme preparation lost over 40% of its original activity when exposed at 60°C and it became completely inactive at temperature above 80°C (Fig. 6.9.3 A).

Both the enzyme preparations were incubated at 85°C for various time points to determine their thermostability at this temperature. The An-KatB protein could withstand 85°C for 30 minutes with minor loss in activity (Fig. 6.9.3 B). In fact it retained around 70% of its original activity at the end of 1 hour of incubation at 85°C.

On the other hand, the commercial catalase lost all of its activity within 10 minutes of incubation at that temperature (Fig. 6.9.3 B).

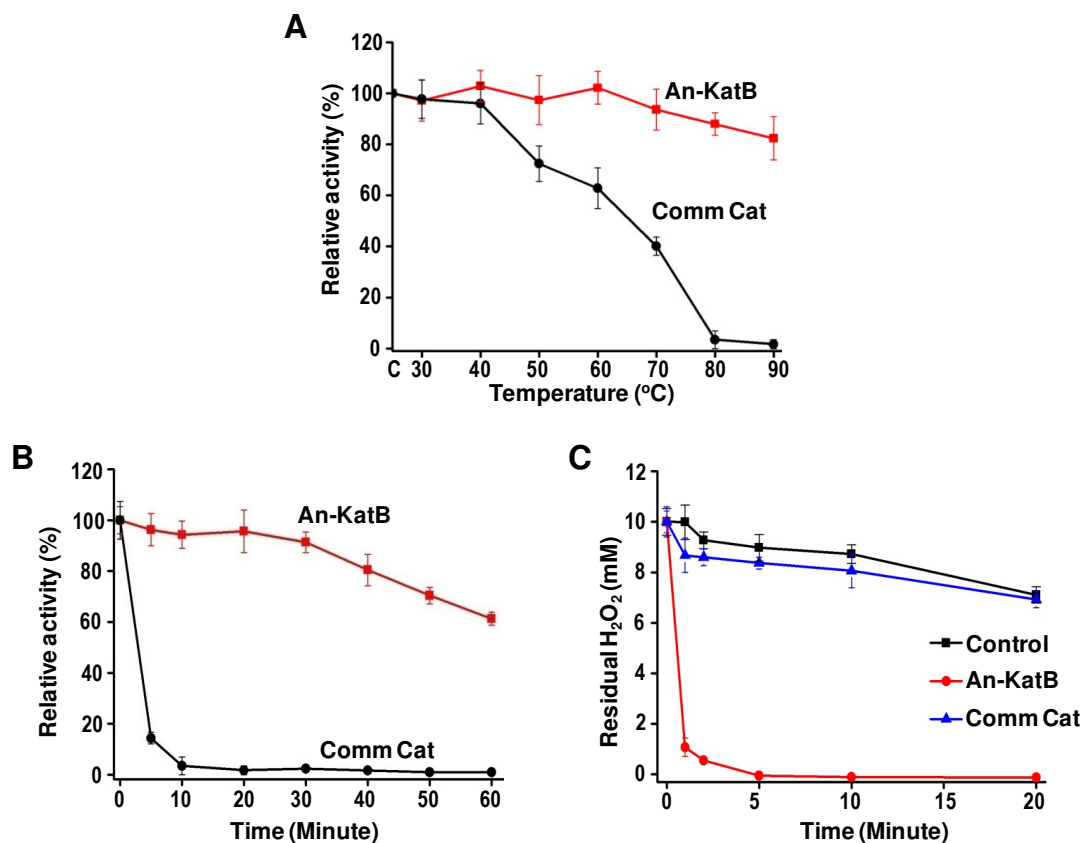


**Fig. 6.9.3 Comparison of thermostability.** (A) Ability of An-KatB or Comm Cat to withstand elevated temperature. Both the proteins were incubated at different temperatures (as indicated) followed by measurement of catalase activity at room temperature. Activity of the sample kept at room temperature was considered to be 100% and other rates were calculated accordingly. Error bars show SE. (B) The An-KatB or Comm Cat protein was incubated at 85°C and catalase activity was measured at the time points indicated. Relative activity of the respective enzymes kept at room temperature was taken as 100% and other rates were calculated accordingly. Error bars represent SE. (C) Activity An-KatB or Comm Cat at 85°C. 10 mM H<sub>2</sub>O<sub>2</sub> substrate was added to the reaction mixture containing proteins at 85°C and aliquots were taken at time points as indicated for determination of residual H<sub>2</sub>O<sub>2</sub> in the reaction mixture. Control, no enzyme added (negative control); An-KatB (20 µg); Comm Cat, Commercial catalase (20 µg). Error bars represent SE.

Ability of these two enzymes to function at high temperature was also assayed. At 85°C, An-KatB could decompose H<sub>2</sub>O<sub>2</sub> efficiently, but the Comm Cat was unable to function

at this temperature (Fig. 6.9.3 C). All these results show that unlike the commercial heme-catalase, An-KatB protein is not only thermostable but also functional at elevated temperatures.

## 6.10 Discussion

In spite of the distinct advantage of photoautotrophy, cyanobacteria are still under exploited as production platforms for generation of high-value products [282]. In most of the cases, heterotrophic micro organisms have been used in bio-industrial processes for the production of variety of commercial products like amino acids, vitamins, recombinant peptides etc. These platforms, including the common ones that utilize *E. coli*, require expensive carbohydrates as nutritional inputs. On the other hand, due to their photosynthetic nature, cyanobacteria can grow on minimal medium containing few salts by harnessing the abundantly available solar energy [283, 284]. As cyanobacteria are more efficient in photosynthesis than plants, they can effectively use solar energy for fixation of atmospheric carbon (CO<sub>2</sub>) into organic matter [285]. As a result, using cyanobacterial biomass for bio-production of high-value compounds also leads to reduction in the atmospheric load of CO<sub>2</sub>, which is a major contributor to global warming [286]. Additionally, nitrogen-fixing strains of cyanobacteria like *Anabaena* can convert the atmospheric N<sub>2</sub> into bio-available form, thereby, circumventing the requirement of nitrogenous compounds for their growth. Moreover, specialized bioreactors are needed for the growth of heterotrophic bacteria, while, for growing cyanobacteria these type of bioreactors are not needed. They can be grown in tanks, pits, raceway ponds etc [287]. For many cyanobacteria, genetic manipulation techniques are well established. Cyanobacteria such as *Synechocystis* sp. PCC 6803,

*Synchococcus* sp. PCC 7002, *Synechococcus elongates* PCC 7942 and *Anabaena* sp. PCC 7120 etc have been genetically modified for expression of transgenes.

Recombinant proteins have been over-expressed in various cyanobacterial hosts in the past. However, most of these reports are confined to unicellular, non-nitrogen fixing strains such as *Synechocystis* or *Synechococcus*. Several proteins have been over-expressed in these cyanobacteria for enhancing their stress tolerance or for production of biofuels/hydrocarbons [288, 289, 290, 291]. Proteins like mosquito larvicidal protein, human superoxide dismutase, metallothionein or lactate dehydrogenase have been successfully over-produced employing cyanobacterial expression systems [292, 293, 294, 270].

More recently, several endogenous proteins (superoxide dismutase A/B; peroxiredoxins All1541, Alr3183 or Alr4641; Mn-catalase KatA etc.) involved in oxidative stress management were overexpressed in *Anabaena* PCC 7120 with an aim to enhance its stress tolerance [198, 159, 95, 191]. Although the above-mentioned proteins were over-produced in good amounts, attempts were not made to purify these from the recombinant *Anabaena* strains. In the present study, we have not only overproduced the KatB protein, but have also demonstrated that the over-expressed protein can be easily purified in its form from *Anabaena* (Fig. 6.3 and Fig. 6.4.3).

For over-expression of a recombinant protein in certain expression host, the choice of promoter element is very crucial. Native or heterologous promoters like  $P_{tac}$  (IPTG-inducible),  $P_{trc}$  (IPTG-inducible),  $P_{psbA1}$  (light-dependent),  $P_{smtA}$  (zinc-inducible),  $P_{petE}$  (copper-inducible) and  $P_{nir}$  (nitrate-inducible) promoters have been used to drive the expression of genes in *Anabaena* [274, 195, 295]. As the  $P_{psbA1}$  is driven by light, this promoter offers a distinct advantage over others as no other chemical inducer is

additionally needed for its induction in *Anabaena*. Since light is the basic requirement for growth of this photosynthetic cyanobacterium, the  $P_{psbAI}$  promoter functions as a strong promoter under the normal conditions of growth. But, it should be noted that this promoter is not stringently regulated. However, this lack of tight regulation can be of distinct advantage when constitutive expression of protein is desired. In current study too, use of  $P_{psbAI}$  promoter resulted in copious production of the recombinant KatB protein in *Anabaena* (Fig. 6.2.3).

One major concern associated with over-expression of proteins in *E. coli* is the partitioning of the over-expressed protein into the insoluble inclusion bodies due to improper folding of the recombinant protein [296]. Results described in the previous chapter (Chapter 4) showed that, when overproduced in *E. coli*, the KatB protein was present in the inclusion body fraction when cells were grown at 37°C. The protein was partly obtained in the soluble fraction only when the incubation temperature was reduced to 20°C. Interestingly, when over-expressed in *Anabaena*, almost the entire amount of over-produced KatB protein was found to be present in the soluble fraction (Fig. 6.2.4). The solubility of the protein was not affected in spite of the fact that the *AnKatB6H<sup>+</sup>* cells were grown at ambient temperature ( $27 \pm 2^\circ\text{C}$ ). Earlier, few proteins like KatA (the other Mn-catalase in *Anabaena*) or Alr4642 (a peroxiredoxin) were over-produced in *E. coli*, but could not be purified as they were completely insoluble in this host. However, these proteins were found to be expressed in their soluble and catalytically active forms when over-expressed in *Anabaena* [200, 190]. It is definitely worthwhile to explore *Anabaena* as an expression system for over-production of proteins that remain completely insoluble when expressed in *E. coli*.

Notably, depending on the expression platform used, distinct differences were observed in the biophysical and biochemical properties of KatB. The *Anabaena* derived KatB (An-KatB) was several-fold more active than the Ec-KatB i.e. the *E. coli*-derived KatB protein (Fig. 6.7 A and Fig. 6.7 B). The An-KatB protein was active in a broader pH range compared to the Ec-KatB protein (Fig. 6.7 C). The exact reason for this phenomenon is not known yet. Results from the previous chapter established that there is a positive correlation between the compactness of KatB oligomer and its catalase activity. Although, An-KatB and Ec-KatB showed similar secondary structure, gel filtration and native PAGE analysis showed An-KatB to be more compact compared to Ec-KatB (Fig. 6.6.1). Another reason for differences in enzyme properties could be the post translational modifications, which are specific to the expression hosts. To shed light on this phenomenon, attempts to crystallize the An-KatB protein for structural characterization are underway.

Although, An-KatB and Ec-KatB showed notable differences in compactness and activity, both the proteins were found to be equally thermostable. Like all Mn-catalases, including KatA from *Anabaena*, An-KatB or Ec-KatB was found to be thermostable. Heme-catalases, on the other hand, are generally heat labile in nature. Heme-catalase, KatG from unicellular cyanobacteria *Synechococcus* PCC 7942 was inactivated when incubated temperature above 50°C [200]. The commercial heme-catalase used in this study too showed a distinct drop in activity above 50°C (Fig. 6.9.4).

Hydrogen peroxide (H<sub>2</sub>O<sub>2</sub>) has widespread use as disinfectant in food or pharmaceutical industries [110]. It is also extensively utilized in textile and paper-pulp industry as universal bleaching agent to increase the whiteness of the substrate [297].

After the process is over, the residual  $\text{H}_2\text{O}_2$  has to be effectively eliminated because the presence of  $\text{H}_2\text{O}_2$  has undesirable effects in the downstream processes. Earlier, repeated washing of the material with water was performed to remove the residual  $\text{H}_2\text{O}_2$ . However, this is not preferred now a days as this is a highly water consuming process. Moreover, direct release of left-over  $\text{H}_2\text{O}_2$  into the environment not acceptable as [111] as  $\text{H}_2\text{O}_2$  *per se* is a toxic reactive oxygen species (ROS), which easily diffuses across cell membranes [298] and threatens cell survival. Therefore, it is essential to detoxify the residual  $\text{H}_2\text{O}_2$  to prevent toxicity to aquatic life and for smooth downstream processing. Hence, in industries, heme-catalases from bovine, fungal or microbial origin are widely used to remove residual  $\text{H}_2\text{O}_2$  after the bleaching process is over [299, 276]. In textile industries, the bleaching process is carried out at high temperature and at alkaline pH. Therefore, the use of heme-catalases poses a major drawback as these enzymes show a steep drop in their activity over  $50^\circ\text{C}$  or at alkaline pH [299]. Hence, a thermostable and alkali tolerant enzyme can offer distinct advantage over currently available heme-catalases in textile industry. Results described in this chapter clearly show that KatB is a robust catalase that can withstand high temperatures and function at alkaline pH (Fig. 6.7 and Fig. 6.9.4). Therefore, thermostable and alkali tolerant catalases such as KatB may prove to be better substitutes for heme-catalases in applications such as bleaching of textiles where  $\text{H}_2\text{O}_2$  is to be decomposed at higher temperatures (over  $60^\circ\text{C}$ ) and alkaline pH [300].

To summarize, the thermostable Mn-catalase KatB, successfully overproduced in *Anabaena* was purified by a simple physical processes. The KatB protein obtained from *Anabaena* had better-quality characteristics than the similar KatB protein purified from *E. coli*. KatB was more thermo-stable than a commercially procured heme catalase.

Thus, *Anabaena* can be an ideal platform for overexpression/purification of proteins, and furthermore, the Mn-catalase KatB may be advantageous over heme-catalases in processes where hydrogen peroxide has to be eliminated at elevated temperatures.

## **CHAPTER 7**

### **Overall Findings of the Thesis and Future Directions**



## 7.1 Overall Findings of the Thesis

Heterocystous, nitrogen-fixing, filamentous cyanobacterium *Anabaena* PCC 7120 is tolerant to stresses like desiccation, radiation, which generate reactive oxygen species (ROS). If ROS level exceeds certain threshold, it can damage all the cellular macromolecules, resulting in cell death. The cyanobacterium *Anabaena* is endowed with an arsenal of ROS scavenging proteins which are deployed under various circumstances to combat oxidative stress. Genome of this ancient photosynthetic organism shows the presence of multiple genes for peroxiredoxins (Prx), Superoxide dismutases (SODs), DPS protein (DNA Protection during starvation), Universal Stress Protein (USP) etc [148]. Notably, typical catalase or bifunctional catalase-peroxidase (KatG) genes are absent in *Anabaena*, but two genes (*katA* and *katB*) encoding a Mn-catalase are present in this organism.

Catalases are ubiquitous ROS scavenging enzymes present in all spheres of life. These enzymes detoxify H<sub>2</sub>O<sub>2</sub>, one of the most important ROS in living organisms. If not scavenged, H<sub>2</sub>O<sub>2</sub>, in presence of Fe<sup>2+</sup>, undergoes Fenton reaction to generate the hydroxyl radical (·OH), the most deleterious ROS that can damage all biomolecules. In *Anabaena*, peroxidases and catalases are the enzymes dedicated to detoxify H<sub>2</sub>O<sub>2</sub>. Induction of peroxidases in response to H<sub>2</sub>O<sub>2</sub> challenge has been reported in past [95]. On the other hand, expression of catalase was not detected in *Anabaena* even on treatment with H<sub>2</sub>O<sub>2</sub> [200]. Among the two Mn-catalases, KatB (230 amino acids in length) was found to be expressed in response to iron starvation, arsenic stress or UV-B stress [206, 207, 208]. It is also up-regulated in desiccation stress [205]. However, detailed physiological analysis or structural characterization of this important stress-responsive protein had not been performed when this work was initiated.

Interestingly, as described in Chapter 3, the wild-type *Anabaena*, pre-treated with NaCl, showed unusual resistance to H<sub>2</sub>O<sub>2</sub> compared to the control cells (i.e. not pre-treated with NaCl). After exposure to H<sub>2</sub>O<sub>2</sub>, the NaCl pre-treated cultures exhibited less formation of ROS and peroxides, decreased malonaldehyde formation and reduced content of oxidized proteins, indicating diminished levels of oxidative stress as compared to control cultures. Interestingly, the NaCl pre-treatment was found to be associated with increased accumulation of Mn-catalase, KatB.

To conclusively prove the role of KatB in the above-mentioned protective effect, production of the KatB protein in *Anabaena* was modulated by genetic manipulation and the response of these genetically altered strains to H<sub>2</sub>O<sub>2</sub> was carefully analyzed. When KatB was over-expressed, the recombinant *Anabaena* strain showed better tolerance to H<sub>2</sub>O<sub>2</sub> than the wild-type cells, indicating that elevated levels of the KatB protein makes this organism resistant to H<sub>2</sub>O<sub>2</sub>. To prove the involvement of KatB in NaCl-mediated cross protection, KatB deficient *Anabaena* strain was generated. The mutant strain could not tolerate H<sub>2</sub>O<sub>2</sub> stress after pre-treatment with NaCl, thereby, proving that it was indeed the *katB* gene that was responsible for NaCl-induced cross-protection. Moreover, the mutant strain was also found to be very susceptible to the oxidative effects of salt stress.

KatB was found to be up-regulated under conditions of osmotic or desiccation stress. However, surprisingly, it was not induced by H<sub>2</sub>O<sub>2</sub>, the direct substrate of the enzyme. In nature, cyanobacteria are periodically exposed to stresses like salinity or desiccation which are known to increase the intracellular levels of H<sub>2</sub>O<sub>2</sub>. Apparently, nature has tuned expression of *katB* gene in such a way that the protein is produced in response to

salinity or desiccation, making the cells competent to combat the  $\text{H}_2\text{O}_2$  that is eventually generated due to these stresses.

The promoter region of this gene ( $P_{katB}$ ), identified by 5'RACE analysis, was ligated upstream of the *gfp* reporter gene in pAM1956 vector and the construct was transferred to *Anabaena*. Analyses of this *Anabaena* strain revealed that the promoter was a genuine osmo-inducible one and that its expression was limited to only vegetative cells, but absent in the heterocysts i.e. the site of nitrogen-fixation.

The KatB protein was over-produced in *E. coli* and purified therefrom by affinity chromatography. The protein was found to be largely  $\alpha$ -helical with a single oligomeric form. Purified protein showed catalase activity and its enzyme kinetic parameters were determined. Sensitivity to hydroxylamine and resistance to sodium azide-mediated inhibition proved that the purified protein was indeed a Mn-catalase. The protein was found to be highly thermostable and could function under conditions of high ionic strength or under alkaline conditions.

The crystal structure revealed that the KatB protein to be hexameric in nature with the individual monomers adopting a four-helix bundle fold architecture specific to the ferritin-like superfamily. Two monomers come together to form the core dimer and the trimer of dimers forms the hexameric assembly of KatB. The two manganese ions at the active site are held together at the centre of the helix core by a  $\text{Glu}_4\text{His}_2$  coordination geometry. The active site of KatB is distinctly different from LPC or TTC in terms of coordination environment with two unique amino acids (Tyr-140 and Glu-163) in the active site region.

The N-terminal region of KatB is extensively involved in oligomerization. The first few residues of the N-terminus form a  $\beta$ -strand, which interacts (in antiparallel fashion)

with the corresponding  $\beta$ -strand of the neighbouring subunit, creating a  $\beta$ -sheet at the dimer interface. Moreover, these residues are relatively conserved in all cyanobacterial Mn-catalases, indicating the N-terminal  $\beta$ -sheet to play an important structural role. To decipher the role of this structural element, the 2<sup>nd</sup> to 7<sup>th</sup> amino acid residues from the N-terminal end were deleted to generate an N-terminally truncated version of KatB. The truncated protein was found to be less compact than the wild-type protein and importantly, did not show any catalase activity. To investigate the contribution of the individual amino acids within the  $\beta$ -strand, 2<sup>nd</sup> to 7<sup>th</sup> amino acid residues was individually mutated to alanine and the variant proteins were purified after over-expression in *E. coli*. Analyses with the N-terminal variants suggested that alteration in the 2<sup>nd</sup> or 4<sup>th</sup> residue affected the biochemical and biophysical properties of KatB the most.

Interestingly, the N-terminal 2<sup>nd</sup> amino acid was always a bulky aromatic amino acid (Phe, Tyr or Trp) in all Mn-catalases across the genera. Our initial mutagenesis also indicated that among the 6 residues in the  $\beta$ -strand, mutation of the second residue (Phe) affected the enzyme most. Hence, the Phe-2 residue was replaced by smaller (Gly or Ala), intermediate (Val) or bulky aromatic (Tyr or Trp) amino acids and corresponding variant proteins were purified after over-expression in *E. coli*. Analyses with the 2<sup>nd</sup> amino acid variants revealed that KatB with smaller or intermediate (Gly, Ala or Val) 2<sup>nd</sup> amino acid were less compact and less stable to thermal or chemical denaturation compared to the wild-type protein. Variant with Val at 2<sup>nd</sup> position showed only marginal catalase activity but, the ones with Gly or Ala were totally inactive. On the other hand the variants with Tyr or Trp at the second position showed appreciable catalase activity with compactness and stability comparable to the wild-type protein.

Also, *Anabaena* strain over-expressing a 2<sup>nd</sup> amino acid variant (KatBF2V) was inefficient in decomposition of externally added H<sub>2</sub>O<sub>2</sub> when compared to the strain over-expressing the wild-type KatB protein.

To shed light on the implications of the 2<sup>nd</sup> amino acid in KatB structure-function, crystal structure of KatBF2V variant was compared with that of the wild-type protein. In the wild-type protein the second amino acid (Phe) forms extensive hydrophobic interactions at the dimer interface which are important to hold the dimer together. Phe-2 also interacts with structurally important Phe-66 and Trp-43 residues in the active site region through its bulky hydrophobic side chain. In KatBF2V these important interactions were not possible due to the much shorter side chain length of Val-2, leading to the formation of a less compact hexamer and a severe reduction in the catalase activity.

Due to photoautotrophic nature and minimal culture requirements, cyanobacteria offer a distinct advantage over the heterotrophic expression hosts like *E. coli* for over-expression of recombinant proteins. Catalase enzyme has in great demand enzymes in industries pertaining to textile, leather, and food. Attempts were made to over-produce and purify KatB enzyme using *Anabaena* PCC 7120 as the expression host to demonstrate the utility of this nitrogen-fixing cyanobacterium as an alternate and viable protein production platform. Using suitable genetic manipulation techniques, *Anabaena* was bioengineered to produce the KatB protein (An-KatB). Interestingly, the over-produced protein could be easily purified by a simple downstream process involving heat treatment followed by ammonium sulphate precipitation thereby obviating the need of chromatographic steps. The purified An-KatB protein retained all the properties of Mn-catalases and showed a robust ability to decompose H<sub>2</sub>O<sub>2</sub>. Interestingly, An-KatB

showed four-fold more activity compared to the KatB protein (Ec-KatB) purified after over-expression in *E. coli*. An-KatB was found to be active in a broader range of pH than Ec-KatB. An-KatB was stable and functioned at temperature as high as 85°C, whereas a commercially procured heme-catalase showed significant drop at temperature above 50°C. Unlike the heme-catalase which showed maximal activity around neutral pH, An-KatB was active at alkaline pH. The study demonstrated that *Anabaena* can be used as a competent microbial platform for overproduction of proteins and also highlighted the advantages of An-KatB over heme-catalases in processes where H<sub>2</sub>O<sub>2</sub> has to be removed at elevated temperatures and pH (e.g. textile industry).

## **7.2 Future Directions**

Although, a detailed characterization of KatB was carried out in this study, several interesting questions remain to be answered. Firstly, the transcriptional regulation of this important salt and desiccation-inducible gene needs to be explored. Our study has revealed that osmotic stress in general is able to induce *katB*. But, the presence of combined nitrogen is also an important factor that modulates *katB* expression. Other studies show that iron starvation, arsenic stress or UV-B stress also up-regulates *katB* expression [206, 207, 208]. Clearly, regulation of this gene expression is complex and several environmental cues are integrated in the process. In unicellular cyanobacterium *Synechocystis* PCC 6803, a bulk of the osmo-inducible genes are regulated by two component systems comprising of sensor histidine kinases and response regulators. Homologues of many of those kinases and regulators are present in *Anabaena* too. Role of these systems in perceiving environmental stimuli and subsequently transmission of those signals to gene level is worth pursuing. Another interesting area for research is to

understand the regulatory mechanisms which suppress expression of *katB* in heterocysts.

The unique active site of Mn-catalase KatB offers a scope to study detailed mechanisms of catalase reaction. The active site region of Mn-catalase is thought to be the precursor of the oxygen evolving complex (OEC) in photosystem II (PSII) [301]. Earlier, the Mn-catalase active site was probed to understand the complexities of chemistry behind the OEC [138]. With a novel type of active site configuration, KatB can offer new understandings related to OEC. Also, the active site can be studied and modified to design novel catalase mimetics for potential therapeutic usage.

Although a comprehensive study was done to decipher the role of the Phe-2 residue, more detailed analyses of the other residues in the N-terminal region needs to be carried out. Structural biology-based analyses can also answer the reason for biophysical and biochemical differences between An-KatB and Ec-KatB.

The unique properties of KatB, like thermostability or ability to function at high pH or at high ionic strength, make this enzyme a suitable candidate for industrial applications. Use of this enzyme may offer benefit over the conventional heme-catalases for applications where H<sub>2</sub>O<sub>2</sub> has to be decomposed at elevated temperatures or at high pH (e. g. textile industry). Other than industrial applications, KatB can be used for biotechnological purposes such as improvement of environmental stress resistance in plants. Heterologous expression of *E. coli* KatE (a hemecatalase) increased tolerance of rice to withstand salt stress [302]. However, in many parts of the world, the temperature reaches 40-45°C regularly during summer months, limiting the activity of the thermolabile heme catalases. Thus, being a thermo and halo-tolerant enzyme, KatB

may be a promising option for transfer to crop plants for improving their stress resistance capabilities.

## SUMMARY

Of the two Mn-catalases (KatA and KatB) present in the cyanobacterium *Anabaena* PCC 7210, KatB was found to be induced under NaCl stress. Interestingly, pre-treatment with NaCl provided enhanced resistance to *Anabaena* cells to externally added H<sub>2</sub>O<sub>2</sub>. Analysis with the KatB deficient *Anabaena* strain showed that *katB* was indeed responsible for NaCl-induced cross-protection. Moreover, the *katB* mutant was found susceptible to the oxidative effect of NaCl stress. Conversely, addition of NaCl sharply increased the ROS levels in the *Anabaena katB* mutant as compared to the corresponding wild-type strain.

Northern-blotting hybridization or Western blotting and immunodetection techniques along with the promoter-*gfp* analyses demonstrated that the *katB* gene was indeed a genuine osmo-inducible gene. The *katB* promoter was active only in vegetative cells but not in the heterocysts. These results demonstrate the role of Mn-catalase KatB in overcoming salt/oxidative stress and furthermore show that the oxidative stress resistance of an organism can be modulated by a simple molecule such as NaCl.

The KatB protein, purified after over-expression in *E. coli*, was found to be a thermostable robust Mn-catalase that functioned at high ionic strength and at alkaline pH. Crystal structure of the protein showed the protein to adopt a hexameric assembly with four-helix bundle type architecture which was specific to ferritin-like super family. With a different Mn-coordination environment, the active site was found to be distinctly different from other Mn-catalases with available crystal structures. Surprisingly, the active site was almost identical to that of bacterioferritin, which contains iron in its active site.

The N-terminal region of KatB, which is involved in oligomerization, was shown to be important for structure-function. Within this  $\beta$ -strand, 2<sup>nd</sup> and 4<sup>th</sup> amino acids were the most crucial residues. Systematic mutagenesis studies revealed that a bulky aromatic acid (Phe, Tyr or Trp) was necessary at the second position for optimal compactness, stability and activity under *in vitro* or *in vivo* conditions. Crystal structure revealed that only a bulky second amino acid could form optimal hydrophobic interactions at the oligomer interface or the proper active site configuration. As these interactions are critical, nature has selected only bulky hydrophobic amino acids (Phe, Tyr, Trp) at the second position in all Mn-catalases.

The photoautotrophic, nitrogen-fixing cyanobacterium *Anabaena* PCC 7120 was used as an expression platform for production of recombinant proteins. The KatB protein could be purified by simple physical processes after over-production in *Anabaena*. The KatB protein purified from *Anabaena* was more compact with better enzymatic characteristics than the KatB protein purified after over-expression in *E. coli*. Unlike a commercially procured heme-catalase, the KatB from *Anabaena* was stable and active at high temperature and alkaline pH, thus demonstrating its use in applications where H<sub>2</sub>O<sub>2</sub> is to be degraded at elevated temperature or pH.

## LIST OF FIGURES

Fig. No.	Title of the figure	Page
1.1.1	Generation of ROS due to stepwise partial reduction of molecular oxygen	28
1.1.2.2	ROS generation in chloroplasts, peroxisomes, mitochondria, and the apoplast in response to different environmental stresses	31
1.6.1	Radial phylogenetic tree for putative manganese catalases in genomic databases	48
1.6.2	Structure of manganese catalase subunits	50
1.6.3	Reaction mechanism of <i>Lactobacillus plantarum</i> Mn-catalase	52
1.7.1	Morphological diversity in cyanobacteria belonging to various orders	54
1.8	Filaments of <i>Anabaena</i> PCC 7120 under microscope	59
1.9	Schematic representation of major ROS removal pathways in <i>Anabaena</i>	61
3.2.1	NaCl induced H <sub>2</sub> O <sub>2</sub> stress tolerance in <i>Anabaena</i> PCC 7120	99
3.2.2	Molecular changes associated with H <sub>2</sub> O <sub>2</sub> treatment in control or NaCl pre-treated <i>Anabaena</i> cells	101
3.3	Expression of catalase and Prx in NaCl and/or H <sub>2</sub> O <sub>2</sub> stressed <i>Anabaena</i>	102

<b>3.4</b>	KatB over-expression in <i>Anabaena</i>	104
<b>3.5.1</b>	Schematic diagram of the pRLkatBKan	106
<b>3.5.2</b>	Generation of <i>Anabaena katB</i> mutant	107
<b>3.6.1</b>	Sensitivity of the <i>AnKatB<sup>-</sup></i> strain to NaCl stress.	109
<b>3.6.2</b>	Molecular changes associated with NaCl treatment in <i>katB</i> mutant	110
<b>3.7</b>	Exposure of the NaCl pre-treated <i>katB</i> mutant <i>Anabaena</i> to H <sub>2</sub> O <sub>2</sub>	112
<b>3.8</b>	Ultrastructural changes associated with NaCl and H <sub>2</sub> O <sub>2</sub> treatment	113
<b>3.9.1</b>	Detection of <i>katB</i> transcript in <i>Anabaena</i> in response to various abiotic stresses	114
<b>3.9.2</b>	Expression of KatB protein under various abiotic stresses	115
<b>3.10</b>	Nitrogen status dependent expression of <i>katB</i> /KatB in <i>Anabaena</i>	117
<b>3.11</b>	RACE analysis and identification of <i>katB</i> promoter	118
<b>3.12.1</b>	Generation of <i>katB</i> promoter- <i>gfp</i> fusion <i>Anabaena</i> strain	119
<b>3.12.2</b>	Expression of <i>katB</i> promoter in response to different osmotic stimuli	121
<b>3.13</b>	Lack of P <sub><i>katB-gfp</i></sub> expression in heterocysts	122
<b>3.14.1</b>	Schematic representation showing the NaCl mediated KatB induction and consequent protection of the organism against oxidative damage	126
<b>3.14.2</b>	Schematic representation of H <sub>2</sub> O <sub>2</sub> detoxification pathways	127

	in vegetative cells and heterocysts	
<b>4.2</b>	Cloning of <i>katB</i> ORF in pET21a expression vector and heterologous over expression of recombinant KatB in <i>E. coli</i>	134
<b>4.3</b>	Effect of low temperature on solubility of over-produced protein and its subsequent purification	136
<b>4.4</b>	Effect of Mn <sup>2+</sup> supplementation on solubility and activity of over-produced KatB protein	137
<b>4.5.1</b>	Gel filtration and native PAGE analysis of purified KatB protein	138
<b>4.5.2</b>	CD spectra of the KatB protein	139
<b>4.5.3</b>	Dynamic Light Scattering (DLS) profile of KatB protein in 20 M Tris buffer, pH 8.0	140
<b>4.6.1</b>	Activity of the purified KatB protein	141
<b>4.6.2</b>	Kinetic properties of KatB enzyme	142
<b>4.6.3</b>	pH dependent activity of KatB	143
<b>4.6.4</b>	Inhibition of KatB activity by hydroxylamine or sodium azide	143
<b>4.6.5</b>	Effect of NaCl on KatB activity	144
<b>4.7</b>	Thermostability of KatB	145
<b>4.8</b>	Sensitivity of the KatB protein to guanidium hydrochloride (GuHCl)	146
<b>4.9.2</b>	Structure of an individual KatB monomer	148
<b>4.9.2</b>	Crystal structure of KatB	149

<b>4.9.3</b>	Active site configuration of KatB	150
<b>4.9.4</b>	Active site comparison	151
<b>4.10.1</b>	Site directed mutagenesis of Tyr-42 in KatB	153
<b>4.10.2</b>	Site directed mutagenesis of Tyr-140 in KatB	154
<b>4.11</b>	Phylogenetic analysis of catalases present among various texa	160
<b>5.2</b>	The N-terminal $\beta$ -sheet and hydrophobic interactions of the relevant residues	169
<b>5.3</b>	Sequence analysis of the N-terminal region of Mn- catalases	170
<b>5.4</b>	Site directed mutagenesis to generate N-terminal variants of KatB	171
<b>5.5</b>	Compactness of the N-terminal variants of KatB	172
<b>5.6</b>	Catalase activity of the N-terminal variants	174
<b>5.7</b>	Sensitivity of the N-terminal variants towards GuHCl mediated chemical denaturation	175
<b>5.8.1</b>	Conservation of the second amino acid in Mn-catalases	176
<b>5.8.2</b>	Purification of the second amino acid variants of KatB	177
<b>5.8.3</b>	Effect of the N-terminal second amino acid on compactness of the KatB oligomer	178
<b>5.8.4</b>	H <sub>2</sub> O <sub>2</sub> decomposition activity of the N-terminal second amino acid variants of KatB	180
<b>5.8.5</b>	Lineweaver-Burk plot for the catalytically active second amino acid variants, KatBF2Y (A), KatBF2W (B) or	181

	KatBF2V (C)	
<b>5.8.6</b>	Sensitivity of the KatB variants to thermal or chemical denaturation	182
<b>5.9.1</b>	Over-expression of KatBF2V variant in <i>Anabaena</i>	186
<b>5.9.2</b>	Expression of KatB in <i>Anabaena</i> strain over-expressing KatBWT or KatBF2V	187
<b>5.9.3</b>	Decomposition of externally added H <sub>2</sub> O <sub>2</sub> by <i>AnKatBF2V</i> <sup>+</sup> , <i>AnKatB</i> <sup>+</sup> or the wild-type <i>Anabaena</i> strain	188
<b>5.10</b>	Crystal structure of the KatBF2V protein	190
<b>5.11.1</b>	Hydrophobic interactions at the dimer interface	191
<b>5.11.2</b>	Interaction between the second amino acid and Phe-66	192
<b>5.11.3</b>	Interaction of the N-terminal second residue with Trp-43	193
<b>6.2.1</b>	Schematic diagram of the vectors generated for KatB over-expression in <i>Anabaena</i>	205
<b>6.2.2</b>	Micrograph of recombinant <i>AnKatB6H</i> <sup>+</sup> strain (400 X)	207
<b>6.2.3</b>	Expression of recombinant his-tagged An-KatB protein in <i>AnKatB6H</i> <sup>+</sup> strain	208
<b>6.2.4</b>	Localization of over-produced An-KatB protein in the soluble fraction	209
<b>6.3</b>	Purification of An-KatB protein by NiNTA affinity chromatography	210
<b>6.4.1</b>	Partial purification of An-KatB with elevated temperature	211
<b>6.4.2</b>	Optimization of incubation time at 80°C	213
<b>6.4.3</b>	Purification of An-KatB by ammonium sulphate	214

	precipitation	
<b>6.5.1</b>	Activity of An-KatB-H-A and An-KatB-N	216
<b>6.5.2</b>	Secondary structure and melting curve analysis	217
<b>6.6.1</b>	Oligomeric compactness of An-KatB or Ec-KatB	218
<b>6.6.2</b>	Circular dichroismspectropolarimetry of An-KatB or Ec- KatB	219
<b>6.7</b>	Comparison of KatB purified from <i>Anabaena</i> (An-KatB) or from <i>E. coli</i> (Ec-KatB)	220
<b>6.9.1</b>	Comparison of specific activity and effect of pH on An- KatB and Comm Cat	222
<b>6.9.2</b>	CD spectropolarimetric analysis of An-KatB or Comm Cat	223
<b>6.9.3</b>	Comparison of thermostability	224

## LIST OF TABLES

<b>Table. No.</b>	<b>Title of the table</b>	<b>Page</b>
<b>2.1</b>	List of chemicals used in the study	67
<b>2.2</b>	List primers used in the study	68
<b>2.3</b>	List plasmids used or generated in the study	71
<b>2.4</b>	List of restriction enzymes used in the study	74
<b>2.5</b>	List of <i>E. coli</i> strains used or generated in the study	74
<b>2.6</b>	List of <i>Anabaena</i> strains used or generated in the study	76
<b>4.1</b>	Kinetic parameters of biochemically characterized Mn-catalases	157
<b>5.1</b>	Kinetic parameters of the catalytically active KatB variants	181
<b>5.2</b>	T <sub>m</sub> of the second amino acid variants	183

### **Highlights of the thesis**

1. Mn-catalase KatB plays a major role in adaptation to salinity and oxidative stress in heterocystous filamentous cyanobacterium *Anabaena* PCC 7120.
2. The *katB* gene is induced by osmotic stress and the *katB* promoter is active only in vegetative cells but not in heterocysts.
3. The KatB protein is a thermostable, robust Mn-catalase that functions in alkaline pH and in high ionic strength.
4. Crystal structure of the protein shows the protein to be a compact hexamer with four-helix bundle type architecture and active site that is distinctly different from other Mn-catalases.
5. The N-terminal region of KatB is involved in oligomerization and in particular, the second residue (a non-active site residue) is essential for inter-subunit interactions and for the formation of the proper hydrophobic pocket that held the active site together.
6. The KatB protein, over-produced using *Anabaena* as expression host, can be purified by simple physical processes.
7. KatB purified from *Anabaena* shows better enzyme characteristics compared to KatB purified after over-expression in *E. coli*.